e-ISSN: 2147-2092

GAZI MEDICAL JOURNAL

2024
October
Volume 35 • Issue 4

galenos yayınevi

medicaljournal.gazi.edu.tr

GAZI MEDICAL JOURNAL

medicaljournal.gazi.edu.tr

Editorial Team

GAZI MEDICAL JOURNAL

medicaljournal.gazi.edu.tr

Please refer to the journal's webpage (https://medicaljournal.gazi.edu.tr/) for "About the Journal" and "Submissions".

The editorial and publication process of Gazi Medical Journal are shaped in accordance with the guidelines of the International Committee of Medical Journal Editors (ICMJE), World Association of Medical Editors (WAME), Council of Science Editors (CSE), Committee on Publication Ethics (COPE), European Association of Science Editors (EASE), and National Information Standards Organization (NISO). The journal is in conformity with the Principles of Transparency and Best Practice in Scholarly Publishing.

Gazi Medical Journal is indexed in Emerging Sources Citation Index, Scopus, Directory of Open Access Journals, EuroPub, Islamic World Science Citation Center, ABCD Index.

The online published articles are freely available on the public internet.

Owner: Musa Yıldız on Behalf of Gazi University

Responsible Manager: Mehmet Ali Ergün

Publisher Contact
Address: Molla Gürani Mah. Kaçamak Sk. No: 21/1
34093 İstanbul, Türkiye
Phone: +90 (539) 307 32 03

E-mail: info@galenos.com.tr/yayin@galenos.com.tr
Web: www.galenos.com.tr
Publisher Certificate Number: 14521

Publication Date: October 2024
e-ISSN: 2147-2092
International scientific journal published quarterly.

GAZI MEDICAL JOURNAL

medicaljournal.gazi.edu.tr

CONTENTS

Original Investigations - Özgün Araştırmalar

GAZI MEDICAL JOURNAL

medicaljournal.gazi.edu.tr

CONTENTS

GAZI MEDICAL JOURNAL

medicaljournal.gazi.edu.tr

CONTENTS

GMJ 2024;35:342-350

DOI: http://dx.doi.org/10.12996/gmj.2024.3621

Educational Needs During COVID-19: MOOCs Experiences Among Global Family Physicians

COVID-19 Sırasında Eğitim İhtiyaçları: Küresel Aile Hekimlerinin KAÇD Deneyimleri

Özden Gökdemir[1], Halime Seda Küçükerdem[2], Sudip Bhattacharya[3], Maria Bakola[4], Mohammed Idris Shariff[5]

[1]Department of Family Medicine, İzmir University of Economics Faculty of Medicine, İzmir, Türkiye
[2]Clinic of Family Medicine, Bozyaka Training and Research Hospital, İzmir, Türkiye
[3]Department of Community Medicine, All India Institute of Medical Sciences Deoghar, Jharkhand, India
[4]Department of Public Health, Medical School, University of Patras, Patras, Greece
[5]Family Health Center, Family Medicine, Dhaman, Kuwait

ABSTRACT

Objective: Family physicians (FPs) worldwide have rallied to minimize the indirect effects of the disease. FPs are always on the frontline, "first in- last out", and took the lead in fighting the virus-caused disease in the acute phase of the coronavirus disease-2019 (COVID-19) epidemic. They played a vital role in examining, informing, and monitoring patients in primary care health centers, as well as in centers set up specifically for COVID-19. However, due to poor knowledge of COVID-19, which changes rapidly, FPs had to update their practical and theoretical knowledge about this novel coronavirus on a daily. Massive open online courses (MOOCs) are courses that use an online application and can reach the entire world. In this study, we aimed to determine the opinions and suggestions of FPs in meeting their educational needs related to COVID-19 through MOOCs and to create solutions.

Methods: The study was planned to be held with FPs who completed MOOCs training and completed the questionnaire. Due to international participation, the survey was conducted in English. Ethical approval was obtained from the Ethics Committee of İzmir University of Economics. Participation was entirely voluntary.

Results: Our study revealed that as the age of FPs increases, their confidence in their ability to treat patients also increases. FPs showed a positive attitude toward MOOCs as sources of continuous medical education and group activity ($p<0.005$). For the qualitative part of the study, three themes were significant: "i) opinions about concerns about changes of primary care, ii) views and attitudes about the information need and access to information, iii) attitudes and beliefs about MOOCs".

ÖZ

Amaç: Aile hekimleri (AH) dünya genelinde hastalığın dolaylı etkilerini en aza indirmek için seferber olmuştur. AH'leri her zaman ön saflarda yer almakta, "ilk giren-son çıkan" olarak hareket etmektedir ve koronavirüs hastalığı-2019 (COVID-19) salgınının akut evresinde virüs kaynaklı hastalıkla mücadelede öncülük etmiştir. Birinci basamak sağlık merkezlerinde ve COVID-19 için özel olarak kurulmuş merkezlerde hastaları muayene etme, bilgilendirme ve izleme konusunda hayati bir rol oynadılar. Ancak hızla değişen COVID-19 konusundaki yetersiz bilgi nedeniyle, AH'leri bu yeni koronavirüs hakkında pratik ve teorik bilgilerini günlük olarak güncellemek zorunda kalmıştır. Kitlesel açık çevrimiçi dersler (KAÇD), çevrimiçi bir uygulama kullanarak dünya çapında erişim sağlayan kurslardır. Bu çalışmada, AH'lerinin COVID-19 ile ilgili eğitim ihtiyaçlarını KAÇD'ler aracılığıyla karşılama konusundaki görüş ve önerilerini belirlemeyi ve çözüm önerileri geliştirmeyi amaçladık.

Yöntemler: Çalışma, KAÇD eğitimini tamamlamış ve anketi doldurmuş AH'lerle gerçekleştirilmek üzere planlanmıştır. Uluslararası katılım nedeniyle anket İngilizce olarak yapılmıştır. Etik onay, İzmir Ekonomi Üniversitesi Etik Kurulu'ndan alınmıştır. Katılım tamamen gönüllülük esasına dayanmaktadır.

Bulgular: Çalışmamız, AH'lerin yaşı arttıkça hastaları tedavi etme konusundaki güvenlerinin de arttığını ortaya koymuştur. AH'ler, KAÇD'lere sürekli tıp eğitimi ve grup etkinliği olarak olumlu bir yaklaşım sergilemişlerdir ($p<0,005$). Çalışmanın nitel kısmında üç tema öne çıkmıştır: "i) birinci basamak sağlık hizmetlerindeki değişikliklere dair endişeler hakkında görüşler, ii) bilgi ihtiyacı ve bilgiye erişim konusundaki görüşler ve tutumlar, iii) KAÇD'ler hakkında tutumlar ve inançlar".

Address for Correspondence/Yazışma Adresi: Özden Gökdemir, Assoc Prof, MD, Department of Family Medicine, İzmir University of Economics Faculty of Medicine, İzmir, Türkiye
E-mail / E-posta: gokdemirozden@gmail.com
ORCID ID: orcid.org/0000-0002-0542-5767

Received/Geliş Tarihi: 19.07.2022
Accepted/Kabul Tarihi: 29.08.2024

ABSTRACT

Conclusion: By completion of this course, FPs broadened their knowledge about COVID-19 management. This gave them capacity to save and improve the lives of countless patients infected by the novel coronavirus worldwide. Sharing their experiences with COVID-19 could be a way to cope with stress.

Keywords: Primary care, education, MOOCs, family physician

ÖZ

Sonuç: Bu kursun tamamlanmasıyla birlikte AH'ler, COVID-19 yönetimi konusunda bilgilerini genişletmişlerdir. Bu, onlara dünya genelinde yeni koronavirüsle enfekte olmuş sayısız hastanın hayatını kurtarma ve iyileştirme kapasitesi sağlamıştır. COVID-19 ile ilgili deneyimlerini paylaşmak, stresle başa çıkmanın bir yolu olabilir.

Anahtar Sözcükler: Birinci basamak, eğitim, KAÇD, aile hekimi

INTRODUCTION

The appearance of the novel coronavirus, which was later named severe acute respiratory syndrome coronavirus 2, was the beginning of one of the most serious challenges that our world faces in our lifetime. The coronavirus disease-2019 (COVID-19) outbreak was declared on January 30, 2020, by the Director-General of the World Health Organization (WHO) as public health (A Joint Statement on Tourism and COVID-19-UNWTO and WHO Call for Responsibility and Coordination) (1). At the time of this writing, in late November 2020, the number of COVID-19 cases was 61.5 million worldwide, with almost 1.5 million deaths recorded in 220 countries, areas and territories (2). The COVID-19 pandemic continues to spread around the world with an overwhelming loss of life, forcing healthcare systems to their limits and forcing more than 3 billion people to follow orders to stay at home (3). Since there is still no adequate treatment at present, this disease increases the number of hospital admissions and the need for intensive care units. Many countries have sought solutions to health system-related equipment-related problems by increasing the number of health workers and the amount of respiratory equipment.

The appearance of COVID-19 pandemic was the beginning of one of the most serious challenges facing our world in our lifetime. Many people mourned their loved ones, and those who survived COVID-19 struggled with the long-term effects of the disease. Although the medical community now has COVID-19 vaccines to prevent deaths from different variants, countries are still struggling with the new waves of COVID-19. FPs are always on the frontline, "first in-last out", and took the lead in fighting the virus-caused disease in the acute phase of the COVID-19 epidemic. They played a vital role in examining, informing, and monitoring patients in primary care health centers, as well as in centers specifically set up for COVID-19. At the same time, they were trying to maintain the follow-up of chronic diseases, deal with the emotional side of medicine, and ease the escalation of the COVID-19 pandemic into a syndemic (4,5). At the beginning of the pandemic, FPs were poorly informed by policy makers about their new roles and how to perform their continuing responsibilities (6). Moreover, primary care had a duty to transform rapidly and protect healthcare workers and patients while at the same time remaining connected to patients (7). Family physicians (FPs) around the world continue to rally to minimize the indirect effects of the disease.

In the early stages of the COVID-19 pandemic, the roles of FPs were ill-defined, but as time went on, their responsibility areas and roles became clearer. FPs were assigned to the hospitals to help meet inpatient COVID-19 admissions, before the administration of COVID-19 prevention measures, isolation, and protective measures were structured. Later on, FPs took on different tasks in the management of outpatient COVID-19 patients in primary care (8). They performed this by monitoring those with close contact with patients with confirmed or probable COVID-19, treating outpatients, and providing information about the importance of isolation. In this way, FPs helped slow the spread of the epidemic (6,9). However, due to difficulties in keeping pace with rapidly changing knowledge about COVID-19, FPs had to update their practical and theoretical knowledge about this novel coronavirus daily. Massive open online courses (MOOCs) are courses that use an online application to reach the entire world (10). These courses aim to increase the quality of education, facilitate access to information, and at the same time enhance the collaboration between doctors and institutes for the benefit of patients and public health (11-13).

In this study, we aimed to determine FPs'opinions about and suggestions for meeting their educational needs related to COVID-19 through MOOCs and to create solutions accordingly.

MATERIALS AND METHODS

Many participants from different countries and different age groups participated in the "Fighting COVID-19 with epidemiology: A Johns Hopkins Teach-Out by Johns Hopkins University" program in 2020, which created a worldwide community of FPs [Fighting COVID-19 with Epidemiology: A Johns Hopkins Teach-Out | Coursera (cited 2020 Nov 29). Available from: https://www.coursera.org/learn/covid19-epidemiology].

The course consisted of three hours of visual and written material. The program shared epidemiological information on epidemic identification, evaluation, epidemic investigation, and epidemic control. Participants followed the course material at their own pace in any time zone, and the discussion environment and information exchange were supported by administrators on the community-created information exchange platform. Calls to join the course were made on various social media platforms (Facebook, WhatsApp, Twitter) and 208 FPs participated. First, we applied the questionnaire, following which a qualitative research design was used to determine motivation for participation in the course, educational achievements, and views and suggestions, as well as training needs. The participants in this study were FPs who completed the MOOCs training and completed the questionnaire. Each participant followed the course material in their time zone. After the completion of the course, the survey was sent via email and WhatsApp messages. The questions were created by the researchers using both open-ended and multiple-choice questions.

Statistical Analysis

The SPSS 21.0 package was used to analyze the data. Parametric or nonparametric analysis methods were preferred for testing number and percentage values, normal distribution, and co-variance fit

for sociodemographic characteristics. The data analysis involved frequency and percentage distributions, chi-square analysis, and t-test in independent groups. In this study, p <0.05 was considered statistically significant, and the results were evaluated accordingly. The "thematic analysis" method developed by Braun and Clarke (14) in 2006 was used as the assessment method for the qualitative study. With the "investigator triangulation" method, it was planned to prevent possible side stiffness (15).

Ethical approval was given from the Ethics Committee of İzmir University of Economics to conduct the study (approval number: B.30.2.İEÜSB.0.05.05-20-073, date: 06.07.2020). FPs who participated were advised in the information provided that by completing and submitting the survey, they were indicating their consent to participate in the study.

RESULTS

Out of 208-FPs in the course, 51 participated in the online survey during the pandemic. Of the 51 participants, 28 were male (54.9%). The mean age of the participants was 37.12±7.557 (Table 1). Among the participants, 31 (60.8%) worked in a dedicated COVID clinic. The largest group of FPs, 21 (41.2%) had 6-10 years of work experience. Nineteen (37.3%) of our participants worked less than 48 hours/week. During their working hours, 13 (25.5%) attended 1-10 patients. We found that the countries most represented were India (27 (52.9%), followed by Türkiye 11 (21.6%), Spain 2 (2%), Mexico, 2 (2%) and the rest, 9 (18%) were from other countries (Table 2). The main way of hearing about the course was through colleagues 17 (33.3%), followed by social media 13 (25.5%), the WhatsApp group of the previous MOOCs 13 (25.5%), and coursera website 7 (13.7%). Most, 35 (68.6%) participants had never attended any MOOCs

Table 1. Descriptive characteristics of the FPs

Descriptive statistics					
	n	**Minimum**	**Maximum**	**Mean**	**SD**
Age	51	20	57	37.12	7.557
How do you feel about MOOC courses as part of continuous medical education?	51	4	10	8.02	1.667
How do you feel about MOOC courses as group activities?	51	4	10	8.06	1.593
Overall confidence	51	3.77	9.62	7.0415	1.22927

SD: Standard deviation, FPs: Family physicians, MOOC: Massive open online courses.

Table 2. Descriptive characteristics of FPs about workplaces

		Frequency	**Adjustedmean**	**95% CI**	**p-value**
Are you working at a dedicated COVID-19 clinic?	Yes	31 (60.8%)	7.096	(6.662, 7.530)	0.689721
	No	20 (39.2%)	6.957	(6.417, 7.498)	
Country	Angola	1 (2.0%)	8.918	(6.763, 11.073)	0.009001
	Bangladesh	1 (2.0%)	5.242	(3.012, 7.472)	
	France	1 (2.0%)	7.796	(5.770, 9.822)	
	India	27 (52.9%)	7.277	(6.881, 7.673)	
	Italy	1 (2.0%)	6.813	(4.797, 8.829)	
	Mexico	2 (3.9%)	8.948	(7.513, 10.383)	
	Nigeria	1 (2.0%)	6.417	(4.399, 8.436)	
	Pakistan	1 (2.0%)	5.907	(3.824, 7.989)	
	Peru	1 (2.0%)	8.346	(6.329, 10.363)	
	Spain	2 (2.0%)	7.153	(5.722, 8.585)	
	Türkiye	11 (21.6%)	5.994	(5.383, 6.604)	
	UAE	1 (2.0%)	6.972	(4.955, 8.989)	
	USA	1 (2.0%)	8.088	(5.979, 10.197)	
How did you hear about the course?	Colleagues	17 (33.3%)	6.684	(6.089, 7.279)	0.666168
	Coursera website	7 (13.7%)	7.322	(6.392, 8.253)	
	I don't know	1 (2.0%)	6.812	(4.376, 9.249)	
	Social media	13 (25.5%)	7.146	(6.468, 7.824)	
	WhatsApp group of the last MOOCs	13 (25.5%)	7.270	(6.591, 7.950)	

FPs: Family physicians, MOOC: Massive open online courses, COVID-19: Coronavirus disease-2019, CI: Confidence interval.

before the pandemic. More than half, 27 (52.9%), attended other MOOCs during the pandemic.

The majority, 38 (74.5%) considered that MOOCs has contributed to their primary care services during the pandemic by increasing their knowledge. The majority 28 (54.9%) of our participants reported never using antidepressants or anxiolytic drugs during the pandemic. Of the 51 participants, 11 (21.6%) had a history of psychiatry consultation. The 11 participants had used antidepressant/anxiolytic drugs at some time and, interestingly, 5 (9.8%) of them started taking them during the pandemic. We calculated the overall confidence as the cumulated mean score of all 26 questions on confidence. To test whether any statistical difference was present in the cumulated mean score among the different categories after controlling for the effect of age on overall confidence, we applied the one-way Analysis of covariance (ANCOVA) statistical test. Age can affect the overall confidence; thus, it is important to control for its effects. In this analysis, age was now considered a covariate in ANCOVA. In the next step, the 95% confidence interval of this adjusted mean and p-value were also calculated to test for any statistically significant difference in the adjusted mean score among different categories of independent variables (Table 3). We found that the p-value was greater than 0.05 for gender, implying no statistical difference in the

Table 3. Univariate ANCOVA (age adjusted)

		Frequency	Adjusted mean	95% CI	p-value
Gender	Female	23 (45.1%)	6.909	(6.403, 7.414)	0.482563
	Male	28 (54.9%)	7.151	(6.693, 7.608)	
Have you ever attended any MOOC events before?	No	35 (68.6%)	6.960	(6.553, 7.366)	0.475516
	Yes	16 (31.4%)	7.220	(6.618, 7.822)	
Did you attend more MOOCs during the pandemic?	No	24 (47.1%)	6.517	(6.068, 6.965)	0.002277
	Yes	27 (52.9%)	7.508	(7.085, 7.931)	
Is this course contributed to your primary care services during the pandemic?	No	13 (25.5%)	6.173	(5.570, 6.776)	0.001564
	Yes	38 (74.5%)	7.339	(6.986, 7.692)	
How many years do you have worked as a FP or general practitioner?	0-5 years	18 (35.3%)	6.369	(5.784, 6.955)	0.006481
	6-10 years	21 (41.2%)	6.836	(6.368, 7.303)	
	11-15 years	6 (11.8%)	7.800	(6.882, 8.718)	
	16-20 years	4 (7.8%)	8.718	(7.492, 9.943)	
	>21 years	2 (3.9%)	9.622	(7.897, 11.348)	
How many working hours have you been doing during COVID-19?	Less than 48 hours/ week	19 (37.3%)	7.452	(6.920, 7.984)	0.040066
	48 hours/week	15 (29.4%)	7.189	(6.600, 7.778)	
	More than 48 hours/ week	17 (33.3%)	6.452	(5.889, 7.015)	
How many patients are examined per day?	0	2 (3.9%)	7.972	(6.342, 9.601)	0.040275
	1-10	13 (25.5%)	7.481	(6.864, 8.098)	
	11-20	9 (17.6%)	6.712	(5.974, 7.450)	
	21-30	11 (21.6%)	7.415	(6.740, 8.089)	
	31-40	7 (13.7%)	7.112	(6.271, 7.954)	
	41-50	3 (5.9%)	6.591	(5.284, 7.897)	
	More than 50	6 (11.8%)	5.732	(4.823, 6.642)	
Did you ever use antidepressants or anxiolytic drugs?	I have used before COVID-19	11 (21.6%)	6.129	(5.462, 6.796)	0.023232
	I used it before COVID-19 and still use it	4 (7.8%)	7.135	(6.024, 8.246)	
	I have 5 (9.8%)	5 (9.8%)	7.942	(6.948, 8.937)	
	I haven't used any drugs	28 (54.9%)	7.268	(6.849, 7.686)	
	I don't want to answer	3 (5.9%)	6.650	(5.330, 7.971)	
Do you have any previous psychiatric treatment history?	No	40 (78.4%)	7.304	(6.958, 7.650)	0.001957
	Yes	11 (21.6%)	6.087	(5.426, 6.748)	

FPs: Family physicians, ANCOVA: Analysis of covariance, CI: Confidence interval, COVID-19: Coronavirus disease-2019.

adjusted mean scores. There was no statistically significant difference in whether the participant had attended any MOOCs before (p>0.05). However, there was a statistically significant difference (p=0.0022) in the participants' overall confidence regarding whether they had attended other MOOCs during the pandemic. In other words, the overall confidence of FPs increased after attending multiple MOOCs. Overall, this course boosted the confidence of FPs who provided primary care services during the pandemic (p=0.001). We also found that FPs' overall confidence had been significantly low for those attending 11-20 patients, increased for those attending 21-30 patients, and then started declining with increasing number of patients. We found that overall confidence was positively correlated with other variables (Table 4). This indicates that as the age increases, confidence about treating patients increases, and they have a more positive attitude toward MOOCs as sources of continuous medical education, as well as group activity (p<0.005). This can be explained by the theory of Kern et al. (16); "Significant personal growth was preceded by powerful experiences, supportive relationships, and introspection. These findings are in line with the theoretical and empirical research on adult learning and may have implications for medical education and practice. They need to be replicated in other physician groups." Self-assessment is also required to improve knowledge and behavior (17). As quantitative research is insufficient to discover deep meanings, the second part of the study was conducted as a qualitative phenomenology study. Phenomenology aims at gaining an in-depth understanding of the meaning or nature of our daily experiences, which, although familiar, may not be fully grasped (18,19).

Participants

The qualitative part of the research was conducted with 8 FPs who completed the course and agreed to participate. All participants worked in primary healthcare during the research period. Attention was paid to ensuring that the interview questions gave the same meaning after translation and were comprehensible. Interviews were conducted online with participants due to the different locations and pandemic conditions. Interviews were recorded with the participants' permissions.

Data Collection Process

Online face-to-face interviews were planned as a data collection tool to obtain the desired information in depth and to adapt to different and instantly changeable conditions (18,19).

After the literature review, the following five research questions were created within the framework of the study:

1. How do you think COVID-19 affects family medicine practice?

2. How has access to essential, reliable, and up-to-date information developed during the pandemic's changing conditions?

3. How did you decide to attend the MOOC?

4. What was your motivation to take the course offered by John Hopkins?

5. If you need regular information on topics other than COVID, how can an international organization like World Organization of Family Doctors (WONCA) help?

The interviews followed a semi-structured interview protocol, and the questions were related to the research questions of this study. Two researchers were present at the interviews: one asked the questions, and the other observed and took notes. The interviews were conducted between November and December 2020 and took between 20 and 30 minutes. The researchers asked questions, but no restrictions were placed on the participants' freedom to express themselves.

Data Analysis

The interview audio recordings were decoded verbatim. After the interviews were transcribed, codings were done by 3 researchers independently, then open codes agreed. Similar codes were divided into groups. The interconnected open codes were collected under "Sub-Themes". More comprehensive common titles, "Themes", were created by evaluating the sub-themes among themselves.

Table 4. Effect of age on MOOC perception

Spearman's correlations				
		Age	**How do you feel about MOOC courses as part of continuous medical education?**	**How do you feel about MOOC courses as group activities?**
Overall confidence	Correlation coefficient	0.367	0.530	0.409
	Sig. (2-tailed)	0.008087	0.000064	0.002910
	n	51	51	51

MOOC: Massive open online courses.

Table 5. Themes determined by the investigation

Theme 1	Opinions and concerns regarding changes in primary care
Theme 2	Views and attitudes about information needs and access to information
Theme 3	Attitudes and beliefs about MOOCs

MOOC: Massive open online courses.

Thematic analysis was used to analyze the data. Synonyms were used for anonymity. Analyses were performed manually rather than through a software. The evaluation of the results was carried out within the framework of the themes.

Results

In the qualitative part of the study, eight participants (who agreed to participate and could spare time) were interviewed. From the created codes, the themes represented were reached. These are listed in the Table 5:

The feeling of loneliness was included as an open code. It was mentioned separately in all themes by most participants. Loneliness was repeatedly expressed in different contexts, such as in a struggle with an unknown situation, accessing information, and communication with colleagues.

Theme 1: Opinions and concerns about changes in primary care:

The sub-headings comprising this theme can be listed as follows:

1. Primary care applications and differences in implementation

2. Disruptions due to contamination anxiety

a. Vaccination

b. Chronic disease follow-up

c. Scans

3. Anxiety associated with an unknown disease: confidence

All FPs stated that there were changes in the content of health services they generally offered. They described the changes in the number of outpatient clinics in the context of patient avoidance due to concerns about contamination and the variability in information and practices.

> I2: There have been constant changes in department by department; the number of patients first decreased and then increased.
>
> I3: .. it has a profound effect on outpatient services.
>
> I4: There was a new process every time, there were sudden changes. It is a period of confusion, and we cannot sit still.

Participants stated that some of their patients hesitated to visit the clinic due to contamination concerns and that they experienced problems during routine healthy child follow-up and vaccination, cancer screening, and chronic disease follow-up.

> I1: "They come with suspicion during pregnancy and during infant and child follow-ups. Will I get COVID from inside?"
>
> I2: "The problem with early diagnostic tests, especially cancer screening, seems to persist."
>
> I2: "… they especially refused to come for vaccines, especially to follow-up on chronic diseases."
>
> I3: "We had to completely postpone or cancel our activities for preventive medicine"
>
> I7: "Where did the other diseases go? What were we doing before COVID-19?"

In some interviews, statements were made about the anxiety of making mistakes in the differential diagnosis, treatment, and management of a new and unknown disease. At the same time, statements indicating malpractise concerns and a lack of confidence were encountered due to the changing 1st level operation, new job descriptions, and additional jobs. There are reports of inadequacies in self-confidence due to uncertainty caused by the lack of clear information.

> I1: "...we had serious difficulties in diagnosis and treatment. We're afraid of malpractise. I wonder if it was COVID or not, and I was worried if I gave another treatment".
>
> I2: "I needed to look over and over for drug interactions to see if I was skipping something."
>
> I3: "…who to refer and who to test remains unclear." We were dealing with more complex cases."
>
> I7: "…this is totally different from the way we understood primary care at the first days… but now it became usual …"

It was found that there were changes in the patient-physician relationship and communication due to the arrangements made in the polyclinics due to the preventive measures for the disease and the changes in the duration and content of the interviews with patients.

> I2: "Unfortunately, it was not possible to carry out that standard meeting… so it was not possible to continue our old communication."
>
> I3: "We work in an unfamiliar environment, not specific to our own discipline."
>
> I7: "…the position of the table and the patients, etc, everything has changed."
>
> I8: "I'm now working in a new place and so I need to see my patients' faces to know them and also the patients…but we all have masks"

Theme 2: Views and attitudes about the need for and access to information

The sub-themes listed below were used in the formation of this theme:

1. Lack/need for information

2. Variability in knowledge

3. Accumulation of knowledge

4. Methods to access information

In the interviews, participants generally expressed negative beliefs about their sense of competence. It was found that respondents did not feel sufficiently informed about disease prevention when answering questions from patients and treatment schemes.

I1: "I questioned my own suggestions, I was hesitant to say something to the patients, because the disease was completely unknown."

I2: "What are the symptoms that will alert us, what should we do for protection, how should we strengthen immunity?"

I3: "I followed the ministry's updates, but they did not meet the needs in the field. Conditions are so dynamic!"

I4: "When it first started in China, I was experiencing anxiety even before we had a single case because there was an object approaching."

I6: "…the ministry and associations had informed us first… now everything is changing quickly, chaotic"

All participants stated in their interviews that no specific training was given, especially to primary healthcare workers.

I1: "the ministry of health did not have a training for us"

I2: "no guide was published directly for the primary level; no direct training was provided to us."

I3: "published studies with a relatively high level of evidence were not primary care studies. It was the 2nd and 3rd step studies; there isn't an adequate, satisfactory answer in the primary care literature yet."

I4: "We did not receive any special training for FPs, except for the nationwide published guidelines."

I6: "No guideline or education was made during the early times for the primary care"

I8. "No education was carried out for the primary care associations and some universities performed how to use PPE, etc, but not more than this"

Participants expressed a variety of feelings and thoughts about their experience of a constant change in the information published throughout the process. Because of this variability, they felt pressure to seek out reliable information and stay up-to-date.

I1: "The resources were frequently updated; it was difficult to follow. The content of the treatment, the scheme of application, the reports to be given to the patients, and the number of filiations were constantly changing."

I2: "There was probably a lot of information pollution".

I3: "Gaps remain constantly in the process of monitoring patients."

I4: "It has transformed, from the thought of reading what I find relevant, to a selection period of thinking about which is correct information, and which one I will trust."

I7: "There were lots of information and I was trying to listen to them all but now I'm only looking for what I need to learn"

Participants were looking for alternative ways to meet their perceived need for information to manage a new disease process. They stated that they encountered many different trainings and sources of information and that they made choices by determining their needs. Among the ways to access information in interviews. they mentioned many different sources, such as online training sessions of professional organizations, webinars, and university messaging groups. Messaging groups of universities and professional organizations, where colleagues share information, were the most frequently used means of access to information.

I1: "…current articles, article sharing on social media by infection teachers I trust"

I2: "I was attending the zoom meetings and google meetings when we were locked down for the first time. There were webinars supported by pharmaceutical companies. Our trade associations had their training."

I3: "Online training is very popular in this period. ...associations and professional organizations have publications."

I4: "I followed the teachers I trusted, participated in sharing groups of different professions, from pulmonology and virology."

I8: "Colleague groups are more effective and quicker"

Theme 3: Attitudes and beliefs about MOOCs:

The following subthemes were used to create this theme:

1. Determination of needs
2. Motivation to join the MOOCs
3. Time
4. Post-MOOCs evaluations
5. International interaction

This study examines the course, "Fighting COVID-19 with Epidemiology: A Johns Hopkins Teach-Out by Johns Hopkins University", and the reasons for participants' enrollment, including a trusted colleague's recommendation, and testing their own limits.

I1: "I also trust her/his medical knowledge on this subject and because it is a doctor's recommendation that I like. I agreed with the priorities of the proposer and whether she/he knew me or not, thinking that the training he offered me would be useful."

I3: "I learned through the communication network of the university where I specialized. I currently have a field of activity in rural medicine. I am now at the center of the organization, in a position at its core. So, I thought it might be useful to me."

I4: "After a little bit of quarantine, we saw that everything worked online. I also joined in to feel closer to such new methods."

I7: "Now working online is a choice, so is education, too. Epidemiology is also a topic of interest to learn together."

I8: "I have learned from my colleagues and thought could be useful."

The interviewees stated that in the process of deciding to enroll in MOOCs training, they mostly considered their current information needs. They stated that they would consider the effect of the language of instruction as a constraint if not in their native language or in English, or if it was difficult to understand. At the end of these training sessions, there were statements that certification was not expected while working in the field, but perhaps for academic

studies or at the end of the training, and if the certificate gives the chance to become with more improved skills, it could make sense. They stated that they did not decide based on salary alone and that they could pay if they needed education, unless it involved very high amounts.

I1: "I determine my needs. If there is something that I am looking for and I need to improve, I do not hesitate to pay, but if not, I prefer the free one. I may be more motivated to attend and finish a paid course; "like registering to the gym and giving money to do sports."

I2: "Do I need training on this topic? Is there a need for my patients? The certificate is not very important; it is more important to be informed."

I3: "My decision to participate is not limited only by the fee; it is important to improve myself, whether or not I will use it in my clinical activities. Certification is effective in my decision-making, and the promise of certification makes us think that the course will be more serious and will yield meaningful results."

I4: "If it's a language I don't know at all, it affects my decision."

I6: "Most of the courses are in English, so there is no problem for me. If it was in another, then maybe a problem. The knowledge that I could use is more important than certificate."

I8: "I can speak in many languages you know, so the language is not a problem for me. A certificate is important and to learn is important too."

One of the main points that the participants paid attention to while deciding on all other trainings and MOOCs trainings was "time."

I1: "There is too much training, I have difficulty keeping up with them."

I2: "Do I need this training; do I have free time?"

I3: "I participate according to my daily practice needs and personal agenda."

I7: "If I had time, I would attend the training programs."

When John Hopkins evaluated the education, after participants' epidemiology training, feedback statements stated that it formed a knowledge base, but participants could not fully benefit from it in the daily practice of family medicine, or that it was very useful in jobs such as filiation.

I1: "I can say that it is more useful in terms of general knowledge development than practice." It laid the foundation."

I2: "I attended this training because I had not participated in this type of training before, because I was directed to attend the course, and it was a period when I was thinking of preparing myself during a febrile period of my illness."

I3: "I found it largely able to meet my expectations regarding its content. In particular, it created data that provide new perspectives. The ideas that the course provided in planning quarantine decisions where I worked enabled me to recover quickly."

I4: "The information you get from here does not immediately come to mind in daily practice. There are seated molds."

I8: "Of course, I used the knowledge that I learnt from the course, but not all of it."

The physicians interviewed expressed positive feelings and thoughts about international interactions in many primary care practices, in which no cultural differences were observed. This was believed to have a positive effect on dealing with feelings of loneliness. Their views revealed that the pandemic was an international situation and that interaction facilitated knowledge and struggle. They expressed that they expect continuous, up-to-date, and beneficial trainings at the primary level from international organizations.

I1: "For those who do not have the opportunity to participate in the trainings, the importance of international institutions increases even more, they can support them in providing a participatory environment and sharing international experiences."

I2: "We expect organizations such as WONCA to meet our needs for information and continue to publish updated information, even if we do not request it. We can sometimes feel lonely constantly, both in the field and for active disease."

I3: "Not a specific area in primary care, I have to somehow accept anyone who enters the door. In particular, the activities of the sub-working groups are important for producing more practical guides.

I4: "Our problems are very dynamic, changeable and urgent. Postgraduate training is very important for our discipline".

I5: "We need regular information on issues that we encounter constantly and rarely come across in practice. I think WONCA can lay the groundwork for a more international platform for a common learning network."

I6: "It's up to my daily practice needs.... now time is limited so summaries, algorithms could be more useful"

I7: "WONCA has more opportunities to reach FPs all over the world… sub working groups are useful too, webinars are made…"

DISCUSSION

The feeling of loneliness was remarkably common while analysing the interviews. For this reason, more in-depth information on this subject can be obtained by designing separate qualitative studies that deal with the relationship between loneliness and pandemics, education, or changing situations. Physicians were working outside the conditions they are accustomed to and in areas where it takes time for knowledge to accumulate. It was thought that this might have caused them a feeling of inadequacy. It is interesting that FPs who are working with 21-30 patients were more likely to attend the course. Appropriate workload could be a factor in attending courses; therefore, it is important to define educational needs and attain essential knowledge. Our research revealed that pandemics had a positive effect on attending online courses, similar to other studies (20,21).

Although countries have diverse strategies, the need for well-structured primary care has been revealed among not only undeveloped countries but also developed countries. The "lockdowns" may reduce the health burden of direct morbidity and mortality from COVID-19, but the new burden "economic status" has added and syndemy has begun (22). Apart from the topics discussed under these headings, G3 drew attention to a different aspect of the disease: COVID-19 causes stigma, and therefore, patients

are hesitant to apply for a diagnosis, which becomes difficult. By completion of this course, FPs broadened their knowledge about COVID-19 management. This enabled them to save and improve the lives of countless patients infected by the novel coronavirus worldwide. Sharing their experiences with COVID-19 could be a way to cope with stress.

Ethics

Ethics Committee Approval: Ethical approval was given from the Ethics Committee of İzmir University of Economics to conduct the study (approval number: B.30.2.İEÜSB.0.05.05-20-073, date: 06.07.2020).

Informed Consent: FPs who participated were advised in the information provided that by completing and submitting the survey, they were indicating their consent to participate in the study.

Authorship Contributions

Concept: Ö.G., H.S.K., S.B., M.B., M.I.S., Design: Ö.G., H.S.K., S.B., M.B., M.I.S., Data Collection or Processing: Ö.G., H.S.K., S.B., M.B., M.I.S., Analysis or Interpretation: Ö.G., H.S.K., S.B., M.B., M.I.S., Literature Search: Ö.G., H.S.K., S.B., M.B., M.I.S., Writing: Ö.G., H.S.K., S.B., M.B., M.I.S.

Conflict of Interest: No conflict of interest was declared by the authors.

Financial Disclosure: The authors declared that this study received no financial support.

REFERENCES

1. World Health Organization. A joint statement on tourism and COVID-19—UNWTO and WHO call for responsibility and coordination. Published, February 27, 2020. Accessed, September, 2021. Available from: https://www.who.int/news/item/27-02-2020-a-joint-statement-on-tourism-and-covid-19---unwto-and-who-call-for-responsibility-and-coordination.
2. World Health Organization. COVID-19: rights, roles and responsibilities of health workers, including key considerations for occupational safety and health. Published, 2019; (December):1-3. Accessed, September, 2021. Available from: https://www.who.int/docs/default-source/coronaviruse/who-rights-roles-respon-hw-covid-19.pdf?sfvrsn=bcabd401_0
3. On being human in the face of a pandemic. Nat Cancer. 2020; 1: 371.
4. Horton R. Offline: COVID-19 is not a pandemic. Lancet. 2020; 396: 874.
5. Gokdemir O, Pak H, Bakola M, Bhattacharya S, Hoedebecke K, Jelastopulu E. Family Physicians' Knowledge about and Attitudes towards COVID-19 - A Cross-sectional Multicentric Study. Infect Chemother. 2020; 52: 539-49.
6. Rawaf S, Allen LN, Stigler FL, Krignos D, Yamamto HQ, Weel CV, et al. Lessons on the COVID-19 pandemic, for and by primary care professionals worldwide. Eur J Gen Pract. 2020; 26: 129-33.
7. Krist AH, DeVoe JE, Cheng A, Ehrlich T, Jones SM. Redesigning Primary Care to Address the COVID-19 Pandemic in the Midst of the Pandemic. Ann Fam Med. 2020; 18: 349-54.
8. Lee JQ, Loke W, Ng QX. The Role of Family Physicians in a Pandemic: A Blueprint. Healthcare (Basel). 2020; 8: 198.
9. Kearon J, Risdon C. The Role of Primary Care in a Pandemic: Reflections During the COVID-19 Pandemic in Canada. J Prim Care Community Health. 2020; 11: 2150132720962871.
10. McAuley A, Stewart B, Siemens G, Cormier D. The MOOC model for digital practice. University of Prince Edward Island; 2010.
11. Christensen G, Steinmetz A, Alcorn B, Bennett A, Woods D, Emanuel EJ. The MOOC Phenomenon: Who Takes Massive Open Online Courses and Why? SSRN Electron J. 2013.
12. Hoedebecke K, Mahmoud M, Yakubu K, Kendir C, D'Addosio R, Maria B, et al. Collaborative global health E-learning: A Massive Open Online Course experience of young family doctors. J Family Med Prim Care. 2018; 7: 884-7.
13. Breslow L, Pritchard D, DeBoer J, Stump G, Ho AD, Seaton DT. Studying learning in the worldwide classroom: Research into edX's first MOOC.2013.
14. Braun V, Clarke V. Using thematic analysis in psychology. Qual Res Psychol. 2006; 3: 77-101.
15. Carter N, Bryant-Lukosius D, Dicenso A, Blythe J, Neville AJ. The use of triangulation in qualitative research. Oncol Nurs Forum. 2014; 41: 545-7.
16. Kern DE, Wright SM, Carrese JA, Jr ML, Simmons JM, Novack DH, et al. Personal growth in medical faculty: A qualitative study. West J Med. 2001; 175: 92-8.
17. Duffy FD, Holmboe ES. Self-assessment in lifelong learning and improving performance in practice: Physician know thyself. J Am Med Assoc. 2006; 296: 1137-9.
18. Yıldırım A, Şimşek H. Sosyal Bilimlerde Nitel Araştırma Yöntemleri. 2011.
19. Patton MQ. Nitel araştırma ve değerlendirme yöntemleri. 3. baskı. Bütün M, Demir SB, (Translation editors). Pegem Akademi; 2014. p. 1-598.
20. Camargo CP, Tempski PZ, Busnardo FF, Martins MA, Gemperli R. Online learning and COVID-19: a meta-synthesis analysis. Clinics (Sao Paulo). 2020; 75: e2286.
21. Elzainy A, El Sadik A, Al Abdulmonem W. Experience of e-learning and online assessment during the COVID-19 pandemic at the College of Medicine, Qassim University. J Taibah Univ Med Sci. 2020; 15: 456-62.
22. Goodyear-Smith F, Kinder K, Eden AR, Strydom S, Bazemore A, Philips R, et al. Primary care perspectives on pandemic politics. Glob Public Health. 2021; 16: 1304-19.

GMJ 2024;35:351-356

DOI: http://dx.doi.org/10.12996/gmj.2024.3624

Pathogenic and Genetic Characteristics of *Helicobacter Pylori*, and its Relationship with Drug-Resistance

Helicobacter pylori'nin Patojenik ve Genetik Özellikleri ve İlaç Direnciyle İlişkisi

Nilgün Uyduran Ünal[1], Adnan Barutçu[1], Toğrul Nagiyev[2], Mehmet Ağın[3], Tülay Kandemir[2], Oğuz Üsküdar[4], Figen Doran[5], Fatih Köksal[2], Gökhan Tümgör[3]

[1]Department of Pediatrics, Çukurova University Faculty of Medicine, Adana, Türkiye
[2]Department of Medical Microbiology, Çukurova University Faculty of Medicine, Adana, Türkiye
[3]Department of Pediatric Gastroenterology, Çukurova University Faculty of Medicine, Adana, Türkiye
[4]Department of Gastroenterology, Çukurova University Faculty of Medicine, Adana, Türkiye
[5]Department of Pathology, Çukurova University Faculty of Medicine, Adana, Türkiye

ABSTRACT

Objective: This study aimed to determine the epidemiological characteristics of *Helicobacter pylori (H. pylori)* infection at the genotype level in patients presenting with dyspeptic complaints, and to show the distribution of virulence factors, importance of intrafamilial transmission, as well as the distribution of resistance to macrolide and quinolone antibiotics.

Methods: The study comprised 110 patients with dyspeptic complaints who were admitted to our hospital between January 13, 2015, and December 31, 2016. Through histopathology, culture, and glmM-polymerase chain reaction (PCR) techniques, we detected *H. pylori*. The *vacA*, *cagA*, and *cagE* genes were determined in patients with positive PCR results were positive.

Results: *H. pylori* strains and clinical results were not found to be significantly correlated in the study. Both genetic variants *A2142G* and *A2143G* were discovered to be present in the individuals. Eight patients had clarithromycin resistance (34.7%). All patients with a positive A2142G mutation and 55% of patients with a positive A2143G mutation were found to have clarithromycin resistance. Levofloxacin resistance was present in only one (4.3%) patient who could produce *H. pylori* in culture.

Conclusion: Approximately 1/3 of the children with dyspeptic complaints were positive for *H. pylori* infection. The most common genotype was observed to be vacAs2. Even individuals with at least one of the genetic mutations A2142G and A2143G have the potential for antibiotic resistance. High resistance was found against clarithromycin in the standard triple therapy regimen used in children for treating *H. pylori* infection.

Keywords: *Helicobacter pylori*, children, virulence, antibiotic resistance, endoscopy, genetic

ÖZ

Amaç: Çalışma, dispeptik şikayetleri olan çocuk hastalarda *Helicobacter pylori (H. pylori)* enfeksiyonlarının sıklığını belirlemeyi ve aile içi geçişin önemini, virülans faktörlerinin dağılımını, ayrıca kinolon ve makrolid grubu antibiyotiklere karşı direncin epidemiyolojik özelliklerini genotip düzeyinde belirleyerek ortaya koymayı amaçlamaktadır.

Yöntemler: Çalışmaya 13 Ocak 2015-1 Aralık 2016 tarihleri arasında hastanemize dispeptik şikayetlerle başvuran 110 hasta dahil edildi. *H. pylori*; histopatolojik, kültür ve glmM-polimeraz zincir reaksiyonu (PZR) yöntemleri ile araştırıldı. PZR'si pozitif saptanan hastalarda *vacA, cagA* ve *cagE* genlerinin tespiti yapıldı.

Bulgular: Çalışmada *H. pylori* suşları ile klinik bulgular arasında anlamlı bir ilişki saptanmamıştır. Etkilenen hastalarda hem A2142G hem de A2143G'nin genetik mutasyonları pozitif bulundu. Sekiz hastada (%34,7) klaritromisin direnci saptandı. A2142G mutasyonu pozitif saptanan hastaların tümünde, A2143G mutasyonu pozitif saptananların %55'inde klaritromisin direnci gözlendi. Kültürde *H. pylori* üretebilen hastaların sadece birinde (%4,3) levofloksasin direnci gözlendi.

Sonuç: Dispeptik şikayetleri olan çocukların yaklaşık 1/3'ünde *H. pylori* enfeksiyonu pozitif saptanmıştır. En çok görülen genotip vacAs2 olduğu gözlenmiştir. A2142G ve A2143G genetik mutasyonlarından en az birine sahip olmak bile antibiyotik direnci potansiyeli taşımaktadır. *H. pylori* enfeksiyonu tedavisinde çocuklarda kullanılan standart üçlü tedavi rejiminde bulunan klaritromisine karşı yüksek direnç saptanmıştır.

Anahtar Sözcükler: *Helicobacter pylori*, çocuklar, virülans, antibiyotik direnci, endoskopi, genetik

Address for Correspondence/Yazışma Adresi: Adnan Barutçu, MD, Department of Pediatrics, Çukurova University Faculty of Medicine, Adana, Türkiye
E-mail / E-posta: adnan_barutcu@hotmail.com
ORCID ID: orcid.org/0000-0001-8930-1122

Received/Geliş Tarihi: 20.07.2022
Accepted/Kabul Tarihi: 10.06.2024

INTRODUCTION

Helicobacter pylori (H. pylori) is the most important cause of gastroduodenal pathology, ranging from non-ulcer dyspepsia to gastric ulcer and mucosa-associated lymphoid tissue lymphoma, to atrophic gastritis to lower-gastrointestinal system (GIS) carcinomas (1-4). Epidemiological studies have suggested that *H. pylori* is usually transmitted from the family in childhood; more than one strain initiated the infection in the first transmission, but one of the strains adapted to the gastric mucosa in the subsequent period (3).

Although many factors belonging to bacteria and the host have been suggested in the possible relationship between gastroduodenal pathology and *H. pylori*, it can be said most crucial evidence in this context is the clinical cure after *H. pylori* eradication therapy. The frequent occurrence of reactivations due to resistance to various antibiotic regimens applied in recent years in bacteria can be considered the second vital data that strengthens the relationship. Developing more rational treatments will only be possible by identifying colonized strains and knowing the movement of resistance in society by identifying resistant strains.

This study aimed to determine the epidemiological characteristics of *H. pylori* infection at the genotype level in childhood gastroduodenal pathologies. In addition, this study aimed to evaluate the initial period of the *H. pylori*-human relationship, the characteristics of the colonized strain(s), the distribution of virulence factors, the importance of intra-familial transmission, and the primary/secondary resistance distribution to macrolide and quinolone group antibiotics.

MATERIALS AND METHODS

A total of 110 cases admitted with dyspeptic complaints between 13 February 2015 and 1 December 2016 were included in the study. The criteria for inclusion in the study; cases between the ages of 3 and 18 years were identified as cases in which upper GIS endoscopy was planned due to dyspepsia and patients who had not previously received eradication treatment for *H. pylori*. Patients with upper gastrointestinal tract bleeding, patients with a history of gastroduodenal surgery, patients who did not agree to participate in the study, patients with a history of antibiotic and/or proton pump inhibitor use up to 1 month before the study, and patients with chronic diseases were excluded from the study.

After upper GIS endoscopy were performed and the findings were recorded, three biopsy samples were collected from the antrum region of the patients included in the study. The first sample was used for pathological examination, the second was used for *H. pylori* isolation in culture medium and for determining antibiotic susceptibility, and the third was used for genotypic examination. The E-test was performed to assess antibiotic susceptibility to *H. pylori* strains isolated in culture, and the minimum inhibitory concentration (MIC) values were determined. In our study, clarithromycin and levofloxacin E-test strips (Biotests, Ankara, Türkiye, and Liofilche, Italy) were used. The MICs were accepted as determined by the European Committee on Antimicrobial Susceptibility Testing in 2016 (5). For genotypic examinations, DNA extraction was performed from gastric biopsy samples, and these extracts were first examined by polymerase chain reaction (PCR) with the help of specific primers to determine the *glmM* gene sequence. The samples with positive *glmM* gene were accepted as *H. pylori*-positive, and their DNA extracts were evaluated by PCR for the detection of vacA, cagA, and cagE, PCR-RFLP for the detection of clarithromycin resistance, and DNA Sequence analysis for the detection of levofloxacin resistance. Additionally, to detect familial genetic and pathogenic inheritance, upper GIS endoscopy was performed by an adult gastroenterologist in 7 parents of 6 *H. pylori*-positive cases.

Ethics Committee approval was obtained from the Non-Interventional Clinical Research Ethics Committee of Çukurova University Faculty of Medicine (approval number: 37, date: 05.12.2014). The relatives of all the children included in the study were interviewed. After providing information about the interventional procedures to be applied to patients, the purpose of the research, and where to use the data, verbal and written consent was obtained.

Statistical Analysis

Statistical evaluations were performed using the SPSS 21.0 package program. Descriptive data are presented as percentage distributions. The chi-square test was used to compare the gender distribution, endoscopic and genotypic findings. Fischer's exact test was used to compare categorical variables. The statistical significance level was established as 0.05 in all tests.

RESULTS

The mean age of the cases was 12.2±4.39 years (3-18 years), as 38 were male (34.5%) and 72 were female (65.5%). *H. pylori* was found to be positive in 30 cases (27.3%) by PCR method. 18.8% of *H. pylori*-positive patients were between 3-6 years old, 33.3% were between 7-12 years old, and 25.9% were between 13-18 years old. No statistically significant difference was found between the *H. pylori*-positive and *H. pylori*-negative groups in terms of gender and age (p=0.235, p=0.519, respectively).

Of 30 PCR-positive patients, 29 (96.6%) were found to be vacA positive, and vacAs1+cagA+cagE association was found in 16.6% (Table 1).

Among the virulence factors, cagA was found to be positive in 50% of vacAs1-positive patients and 29.4% of vacAs2-positive patients. When the association between vacA subtypes and cagA was examined, no statistically significant difference was found (p=0.390).

Table 1. Distribution of virulence genes in 30 patients with *H. pylori* detected by PCR method

***Virulence* genes**	**n=30 (%)**
vacA	29 (96.6)
vacAs1	12 (40)
vacAs2	17 (56.6)
cagA	11 (36.7)
cagE	7 (23.3)
vacAs1 + cagA	1 (3.3)
vacAs1 + cagE	2 (6.6)
vacAs1 + cagA + cagE	5 (16.6)
vacAs2 + cagA	5 (16.6)

PCR: Polymerase chain reaction

It was found that 58.3% of the vacAs1-positive patients were cagE-positive. No association was observed between vacAs2 and cagE in any of the patients. When the distribution of virulence genes in *H. pylori* PCR-positive cases was examined, no statistically significant relationship was found (p>0.05).

It was observed that vacAs2, one of the less virulent vacA alleles, was found in all cases with normal histopathology, cagA was positive in 66.6% of these cases, and vacAs1 and cagE were not found in these cases. In patients with active chronic gastritis, the *vacAs1*, *vacAs2*, *cagA*, and *cagE* virulence genes were found to be 44.4%, 51.8%, 33.3%, and 25.9%, respectively.

Antibiogram was performed in 23 (20.9%) cases with positive *H. pylori* culture. Clarithromycin resistance was found in 8 (34.7%) patients, and no significant difference was found between genders in terms of clarithromycin resistance (p=0.342). Of clarithromycin-resistant cases, vacAs1 was found to be positive in 50%, vacAs2 in 36.4%, cagA in 40%, and cagE in 66.7%. However, no statistically significant intergroup difference was observed regarding the relationship between virulence genes and clarithromycin resistance (Table 2). Levofloxacin resistance was observed in only one case (4.3%), and vacAs1 was positive; vacAs2, cagA, and cagE were negative in this case.

When the *A2142G* gene mutation distribution was examined according to the age groups of the patients, it was found that there were no genetic mutations between the ages of 3-6 and the presence of genetic mutations at a rate of 16.7% between the ages of 7-12 and 20% between the ages of 13-18. When the *A2143G* gene mutation distribution was examined by age groups, it was observed with a rate of 33.3% between ages 3-6, 25% between ages 7-12, and 53.3% between ages 13-18. Per age group, no statistically significant difference was found in terms of *A2142G* and *A2143G* gene mutation positivity (p=0.698, p=0.318, respectively).

It was found that all patients with the positive A2142G mutation were clarithromycin-resistant, and clarithromycin resistance was found to be significantly higher than those who were negative (p=0.023). No significant difference was found in clarithromycin resistance between the A2143G mutation-positive patients than the negative ones (p=0.054) (Table 3). Both *A2142G* and *A2143G* genetic mutations were found to be positive in a single patient with levofloxacin resistance.

In our study, endoscopy was performed in 7 parents of 6 PCR-positive patients with clinical symptoms, and different *H. pylori* strains were found in the children and parents (Table 4).

Table 2. The relationship of *H. pylori* virulence genes with clarithromycin resistance

***Virulence* genes**	**Clarithromycin-susceptible, n (%)**	**Clarithromycin-resistant, n (%)**	**p**
vacA (-)	0 (0)	1 (100)	
vacAs1 (+)	3 (50)	3 (50)	0.446
vacAs2 (+)	7 (63.6)	4 (36.4)	
cagA (-)	7 (53.8)	6 (46.2)	1.000*
cagA (+)	3 (60)	2 (40)	
cagE (-)	9 (60)	6 (40)	0.559*
cagE (+)	1 (33.3)	2 (66.7)	

*Fisher exact test.

Table 3. Distribution of *A2142G* and *A2143G* genetic mutations in clarithromycin-susceptible and clarithromycin-resistant patients

Genetics mutations	**Clarithromycin-susceptible, n (%)**	**Clarithromycin-resistant, n (%)**	**p**
A2142G negative	15 (83.3)	3 (16.7)	0.023*
A2142G positive	0 (0)	5 (100)	
A2143G negative	10 (83.3)	2 (16.7)	0.054*
A2143G positive	5 (45)	6 (55)	

*Fisher exact test

DISCUSSION

H. pylori is one of the most common pathogens in humans (6). In addition to virulence factors such as urease activity and motility, immunogenic cross-reactivity in gastric cells plays an essential role in the pathogenesis of *H. pylori* (7). In addition, it is thought that some of the *H. pylori* virulence genes increase the risk of developing gastric lesions, and the pathogenic effect of bacteria virulence factors is affected by many factors belonging to the environment and host (8).

In our country, the number of studies evaluating *H. pylori* virulence genes in children is extremely low. Looking at *vacA* isolates from virulence genes, in 2013, Ozbey et al. (9) reported that 91.8% of vacAs1 isolates in *H. pylori*-positive children, and in 2014, Karabiber et al. (10) reported that 81.6% of them were vacAs1 subtype, and

Table 4. Comparison of PCR-positive patients and their parents' virulence genes and genetic mutations

Patients and parents	**vacAs1**	**vacAs2**	**cagA**	**cagE**	**A2142G**	**A2143G**
Patient A	+	-	-	+	-	-
Mother of patient A	+	-	+	+	-	-
Father of patient A	+	-	+	+	-	-
Patient B	-	+	+	-	-	-
Mother of patient B	-	+	-	-	-	-
Patient C	+	-	-	-	-	+
Father of patient C	+	-	+	-	-	-
Patient D	-	+	+	-	-	-
Mother of patient D	-	+	-	-	-	-
Patient E	+	-	-	-	-	+
Mother of patient E	-	+	-	-	-	+
Patient F	+	-	-	-	-	-
Mother of patient F	-	+	-	-	-	-

PCR: Polymerase chain reaction.

the most common vacA subtype was vacAs1a/m2, at a rate of 32.7%. vacAs1/m1 was the most common allele in 85% of symptomatic children in Venezuela and vacAs1 in 82.5% of asymptomatic children in Brazil (11,12). In a study conducted by Erdoğdu et al. (13) in 120 children, it was found that 70.1% of *H. pylori* isolates had vacAs1a, 2.8% had vacAs1b, and 27.1% had the vacAs2 subtype, and reported that vacA genotype was not associated with endoscopic findings. While the most common genotype in Iranian children is vacAs1/m2; it was found that nodular gastritis is common in endoscopic findings, and this is significantly associated with the presence of vacAm1 (14). In our study, the vacAs1 allele was found to be positive in 40% of *H. pylori*-positive cases, and the vacAs2 allele, which is known to be less virulent, in 56.6%. Compared with these two studies, it was observed that the vacAs2 allele was higher in our study. In our research, no statistically significant difference was found in the evaluation of the vacAs1 and vacAs2 genotypes according to endoscopic findings and histopathological data.

In our study, cagA was found with a rate of 36.7%. In symptomatic children, *H. pylori* cagA strains and serum cagA antibodies are found at the rate of 33% -80% (15-17). In a study by Kato et al. (18) conducted on 25 children with the ulcer, it was reported that cagA was detected in 81.8% of asymptomatic children, 93.3% of patients with gastritis, and 80% of patients with gastric ulcers. In a study conducted by Saltik et al. (19), 45 children were evaluated for abdominal pain and tested only for cagA, which is one of the virulence factors. They found cagA positivity at a rate of 55.6%, and they reported that there was no relationship between the severity of gastrointestinal findings.

When *cagE*, a virulence gene, was examined, 23.3% of the 30 PCR-positive patients in our study were found to be cagE positive. A vacAs1+cagE association was found in 6.6% of these, and a vacAs1+cagA+cagE association was found in 16.6%. Because there were not enough studies on this subject in children, cagE positivity was found at a low rate in our study compared to adult studies conducted in our country, whereas a similar rate of cagE positivity was found when compared to the study conducted by Ozbey et al. (9).

In our study, active chronic gastritis was detected in 90% of *H. pylori* PCR-positive 30 patients, and histopathological evaluation of 14.3% of these patients was found to be normal. Among these *H. pylori* PCR-positive cases, it was observed that all of the vacA alleles with normal histopathology were vacAs2, one of the less virulent vacA alleles, and 66.6% of these patients with normal histopathology had cagA and no vacAs1 and cagE, which play an important role in virulence. In patients with active chronic gastritis, the *vacAs1*, *vacAs2*, *cagA*, and *cagE* virulence genes were found to be 44.4%, 51.8%, 33.3%, and 25.9%, respectively. While less virulent genes were detected in cases with normal histopathological evaluation, the positivity of genes known to be more virulent in active chronic gastritis cases was remarkable.

In countries where clarithromycin, metronidazole, and amoxicillin, which are the first-choice antibiotics, are used extensively in eradication treatment, the development of increasing resistance against these drugs causes treatment failure. Therefore, resistance determination has gained importance in the establishment of treatment protocols (20-22). Although many adult studies aimed at determining antibiotic resistance, there are not enough studies on children. Recent data on clarithromycin resistance in our country are generally obtained from studies conducted in adults, and resistance rates vary between 40.2% and 48% (23-25). The use of macrolide group antibiotics, especially in respiratory tract infections, is one of the most important reasons for the development of clarithromycin resistance. It is thought that clarithromycin resistance is a much more critical problem in developed countries, such as our country, where antibiotic use rates are high, or especially in developed countries where macrolide group antibiotics are prescribed for the treatment of respiratory tract infections (26-28).

In the study of Ozçay et al. (29), which was performed on 102 children diagnosed with *H. pylori* infection by urea breath test, serology, or culture, the rate of clarithromycin resistance was found as 18.1%. Karabiber et al. (10) reported that 51 (52%) of 98 PCR-positive children with *H. pylori* gastritis were culture-positive, and clarithromycin, metronidazole, and amoxicillin resistance were 23.5%, 11.7%, and 3.9%, respectively. In the same study, no relationship was found between the presence of cagA, and clarithromycin and metronidazole resistance. Clarithromycin resistance was found at a rate of 83.3% in cagE-positive patients, while this rate decreased to 16.7% in cagE-negative patients (10). In a study conducted on 118 patients, 52.7% of whom were children, in Spain in 2008, it was reported that the clarithromycin resistance measured by the E-test method was 35.6% (30). It was found that metronidazole and clarithromycin resistance tended to increase among children infected with *H. pylori* in China at rates of 49.2% and 34.9%, respectively (31). In Japan, resistance rates to metronidazole and clarithromycin were found to be 43.3% and 21.9%, respectively (32). Levofloxacin, which is effective against *H. pylori in vitro*, has more limited effects in vivo. Wong et al. (33) reported 18%, and Perna et al. (34) reported 30.3% levofloxacin-resistance. In another study, resistance to fluoroquinolone group drugs, which are not commonly used in children, was shown as 30.8% at the age of 0-6, and it was thought that resistance to these drugs was probably acquired from parents (35). The clarithromycin resistance observed in our study is compatible with studies in the literature. However, more meaningful results can be obtained by increasing the number of patients. If *H. pylori* cannot be destroyed sufficiently due to clarithromycin resistance, which is thought to be caused by unnecessary antibiotic use, triple and sequential treatments containing the fluoroquinolone group instead of the macrolide group are promising for older children. The rapid development of resistance to fluoroquinolone group antibiotics is worrying in this respect (35-38).

H. pylori is a microorganism with a high degree of genetic variability. While some studies reported a relationship between virulence genes and antibiotic resistance, some studies reported no such relationship (10,39,40). In our study, no relationship was found between vacA subtypes, cagA and cagE, and antibiotic resistance.

In the study conducted by Caliskan et al. (41) isolate a total of 98 *H. pylori* strains, 36 (36.7%) patients had clarithromycin resistance, 34 (35.5%) had metronidazole resistance, 29 (29.5%) had levofloxacin resistance, and multiple antibiotic resistance was detected in 19.3% of the patients. In the same study, the A2143G and A2144G genetic mutations were detected in 100% of clarithromycin-resistant strains. In our study, clarithromycin resistance was detected in 100% of the five patients who were found to be positive for the A2142G mutation

and underwent antibiogram, and in 6 (55%) of the patients who were A2143G positive. Both mutations were found in male patients with levofloxacin resistance. Even at least one of these genetic mutations has the potential to become resistant to antibiotics.

A comparison of the *vacAs1*, *vacAs2*, *cagA*, and *cagE* virulence genes and *A2142G* and *A2143G* genetic mutations were made PCR-positive six patients with and seven parents of these patients. It has been shown that the *H. pylori* strains of the patient and their parents are different, and in 4 of the six patients we compared, the *H. pylori* strain with the same vacA allele as their parents was detected, whereas bacteria with different cagE and *cagA* genes were detected in these patients. It is known that the *cagA* and *cagE* genes located on the Cag Pathogenicity Island (cagPAI) of *H. pylori* may be acquired later or that existing genes may be lost in the future. While evaluating the differences in *H. pylori* strains between patients and parents, it should be kept in mind that there may be changes in cagPAI in the future. In addition, children can be infected with more than one strain of H. pylori at the same time. By increasing the number of biopsy samples, the possibility of detecting other strains of *H. pylori* can be increased.

Since the PCR-RFLP method, which examines the 1162 bp specific region of the *vacA* gene in our study to detect point mutations effective in clarithromycin resistance, is a sensitive method that gives a very heterogeneous band profile, as shown in other studies, it has been concluded that *H. pylori* isolation in gastric biopsy samples taken from pediatric patients is not a suitable method for determining kinship transmission (42).

CONCLUSION

In conclusion, *H. pylori* infection was positive in approximately one-third of the children with dyspeptic complaints. It was observed that these patients mostly had the vacAs2 genotype. Even individuals with at least one of the genetic mutations A2142G and A2143G genetic mutations have the potential to be resistant to antibiotics. A high rate of resistance has been found against clarithromycin used in the standard triple therapy for *H. pylori* in children in our country. *H. pylori* infection eradication rates are also low with standard triple therapy in clinical studies. Therefore, it is appropriate to develop new treatment modalities for treating *H. pylori* infection in children.

Ethics

Ethics Committee Approval: Ethics Committee approval was obtained from the Non-Interventional Clinical Research Ethics Committee of Çukurova University Faculty of Medicine (approval number: 37, date: 05.12.2014).

Informed Consent: The relatives of all the children included in the study were interviewed. After providing information about the interventional procedures to be applied to patients, the purpose of the research, and where to use the data, verbal and written consent was obtained.

Authorship Contributions

Surgical and Medical Practices: N.U.Ü., A.B., M.A., O.Ü., F.D., G.T., Concept: N.U.Ü., A.B., G.T., Design: N.U.Ü., G.T., Data Collection or Processing: N.U.Ü., A.B., T.N., M.A., T.K., O.Ü., F.D., F.K., G.T., Analysis or Interpretation: N.U.Ü., A.B., T.N., M.A., T.K., O.Ü., F.D., F.K., G.T., Literature Search: N.U.Ü., A.B., G.T., Writing: N.U.Ü., A.B., G.T.

Conflict of Interest: The authors declare no conflict of interest.

Financial Disclosure: This study was supported by Çukurova University Rectorate Research Fund TTU-2015- 3550 project.

REFERENCES

1. Ryan, Kenneth J. Topley and Wilson's Principles of Bacteriology, Virology and Immunity, vol 1: General Bacteriology and Immunity. JAMA. 1991; 266: 2621.
2. Baltrus DA, Amieva MR, Covacci A, Lowe TM, Merrel DS, Ottemann KM, et al. The complete genome sequence of Helicobacter pylori strain G27. J Bacteriol. 2009; 191: 447-8.
3. Marshall BJ, Warren JR. Unidentified curved bacilli in the stomach of patients with gastritis and peptic ulceration. Lancet. 1984; 1: 1311-5.
4. van Amsterdam K, van Vliet AH, Kusters JG, van der Ende A. Of microbe and man: determinants of Helicobacter pylori-related diseases. FEMS Microbiol Rev. 2006; 30: 131-56.
5. EUCAST T. European Committee on Antimicrobial Susceptibility Testing, Breakpoint tables for interpretation of MICs and zone diameters. European Society of Clinical Microbiology and Infectious Diseases Basel; 2015.
6. Suerbaum S, Michetti P. Helicobacter pylori infection. N Engl J Med. 2002; 347: 1175-86.
7. Dunn BE. Pathogenic mechanisms of Helicobacter pylori. Gastroenterol Clin North Am. 1993; 22: 43-57.
8. Höcker M, Hohenberger P. Helicobacter pylori virulence factors--one part of a big picture. Lancet. 2003; 362: 1231-3.
9. Ozbey G, Dogan Y, Demiroren K. Prevalence of Helicobacter pylori virulence genotypes among children in Eastern Turkey. World J Gastroenterol. 2013; 19: 6585-9.
10. Karabiber H, Selimoglu MA, Otlu B, Yildirim O, Ozer A. Virulence factors and antibiotic resistance in children with Helicobacter pylori gastritis. J Pediatr Gastroenterol Nutr. 2014; 58: 608-12.
11. Braga LL, Oliveira MA, Gonçalves MH, Chaves FK, Benigno TGS, Gomes AD, et al. CagA phosphorylation EPIYA-C motifs and the vacA i genotype in Helicobacter pylori strains of asymptomatic children from a high-risk gastric cancer area in northeastern Brazil. Mem Inst Oswaldo Cruz. 2014; 109: 1045-9.
12. Ortiz-Princz D, Daoud G, Salgado-Sabel A, Cavazza ME. Helicobacter pylori infection in children: should it be carefully assessed? Eur Rev Med Pharmacol Sci. 2016; 20: 1798-813.
13. Erdoğdu C, Saribaş Z, Akyön Yilmaz Y. Detection of cagA and vacA genotypes of Helicobacter pylori isolates from a university hospital in Ankara region, Turkey. Turk J Med Sci. 2014; 44: 126-32.
14. Rafeey M, Ghotaslou R, Milani M, Farokhi N, Ghojazadeh M. Association between Helicobacter pylori, cagA, and vacA Status and Clinical Presentation in Iranian Children. Iran J Pediatr. 2013; 23: 551-6.
15. Camorlinga-Ponce M, Torres J, Perez-Perez G, Leal-Herrea Y, Gonzalez-Ortiz B, Madrazp de la Garza A, et al. Validation of a serologic test for the diagnosis of Helicobacter pylori infection and the immune response to urease and CagA in children. Am J Gastroenterol. 1998; 93: 1264-70.
16. Elitsur Y, Neace C, Werthammer MC, Triest WE. Prevalence of CagA, VacA antibodies in symptomatic and asymptomatic children with Helicobacter pylori infection. Helicobacter. 1999; 4: 100-5.
17. Rutigliano V, Ierardi E, Francavilla R, Castellaneta S, Margiotta M, Amoruso A, et al. Helicobacter pylori and nonulcer dyspepsia in childhood: clinical pattern, diagnostic techniques, and bacterial strains. J Pediatr Gastroenterol Nutr. 1999; 28: 296-300.

18. Kato S, Sugiyama T, Kudo M, Ohnuma K, Ozawa K, Iinuma K, et al. CagA antibodies in Japanese children with nodular gastritis or peptic ulcer disease. J Clin Microbiol. 2000; 38: 68-70.
19. Saltik IN, Demir H, Engin D, Ertunç OD, Akyön Y, Koçak N. The cagA status of Helicobacter pylori isolates from dyspeptic children in Turkey. FEMS Immunol Med Microbiol. 2003; 36: 147-9.
20. Sharara AI, Chedid M, Araj GF, Barada KA, Mourad FH. Prevalence of Helicobacter pylori resistance to metronidazole, clarithromycin, amoxycillin and tetracycline in Lebanon. Int J Antimicrob Agents. 2002; 19: 155-8.
21. Lang L, García F. Comparison of E-test and disk diffusion assay to evaluate resistance of Helicobacter pylori isolates to amoxicillin, clarithromycin, metronidazole and tetracycline in Costa Rica. Int J Antimicrob Agents. 2004; 24: 572-7.
22. Alarcón T, Domingo D, Sánchez I, Díaz de Rojas F, López-Brea M. In vitro activity of omeprazole in combination with several antimicrobial agents against clinical isolates of Helicobacter pylori. Eur J Clin Microbiol Infect Dis. 1996; 15: 937-40.
23. Bakir Ozbey S, Ozakin C, Keskin M. Antibiotic resistance rates of Helicobacter pylori isolates and the comparison of E-test and fluorescent in situ hybridization methods for the detection of clarithromycin resistant strains. Mikrobiyol Bul. 2009; 43: 227-34 (Turkish).
24. Onder G, Aydin A, Akarca U, Tekin F, Ozutemiz O, Ilter T. High Helicobacter pylori resistance rate to clarithromycin in Turkey. J Clin Gastroenterol. 2007; 41: 747-50.
25. Sezgin O, Aslan G, Altintaş E, Tezcan S, Serin MS, Emekdaş G. Detection of point mutations on 23S rRNA of Helicobacter pylori and resistance to clarithromycin with PCR-RFLP in gastric biopsy specimens in Mersin, Turkey. Turk J Gastroenterol. 2008; 19: 163-7.
26. Kalach N, Serhal L, Asmar E, Campeotto F, Bergeret M, Dehecq E, et al. Helicobacter pylori primary resistant strains over 11 years in French children. Diagn Microbiol Infect Dis. 2007; 59: 217-22.
27. Vécsei A, Kipet A, Innerhofer A, Graf U, Binder C, Gizci H, et al. Time trends of Helicobacter pylori resistance to antibiotics in children living in Vienna, Austria. Helicobacter. 2010; 15: 214-220.
28. Garcia GT, Aranda KR, Gonçalves ME, Graf U, Binder C, Gizci H, et al. High prevalence of clarithromycin resistance and cagA, vacA, iceA2, and babA2 genotypes of Helicobacter pylori in Brazilian children. J Clin Microbiol. 2010; 48: 4266-8.
29. Ozçay F, Koçak N, Temizel IN, Demir H, Ozen H, Yüce A, et al. Helicobacter pylori infection in Turkish children: comparison of diagnostic tests, evaluation of eradication rate, and changes in symptoms after eradication. Helicobacter. 2004; 9: 242-8.
30. Agudo S, Pérez-Pérez G, Alarcón T, López-Brea M. High prevalence of clarithromycin-resistant Helicobacter pylori strains and risk factors associated with resistance in Madrid, Spain. J Clin Microbiol. 2010; 48: 3703-7.
31. Li L, Ke Y, Yu C, Li G, Yang N, Zhang J, Li Y. Antibiotic resistance of Helicobacter pylori in Chinese children: A multicenter retrospective study over 7 years. Helicobacter. 2017; 22.
32. Okuda M, Kikuchi S, Mabe K, Osaki T, Kamiya S, Fukuda Y, et al. Nationwide survey of Helicobacter pylori treatment for children and adolescents in Japan. Pediatr Int. 2017; 59: 57-61.
33. Wong W, Gu Q, CHU KM, Yee YK, Fung FMY, Tong TSM, et al. Lansoprazole, levofloxacin and amoxicillin triple therapy vs. quadruple therapy as second-line treatment of resistant Helicobacter pylori infection. Aliment Pharmacol Ther. 2006; 23: 421-7.
34. Perna F, Zullo A, Ricci C, Hassan C, Morini S, Vaira D. Levofloxacin-based triple therapy for Helicobacter pylori re-treatment: role of bacterial resistance. Dig Liver Dis. 2007; 39: 1001-5.
35. Liu G, Xu X, He L, Ding Z, Gu Y, Zhang J, et al. Primary antibiotic resistance of Helicobacter pylori isolated from Beijing children. Helicobacter. 2011; 16: 356-62.
36. Nista EC, Candelli M, Zocco MA, Creomini F, Ojetti V, Finizo R, et al. Levofloxacin-based triple therapy in first-line treatment for Helicobacter pylori eradication. Am J Gastroenterol. 2006; 101: 1985-90.
37. Cheng H, Hu FL, Zhang GX, Shi RH, Du YQ, Li ZS, et al. [Levofloxacin-based triple therapy for first-line Helicobacter pylori eradication treatment: a multi-central, randomized, controlled clinical study]. Zhonghua Yi Xue Za Zhi. 2010; 90: 79-82.
38. Cuadrado-Lavín A, Salcines-Caviedes JR, Carrascosa MF, Mellado P, Monteagudo I, Llorca J, et al. Antimicrobial susceptibility of Helicobacter pylori to six antibiotics currently used in Spain. J Antimicrob Chemother. 2012; 67: 170-3.
39. Elviss NC, Owen RJ, Xerry J, Walker AM, Davies K. Helicobacter pylori antibiotic resistance patterns and genotypes in adult dyspeptic patients from a regional population in North Wales. J Antimicrob Chemother. 2004; 54: 435-40.
40. Boyanova L, Nikolov R, Gergova G, Evstatiev I, Lazarova E, Kamburov V, et al. Two-decade trends in primary Helicobacter pylori resistance to antibiotics in Bulgaria. Diagn Microbiol Infect Dis. 2010; 67: 319-26.
41. Caliskan R, Tokman HB, Erzin Y, Saribas S, Yuksel P, Bolek BK, et al. Antimicrobial resistance of Helicobacter pylori strains to five antibiotics, including levofloxacin, in Northwestern Turkey. Rev Soc Bras Med Trop. 2015; 48: 278-84.
42. Han SR, Schreiber HJ, Bhakdi S, Loos M, Maeurer MJ. vacA genotypes and genetic diversity in clinical isolates of Helicobacter pylori. Clin Diagn Lab Immunol. 1998; 5: 139-45.

Original Investigation | Özgün Araştırma

GMJ 2024;35:357-363

DOI: http://dx.doi.org/10.12996/gmj.2024.3965

The Relationship Between Postpartum Physical Symptom Severity and Sleep Quality in Women with Cesarean Section

Sezaryen ile Doğum Yapmış Kadınlarda Postpartum Fiziksel Semptom Şiddet Yaşama Durumları ile Uyku Kalitesi Arasındaki İlişki

Melike Yılmaz, Nuriye Erbaş

Department of Obstetrics and Gynecology Nursing, Sivas Numune Hospital, Sivas, Türkiye

ABSTRACT

Objective: This study was conducted to examine the relationship between postpartum physical symptom severity and sleep quality among women undergoing cesarean section.

Methods: This descriptive cross-sectional study was conducted with a total of 193 women with cesarean section in a city hospital between October 14, 2019 and May 30, 2020. Data were collected using an individual characteristics form, the postpartum physical symptom severity scale (PPSSS) and Pittsburgh sleep quality index (PSQI). Data were evaluated using descriptive statistics, such as number and percentage distributions, t-test, analysis of variance (ANOVA), Mann-Whitney U test, Kruskal-Wallis H test, Pearson's correlation analysis, and linear regression analysis.

Results: The women's PPSSS mean score was 10.38±5.92, suggesting low postpartum physical symptom severity. However, the most common physical symptoms in the fourth postpartum week were poor sleep quality/lack of sleep (85.5%) and perineal/incision pain (82.9%); and their least common physical symptoms were vaginal infection (9.8%) and urinary incontinence (11.4%). In addition, the women's PSQI mean score was 8.57±3.53, and 83.9% of them had poor sleep quality.

Conclusion: There was a statistically significant, positive, moderate relationship between postpartum physical symptom severity and sleep quality in women who underwent cesarean section (r=0.438; p=0.000) (p<0.05), whereby sleep quality decreased as postpartum physical symptom severity increased.

Keywords: Cesarean section, postpartum physical symptom severity, sleep quality, obstetrics and gynecology nursing

ÖZ

Amaç: Araştırma, sezaryen ile doğum yapmış kadınlarda postpartum fiziksel semptom şiddet yaşama durumları ile uyku kalitesi arasındaki ilişkiyi incelemek amacıyla gerçekleştirilmiştir.

Yöntemler: Tanımlayıcı ve kesitsel nitelikteki bu araştırma, 14 Ekim 2019-30 Mayıs 2020 tarihleri arasında, Sivas Numune Hastanesi'nde sezaryen doğum yapan 193 kadın ile gerçekleştirilmiştir. Veriler bireysel özellikler formu, postpartum fiziksel semptom şiddeti ölçeği ile Pittsburgh uyku kalitesi indeksi (PUKİ) uygulanarak toplanmıştır. Verilerin değerlendirilmesinde, tanımlayıcı istatistik testleri ile sayı ve yüzdelik dağılımlar, t-testi, ANOVA varyans analizi, Mann Whitney U testi, Kruskal Wallis H testi, Pearson korelasyon analizi ve Lineer regresyon analizi kullanılmıştır.

Bulgular: Araştırmada, kadınların postpartum fiziksel semptom şiddeti ölçeğinden 10,38±5,92 puan aldığı ve postpartum fiziksel semptom şiddetinin düşük düzeyde olduğu saptanmıştır. Bununla birlikte, kadınların postpartum döneminin dördüncü haftasında en çok yaşadıkları fiziksel semptomların yetersiz uyku kalitesi/uykusuzluk (%85,5) ve sezaryen bölgesi/perinede ağrı (%82,9) olduğu; en az yaşadıkları fiziksel semptomların ise vajinal enfeksiyon (%9,8) ve idrar kaçırma (%11,4) olduğu, bu semptomları ise çoğunlukla hafif şiddette yaşadıkları belirlenmiştir. Araştırmada, kadınların PUKİ'den ortalama 8,57±3,53 puan aldığı ve %83,9'unun uyku kalitesinin kötü düzeyde olduğu tespit edilmiştir.

Sonuç: Araştırmada, postpartum fiziksel semptom şiddeti ile uyku kalitesi arasında pozitif yönde orta düzeyde (r=0,438; p=0,000) anlamlı ilişki olduğu (p<0,05), postpartum fiziksel semptom şiddeti arttıkça uyku kalitesinin azaldığı sonucuna ulaşılmıştır.

Anahtar Sözcükler: Sezaryen, postpartum fiziksel semptom şiddeti, uyku kalitesi, kadın doğum hemşireliği

Address for Correspondence/Yazışma Adresi: Melike Yılmaz, Department of Obstetrics and Gynecology Nursing, Sivas Numune Hospital, Sivas, Türkiye

E-mail / E-posta: melikeyilmaz5894@gmail.com

ORCID ID: orcid.org/0000-0002-7524-8700

Received/Geliş Tarihi: 20.07.2022

Accepted/Kabul Tarihi: 10.06.2024

This article was presented as a summary presentation at the first International Health Sciences and Biomedical Congress on January 23-24, 2021.

INTRODUCTION

All changes occurring in the body during pregnancy return to a non-pregnant state within six weeks after childbirth (1), but can cause physical symptoms that negatively affect their quality of life. In addition, the mode of delivery also affects these physical symptoms (2). Studies have reported that health problems are more common after cesarean section than after vaginal delivery (3). Especially after cesarean section, several health issues, such as surgical wounds, long-term oral stop, delayed mobilization, delayed onset of mother-infant bonding, breastfeeding, and milk secretion problems, can occur, and the risk of getting infection increases the mother's anxiety, making it difficult for her to adapt to the postpartum period (3). During pregnancy and childbirth, increased need for strength, physical fatigue due to labor, blood loss at birth, and tissue trauma increase postpartum health issues and adversely affect maternal well-being (4). Studies have reported that mothers mostly undergo episiotomy, breast fullness, pain due to cesarean section or hemorrhage, constipation, fatigue, and psychological problems during the postpartum period (5,6). Decreased sleep quality and lack of sleep are also the main problems mothers experience during the postpartum period (7). After childbirth, sleep disorders increase due to sudden decreases in estrogen and progesterone, and women experience drowsiness and insomnia more frequently (8). It was observed that mothers who were in the recovery period after cesarean section were more vulnerable to insufficient sleep due to discomfort and other factors related to surgical recovery, experienced more frequent awakenings at night, and had decreased total sleep time (9). Sleep quality is very important in the process of adaptation to the post-cesarean period, during which physical and psychological problems are experienced, as well as in the process of adaptation to the care of the newborn (10). In this period, women need to sleep more because they struggle with physical and psychological changes on the one hand and try to breastfeed the newborn, care for the newborn, and carry out housework on the other (7,11). The combination of good levels of healthy sleep and quality of life positively affect maternal and infant health (11). Mothers need 20% more sleep at night after giving birth, but they cannot meet this need because of postpartum physical problems (7). Mothers may experience sleep problems, especially in the first months, due to the baby's night care, feeding, and sleep irregularity, or changes in their hormone levels (2). A previous study concluded that 79.5% of mothers had problems sleeping and resting after childbirth (12). In another study, 87.5% of mothers had low sleep quality, which was negatively affected by physical symptoms, frequent waking up at night, inability to sleep with the spouse, stress, and the baby's irregular sleep pattern (13). In the literature, studies on maternal health are mostly conducted on pregnancy and childbirth, and they do not mention the physical symptoms and care needs during postpartum period (4). Studies on mothers' health issues during the postpartum period have examined diverse parameters, such as quality of life, comfort, pain, depression, and fatigue (5,14,15). Sleep disorders are also associated with the postpartum period (8), and they have not been adequately studied in the literature. In addition, the first month postpartum, especially after cesarean section, is a period in which mothers experience anxiety about sleep hygiene because of their recovery after surgery, their adaptation to maternal roles, and their responsibility for taking care of their babies (16). Accordingly, physical symptoms and sleep problems are intensely experienced in women after cesarean section, and there is limited research on the subject in the literature. Therefore, this study was conducted to examine all health problems during the period after cesarean delivery and the relationship between these problems and sleep quality.

MATERIAL AND METHODS

The Universe and Samples of the Research

The universe of the study consisted of 1,865 women between January 01, 2018 and June 11, 2019 who underwent cesarean section. The sample of the study comprised those with cesarean section in the obstetrics and gynecology service of the hospital between October 14, 2019 and May 30, 2020, using sampling with a known population size and benefiting from previous studies. In total, 193 women were studied in the research. The power of the test was found as p=0.9921818 (0.99) according to post hoc analysis using the G Power program.

Tools

Data were collected using an individual characteristics form, the Postpartum Physical Symptom Severity Scale (PPSSS) and Pittsburgh Sleep Quality Index (PSQI).

1. Individual Characteristics Form: This form was prepared by the researcher and consisted of 15 questions including the mothers' sociodemographic characteristics and information about pregnancy, childbirth, and the postpartum period (2,7,12,17).

2. Postpartum Physical Symptom Severity Scale (PPSSS): The scale was improved by Chien et al. (18) to identify the prevalence and persistence of postpartum physical symptoms. The game consists of a total of 18 items, scoring as 0 (none), 1 (mild), 2 (moderate), and 3 (high). The Turkish validity and reliability of the scale was conducted by Arkan (2). The scale evaluates physical symptoms and their severity, including postpartum perineal/incision pain, lack of sleep, constipation, backache, headache, hemorrhoids, joint pain, vaginal bleeding, vaginal discharge, and infection, numbness in hands and feet, urinary tract infection, urinary incontinence, dizziness, varicose veins, and coldness in hands and feet. Total scale scores range from 0 to 54. Higher scores indicate greater severity of postpartum physical symptoms. For the Turkish version of the scale, internal consistency (Cronbach's alpha) was found as 0.77 at the postpartum 1st month and 0.69 at the postpartum year (2). In this study, the reliability coefficient (Cronbach alpha) of the scale was calculated as 0.74.

3. Pittsburgh Sleep Quality Index (PSQI): The scale was improved by Buysse et al. (19), and its Turkish validity and reliability studies were conducted by Ağargün et al. (20). The PSQI consists of a total of 24 items to evaluate sleep quality over the past 4 weeks, including 19 self-reported items for respondents and five items for their spouses or roommates. These five items to be answered by the roommate or partner were not included in the scoring. The 19 self-rated items generate seven "component" scores: subjective sleep quality (component 1), sleep latency (component 2), sleep duration (component 3), habitual sleep efficiency (component 4), sleep disturbance (component 5), use of sleeping medication (component 6), and daytime dysfunction (component 7). Each component is

evaluated between 0 and 3 points. The sum of the seven-component scores gives the overall PSQI score, which ranges from 0 to 21 (20). A high total score indicates poor sleep quality, where a score between 0-4 refers to good sleep quality and between 5-21 to poor sleep quality. The scale scores are compared and interpreted for different groups. The Cronbach's alpha internal consistency coefficient of the scale was found as 0.80 (19,20). In this study, the reliability coefficient (Cronbach's alpha) of the scale was calculated as 0.59.

Data Collection

The data were gathered in two stages. First, the individual characteristics form was implemented for women within 48 hours of their cesarean section operation. Second, home visits were made to women after hospital discharge. Before starting the second stage, the patients' addresses, visiting dates, and times were decided for home visits within one month of discharge, considering their date of cesarean section surgery. Before home visits, women were invited to discuss their availability. During the home visit, the PPSSS and PSQI were applied to the women between October 14, 2019 and May 30, 2020.

Statistical Analysis

The data were analyzed using the SPSS 23.0 program and appraised using descriptive statistics, such as the number, percentage distribution, mean, range, standard deviation, and maximum and minimum values. Reliability analysis was performed to determine the Cronbach's alpha coefficient of the scales. To determine whether there was a difference between the averages of the independent groups, the t-test was used for two groups with data matching the normal distribution, and ANOVA was used for more than two groups. The Mann-Whitney U test and Kruskal-Wallis H one-way analysis of variance test were used for data that did not match the normal distribution and for more than two independent groups. In this study, Pearson's correlation coefficient analysis was performed to the variables with normal distribution to reveal the relationship between them. Linear regression analysis was used to determine whether postpartum physical symptom severity affected sleep quality. The grade of significance was accepted as $p<0.05$.

Ethics Approval and Consent to Participate of the Research

Before collecting the data, two ethics committee approvals, including (approval number: 2019-08/04, date: 07.08.2019 and approval number: 2021-03/64, date: 10.03.2021), were obtained from the Sivas Cumhuriyet University Non-interventional Clinical Research Ethics Committee. In addition, permits have been obtained from the institution where the research was conducted and from the provincial health directorate. Verbal/written approval was obtained from all women who attended in the research.

RESULTS

The women participating in the study; 45.6% were between the ages of 30-35 years with a mean of 28.75±4.55 years, and 49.2% were primary school graduates. Women, 69.9% had 1-3 pregnancies, it was determined that 82.4% had 1-3 births. It was determined that 76.2% of the women did not go for health control while pregnant, 45.1% accepted prenatal education, 74.7% received education from health personnel and at a pregnant school in Table 1.

Table 1. Distribution of sociodemographic and fertility characteristics of women after cesarean section

Characteristics	n	%
Age (mean ± SD: 28.75±4.55)		
20-24 ages	40	20.7
25-29 ages	65	33.7
30-35 ages	88	45.6
Educational level		
Literacy	6	3.2
Primary school-middle school	95	49.2
High school	46	23.8
University	46	23.8
Job		
Housewife	135	69.9
Officer	49	25.4
Self-employed	9	4.7
Number of pregnancies (mean ± SD: 2.98±1.68)		
1-3 pregnancies	135	69.9
4-6 pregnancies	49	25.4
7-9 pregnancies	9	4.7
Number of births (mean ± SD: 2.49±1.17)		
1-3 births	159	82.4
4 or more births	34	17.6
Gestational week at delivery (mean ± SD: 38.59±1.31)		
36th week and before	14	7.2
Between the 37th and 39th weeks	136	70.5
40th week and later	43	22.3
Newborn weight (mean ± SD: 3.345±441.60)		
2500-3000 g	41	21.2
3001-3500 g	93	48.2
Over 3501 g	59	30.6
Having had regular health follow-ups during pregnancy		
Yes	46	23.8
No	147	76.2
Having had prenatal education		
Yes	87	45.1
No	106	54.9
Source of prenatal education* (s=87)		
Medical staff and pregnant school	65	74.7
Internet	32	36.8
From my environment (mother, friend, relative)	13	15.0
Book	11	12.7
Total	**193**	**100**

*More than one option was selected by 87 women who were reported to have received prenatal education. SD: Standard deviation.

Mean PPSSS scores of women undergoing cesarean section ranged between 0.14 and 1.45. Their highest and lowest mean scores were 1.45±0.94 for item 2 [poor sleep quality/lack of sleep and 0.14±0.46 for item 10 (vaginal infection)]. Their mean PFSSS score was 10.38±5.92.

The most common physical symptoms in women at the fourth postpartum week were poor sleep quality/lack of sleep (85.5%) and cesarean section/perineal pain (82.9%), whereas the least common physical symptoms were vaginal infection (9.8%) and urinary incontinence (11.4%), and these symptoms were mostly experienced in mild severity in Table 2.

The women's sleep quality was poor with a mean PSQI score of 8.57±3.53, and 83.9% of them had poor sleep quality. The PSQI components mean scores were 1.50±0.76 for subjective sleep quality, 0.69±0.72 for sleep latency, 1.73±1.13 for sleep duration, 1.52±1.48 for habitual sleep activity, 1.53±0.59 for sleep disorder, 0.0±0.000 for use of sleeping medication, and 1.60±0.99 for daytime dysfunction in Table 3. There was a statistically significant positive correlation between the PPSSS and the PSQI total mean scores of women who underwent cesarean section (r=0.438; p=0.000) (p<0.05). There was a statistically significant moderately positive correlation between their PPSSS and subjective sleep quality scores (r=0.464; p=0.000) (p<0.05). There was a statistically significant weak correlation between their PPSSS and sleep latency scores (r=0.192; p=0.008) (p<0.05) and between their PPSSS and sleep duration scores in Table 4 (r=0.215; p=0.003) (p<0.05).

DISCUSSION

In this study, the mean PPSSS score of women was 10.38±5.92 and their postpartum physical symptom severity was low. In the literature, a limited number of studies about the severity of postpartum physical symptoms in women with cesarean section. In contrast to our study, this study found that women who underwent cesarean section had statistically significantly higher postpartum physical symptom severity than those who underwent vaginal delivery (21). Reducing the severity of physical symptoms among postpartum women is important because severe physical symptoms can negatively affect their ability to perform daily activities (21-23). The low severity of physical symptoms in women with cesarean section in our study may be because the majority of them had previous cesarean section and postpartum experiences. In our study, the most common physical symptoms in women were determined as poor sleep quality/lack of sleep (85.5%) and cesarean section/perineal pain (82.8%), and it was understood that these symptoms were mostly experienced with mild severity. In the first study to document that sleep is significantly more important for women hospitalized after cesarean delivery, it was identified that hospitalized mothers who were recovering after cesarean section were more susceptible to insufficient sleep (9). Erbaş (24) concluded that 97% of women who had cesarean section had sleep and resting problems on the second day after discharge, 81.8% at the second postpartum week, and 15.2% at the eighth postpartum week. Studies in the literature support our results. In the postpartum period, women often struggle with both physical and psychological changes and try to breastfeed their newborn babies, take care of them, and fulfill their domestic responsibilities. Therefore, women's nighttime sleep is interrupted by physical symptoms, thereby

Table 2. Distribution of postpartum physical symptom severities in women after cesarean section

Symptoms	Severity of symptoms (%)			
	No semptom	Mild severity	Moderate severity	High severity
Poor sleep quality or insomnia	14.5	42.5	26.4	16.6
Pain at the site of cesarean section or perineum	17.1	43.5	26.9	12.5
Back pain	22.3	30.6	29.0	18.1
Headache	39.9	31.1	19.7	9.3
Constipation	48.2	20.7	20.2	10.9
Cold hands and feet	64.8	23.8	8.8	2.6
Feeling cold	65.3	24.4	7.7	2.6
Dizziness	69.4	21.2	8.8	0.6
Joinr pain	72.0	17.2	9.8	1.0
Hemorrhoids	72.0	13.0	9.8	5.2
Numbness in hands	74.1	18.7	6.2	1.0
Excessive vaginal bleeding	76.2	17.6	6.2	0.0
Varicose veins in the legs	79.8	14.0	4.1	2.1
Urinary tract infection	80.8	11.4	4.7	3.1
Excessive vaginal discharge	81.3	13.0	4.7	1.0
Numbness in feet	83.9	11.9	4.2	0.0
Urinary incontinence	88.6	8.8	1.6	1.0
Vaginal infection	90.2	6.2	3.1	0.5

Table 3. Distribution of mean PSQI scores among women with cesarean section

PSQI and its components	Mean ± SD	Median	Min.-max.
Subjective sleep quality	1.50±0.76	1	0-3
Sleep latency	0.69±0.72	1	0-3
Sleep duration	1.73±1.13	2	0-3
Habitual sleep efficiency	1.52±1.48	2	0-3
Sleep disturbances	1.53±0.59	1	0-3
Use of sleep medication	0.0±0.000	0	0-0
Daytime dysfunction	1.60±0.99	3	0-3
PSQI total	8.57±3.53	15	1-17
Sleep quality level		**Number**	**Percentage**
Good sleep quality		31	16.1
Poor sleep quality		162	83.9

SD: Standard deviation, PSQI: Pittsburgh sleep quality index, Min.: Minimum, max.: Maximum.

Table 4. Relationship between the PPSSS and PSQI Scores of women after cesarean section

Characteristics		Postpartum physical symptom severity scale	
	S	r[a]	p
Subjective sleep quality	193	0.464	**0.000***
Sleep latency	193	0.192	**0.008***
Sleep duration	193	0.215	**0.003***
Habitual sleep efficiency	193	0.116	0.110
Sleep disturbances	193	0.545	**0.000***
Use of sleep medication	193	0.327	**0.000***
PSQI total	193	0.438	**0.000***

[a]Pearson's correlation analysis was applied, *p<0.05.
PPSSS: Postpartum physical symptom severity scale, PSQI: Pittsburgh sleep quality index.

decreasing their sleep quality. One of the most common physical symptoms experienced by women in our study was pain in the cesarean section/perineal (82.8%). A previous study found that all women described pain of varying severity, from mild to unbearable, after cesarean section (25). Another study also reported that all women experienced pain at the incision site after cesarean section on the second day after discharge and in the second week postpartum, and 30.3% of them experienced this pain even in the eighth postpartum week (24). Studies support our study, suggesting that post-cesarean pain is common in women. This result may be attributed to uterine contractions, postoperative pain, and incision size due to increased vessel and nerve damage as the incision length increases. Therefore, both pharmacological and non-pharmacological methods should be used to relieve pain experienced by women. In our study, the least common physical symptoms in women were vaginal infection (9.8%) and urinary incontinence (11.4%), and it was understood that these symptoms were mostly experienced with mild severity. There are only a limited number of studies on this subject. A previous study found that 40.7% of women who underwent cesarean section had urinary incontinence after delivery, which was significantly higher in our study (26). In another study, urinary incontinence was the most common symptom experienced by women who underwent cesarean section (27). The results in the literature differ from those of our study. This may be because elective cesarean section has a positive effect on urinary incontinence as it protects pelvic tissues and because the women who did not have incontinence problems before delivery were included in the study. In our study, women who underwent cesarean section had poor sleep quality, with a PSQI mean score of 8.57±3.53, and 83.9% of them had poor sleep quality. Tzeng et al. (16), found that postpartum mothers' sleep duration, subjective sleep quality, and daytime dysfunction scores of postpartum mothers were highest in the first month after cesarean section. A previous study reported the PSQI total mean score of postpartum women as 10.1±3.5 (11). Another study reported that 83.6% of mothers had poor sleep quality (17). In another study, found the prevalence of poor sleep quality in postnatal women was 67.2% (28). Both the literature and our study suggest that postpartum women have poor sleep quality. These results may be because women had physical and hormonal changes that occurred in the postpartum period after cesarean section, the lack of sufficient time to rest, the wake up more frequently at night due to the care needs of the newborn, and experienced postpartum stress. These results may also be because the majority of women in our study had nuclear family, therefore they had inadequate number of family members who could support them during the postpartum period. Our study found a significant positive correlation between the PPSSS and PSQI total mean scores of women undergoing

cesarean section (r=0.438; p=0.000) (p<0.05). This result suggests that as the severity of postpartum physical symptoms of women with cesarean section increases, their sleep quality decreases. Postpartum mothers need 20% more sleep at night after delivery, but this need cannot be met due to postpartum physical problems (7). A study on sleep quality in the postpartum period has concluded that sleep problems complicated the mother's health status and negatively affected the care needs of the newborn (8). Ko et al. (13) found that 87.5% of mothers had poor sleep quality due to physical symptoms, frequent waking up at night, inability to sleep with the spouse, stress, and the baby's sleep pattern. Another study found that poor sleep quality was positively correlated with the severity of postpartum physical symptoms, sharing a room with the babies, and lack of exercise (29). The literature results support our study, suggesting that the severity of physical symptoms in women during the postpartum period negatively affects their sleep quality. Our study found a significant positive correlation between the PPSSS and mean subjective sleep quality scores of women who underwent cesarean section (r=0.464; p=0.000) (p<0.05). This result suggests that as the severity of postpartum physical symptoms of women increases, their subjective sleep quality decreases. Our study found a significant positive weak correlation between the mean PPSSS and sleep latency scores (r=0.192; p=0.008) (p<0.05). This result indicates that as the severity of postpartum physical symptoms increases, sleep latency decreases. There was a weak positive correlation between the PPSSS and mean sleep duration scores of women (r=0.215; p=0.003) (p<0.05). This result indicates that as the severity of postpartum physical symptoms of women increases, their sleep duration decreases. There was a moderately significant positive correlation between the mean scores of the PPSSS and sleep disorder in women (r=0.545; p=0.000) (p<0.05). This result demonstrates that as the severity of postpartum physical symptoms increases, sleep disturbance also increases. Our study concluded that there is a relationship between postpartum physical symptom severity and sleep quality in women who have undergone cesarean section, whereby sleep quality decreases as postpartum physical symptom severity increases. More studies are needed to better comprehend the relationship between sleep quality and postpartum physical symptom severity, which affects maternal health (9). It is necessary to determine the factors affecting postpartum sleep quality and the problems that postpartum mothers may encounter in advance (17). Therefore, determining the causes that negatively affect sleep quality in the postpartum period and developing solutions by nurses in parallel can provide significant gains for maternal and newborn health (17). Sleep quality should be evaluated with nursing interventions, especially in women in the postpartum period, and postpartum women should be trained to manage their postpartum physical symptoms and improve sleep quality (29).

CONCLUSION

As a result of our study, the mean PSQI score of women was found to be 8.57±3.53 and 83.9% of them had poor sleep quality. In addition, it was concluded that there is a significant relationship between postpartum physical symptom severity and sleep quality (p<0.05) and sleep quality decreased as postpartum physical symptom severity increased. In line with these results, as postpartum physical symptom severity affects sleep quality in with cesarean section, it may be recommended to teach postpartum women and other family members coping methods to reduce the severity of physical symptoms and to plan training programs for healthcare professionals who care for postpartum women.

Ethics

Ethics Committee Approval: Before collecting the data, two ethics committee approvals, including (approval number: 2019-08/04, date: 07.08.2019 and approval number: 2021-03/64, date: 10.03.2021), were obtained from the Sivas Cumhuriyet University Non-interventional Clinical Research Ethics Committee.

Informed Consent: Verbal/written approval was obtained from all women who attended in the research.

Authorship Contributions

Concept: M.Y., N.E., Design: M.Y., Supervision: M.Y., N.E., Materials: M.Y., Analysis or Interpretation: M.Y., N.E., Literature Search: M.Y., N.E., Writing: M.Y., Critical Review: M.Y., N.E.

Conflict of Interest: The authors declare there are no conflicts of interest.

Financial Disclosure: The authors declared that this study received no financial support.

REFERENCES

1. Taşkın L. Obstetrics and womens health nursing. Ankara, 13th edition ISBN:975-94661-0-04, 2016.
2. Arkan G. Validity and reliability study of postpartum physical symptom severity scale (Master's Thesis). İzmir, İzmir Katip Celebi University, 2016.
3. Erbaş N. Determination of the health problems among women in postpartum period depending on the way of giving birth: An example from Sivas for the year 2012. Journal of Continuing Medical Education. 2017; 26: 133-8.
4. Arkan G, Egelioğlu Çetişli N. Validity and reliability study of postpartum physical symptom severıty scale. JASCD. 2017; 4: 18-34.
5. Bağcı S, Altuntuğ K. Problems experienced by mothers in postpartum period an their associations with quality of life. International Journal of Human Sciences. 2016; 13: 3266-79.
6. Şimşek Ç, Yılmaz Esencan T. Nursing care during the postpartum period. Zeynep Kamil Medical Bulletin. 2017; 48: 183-9.
7. Boz İ, Selvi N. Testing the Psychometric Properties of the Postpartum Sleep Quality Scale in Turkish Women. J Nurs Res. 2018; 26: 385-92.
8. Özen ME, Örüm HM, Kalenderoğlu A, Karaçor T, Bucak İH, Atmaca M. Investigation of sleep quality and excessive daytime sleepiness in puerperium women. FNG & Science Medical Journal. 2018; 4: 111-4.
9. Lee SY, Lee KA. Early postpartum sleep and fatigue for mothers after cesarean delivery compared with vaginal delivery: an exploratory study. J Perinat Neonatal Nurs. 2007; 21: 109-13.
10. Şeker A. The relationship between sleep quality and breastfeeding self-efficacy of mothers in the postpartum period. (Master's Thesis), Mersin, Mersin University, 2018.
11. Erçel Ö, Kâhyaoğlu Süt H. Sleep and quality of life in postpartum women. Journal of Turkish Sleep Medicine. 2020; 1: 23-30.
12. Bağcı S. Problems experienced by mothers in postpartum period and their associations with quality of life. (Master's Thesis). Konya, Selcuk University, 2018.

13. Ko SH, Chen CH, Wang HH, Su YT. Postpartum women's sleep quality and its predictors in Taiwan. J Nurs Scholarsh. 2014; 46: 74-81.
14. Ay F, Tektaş E, Mak A, Aktay N. Postpartum depression and the factors affecting it: 2000-2017 study results. Journal of Psychiatrıc Nursing. 2018; 9: 147-52.
15. Birgili F. The Birth of Comfortable Women and The Effective Factors. Journal of Anatolia Nursing and Health Sciences. 2020; 23: 351-60.
16. Tzeng YL, Chen SL, Chen CF, Wang FC, Kuo SY. Sleep Trajectories of Women Undergoing Elective Cesarean Section: Effects on Body Weight and Psychological Well-Being. PLoS One. 2015; 10: e0129094.
17. Bay H, Soğukpınar N. The relationship between perceived social support and maternal sleep quality in postpartum period. Turkiye Klinikleri Journal of Health Sciences. 2019; 4: 242-50.
18. Chien LY, Tai CJ, Hwang FM, Huang CM. Postpartum physical symptoms and depressive symptomatology at 1 month and 1 year after delivery: A longitudinal questionnaire survey. Int J Nurs Stud. 2009; 46: 1201-8.
19. Buysse DJ, Reynolds CF 3rd, Monk TH, Berman SR, Kupfer DJ. The Pittsburgh Sleep Quality Index: a new instrument for psychiatric practice and research. Psychiatry Res. 1989; 28: 193-213.
20. Ağargün YM, Kara H, and Anlar Ö. The reliability and validity the Pittsburgh sleep quality index. Turkish Journal of Psychiatry. 1996; 7: 107-15.
21. Egelioğlu Çetişli N, Kahveci M, Hacılar A. Postpartum physical symptom severity and breastfeeding behaviour of primipar mother according to their birth type. Koç University Journal of Education and Research in Nursing. 2020; 17: 98-103.
22. Hobbs AJ, Mannion CA, McDonald SW, Brockway M, Tough SC. The impact of caesarean section on breastfeeding initiation, duration and difficulties in the first four months postpartum. BMC Pregnancy Childbirth. 2016; 16: 90.
23. Pereira TRC, Souza FG, Beleza ACS. Implications of pain in functional activities in immediate postpartum period according to the mode of delivery and parity: an observational study. Braz J Phys Ther. 2017; 21: 37-43.
24. Erbaş N. Determination of the nursing diagnoses and the problems experiencing by women in the care given according to functional health patterns model after cesarean. Turkish Clinics Journal of Nursing Science. 2017; 9: 15-29.
25. Karaman Özlü Z, Soydan S, Çapık A, Ejder Apay S, Avşar G, Özer N, et al. The effect of progressive relaxation exercises on pain control in postpartum women having a cesarean section. Journal of Anatolia Nursing and Health Sciences. 2016; 2: 1.
26. Keskin E. Urinary incontinence in pregnancy and its effect on quality of life. (Master's Thesis). Ordu, Ordu University, 2019.
27. Triviño-Juárez JM, Romero-Ayuso D, Nieto-Pereda B, Forjaz MJ, Criado-Alvarez JJ, Arruti-SevillanB, et al. Health related quality of life of women at the sixth week and sixth month postpartum by mode of birth. Women Birth. 2017; 30: 29-39.
28. Yang Y, Li W, Ma TJ, Zang L, Hall BJ, Ungvari GS, et al. Prevalence of Poor Sleep Quality in Perinatal and Postnatal Women: A Comprehensive Meta-Analysis of Observational Studies. Front Psychiatry. 2020; 11: 161.
29. Wen SY, Ko YL, Jou HJ, Chien LY. Sleep quality at 3 months postpartum considering maternal age: A comparative study. Women Birth. 2018; 31: e367-73.

GMJ 2024;35:364-368

DOI: http://dx.doi.org/10.12996/gmj.2024.4023

Normal Ranges of Left Atrial Strain and 3D Echocardiographic Volume Measurements in Türkiye

Türkiye'de Sol Atriyal Strain ve 3D Ekokardiyografik Hacim Ölçümlerinin Normal Değer Aralıkları

Özden Seçkin Göbüt, Serkan Ünlü, Burcu Cihan Talay

Clinic of Cardiology, Gazi University Hospital, Ankara, Türkiye

ABSTRACT

Objective: The clinical importance of left atrial (LA) remodeling and function have been shown in various cardiovascular diseases, such as heart failure and atrial fibrillation. The LA dimension and volume index are the currently recommended parameters for evaluation of LA. Speckle tracking echocardiography makes it possible to evaluate the physio-mechanics of the LA method and threedimensional echocardiography have been shown to provide robust calculations of LA volume. However, there is still a lack of reference values regarding the LA longitudinal strain (LS) and three-dimensional (3D) volumetric measurements in Türkiye. Thus, we sought to investigate and determine normal references for mentioned echocardiographic methodologies by examining healthy individuals.

Methods: The echocardiographic data of one-hundred and forty-six volunteers without known cardiovascular pathologies were analyzed. 3D volume measurements and LA longitidinal strain in the reservoir, conduit, and contraction phase were investigated. Trigger points were placed on the R-waves on the electrocrocardiogram, as suggested by recent recommendations.

Results: Our study revealed a normal reference range for LA reservoir LS [40% (95% confidence interval (CI): 38-43%)], LA conduit LS [24% (95% CI: 22-26%)], LA contraction phase LS [16% (95% CI: 13-18%)] and for 3D maximal LA volume of 28 mL/m^2 (95% CI: 25-32).

Conclusion: We have provided normal reference ranges for phasic LA LS and 3D volume measurements. Having normal reference ranges for Turkish population carries importance as regional difference can occur.

Keywords: Adult echocardiography, left atrial function, left atrial volume, deformation imaging, 3D echocardiography, reference values

ÖZ

Amaç: Sol atriyum (SA) yeniden şekillenmesinin ve işlevinin klinik önemi, kalp yetmezliği ve atriyal fibrilasyon gibi çeşitli kardiyovasküler hastalıklarda gösterilmiştir. SA boyutu ve hacim indeksi, SA'nın değerlendirilmesi için halen önerilen parametrelerdir. Speckle tracking ekokardiyografi, SA'nın fizyomekanik özelliklerinin değerlendirilmesine olanak tanırken, üç boyutlu (3D) ekokardiyografinin SA hacminin sağlam bir şekilde hesaplanmasını sağladığı gösterilmiştir. Ancak, Türkiye'de SA longitudinal strain (LS) ve 3D hacim ölçümleri ile ilgili referans değerler konusunda hala bir eksiklik vardır. Bu nedenle, sağlıklı bireyleri inceleyerek, bahsedilen ekokardiyografik metodolojiler için normal referans değerlerini araştırmayı ve belirlemeyi amaçladık.

Yöntemler: Bilinen kardiyovasküler patolojisi olmayan yüz kırk altı gönüllünün ekokardiyografik verileri analiz edildi. Rezervuar, iletken ve kasılma fazlarında 3D hacim ölçümleri ve SA LS incelendi. Tetikleme noktaları, güncel öneriler doğrultusunda elektrokardiyogramdaki R dalgaları üzerine yerleştirildi.

Bulgular: Çalışmamız, SA rezervuar LS için normal referans aralığını [%40 (%95 güven aralığı (GA): %38-43)], SA iletken LS [%24 (%95 GA: %22-26)], SA kasılma fazı LS [%16 (%95 GA: %13-18)] ve 3D maksimum SA hacmi için 28 mL/m^2 (%95 GA: 25-32) olarak ortaya koymuştur.

Sonuç: Fazik SA LS ve 3D hacim ölçümleri için normal referans aralıkları sağladık. Türk popülasyonu için normal referans aralıklarının belirlenmesi, bölgesel farklılıklar olabileceğinden önem taşımaktadır.

Anahtar Sözcükler: Yetişkin ekokardiyografi, sol atriyal işlev, sol atriyal hacim, deformasyon görüntüleme, 3D ekokardiyografi, referans değerler

Address for Correspondence/Yazışma Adresi: Özden Seçkin Göbüt, MD, Clinic of Cardiology, Gazi University Hospital, Ankara, Türkiye
E-mail / E-posta: ozden-seckin@hotmail.com
ORCID ID: orcid.org/0000-0001-7385-4419

Received/Geliş Tarihi: 15.10.2023
Accepted/Kabul Tarihi: 13.05.2024

INTRODUCTION

Numerous cardiovascular conditions, including heart failure and atrial fibrillation, induce alterations in the morphology and function of the left atrium. Left atrial (LA) remodeling, characterized by structural and functional changes, holds diagnostic and prognostic significance in various critical diseases (1). Presently, LA assessment primarily relies on two-dimensional (2D) echocardiography for measuring LA size and volume index (2). Nevertheless, 2D measurements have limitations, such as susceptibility to foreshortening and dependence on geometric assumptions. In contrast, three-dimensional (3D) echocardiography, owing to its increasing use and demonstrated accuracy and reproducibility, provides precise measurements without the need for geometric assumptions (3). Volumetric measurements derived from 3D echocardiography exhibit strong correlations with computed tomography and cardiac magnetic resonance measurements. Assessing the functional aspect of the left atrium is as crucial as understanding its anatomy in managing various diseases. The left atrium fulfills multiple roles in cardiac function, acting as a reservoir during left ventricular systole, a conduit in early diastole, and a pump in late diastole (4). Speckle tracking echocardiography facilitates a comprehensive evaluation of LA physio-mechanics (5). Initial reservations regarding LA strain assessment due to the thin myocardial wall have been dispelled by subsequent studies, demonstrating robust correlations between LA strain and atrial fibrosis rates. LA strain has shown diagnostic value in conditions such as heart failure with preserved ejection fraction, predictive value for thromboembolic events, and prognostic value for mitral regurgitation and atrial fibrillation (6-9). Moreover, strain analysis obtained through speckle tracking echocardiography is angle-independent and minimally affected by loading conditions, rendering it a potent tool for detecting subclinical dysfunction (4).

Technical standardization: A significant challenge arises from the lack of a technical consensus on LA strain analysis, primarily due to variations in software used by different vendors. Standardization within a specific vendor's system and conducting serial follow-ups with the same system are recommended to reduce measurement variability. Imaging from both apical four-chamber and two-chamber views is essential, and the region of interest (ROI) should be adjusted to avoid pericardial inclusion-related errors.

Reference values: The absence of established reference values for LA strain complicates its clinical application. Previously reported normal LA peak values vary significantly, partly due to differences in study populations and the definition of a "healthy subject group." Establishing specific reference values is essential for reducing regional variations (2,3).

Left atrial cycle definition: Two different definitions for the LA cycle exist: RR gating and PP gating. PP gating initiates the cycle with atrial contraction, resulting in a biphasic strain curve. RR gating, conversely, defines the cycle from the R-wave peak to the same point in the next cycle, yielding a monophasic curve that clearly delineates the reservoir phase. Recent studies recommend RR gating because it can be employed during atrial fibrillation (10).

While LA strain assessment via speckle tracking echocardiography provides valuable insights into cardiac function and holds significant potential for clinical application, several challenges necessitate further exploration and standardization. These include technical standardization, the establishment of reference values and the choice of LA cycle definition. This study seeks to investigate normal reference values of LA strain and 3D echocardiographic volume measurements in healthy individuals in Türkiye, thereby contributing to a better understanding of this emerging tool in cardiac assessment.

MATERIALS AND METHODS

Study Participants

Patients over 18 years of age, without known cardiac disease and in sinus rhythm were included in the study. Patients with a history of heart failure, moderate or severe valvular heart disease, pericardial disease, coronary artery disease and pulmonary embolism were excluded from the study. Patients with poor image quality were also excluded. Finally, 146 patients were analyzed. The study protocol was approved by the Gazi University Clinical Research Ethics Committee (approval number: 753, date: 09.11.2020). Informed consent was obtained.

Echocardiographic evaluation: Echocardiographic evaluations of the patients at rest were performed by the same cardiologist using a General Electrics Vivid E95 device with a 2D M5Sc-D probe (GE Vingmed Ultrasound) according to the American Society of Echocardiography guidelines. For LA strain analysis, LA-focused images avoiding foreshortening were recorded.

3D imaging was performed with the GE Vivid E95 4V-D Probe (GE Vingmed Ultrasound). To obtain data sets of appropriate image quality, multi-beat images were recorded consecutively over 6 beats.

The acquired ECG-linked images were transferred to an offline EchoPac v201 (GE Vingmed Ultrasound) station for analysis.

Left atrial strain analysis with 2D STE: The LA ROI was determined in the obtained images. The full-wall ROI was manually adjusted for each image with an average thickness of 3 mm, optimally excluding the pericardium, pulmonary veins, and LA appendage. LA longitidinal strain curves were obtained from RR gating. The left atrial reservoir strain (LASr), left atrial conduit strain (LAScd), and left atrial contraction strain (LASc) were calculated from the obtained curve (11).

Reservoir strain (LASr): Describes the deformation of the left ventricle during isovolumetric contraction, ejection and isovolumetric relaxation. It is calculated as the difference in strain between the peak of the strain curve and the end of diastole. This value is always positive.

Conduit strain (LAScd): It occurs in patients in sinus rhythm from the opening of the mitral valve until the onset of LA contraction. It is calculated by subtracting the peak value of the curve from the strain value at the beginning of atrial contraction and is always negative.

Contraction strain (LASc): Defines the deformation from the beginning of LA contraction to the end of diastole. Therefore, it is calculated as the difference between the tension value at the end of diastole (zero by definition) and the value at the beginning of atrial contraction. LASc occurs only in sinus rhythm and always has a negative value.

3D echocardiographic left atrial volume measurement: The image was aligned to obtain an optimal border delineation of the left atrium. The 3D longitudinal axis was aligned parallel to the axis of the left atrium. The 3D transverse axis was positioned approximately at

the level of the left atrium, where it intersected the 3D longitudinal axis at the geometric center point of the left atrium. For LA border tracking, 4 mitral annular points (lateral, septal, inferior, anterior) and the atrial superior dome point opposite the annulus were marked for semi-automatic LA border tracking. The LA maximum volumes were calculated automatically by the software. Maximum LA volume was measured in the frame just before mitral valve opening and manually indexed to BSA.

Statistical Analysis

Continuous variables have been conveniently summarized as mean values accompanied by their respective standard deviations, whereas categorical data are presented as percentages or frequencies. To assess the normality of the distribution of continuous variables, the Kolmogorov-Smirnov test was employed. A stringent criterion for statistical significance, denoted by a two-tailed p-value of <0.05, was uniformly adopted throughout all analyses. The statistical analysis was conducted using SPSS version 23.0, developed by IBM Corp in Armonk, NY, USA.

RESULTS

We provide normal reference ranges for phasic LA LS and 3D volume measurements. A total of 146 healthy volunteers were included in the study. The mean age of the population was 34.1±7.2 years. 48.6% were female. There were no known diseases that could affect hemodynamics. Arterial blood pressure and heart rate were within the normal range. The demographic, anthropometric, and clinical characteristics of the patients are summarized in Table 1.

Phasic LA longitidinal strain obtained from 2D speckle tracking echocardiography and 3D echocardiographic LA volume measurements are summarized in Table 2. LASr was 40% [confidence interval (CI): 95% 38-43%], conduit strain (LAScd) 24% (CI: 95% 22-26%), and contraction phase strain (LASc) 16% (CI: 95% 13-18%). 3D echocardiographic LA maximum volume was 28 mL/m^2 (25-32 mL/m^2).

Table 1. Demographic anthropometric and clinical features

Parameters	(n=146)
Age (years)	34.1±7.2
Gender (f) (n, %)	71 (48.6%)
SBP (mmHg)	115.7±8.7
DBP (mmHg)	78.1±6.9
Heart rate (bpm)	71.5±9
Weight (kg)	70.7±14.5

SBP: Systolic blood pressure, DBP: Diastolic blood pressure.

Table 2. Comparison of conventional echocardiographic parameters among groups

Parameters	Referance value	95% CI
LASr (%)	40%	38-43%
LAScd (%)	24%	22-26%
LASc (%)	16%	13-18%
LA volume indeks (mL/m^2)	28 mL/m^2	25-32 mL/m^2

LA: Left atrium, LS: Longitudinal strain, LASr: Left atrial reservoir strain, LAScd: Left atrial conduit strain, LASc: Left atrial contraction strain, CI: Confidence interval.

DISCUSSION

In this study, a healthy population in Türkiye was analyzed. The aim was to determine LA phasic strain values and 3D echocardiographic LA volume reference values. The findings of this study can be summarized as follows: (a) LA phasic strain values were 40% for the reservoir phase, 24% for the conduit phase, and 16% for the contraction phase. (b) 3D echocardiographic volume measurements showed a maximum LA volume index of 28 mL/m^2. (c) Our measurements were correlated with other comprehensive studies.

Deformation Imaging and 2D Speckle Tracking Echocardiography for Left Atrial Remodeling

LA remodeling refers to cumulative structural and functional changes due to haemodynamic stress. Given the absence of other structural abnormalities, the main cause of LA remodeling is high LV filling pressure (5). Therefore, the presence of LA remodeling reflects the long-term progression of various cardiovascular diseases. Currently, LAVI is the main parameter of LA remodelling and has its proven clinical advantages of simple measurement and derived from various cardiovascular diseases. However, the LAVI actually represents a static volume. Therefore, LAVI has limitations in reflecting the unique LA mechanics during the cardiac cycle, including reservoir, channel, and contractile functions.

Assessment of phasic atrial function provides an understanding of the complex role of the atria and its various phasic functions (reservoir, channel, and contractile) (1). Assessment of atrial function by speckle tracking echocardiography is a reproducible and accurate method of analysis for the detection of subclinical LA dysfunction that is relatively free from loading conditions and relatively geometric assumptions. The prognostic significance has been demonstrated in many cardiovascular diseases. LA strain values of atrial fibrillation patients have been shown to be associated with increased gadolinium uptake, i.e., fibrosis, in cardiac magnetic resonance (6). Subsequently, many studies have emphasized the relationship between atrial fibrillation frequency and atrial strain (8). LA strain has been shown to be a very strong predictor of atrial fibrillation recurrence. In particular, a peak atrial strain below 23% predicted recurrence after atrial fibrillation ablation. LA strain has also been associated with survival after stroke in patients with chronic atrial fibrillation. In this study, 12% was used as the limit value (9,12,13). Another use of LA strain is in heart failure (14). It has been found to be a prognostic marker in heart failure with low ejection fraction. It has been shown that the prognosis is extremely poor when peak atrial strain is below 13 per cent.

LA strain was also found to be a prognostic parameter in heart failure with preserved ejection fraction with low ejection fraction. The limit values are 31% for patients with sinus rhythm and 35% for patients with atrial fibrillation. In the staging of diastolic dysfunction, LA peak strain was found to be an important marker of diastolic dysfunction in all diastolic dysfunction groups and subgroups, while other echocardiographic parameters did not show continuity between groups (7). However, despite these strong studies, LA strain could

not be included as a basic parameter because a specific reference value could not be determined. Moderately comprehensive studies in different patient groups and lack of technical standardization are the most important obstacles to establishing a clear reference value (11). In addition, there is a high heterogeneity between groups in studies conducted to determine reference values. Regional differences are also one of the biggest obstacles in the clarification of the reference value. Therefore, there is still a need for studies to determine reference values in healthy participant groups. In response to this practical need, this study presents reference values for LA stain obtained from a group of healthy subjects in Türkiye.

The mean LASr in our study was 40% (95% CI: 37-43%). Several previous studies have reported LASr values (also defined as peak LA trains) in healthy groups. Pathan et al. (15) conducted a meta-analysis on 2,542 healthy subjects and found that the mean LASr was 39.4% (95% CI: 38.0%-40.8%). D'Ascenzi et al. (16) performed a meta-analysis on 2,087 subjects and reported a mean LASr of 38±3% (95% CI: 32%-43%). Although these studies reported LASr values similar to our results, Sun et al. (17) reported a mean LAS RES of 35.7±5.8% in a study of 54 healthy Korean subjects. This is substantially different from our results. The main difference in these results seems to be related to regional variation. However, there are few original studies analysing LAScd and LASc. This study additionally provides a reference value for LAScd and LASc.

3D Echocardiographic Volume Assessment for Left Atrium

The prognostic value of LAV as a predictor of morbidity and mortality is well recognized in many cardiovascular disease states and is particularly important for the assessment of LV diastolic function. However, 2DE techniques routinely used to measure LAV in clinical practice are prone to errors due to their 2D nature. Extensive studies have shown a significant underestimation of 2D LAV measurements compared with computed tomography and cardiac magnetic resonance results. Traditional assessment of LA volumes by 2DE is limited by prior abbreviation and reliance on incorrect geometric assumptions for volumetric estimation, leading to underestimation of true LA volumes (18). There are several publications showing that this underestimation is significantly reduced by the use of 3DE imaging. However, there are very few studies on reference values. Determination of reference values with 3D echocardiography, which is a more accessible and inexpensive method compared to cardiac MR, is important for clinical practice (19). In our study, we determined the reference value for the indexed 3D LAV as 28 mL/m^2. Our reference value seems to be more compatible with cardiac MR results obtained in previous comprehensive studies compared to 2D echocardiography (18,19).

Study Limitations

It is important to recognize the limitations of our study. Perhaps the most important limitation was the relatively small sample size and the recruitment of participants from a single center. Although our findings provide valuable information, future research with larger and more diverse cohorts will allow for the clarification and establishment of reference values in clinical practice.

CONCLUSION

In conclusion, we proposed reference values for strain analysis and 3D echocardiographic indexed volume assessment of the LA reservoir, duct, and contractile components in a large group of healthy subjects living in Türkiye. New developments in echocardiography allow non-invasive elucidation of LA physiomechanics. However, more comprehensive studies on reference values are needed to incorporate these parameters in clinical practice.

Ethics

Ethics Committee Approval: The study protocol was approved by the Gazi University Clinical Research Ethics Committee (approval number: 753, date: 09.11.2020).

Informed Consent: It was obtained.

Authorship Contributions

Surgical and Medical Practices: Ö.S.G., S.Ü., B.C.T., Concept: Ö.S.G., S.Ü., B.C.T., Design: Ö.S.G., S.Ü., B.C.T., Data Collection or Processing: Ö.S.G., S.Ü., B.C.T., Analysis or Interpretation: Ö.S.G., S.Ü., B.C.T., Literature Search: Ö.S.G., S.Ü., B.C.T., Writing: Ö.S.G., S.Ü., B.C.T.

Conflict of Interest: No conflict of interest was declared by the authors.

Financial Disclosure: The authors declared that this study received no financial support.

REFERENCES

1. Hoit BD. Evaluation of left atrial function: current status. Structural Heart. 2017; 1: 109-20.
2. Cho GY, Chan J, Leano R, Strudwick M, Marwick TH. Comparison of two-dimensional speckle and tissue velocity based strain and validation with harmonic phase magnetic resonance imaging. Am J Cardiol. 2006; 97: 1661-6.
3. Cameli M, Caputo M, Mondillo S, Ballo P, Palmerini E, Lisi M, et al. Feasibility and reference values of left atrial longitudinal strain imaging by two-dimensional speckle tracking. Cardiovasc Ultrasound. 2009; 7: 6.
4. Vieira MJ, Teixeira R, Gonçalves L, Gersh BJ. Left atrial mechanics: echocardiographic assessment and clinical implications. J Am Soc Echocardiogr. 2014; 27: 463-78.
5. Buggey J, Hoit BD. Left atrial strain: measurement and clinical application. Curr Opin Cardiol. 2018; 33: 479-85.
6. Kuppahally SS, Akoum N, Burgon NS, Badger TJ, Kholmovski EG, Vijayakumar S, et al. Left atrial strain and strain rate in patients with paroxysmal and persistent atrial fibrillation: relationship to left atrial structural remodeling detected by delayed-enhancement MRI. Circ Cardiovasc Imaging. 2010; 3: 231-9.
7. Nagueh SF, Smiseth OA, Appleton CP, Byrd BF 3rd, Dokainish H, Edvardsen T, et al. Recommendations for the Evaluation of Left Ventricular Diastolic Function by Echocardiography: An Update from the American Society of Echocardiography and the European Association of Cardiovascular Imaging. J Am Soc Echocardiogr. 2016; 29: 277-314.
8. Tops LF, Delgado V, Bertini M, Marsan NA, Den Uijl DW, Trines SA, et al. Left atrial strain predicts reverse remodeling after catheter ablation for atrial fibrillation. J Am Coll Cardiol. 2011; 57: 324-31.
9. Shih JY, Tsai WC, Huang YY, Liu YW, Lin CC, Huang YS, et al. Association of decreased left atrial strain and strain rate with stroke in chronic atrial fibrillation. J Am Soc Echocardiogr. 2011; 24: 513-9.

10. Hayashi S, Yamada H, Bando M, Saijo Y, Nishio S, Hirata Y, et al. Optimal Analysis of Left Atrial Strain by Speckle Tracking Echocardiography: P-wave versus R-wave Trigger. Echocardiography. 2015; 32: 1241-9.
11. Voigt JU, Mălăescu GG, Haugaa K, Badano L. How to do LA strain. Eur Heart J Cardiovasc Imaging. 2020; 21: 715-7.
12. Cameli M, Mandoli GE, Loiacono F, Sparla S, Iardino E, Mondillo S. Left atrial strain: A useful index in atrial fibrillation. Int J Cardiol. 2016; 220: 208-13.
13. Tsai WC, Lee CH, Lin CC, Liu YW, Huang YY, Li WT, et al. Association of left atrial strain and strain rate assessed by speckle tracking echocardiography with paroxysmal atrial fibrillation. Echocardiography. 2009; 26: 1188-94.
14. Freed BH, Daruwalla V, Cheng JY, Aguilar FG, Beussink L, Choi A, et al. Prognostic Utility and Clinical Significance of Cardiac Mechanics in Heart Failure With Preserved Ejection Fraction: Importance of Left Atrial Strain. Circ Cardiovasc Imaging. 2016; 9: 10.
15. Pathan F, D'Elia N, Nolan MT, Marwick TH, Negishi K. Normal Ranges of Left Atrial Strain by Speckle-Tracking Echocardiography: A Systematic Review and Meta-Analysis. J Am Soc Echocardiogr. 2017; 30: 59-70.
16. D'Ascenzi F, Piu P, Capone V, Sciaccaluga C, Solari M, Mondillo S, et al. Reference values of left atrial size and function according to age: should we redefine the normal upper limits? Int J Cardiovasc Imaging. 2019; 35: 41-8.
17. Sun BJ, Park JH, Lee M, Choi JO, Lee JH, Shin MS, et al. Normal Reference Values for Left Atrial Strain and Its Determinants from a Large Korean Multicenter Registry. J Cardiovasc Imaging. 2020; 28: 186-98.
18. Mor-Avi V, Yodwut C, Jenkins C, Kühl H, Nesser HJ, Marwick TH, et al. Real-time 3D echocardiographic quantification of left atrial volume: multicenter study for validation with CMR. JACC Cardiovasc Imaging. 2012; 5: 769-77.
19. Figliozzi S, Georgiopoulos G, Pateras K, Sianis A, Previtero M, Tondi L, et al. Normal ranges of left atrial volumes and ejection fraction by 3D echocardiography in adults: a systematic review and meta-analysis. Int J Cardiovasc Imaging. 2022 ;38: 1329-40.

Original Investigation | Özgün Araştırma

GMJ 2024;35:369-375

DOI: http://dx.doi.org/10.12996/gmj.2024.4076

Mitral Valve Repair in Pediatric Patients with Dilated Cardiomyopathy and Mitral Insufficiency: Single-Center Experience and Results

Dilate Kardiyomiyopati ve Mitral Yetmezlikli Çocuk Hastalarda Mitral Kapak Onarımı: Tek Merkezli Deneyim ve Sonuçlarımız

Mustafa Yılmaz[1], Başak Soran Türkcan[1], Ata Niyazi Ecevit[1], İbrahim Ece[2], Hazım Alper Gürsu[2], Atakan Atalay[1]

[1]Clinic of of Pediatric Cardiovascular Surgery, Ankara Bilkent City Hospital, Ankara, Türkiye
[2]Clinic of Pediatric Cardiology, Ankara Bilkent City Hospital, Ankara, Türkiye

ABSTRACT

Objective: Idiopathic dilated cardiomyopathy (DCM) is a serious disease causing mitral regurgitation and contraction defects of the myocardium. Through mitral valve (MV) repair surgery, the clinical status of patients can be improved.

Methods: Pediatric patients with DCM and mitral insufficiency who underwent mitral repair procedures between 2019 and 2023 were retrospectively investigated. The patients' demographic characteristics, preoperative and postoperative clinical conditions, and echocardiographic findings were compared. The techniques used in patient operations were examined. Similarly, data regarding the postoperative intensive care unit processes and mortality data of the patients were recorded.

Results: Mitral repair was performed in 3 patients during the study period. The mean age of the patients was 4.66 months (±3.05) and body weight was 5.25 kg (±0.25). In the preoperative period, left ventricular ejection fraction decreased slightly in all patients [mean: 43.3% standard deviation (SD): ±2.8]. Although the preoperative and postoperative values of left ventricular end-diastolic diameter (LVEDd) and LVEDd Z-scores were above normal, respectively, they showed a decreasing trend after the operation. Although the mitral annulus diameters decreased slightly after the operation in all three patients, they remained high (mean: 17.6 mm SD: ±1.5). A significant decrease in MV insufficiency was observed in postoperative follow-ups after discharge (1^{st}-2^{nd} degree). Wooler annuloplasty and posterior valve pericardial patch augmentation were applied as the primary approach in all patients. The patients did not develop additional morbidities, and no mortality was observed during hospitalization.

Conclusion: Successful surgical interventions to prevent mitral regurgitation in pediatric patients with DCM and mitral regurgitation, may improve the clinical status of these patients.

Keywords: Cardiomyopathy, dilated, mitral valve, infant, mitral valve annuloplasty, heart failure

ÖZ

Amaç: İdiyopatik dilate kardiyomiyopati (DCM), mitral yetersizliğine ve miyokardın kasılma bozukluğuna neden olan ciddi bir hastalıktır. Mitral kapak (MK) onarımı ameliyatı ile hastaların klinik durumu iyileştirilebilir.

Yöntemler: 2019-2023 yılları arasında mitral onarımı yapılan DCM ve mitral yetmezliği olan pediatrik hastalar retrospektif olarak incelendi. Hastaların demografik özellikleri, ameliyat öncesi ve sonrası klinik durumları ve ekokardiyografik bulguları karşılaştırıldı. Hastaların ameliyatlarında kullanılan teknikler incelendi. Benzer şekilde hastaların postoperatif yoğun bakım süreçleri ve mortalite verileri kaydedildi.

Bulgular: Çalışmanın yapıldığı tarih aralığında 3 hastaya mitral tamir uygulandı. Hastaların ortalama yaşı 4.66 ay (±3,05) ve vücut ağırlığı 5.25 kg (±0,25) idi. Preoperatif dönemde hastaların hepsinde sol ventrikül ejeksiyon fraksiyonu hafif azalmıştı [ort.: %43,3±2,8 standart deviasyon (SD)]. Sol ventrikül diyastol sonu çapı (LVEDd) ve LVEDd Z-skorları sırayla preoperatif ve postoperatif değerleri normalin üzerinde olsa da operasyondan sonra azalma trendi göstermiştir. Her üç hastada da mitral annülüs çapları operasyon sonrasında hafif gerileme gösterse de yine yüksek sebat etmiştir (ort.: 17,6 mm ±1,5 SD). Postoperatif taburculuk sonrası takiplerde mitral kapak yetmezliğinde belirgin azalma görülmüştür (1.-2. derece). Tüm hastalarda primer yaklaşım olarak Wooler annüloplasti ve posterior kapak perikardial yama augmentasyonu uygulandı. Hastaların hastanede yatış süreleri boyunca ek morbiditeleri gelişmedi, mortalite izlenmedi.

Sonuç: DCM ve mitral yetmezlikli çocuk hastalarda mitral yetersizliğini önlemeye yönelik başarılı cerrahi girişimler hastaların klinik durumunu iyileştirebilir.

Anahtar Sözcükler: Kardiyomiyopati, dilate, mitral kapak, infant, mitral kapak annüloplasti, kalp yetmezliği

Address for Correspondence/Yazışma Adresi: Mustafa Yılmaz, MD, Department of Pediatric Cardiovascular Surgery, Ankara Bilkent City Hospital, Ankara, Türkiye
E-mail / E-posta: mustafayz1983@gmail.com
ORCID ID: orcid.org/0000-0002-3212-2673

Received/Geliş Tarihi: 16.12.2023
Accepted/Kabul Tarihi: 20.01.2024

INTRODUCTION

Idiopathic dilated cardiomyopathy (DCM) is a myocardial disease in which the left or both ventricles are affected simultaneously, leading to contraction disorders, and the underlying cause cannot be revealed. This condition, which can affect both adults and children, is much less common in children (annual average 1:170,000 vs. 1:2500) (1,2). However, the clinical course of DCM in children is unfortunately more severe than in adults. The rate of death or transplantation requirement of patients during 1 and 5-year follow-ups is 31% to 46%, respectively (1,2). Approximately 30% of pediatric patients with DCM, the disease may regress under medical treatment or spontaneously over the years. However, in the majority of patients, the clinical picture progressively worsens, and they begin to require frequent hospitalization and inotropic therapy. Patients with poor left ventricular contraction, a high degree of mitral insufficiency (MI), lower functional capacity, and those who do not respond to medical treatment have a poor prognosis. These patients may require mechanical support and/or heart transplantation. DCM is the most common cause of heart transplantation in pediatric patients (3). However, today, due to the scarcity of donors, several patients cannot be transplanted in a timely manner, and approximately 30% of patients die while waiting for transplantation (4). In addition, chronic rejection may develop in transplanted patients in the subsequent years, and the 25-year survival rate of the patients may decrease to 37%.

The suboptimal long-term outcomes of heart transplantation, considered the definitive treatment for end-stage heart failure, have prompted clinicians to explore alternative medical and surgical approaches. Especially in the last two decades, repair procedures for MI, frequently observed in patients with DCM, have gained popularity in both adult and pediatric patients. Studies have reported that by eliminating or reducing MI through repair or replacement, the clinical status of some patients improved, and the need for transplantation was postponed. The aim of this study is to investigate changes in the clinical status and echocardiographic (ECHO) data of pediatric patients with DCM and severe MI who underwent mitral valve (MV) repair and to compare the results obtained with those reported in the current literature.

MATERIALS AND METHODS

This study is a retrospective observational study, and its cohort consists of pediatric patients (<18 years old) diagnosed with DCM and severe MI who were referred to mitral repair surgery at Ankara Bilkent City Hospital between August 2019 and August 2023. The study protocol was approved by the Ankara Bilkent City Hospital (approval number: E2-23-5860, date: 06.12.2023).

The diagnosis of DCM was based on the presence of the following signs and symptoms: heart failure symptoms, left ventricular end-diastolic diameter (LVEDd) Z-score >2, a thin-walled left ventricle (LV) with a spherical shape, and left ventricular ejection fraction (LVEF) below 50%. The study included patients with idiopathic DCM, while those with myopathies developing secondary to viral or other factors were excluded to ensure homogeneity.

The indications for the operation in patients were determined as signs of congestive heart failure that could not be diminished with maximum medical treatment, such as tachypnea, tachycardia, intense sweating, difficulty in feeding, and failure to gain weigh as well as poor cardiac function and severe MI. The patients' demographic characteristics, preoperative clinical conditions, ECHO findings, operative details, postoperative intensive care data, and post-discharge follow-up data were retrospectively investigated. In the ECHO assessment, both preoperative and postoperative (after discharge) measurements of patients' LVEF, left ventricular fractional shortening (LVFS), LVEDd and Z-scores, MV annulus diameters and Z-score and MI grading were evaluated. EF and LVEDd measurements were obtained using the biplane Simpson method. In the clinical evaluation, the patient's modified Ross classification, daily diuretic use dose, and the child's ability to gain weight were examined both preoperatively and postoperatively. Post-discharge changes in the patients' MI and whether there was a need for an increase in the diuretic dose were assessed.

Statistical Analysis

Categorical measurements were summarized as numbers and percentages, and numerical measurements were summarized as mean and standard deviation (SD). All statistical analyses were performed using IBM SPSS version 25.

Operative Technique

In all patients, the MV was accessed through median sternotomy. After inducing moderate hypothermia and achieving cardiac arrest, the interatrial groove was dissected, and entry into the left atrium was made through Sondergaard's groove. Improved visualization of the MV was achieved by placing suspension sutures in both trigone and the middle of the posterior annulus. Subsequently, both valves and the subvalvular apparatus were meticulously examined using nerve hooks. The intensity and characteristics of the MI (central or eccentric) were then assessed by applying a saline test. The size of the annulus diameter and anterior mitral leaflet were determined using appropriate scales. Intraoperative examination revealed that the MV and subvalvular apparatus were structurally healthy. No thickening or shrinkage that could be considered pathological was observed. No major finding that could be compatible with rheumatic or infective endocarditis was detected. The scallops on both leaflets of the valve were prominent, and the coaptation surfaces had smooth anatomy. No clefts were observed in the MV leaflets. The primary causes of MI in all patients were annular dilatation and restriction of movement of the posterior leaflet. The anterior MV and its associated subvalvular apparatus move freely. However, it was noted that the configuration of the posteromedial papillary muscle was disturbed by LV dilatation. The LV had thinned free walls, and the chordae of the posteromedial papillary muscle had restricted the movement of the posterior leaflet. In the saline test, it was observed that the posterior leaflet could not completely cover the coaptation surface, leading to functional central insufficiency, especially in the P2-A2 line. Subsequently, Wooler annuloplasty and posterior leaflet augmentation using autologous pericardium were performed in all patients (Figure 1a,b). In patient number 2, upon observing that central MI persisted in the intraoperative saline test, Wooler annuloplasty stitches were removed, and posterior annular shortening plasty reinforced with an autologous pericardial strip was performed on the posterior leaflet. Additionally, in patient number 1, since serious MI was observed on intraoperative transesophageal

echocardiography (TEE), the surgical repair was re-evaluated by applying a cross-clamp for the second time. It was observed that the posterior suture line of the autologous pericardium was detached from the native MV tissue, probably due to weak stitches. The entire anastomosis was re-performed and strengthened. After all these interventions, it was observed that MI decreased to trace or grade 1 in all patients. All patients had moderate tricuspid valve insufficiency. The reason for this was thought to be related to secondary pulmonary hypertension due to severe MI and distortion of the morphology of the right chambers by the enlarged left chambers. Because there were no obvious signs of right heart failure in the patients and it was thought that the existing insufficiency could improve in the long term, no additional intervention was applied to the tricuspid valve.

RESULTS

During the study period, mitral valvuloplasty was performed in three pediatric patients diagnosed with DCM and severe MI. Two of the patients were female, and one was a boy. The mean age of the patients was 4.66 months (±3.05 SD), and their body weight was 5.25 kg (±0.25 SD). In the preoperative period, LVEF slightly decreased in all patients [mean 43.3% (±2.8 SD)]. LVFS was observed at the lower limits of normal in all three patients [mean 24.3% (±2.08 SD)]. Although the preoperative and postoperative values of LVEDd and LVEDd Z-scores were above normal, respectively, they showed a decreasing trend after the operation. In all three patients, MV annuli were observed to be very large in the preoperative period [mean 19.3 mm (±2.08 SD)]. Although these values showed slight regression after the operation, they remained high [mean 17.6 mm (±1.5 SD)]. Similarly, the diameter of the left atrium increased significantly in all patients preoperatively, and some regression was observed after the procedure. Severe (grade 3-4) insufficiency in the MV was observed in all patients before the operation. A significant decrease in MI was observed during postoperative follow-up after discharge. Additionally, the modified Ross score of patients decreased, and the need for diuretic use decreased slightly. The perioperative variables are summarized in Table 1.

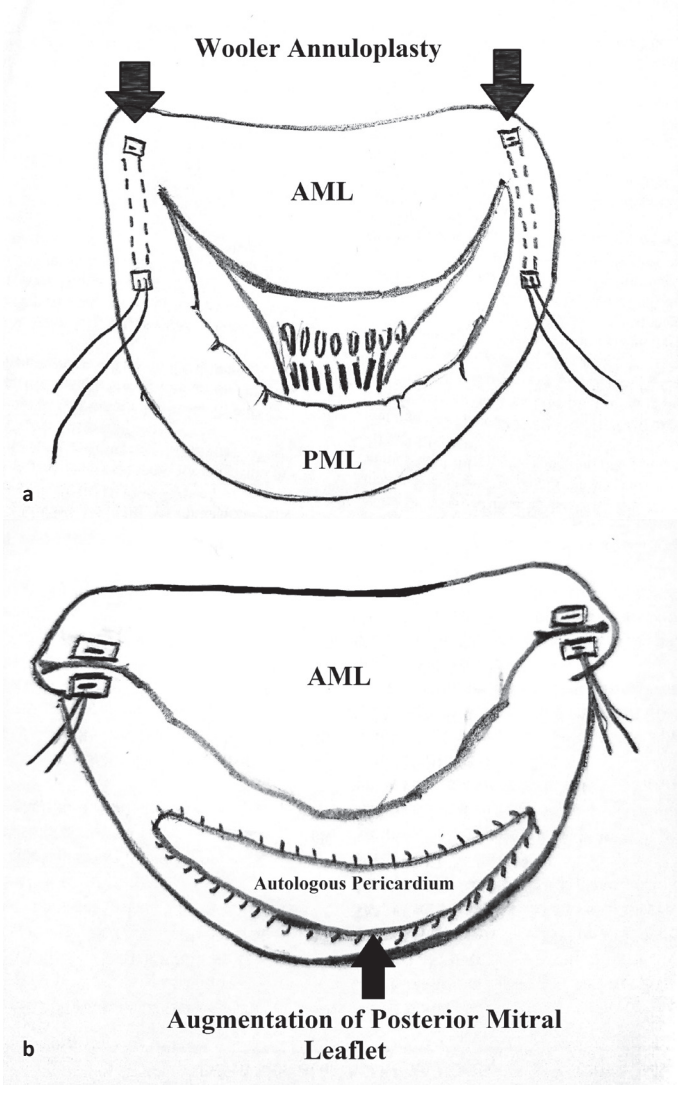

Figure 1. (a, b) Wooler annuloplasty procedure combined with augmentation of posterior mitral leaflet with autologous pericardium.

The operations of the patients were performed in a standard manner, and the cardiopulmonary bypass (CPB) and cross-clamp times of two patients was observed to be under 60 minutes. In one patient, CPB support was needed for the second time after residual severe MI was detected in the control performed with TEE. Wooler annuloplasty and posterior valve augmentation were applied as the primary approach in all patients. In patient number 1, the surgical procedure was revised in the same session, and in patient number 2, the posterior annulus was narrowed little more with modified Paneth annuloplasty reinforced with the untreated autologous pericardial strip technique (5), as the lid coaptation was not to the desired extent after the procedures. Postprocedure intraoperative TEE measurements mostly showed grade 1 MI. In the postoperative period, patient number 1's need for ICU and inotrope due to heart failure lasted significantly longer, and this was not observed in other patients. The patients did not develop additional morbidities, and no mortality was observed during the hospitalization period. Operative and ICU data are summarized in Table 2.

DISCUSSION

Approximately half of the pediatric patients diagnosed with DCM are in the infant age group. When all pediatric cardiomyopathies are evaluated, the rate of patients remaining free from death or heart transplantation over a 5-year period ranges between 46% to 60%. DCM is the most frequently transplanted pathology among all cardiomyopathies in pediatric patients (2).

Pediatric patients diagnosed with DCM may present with different clinical characteristics and ECHO findings. In this disease, myocardial thinning, LV dilatation and functional MI occur mainly secondary to progressive myocardial damage. Functional MI initiates a vicious circle, further increasing LV preload. This leads to LV dilatation, increased LV wall tension, prolongation of the distance between the papillary muscles, and further aggravation of functional MI. Consequently, the increasing MI, stretched, and enlarged left atrium and ventricle, and decreasing LV systolic function contribute to a further increase in MI and a gradual decrease in effective stroke volume. Patients become symptomatic with left heart failure due to this vicious circle. It is stated that the degree of MI at first admission

Table 1. Perioperative variables

	Patient number					
Perioperative variables	**1**		**2**		**3**	
	Preop	**Postop**	**Preop**	**Postop**	**Preop**	**Postop**
Age (month)	8	10	4	10	2	4
Weight (kg)	5.3	5.8	5.5	6.2	5	5.3
LVEF, (%)	45	58	40	57	45	60
LVFS, (%)	25	28	22	28	26	31
LVEDd (mm)	46	35	36	31	28	28
LVEDd Z-score	10.3	6.18	6.34	3.83	3.56	2.33
LVPWt (mm)	6	7	6	9	5	6
Mitral annulus (mm)	21	19	17	16	20	18
Mitral annulus Z-score	15.5	14.8	14.3	13.7	15.3	14.7
Mitral valve Insufficiency	3-4	1	4	1	3-4	1-2
Valve with restricted mobility	PML	-	PML	-	PML	-
Left atrium (mm)	41x35	30x36	35x35	30x30	40x35	35x35
RVSP (mmHg)	45-50	40-45	70-75	30-35	55-60	40-45
Tricuspid insufficiency	2	1-2	1-2	1	2	1
Additional cardiac anomaly	-	-	-	-	Large PDA	
Medication (mg/kg/d)						
- Spirinolacton	2.2	1.1	0.65	-	1	-
- Furosemid	2	1,8	0.72	1.12	2	2
- Captopril	2.2	1.5	0.62	0.5	0.8	0.8
Modified ross classification	3	2	3	1	3	1

LVEF: Left ventricular ejection fraction, LVFS: Left ventricular fractional shortening LVEDd: Left ventricular end diastolic diameter, LVPWt: Left ventricular posterior wall thickness, PDA: Patent ductus arteriosus, PML: Posterior mitral leaflet, RVSP: Right ventricular systolic pressure.

is a very important prognostic factor in the prognosis of patients with DCM, and functional MI is observed in 60-87% of all DCM patients at first admission or during follow-up (6,7).

In their study of 42 patients with DCM, Fernandes et al. (8) found that MI may increase even if EF remains stable in long-term follow-ups. Moreover, they observed that each degree of increase in MI doubled the risk of transplantation and death. Additionally, there is a correlation between a higher degree of MI and the worsening of patients' functional clinical status. However, an inverse relationship was observed between the patient's high degree of MI at the time of the initial diagnosis and exclusion from death or transplantation (8).

While MI develops in some patients with DCM but is not observed in others. The underlying reason for this remains unclear. However, based on these assumptions, it is thought that the disease progresses more severely in the myocardium of patients who develop MI, and dysfunction in the MV rapidly develops as a secondary effect of papillary muscle involvement. Additionally, it is believed that some as-yet-unidentified genetic factors may also influence the MV in certain patients, potentially paving the way for the development of insufficiency (6). The initial step in treating idiopathic DCM and MI involves alleviating congestive heart failure symptoms through medical interventions. Patients who respond successfully to medical treatment undergo close outpatient cardiological examinations for follow-up. Those whose symptoms cannot be adequately controlled through medication are hospitalized, and inotropic treatment is initiated. Individuals whose general condition does not improve despite these interventions, and who suffer from functionally severe heart failure were, are placed on the heart transplant list. If necessary, mechanical support devices can be implemented as a bridge to transplantation. Presently, due to a shortage of donors, patients on the transplant list face prolonged waiting times, leading to a distressing reality in which approximately 30% of these patients succumb to their condition before transplantation. Moreover, transplanted patients inevitably confront chronic rejection over the long term, with less than half of them reaching adulthood (4). The suboptimal results of transplantation treatment in pediatric patients have prompted clinicians to explore alternative surgical procedures that aim to alleviate patients' symptoms, delay the need for transplantation, and potentially eliminate this requirement altogether.

Endovascular or surgical repair techniques for MI are now commonly employed in adult patients with DCM. The perioperative mortality rate for adults with DCM who undergo MV surgery ranges between 2% and 11% (9). Given that this rate is comparable to the 1-year survival of transplanted patients, there is a growing trend in the frequency of interventions for MI in this patient group today. However, experience regarding the applicability and outcomes of these treatment methods in pediatric patients is limited. Few case

Table 2. Operative and ın-hospital follow-up data

	Patient number		
	1	**2**	**3**
CPB duration	108*	61	50
Cross clamp duration	49*	46	43
Mitral valve repair	Wooler annuloplasty, posterior leaflet augmentation	Posterior leaflet augmentation modified paneth annuloplasty†	Wooler annuloplasty, posterior leaflet augmentation
Mitral regurgitation after intraoperative repair (TEE)	1-2	Trivial-1	Trivial-1
Morbidity in the ICU	-	-	-
Duration of mechanical ventilation (h)	34	8	13
Duration of inotropic treatment	266	16	32
ICU stay (d)	12	2	4
Total hospital stay (d)	28	7	8
Mortality	-	-	-

CPB: Cardiopulmonary bypass, TEE: transesophageal echocardiography, ICU: Intensive care unit, *Patient number 1 was cross-clamped for the second time after severe residual central mitral insufficiency was observed in intraoperative TEE, †In patient number 2, modified Paneth annuloplasty was performed after Wooler annuloplasty failed.

series have been described to date, and the long-term results of MV repair surgery in pediatric patients with DCM are still under investigation. Nevertheless, many studies optimistically report that following MV repair, patients experience fewer symptoms, a reduced need for inotrope, and decreased hospitalization requirements. Additionally, it is suggested that this approach is effective in postponing the need for transplantation in such patients.

The primary surgical choice for pediatric patients with DCM and severe MI is MV repair. Studies conducted on adult patients with DCM indicate high mortality rates when direct mitral valve replacement (MVR) is applied in these cases. This finding is attributed to disruption of the subvalvar apparatus and loss of LV function associated with MVR. Preserving annulus and papillary muscle continuity has been demonstrated to play critical roles in maintaining LV geometry and reducing LV wall stress. Consequently, valve repair is preferred over replacement in MI cases in patients with impaired contractile function. Long-term results in both pediatric and adult patients undergoing MV repair show promise in terms of favorable outcomes related to mortality and morbidity (5,7). However, if the desired result cannot be achieved after mitral repair or signs of insufficiency recur in the long term, MVR is recommended as a last resort. The potential risks and disadvantages of MVR in children have been recognized for many years. These include the absence of prostheses designed for patients with a narrow annulus (<15 mm) and the necessity to employ annulus expansion techniques in these patients. Other concerns involve the potential development of patient-prosthesis mismatch due to the patient's growth in the post-implantation period and the likelihood of re-replacement. These challenges encompass the need for replacement, difficulties in applying anticoagulation in pediatric patients, the risk of permanent heart block, and the threat of thromboembolism. Despite these considerations, mechanical valves are still widely used globally in pediatric patients who are not suitable for repair. In a study involving 17 pediatric patients with a mean age and body weight of 3.2 months and 5.2 kg, respectively, MVs that were deemed unsuitable for repair were replaced with a 15 mm STJ mechanical valve. Subsequently, 11 patients required a new valve replacement due to patient-prosthesis incompatibility after an average of 2.9 years. During an average follow-up of 9.6 years, mortality occurred in 2 patients, 1 early and 1 late (12%). Throughout the follow-up period, thromboembolic events developed in 4 patients, and permanent neurological damage occurred in only 1. When no other option was available, the authors concluded that MVR with a 15 mm mechanical valve can be performed safely (10). Unfortunately, to date, there are no prospective controlled studies examining the long-term outcomes of MVR in pediatric patients with DCM.

On the other hand, there are few cases series in the literature about patients with DCM who underwent mitral repair. In a study involving 7 pediatric patients with an average age of 5.5±4.2 years who underwent mitral repair and replacement due to severe MI, it was found that their fractional shortening stabilized, although not significantly improved. Additionally, their LV end-diastolic and end-systolic Z-score significantly decreased in the positive direction. Furthermore, a significant reduction was observed in the need for hospital admission to the heart failure clinic within 1 year in these patients, with no early postoperative mortality reported. Moreover, in 2 patients who underwent transplantation during follow-up after mitral repair, the need for transplantation increased over 2 years. The authors concluded that surgical interventions using MV in patients with DCM and MI are reliable and can be performed to postpone transplantation (9). Sugiyama et al. (11) conducted non-transplant surgical interventions in 6 out of 11 pediatric patients with DCM. Among these, partial left ventriculotomy and Alfieri mitral repair were performed in 5 patients. In 2 of those who underwent repair, severe MI developed during follow-up, leading to MVR. After more than 5 years of clinical follow-up, 3 of these patients (50%) were able to continue education and were followed up without complaint. The authors suggest that partial left ventriculotomy and MVR may play an important role in palliative treatment as a bridge to transplantation. They even propose that in patients in end-stage heart failure clinics

not suitable for transplantation, these interventions could be considered permanent treatment when combined with aggressive medical management (11). Hsu et al. (12) conducted 6 operations on 5 pediatric patients with DCM. Two of these patients underwent elective partial left ventriculotomy and MV repair, respectively, and both successfully underwent orthotopic heart transplantation 7 and 5 months after the operation, respectively. The other three patients underwent surgery under emergency conditions, and all of them died either immediately after the operation or due to heart failure that developed during early follow-up. The authors suggest that non-transplantation cardiac surgery may provide palliation as a biological bridge to heart transplantation in pediatric patients and may serve as an alternative to mechanical support treatments (12).

In their case report, Kobayashi et al. (13) performed MV annuloplasty at the age of 18 months and size 21 MVR at the age of 3 in pediatric patients who developed DCM and severe MI secondary to enteroviral myocarditis in the neonatal period. The patient, on whom they performed debridement due to pannus formation in the mechanical valve in the 4th year after replacement was followed up with an LVEF of 47% and a mean transmitral gradient of 5 mmHg at the age of 7. The authors state that appropriate and timely mitral intervention can delay the need for transplantation (13). Walsh et al. (2) employed different MV repair techniques in 5 pediatric patients with DCM and MI who were aged between 3 months and 4 years and weighed 4.3 to 12.0 kg. Following the repairs, it was observed that the MI in 4 of the patients significantly regressed, their symptoms significantly decreased, and their functional capacity increased. Although no significant increase in LVEF was noted in these patients, the left atrial diameters and LVEDd were significantly decreased. The authors suggest that symptomatic improvement can be achieved in patients who undergo MV repair. However, a clear comment cannot be made regarding whether transplantation will be required in the future after this repair (2).

In this case series, Wooler annuloplasty and posterior leaflet augmentation were used in combination for three patients with DCM and MI. Through these techniques, we achieved symmetrical annular narrowing and expanded the posterior leaflet surface area was expanded, facilitating the coaptation of both leaflets close to normal. In one patient, we incorporated posterior annular shortening plasty reinforced with an autologous pericardial strip because the MI persisted above grade 2 during intraoperative TEE evaluation. As a result, we observed improvements in the clinical conditions of patients during the early postoperative and early postdischarge periods. Additionally, ECHO analysis revealed a regression in LVEDd, left atrial diameter, and MI levels. Diuretic and cardioprotective agents were continually administered to all patients. During follow-up, the patients gained weight, and their Ross scores decreased. Despite the positive findings observed in our patients after mitral repair, the long-term outcomes remained uncertain. Experience from other series indicates that diverse clinical courses may be encountered in these patient groups. While some children may experience a rapid regression of heart failure symptoms and an increase in daily activities, others may continue to require inotrope even if MI is successfully eliminated. MI may reoccur during follow-up in some patients, leading to the necessity of MVR, and eventually, these patients may become candidates for transplantation (9).

Because there are no large case series and controlled studies on this subject, we consider the potential for the recurrence of MI based on previous case series. However, we also believe that patients have the potential to recover at the myocardial level. Some studies have suggested that in certain patients with DCM and MI, reverse remodeling may occur in the LV, and ventricular function may improve after mitral repair. On the other hand, it has been indicated that this reverse remodeling does not occur, and ventricular dilatation progresses in patients in whom MI surgery is unsuccessful. Based on these data, we believe that mitral repair is a method that can be considered for bridging or as treatment before transplantation in patients with DCM and MI.

CONCLUSION

The presence of MI is a poor prognostic finding in pediatric patients with DCM. Successful surgical interventions for MI in this patient group may improve clinical status, reduce the frequency of hospitalization, and postpone the need for transplantation.

Ethics

Ethics Committee Approval: The study protocol was approved by the Ankara Bilkent City Hospital (approval number: E2-23-5860, date: 06.12.2023).

Informed Consent: Retrospective study.

Authorship Contributions

Concept: M.Y., A.A., Design: M.Y., Supervision: İ.E., H.A.G., Resources: M.Y., B.S.T., Material: B.S.T., Data Collection or Processing: İ.E., H.A.G., Analysis or Interpretation: M.Y., A.A., Literature Search: B.S.T., A.N.E., Writing: M.Y., A.A., Critical Review: A.N.E., A.A.

Conflict of Interest: No conflict of interest was declared by the authors.

Financial Disclosure: The authors declared that this study received no financial support.

REFERENCES

1. Puggia I, Merlo M, Barbati G, Rowland TJ, Stolfo D, Gigli M, et al. Natural History of Dilated Cardiomyopathy in Children. J Am Heart Assoc. 2016; 5: e003450.
2. Walsh MA, Benson LN, Dipchand AI, Caldarone CA, Van Arsdell GS, Kantor PF, et al. Surgical repair of the mitral valve in children with dilated cardiomyopathy and mitral regurgitation. Ann Thorac Surg. 2008; 85: 2085-8.
3. Boucek MM, Aurora P, Edwards LB, Christie J, Dobbles F, Edwards LB, et al. Registry of the International Society for Heart and Lung Transplantation: tenth official pediatric lung and heart/lung transplantation report--2007. J Heart Lung Transplant. 2007; 26: 1223-8.
4. Rossano JW, Cherikh WS, Chambers DC, Goldfarb S, Jr HD, Khush KK, et al. The International Thoracic Organ Transplant Registry of the International Society for Heart and Lung Transplantation: Twenty-first pediatric heart transplantation report-2018; Focus theme: Multiorgan Transplantation. J Heart Lung Transplant. 2018; 37: 1184-95.
5. Hetzer R, Walter EBMD, Hübler M, Alexi-Meskishvili V, Weng Y, Nagdyman N, et al. Modified surgical techniques and long-term outcome of mitral valve reconstruction in 111 children. Ann Thorac Surg. 2008; 86: 604-13.

6. Patange A, Thomas R, Ross RD. Severity of mitral regurgitation predicts risk of death or cardiac transplantation in children with idiopathic dilated cardiomyopathy. Pediatr Cardiol. 2014; 35: 232-8.
7. Romano MA, Bolling SF. Update on mitral repair in dilated cardiomyopathy. J Card Surg. 2004; 19: 396-400.
8. Fernandes FP, Manlhiot C, McCrindle BW, Mertens L, Kantor PF, Friedberg MK. Usefulness of mitral regurgitation as a marker of increased risk for death or cardiac transplantation in idiopathic dilated cardiomyopathy in children. Am J Cardiol. 2011; 107: 1517-21.
9. Breinholt JP, Fraser CD, Dreyer WJ, Chang AC, O'Brian Smith E, Heinle JS, et al. The efficacy of mitral valve surgery in children with dilated cardiomyopathy and severe mitral regurgitation. Pediatr Cardiol. 2008; 29: 13-8.
10. IJsselhof RJ, Slieker MG, Hazekamp MG, Accord R, van Wetten H, Haas F, et al. Mitral Valve Replacement with the 15 mm Mechanical Valve: A 20-Year Multicenter Experience. Ann Thorac Surg. 2020; 110: 956-61.
11. Sugiyama H, Hoshiai M, Naitoh A, Kadono T, Suzuki S, Sugita K. Outcome of non-transplant surgical strategy for end-stage dilated cardiomyopathy in young children. Circ J. 2009; 73: 1045-8.
12. Hsu RB, Chen RJ, Wu MH, Wang JK, Wang SS, Chu SH. Non-transplant cardiac surgery for end-stage dilated cardiomyopathy in small children. J Heart Lung Transplant. 2003; 22: 94-7.
13. Kobayashi D, Pettersen MD, Walters HL 3rd, Aggarwal S. Mitral valve surgery for severe mitral regurgitation and dilated cardiomyopathy--a bridge to transplant: case report and a review of literature. Congenit Heart Dis. 2012; 7: E39-65.

GMJ 2024;35:376-381

DOI: http://dx.doi.org/10.12996/gmj.2024.4054

Interleukin-34 as a Robust Predictor of No-Reflow Phenomenon in ST-Elevation Myocardial Infarction: Insights into Inflammatory Mechanisms and Clinical Implications

ST-Yükselmeli Miyokard İnfarktüsünde No-Reflow Fenomeninin Güçlü Bir Belirteci Olarak İnterlökin-34: Enflamatuvar Mekanizmalar ve Klinik Sonuçlar Üzerine Bir Bakış

Mehdi Karasu[1], Hasan Ata Bolayır[2], İbrahim Aktaş[2]

[1]Department of Cardiology, Elazığ Fethi Sekin City Hospital, Türkiye
[2]Department of Cardiology, Malatya Turgut Özal University Faculty of Medicine, Malatya, Türkiye

ABSTRACT

Objective: ST-elevation myocardial infarction (STEMI) poses a significant challenge despite advances in reperfusion strategies. The "no-reflow" phenomenon, characterized by inadequate microvascular blood flow restoration following successful revascularization, remains poorly understood. Inflammation, particularly interleukin-34 (IL-34), is implicated in cardiovascular disease, prompting investigation into its role in no-reflow.

Methods: This observational study included 182 patients with STEMI (32 with no-reflow, 150 without) and 100 controls. Clinical and angiographic data were analyzed, and IL-34 levels were measured. Logistic regression and receiver operating characteristic (ROC) analysis assessed IL-34's predictive value for no-reflow.

Results: Patients with no reflow exhibited elevated IL-34 levels compared with controls and those without no-reflow. Logistic regression identified IL-34 as an independent predictor of no-reflow (odds ratio: 1,020, p<0.001). ROC analysis showed IL-34's significant predictive value (area under the curve: 0.972, p<0.001).

Conclusion: IL-34 emerges as a robust predictor of no-reflow in STEMI, potentially reflecting its role in macrophage activation and the inflammatory response. These findings suggest a novel avenue for understanding and mitigating no-reflow in STEMI, paving the way for targeted therapies. Early identification of high-risk patients could inform tailored interventions, ultimately improving STEMI outcomes. Further research is warranted to elucidate IL-34's mechanistic involvement and validate its predictive value in larger cohorts.

Keywords: Interleukin-34, ST-elevation myocardial infarction, no-reflow phenomenon

ÖZ

Amaç: ST-yükselmeli miyokard enfarktüsü (STEMI), reperfüzyon stratejilerindeki ilerlemelere rağmen önemli bir zorluk teşkil etmektedir. Başarılı revaskülarizasyon sonrasında yetersiz mikrovasküler kan akımının geri kazanılması ile karakterize edilen "no-reflow" fenomeni, henüz tam olarak anlaşılamamıştır. Enflamasyon, özellikle interlökin-34 (IL-34), kardiyovasküler hastalıklarda rol oynamaktadır ve bu, no-reflow'daki rolünün araştırılmasını teşvik etmektedir.

Yöntemler: Bu gözlemsel çalışmaya STEMI olan 182 hasta (32 no-reflow, 150 no-reflow olmayan) ve 100 kontrol grubu dahil edilmiştir. Klinik ve anjiyografik veriler analiz edilmiş ve IL-34 seviyeleri ölçülmüştür. Lojistik regresyon ve alıcı işletim karakteristiği (ROC) analizi, no-reflow için IL-34'ün prediktif değerini değerlendirmiştir.

Bulgular: No-reflow olan hastalar, kontrol grubuna ve no-reflow olmayanlara kıyasla yükselmiş IL-34 seviyeleri göstermiştir. Lojistik regresyon analizi, IL-34'ü no-reflow'nun bağımsız bir öngörücüsü olarak tanımlamıştır (olasılık oranı: 1.020, p<0,001). ROC analizi, IL-34'ün anlamlı prediktif değerini ortaya koymuştur (eğri altındaki alan: 0,972, p<0,001).

Sonuç: IL-34, STEMI'de no-reflow'nun güçlü bir öngörücüsü olarak ortaya çıkmakta olup, makrofaj aktivasyonu ve enflamatuvar yanıt üzerindeki rolünü yansıtıyor olabilir. Bu bulgular, STEMI'de no-reflow'yu anlama ve azaltmada yeni bir yol önererek, hedefe yönelik tedavilere kapı aralamaktadır. Yüksek riskli hastaların erken tanımlanması, özelleştirilmiş müdahaleleri bilgilendirebilir ve sonuçta STEMI sonuçlarını iyileştirebilir. Daha geniş kohortlarda IL-34'ün mekanik katılımını açıklamak ve prediktif değerini doğrulamak için daha fazla araştırma gerekmektedir.

Anahtar Sözcükler: İnterlökin-34, ST-yükselmeli miyokard enfarktüsü, no-reflow fenomeni

Address for Correspondence/Yazışma Adresi: Mehdi Karasu, MD, Department of Cardiology, Elazığ Fethi Sekin City Hospital, Elazığ, Türkiye
E-mail / E-posta: mehdikarasu@yahoo.com
ORCID ID: orcid.org/0000-0003-1713-3451

Received/Geliş Tarihi: 18.11.2023
Accepted/Kabul Tarihi: 20.01.2024

INTRODUCTION

ST-elevation myocardial infarction (STEMI) represents a significant cardiovascular emergency marked by the abrupt blockage of a coronary artery, resulting in substantial and frequently irreversible harm to the heart muscle. The timely recognition and management of STEMI are crucial to mitigate its potentially severe consequences (1). The swift reinstating of blood flow to the oxygen-starved heart muscle using reperfusion methods like primary percutaneous coronary intervention (PCI), has fundamentally transformed the approach to managing STEMI. This intervention has significantly improved patient outcomes and minimized the extent of heart muscle damage in many cases (2). However, despite these advances, a vexing challenge persists - the "no-reflow" phenomenon (NRP).

"No-reflow" represents an intriguing and clinically significant complication in the treatment of STEMI (3). It occurs when, despite successful revascularization of the occluded coronary vessel, there is insufficient restoration of microvascular blood flow within the myocardium (4). This phenomenon is associated with exacerbated myocardial injury, increased infarct size, and a heightened risk of adverse cardiovascular events, making it a subject of keen interest among clinicians and researchers alike (5).

To date, the precise mechanisms underlying no-reflow in the context of STEMI remain incompletely understood. Ongoing research is shedding light on the potential impact of inflammatory processes in the pathophysiology associated with this condition (6). In particular, interleukin-34 (IL-34), a proinflammatory cytokine, has garnered attention for its potential role in cardiovascular disease (7). IL-34 operates by engaging with the colony-stimulating factor-1 receptor present on a spectrum of immune and non-immune cells. Through this interaction, it exerts influence over immune responses and modulates inflammatory processes within the body. This interplay underscores its significance in regulating the immune system and related inflammatory pathways (8). Recent investigations have suggested a potential link between IL-34 and an increased risk of the composite endpoint and cardiovascular death in the context of myocardial infarction (9,10). This finding prompts further exploration of IL-34's role in the context of no-reflow.

This research article seeks to delve into the intricate interplay between the NRP and IL-34 in the context of STEMI, unraveling the underlying mechanisms that govern microvascular dysfunction during acute myocardial infarction (AMI). By scrutinizing IL-34's impact on the coronary microcirculation and its role in associated inflammatory responses, we aim to provide valuable insights that may inform future therapeutic strategies and, ultimately, enhance the prognosis of patients experiencing STEMI.

MATERIALS AND METHODS

Study Design

In this cross-sectional observational study, data were gathered from 182 individuals with STEMI, comprising 32 patients experiencing no-reflow (NRP) and 150 without NRP, constituting the study group. Furthermore, a control group comprising 100 individuals was also incorporated into the study for comparative analysis.

Diagnostic criteria: STEMI diagnosis relied on the presence of typical myocardial ischemia symptoms and specific ST-segment elevation criteria: more than 1 mm in the inferior lead or over 2 mm in the anterior chest lead, observed in a minimum of two adjacent leads. Confirmation included the emergence of a new left bundle branch block, which was subsequently validated by elevated cardiac troponin levels. The exclusion criteria included individuals with a previous history of coronary artery bypass surgery, those experiencing cardiogenic shock, prolonged delays exceeding 12 hours from symptom onset to balloon inflation, individuals treated with fibrinolytic agents, active infectious or inflammatory conditions, and a spectrum of chronic inflammatory or autoimmune disorders.

The study received ethical clearance from the Ethics Committee of Fırat University Faculty of Medicine, ensuring compliance with the principles outlined in the Declaration of Helsinki and maintaining adherence to good clinical practices throughout the research process (approval number: 2022/07-38, date: 26.05.2022). Informed written consent was obtained all of the participants prior to study. Upon the diagnosis of STEMI, all patients received specific medications, including 300 mg of aspirin, accompanied by a loading dose of either 600 mg clopidogrel, 180 mg of ticagrelor, or 60 mg prasugrel as part of their immediate treatment regimen. Initial coronary angiography was performed using standard techniques, followed by an intravenous bolus of unfractionated heparin upon the decision for coronary intervention. Primary PCI procedures utilized 6 F or 7 F guiding catheters, and cineangiography analysis was conducted using an Artis Zee Floor workstation (Siemens Medical Solution, Erlangen, Germany).

Assessment of no-reflow phenomenon: The presence of NRP was determined by visually grading thrombolysis in my ocardial infarction (TIMI) flow grades in peri-procedure angiograms. TIMI flow grades were evaluated by two independent interventional cardiologists blinded to patient data. Grades ranged from 0 (indicating no flow after the culprit lesion) to 3 (representing normal coronary flow). Patients were divided into two distinct groups based on their final angiographic TIMI flow rates: the normal-reflow group and the no-reflow group. This categorization allowed for a comparative analysis between these two subsets based on their observed flow rates.

Laboratory assessments: Blood samples were collected from the antecubital veins before coronary intervention for various laboratory examinations, including troponin I levels, lipid profiles, platelet and white blood cell (WBC) counts, creatinine, plasma glucose, and other biochemical tests. The estimated glomerular filtration rate was determined by applying the modification of diet in renal disease equation for calculation purposes. Medication administration during the perioperative period aligned with clinical guidelines, including the discretionary use of glycoprotein IIb/IIIa inhibitors, intracoronary nitroglycerin, and adenosine, as deemed necessary by the operator.

Statistical Analysis

Statistical analyses were performed using SPSS software (SPSS Inc., Chicago, IL, USA). The Kolmogorov-Smirnov test was used to determine whether continuous variables were normally distributed. Normally distributed variables were given as mean ± standard deviation, and non-normally distributed variables were given as median (minimum-maximum) values. Descriptive statistics are given as percentages and absolute values. The ANOVA test was used to compare the baseline clinical characteristics of 3 groups. A post-hoc

analysis was performed for multiple comparison of groups. When homogenity of variance could not be provided in Levene's test, the Games-Howell test was applied.

Correlation analysis was applied to determine the relationship between IL-34 and NRP. Data were analyzed using logistic regression models to determine whether IL-34 was independently associated with NRP. We performed receiver operating characteristic (ROC) analysis to determine the most sensitive IL-34 cut-off level for predicting the occurrence of NRP following primary PCI in STEMI. Potential confounding factors underwent univariable regression analysis, and confounders with a p<0.25 were further tested in multivariable logistic regression. The threshold for statistical significance was established at a p-value of less than 0.05. We used G-power to detect the study power. The enrollment of 182 patients with STEMI (32 with NRP and 150 without NRP) in the study group, alongside 100 individuals in the control group was aimed at achieving a 99.5% statistical power to detect significant differences in IL-34 levels among patients with NRP, those without NRP, and control subjects.

RESULTS

Table 1 provides a detailed summary of baseline characteristics and laboratory measurements comparing control subjects with patients diagnosed with STEMI, delineating between those with and without the occurrence of the NRP. Cardiovascular risk factors and inflammatory markers appear elevated in STEMI patients, especially those with no reflow. Age did not significantly differ between control subjects (59 years), STEMI patients who underwent successful primary PCI (61 years), and those with no-reflow after STEMI (58 years). There was no statistically significant difference observed in the ratio of females to males between the groups. Body mass index showed a slight increase in both STEMI groups compared to control subjects. Glucose levels exhibited a slightly elevated trend in both STEMI groups when contrasted with the control group; however, this disparity was not significant. Median levels of blood urea nitrogen, creatinine, uric acid, hemoglobin, platelet count, and high-density lypoprotein showed no significant differences across the groups.

When compared with the control group, patients with STEMI, especially those with no reflow, had significantly higher total cholesterol levels. STEMI groups exhibited notably higher levels of triglycerides and low dencity lypoprotein (LDL), showcasing a statistically significant difference between these cohorts. High-sensitivity C-reactive protein (hs-CRP) levels displayed considerable elevation in both STEMI groups when compared with the control group, indicating a notable difference between these sets of patients.

Table 1. Baseline characteristics and laboratory measurements of the study population

Parameters	Control subjects (n=100), mean ± SD or median (min.-max.)	STEMI with successful primary PCI (n=150), mean ± SD or median (min.-max.)	STEMI with NR (n=32), mean ± SD or median (min.-max.)	p
Age, years	59±6.4	61±3.7	58±5.7	NS
Sex, female/male	44/56	69/81	13/19	NS
Body mass index, kg/m^2	28.0±4.4	29.6±4.9	30.1±4.7	NS
Glucose, mg/dL	86.5±5.2	88.3±6.1	92.2±2.7	NS
BUN, mg/dL	14.5 (10-21)	18 (11-27)	13 (9-26)	NS
Creatinine, mg/dL	0.7 (0.5-1.1)	0.7 (0.5-1.2)	0.8 (0.5-1.4)	NS
Uric acid mg/dL	7.6±1.0	7.1±1.8	7.7±1.6	NS
Total cholesterol mg/dL	**219 (111-319)**	**280 (186-366)**	**290 (191-389)**	**<0.05**
Triglyceride, mg/dL	**163.7±99.6**	**182.4±60.4**	**188.4±62.9**	**<0.05**
HDL, mg/dL	45.3±9.9	46.5±11.1	44.5±12.3	NS
LDL, mg/dL	**133.2±43.5**	**172.8±27.3**	**181.1±21.9**	**<0.05**
hs-CRP, mg/dL	**0.3 (0-0.8)**	**4.8 (4.1-6.1)**	**5.9 (4.4-7.7)**	**<0.05**
Hemoglobin, g/dL	13.4±1.0	13.1±1.0	13.7±2.0	NS
Platelet, x10^3/µL	247.4±53.0	253.9±52.7	251.9±47.5	NS
WBC, x10^3/µL	**5.8±1.1**	**8.8±1.6**	**11.4±2.8**	**<0.05**
IL 34, pg/mL	**11±0.9**	**34±5.9**	**51±7.7**	**<0.05**
DM (n)	18	27	8	NS
HT (n)	22	32	8	NS
Smoking (n)	32	48	11	NS
Gensini score, mean	-	34±7.6	37±4.4	NS
Stent length, mm, mean	-	29±3.8	30±5.2	NS
Bifurcation stenting	-	-	-	

BUN: Blood urea nitrogen, HDL: High-density lipoprotein, LDL: Low dencity lipoprotein, WBC: White blood cell, NR: No-reflow, IL: Interleukin, NS: Not significant, STEMI: ST elevated myocardial infarction, PCI: Percutaneous coronary intervention, hs-CRP: High-sensitivity-C-reactive protein.

WBC counts exhibited a notable rise in the no-reflow group compared to both the control group and the successful primary PCI group, showcasing a significant difference among these cohorts. This difference highlights a notable disparity in WBC counts among these patient subsets. IL-34 levels were significantly elevated in both STEMI groups, with the highest levels in the NRP group. There were no significant differences observed in the prevalence of diabetes mellitus, hypertension, and smoking across the groups. The Gensini score, reflecting the severity of coronary artery disease, was not significantly different between the successful primary PCI group and the no-reflow group, though this data was not available for the control group. Stent length did not display any significant differences among the groups.

Those with NRP had significantly increased average serum IL-34 values than controls and STEMI with successful primary PCI (Figure 1).

Table 2 showcases the outcomes derived from logistic regression analyses aimed at pinpointing independent predictors associated with the occurrence of the NRP within the scope of STEMI. While age [odds ratio (OR): 1.018, 95% confidence interval (CI): 0.977-1.062, p=0.388), LDL (OR: 0.940, 95% CI: 0.666-1.328, p=0.727), platelet count (OR: 1.001, 95% CI: 0.995-1.007, p=0.672), and WBC count (OR: 1.007, 95% CI: 0.997-1.018, p=0.173) did not emerge as significant predictors, hs-CRP (OR: 1.039, 95% CI: 1.018-1.060, p=0.004), and IL-34 (OR: 1.020, 95% CI: 1.010-1.030, p<0.001) demonstrated varying degrees of significance. IL-34, in particular, showed a strong association with the NRP in both univariable and multivariable analyses.

A ROC curve was employed to assess the sensitivity and specificity of IL-34 as a diagnostic marker for detecting the NRP within the study population. Results (Figure 2) indicate that plasma IL-34 levels had a significant predictive value for the identification of individuals with NRP (area under the curve: 0.972, 95% CI: 0.950-0.980, p<0.001).

DISCUSSION

In this study, we demonstrated that IL-34, a cytokine involved in macrophage differentiation and activation, emerges as a robust predictor of no-reflow in STEMI patients. The results clearly indicate significantly elevated IL-34 levels in patients who subsequently develop no-reflow following primary PCI. These findings align with a growing body of evidence that underscores the crucial involvement of inflammation in NRP development.

The phenomenon of no-reflow, which is characterized by impaired microvascular perfusion despite successful epicardial vessel reperfusion, is a complex, multifactorial process involving

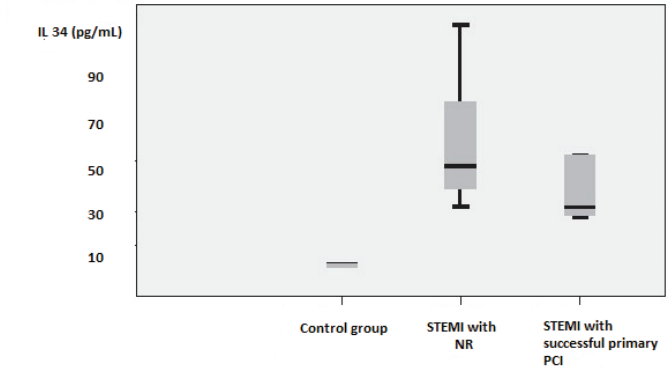

Figure 1. Comparison of IL-34 levels between the groups.

IL-34: Interleukin 34, STEMI: ST-elevation myocardial infarction, PCI: Percutaneous coronary intervention.

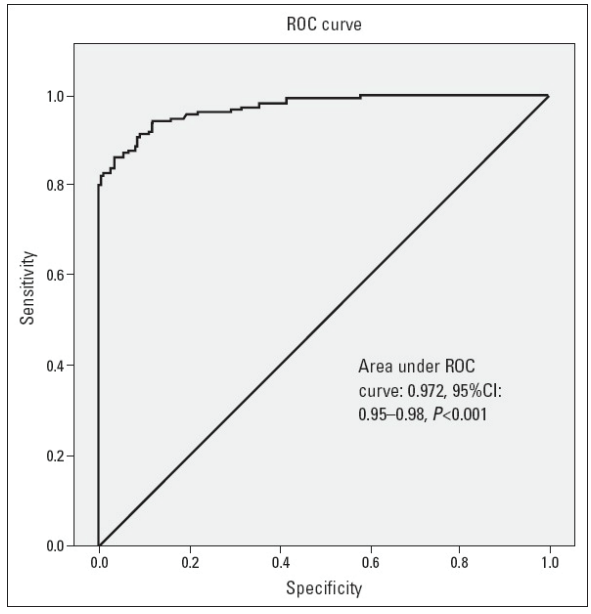

Figure 2. ROC of IL 34 and NRP.

ROC: receiver operating characteristic, NRP: No-reflow phenomenon, CI: Confidence interval.

Table 2. Univariable and multivariable logistic regression analysis representing the independent predictors of NR phenomenon

	Univariable		Multivariable	
Variables	**OR (95% CI)**	**p**	**OR (95% CI)**	**p**
Age	1.027 (0.991-1.064)	0.140	1.018 (0.977-1.062)	0.388
LDL	0.831 (0.631-1.094)	0.187	0.940 (0.666-1.328)	0.727
Platelet	1.004 (0.999-1.008)	0.141	1.001 (0.995-1.007)	0.672
WBC	**1.013 (1.004-1.022)**	**0.006**	1.007 (0.997-1.018)	0.173
hs-CRP	**1.183 (1.143-1.223)**	**0.003**	**1.039 (1.018-1.060)**	**0.004**
IL-34	**1.028 (1.018-1.038)**	**<0.001**	**1.020 (1.010-1.030)**	**<0.001**

CI: Confidence interval, OR: Odds ratio, WBC: White blood cell, hs-CRP: High-sensitivity-C-reactive protein, IL-34: Interleukin 34, LDL: Low-density lipoprotein.

inflammation, endothelial dysfunction, and thrombosis (11,12). Thus, identifying reliable predictors is crucial for improving risk stratification and potentially developing targeted therapeutic interventions.

Previous studies have reported CRP and IL-6 on admission as predictors of the NRP (13). Hs-CRP has the potential to foster the development of the NRP by augmenting the expression of COX-1 and COX-2, a process that is partly regulated through ERK and JNK activity (14). AMI followed by reperfusion led to notable elevations in serum IL-6 levels and an increase in interferon gamma expression within the myocardial tissue (15). Inflammatory markers like platelet-to-lymphocyte ratio (PLR), neutrophil-to-lymphocyte ratio (NLR), mean platelet volume, and platelet distribution width PDW have been associated with the occurrence of NRP (16-19). A recent study by Esenboğa et al. (20) demonstrated that SII is superior to NLR and PLR in NRP prediction. They also showed that SII was better than CRP for NRP prediction (20). Moreover, the present study underscores the importance of looking beyond traditional inflammatory markers in the context of no-reflow.

One possible explanation for the enhanced predictive value of IL-34 could be its direct involvement in the regulation of macrophages, which are key players in the inflammatory response following myocardial infarction. Macrophages, through their diverse phenotypes, can either exacerbate or resolve inflammation, and their imbalance may contribute to microvascular dysfunction. IL-34 plays a role in the differentiation and migration of macrophages and monocytes (21). Being a proinflammatory cytokine, IL-34 stimulates chemokines and cytokines like monocyte chemoattractant protein, IL-6, and IL-8 (22). IL-34 significantly promotes IL-6 and IL-8 expression (23). Furthermore, IL-34 levels are significantly negatively associated with PLT (24). In a study conducted in patients with rheumatoid arthritis, an increased amount of IL-34 in synovial tissue decreased neutrophil recruitment and intra-synovial neutrophil extracellular traps (25). Li et al. (26) showed that in T-lymphocytes cocultured with antigen-presenting cells, IL-34 treatment downregulates the number of effector cells. Elevated concentrations of IL-34 in patients are correlated with ESR, CRP, ds-DNA antibodies, hemoglobin, and complement levels (27).

The specificity of IL-34 to macrophage activation could make it a more relevant marker for the underlying processes that lead to no-reflow. Although, as far as we have seen, there is no study showing the relationship between NRP and IL-34, numerous studies have investigated the correlation between IL-34 and various cardiovascular diseases, aiming to elucidate its potential role and impact within this medical domain.

Xi et al. (28) demonstrated significantly increased serum IL-34 in ischemic cardiomyopathy, correlating with the presence and severity of ischemic heart failure. Preisser et al. (29) linked IL-34 to profibrotic macrophages and released transforming growth factor β, platelet-derived growth factor, and galectin-3-factors impacting heart failure development. Fan et al. (30) associated IL-34 with the presence and severity of CAD. Li et al. (31) noted elevated IL-34 in CAD patients, correlating positively with hs-CRP levels. Zorena et al. (32) underscored IL-34's enhanced discrimination over CRP for vascular diabetes complications. It is worth noting that this study has limitations, including its cross-sectional design and the need for further validation in larger, prospective cohorts. Additionally, the exact mechanisms by which IL-34 influences no-reflow require further investigation.

CONCLUSION

In conclusion, assessing the NRP in STEMI is of paramount importance in guiding clinical management and predicting patient outcomes. While several inflammatory markers have been explored as potential predictors of no-reflow, the results of this study suggest that the potential role of IL-34 in the regulation of macrophages and the inflammatory response post-myocardial infarction makes it a promising candidate for further research in this context. Identifying patients at a higher risk of no-reflow early could pave the way for more targeted therapies and improved outcomes in STEMI management.

Ethics

Ethics Committee Approval: The study received ethical clearance from the Ethics Committee of Fırat University Faculty of Medicine, ensuring compliance with the principles outlined in the Declaration of Helsinki and maintaining adherence to good clinical practices throughout the research process (approval number: 2022/07-38, date: 26.05.2022).

Informed Consent: Informed written consent was obtained all of the participants prior to study.

Authorship Contributions

Concept: H.A.B., Design: H.A.B., Süpervision: H.A.B., Resources: İ.A., Materials: İ.A., Data Collection or Processing: İ.A., Analysis or Interpretation: H.A.B., Literature Search: M.K., Writing: M.K., Critical Review: M.K.

Conflict of Interest: No conflict of interest was declared by the authors.

Financial Disclosure: The authors declared that this study received no financial support.

REFERENCES

1. Ibanez B, James S, Agewall S, Antunes MJ, Bucciarelli-Ducci C, Bueno H, et al. 2017 ESC Guidelines for the management of acute myocardial infarction in patients presenting with ST-segment elevation: The Task Force for the management of acute myocardial infarction in patients presenting with ST-segment elevation of the European Society of Cardiology (ESC). Eur Heart J. 2018; 39: 119-77.
2. O'Gara PT, Kushner FG, Ascheim DD, Casey DE Jr, Chung MK, de Lemos JA, et al. 2013 ACCF/AHA guideline for the management of ST-elevation myocardial infarction: a report of the American College of Cardiology Foundation/American Heart Association Task Force on Practice Guidelines. Circulation. 2013; 127: e362-425.
3. Berg R, Buhari C. Treating and preventing no reflow in the cardiac catheterization laboratory. Curr Cardiol Rev. 2012; 8: 209-14.
4. Niccoli G, Burzotta F, Galiuto L, Crea F. Myocardial no-reflow in humans. J Am Coll Cardiol. 2009; 54: 281-92.
5. Brosh D, Assali AR, Mager A, Porter A, Hasdai D, Teplitsky I, et al. Effect of no-reflow during primary percutaneous coronary intervention for acute myocardial infarction on six-month mortality. Am J Cardiol. 2007; 99: 442-5.

6. Kalogeris T, Baines CP, Krenz M, Korthuis RJ. Ischemia/Reperfusion. Compr Physiol. 2016; 7: 113-70.
7. Kaufmann CC, Ahmed A, Muthspiel M, Rostocki I, Pogran E, Zweiker D, et al. Association of Interleukin-32 and Interleukin-34 with Cardiovascular Disease and Short-Term Mortality in COVID-19. J Clin Med. 2023; 12: 975.
8. Masteller EL, Wong BR. Targeting IL-34 in chronic inflammation. Drug Discov Today. 2014; 19: 1212-6.
9. Fan Q, Tao R, Zhang H, Xie H, Xi R, Wang F, et al. Interleukin-34 Levels Were Associated with Prognosis in Patients with Acute Myocardial Infarction. Int Heart J. 2019; 60: 1259-67.
10. Zhuang L, Zong X, Yang Q, Fan Q, Tao R. Interleukin-34-NF-κB signaling aggravates myocardial ischemic/reperfusion injury by facilitating macrophage recruitment and polarization. EBioMedicine. 2023; 95: 104744.
11. Iwakura K, Ito H, Takiuchi S, Taniyama Y, Nakatsuchi Y, Negoro S, et al. Alternation in the coronary blood flow velocity pattern in patients with no reflow and reperfused acute myocardial infarction. Circulation. 1996; 94: 1269-75.
12. Ito H. No-reflow phenomenon and prognosis in patients with acute myocardial infarction. Nat Clin Pract Cardiovasc Med. 2006; 3: 499-506.
13. A X, Li Z, Luo W, Chai J. Long-term compound danshen dripping pills therapy reduces the no-reflow phenomenon in nondiabetes mellitus patients after primary percutaneous coronary intervention for acute myocardial infarction. Ann Palliat Med. 2020; 9: 1144-51.
14. Jiao Q, Ke Q, Li W, Jin M, Luo Y, Zhang L, et al. Effect of inflammatory factor-induced cyclo-oxygenase expression on the development of reperfusion-related no-reflow phenomenon in acute myocardial infarction. Clin Exp Pharmacol Physiol. 2015; 42: 162-70.
15. Zhao XJ, Liu XL, He GX, Xu HP. Effects of single-dose atorvastatin on interleukin-6, interferon gamma, and myocardial no-reflow in a rabbit model of acute myocardial infarction and reperfusion. Braz J Med Biol Res. 2014; 47: 245-51.
16. Kurtul A, Yarlioglues M, Murat SN, Ergun G, Duran M, Kasapkara HA, et al. Usefulness of the platelet-to-lymphocyte ratio in predicting angiographic reflow after primary percutaneous coronary intervention in patients with acute ST-segment elevation myocardial infarction. Am J Cardiol. 2014; 114: 342-47.
17. Yildiz A, Yuksel M, Oylumlu M, Polat N, Akyuz A, Acet H, et al. The Utility of the Platelet-Lymphocyte Ratio for Predicting No Reflow in Patients With ST-Segment Elevation Myocardial Infarction. Clin Appl Thromb Hemost. 2015; 21: 223-8.
18. Vakili H, Shirazi M, Charkhkar M, Khaheshi I, Memaryan M, Naderian M. Correlation of platelet-to-lymphocyte ratio and neutrophil-to-lymphocyte ratio with thrombolysis in myocardial infarction frame count in ST-segment elevation myocardial infarction. Eur J Clin Invest. 2017; 47: 322-7.
19. Zhang Q, Hu M, Sun J, Ma S. The combination of neutrophil-to-lymphocyte ratio and platelet correlation parameters in predicting the no-reflow phenomenon after primary percutaneous coronary intervention in patients with ST-segment elevation myocardial infarction. Scand Cardiovasc J. 2020; 54: 352-7.
20. Esenboğa K, Kurtul A, Yamantürk YY, Tan TS, Tutar DE. Systemic immune-inflammation index predicts no-reflow phenomenon after primary percutaneous coronary intervention. Acta Cardiol. 2022; 77: 59-65.
21. Robbins CS, Chudnovskiy A, Rauch PJ, Figueiredo JL, Iwamoto Y, Gorbatov R, et al. Extramedullary hematopoiesis generates Ly-6C(high) monocytes that infiltrate atherosclerotic lesions. Circulation. 2012; 125: 364-74.
22. Masteller EL, Wong BR. Targeting IL-34 in chronic inflammation. Drug Discov Today. 2014; 19: 1212-6.
23. Zhou J, Sun X, Zhang J, Yang Y, Chen D, Cao J. IL-34 regulates IL-6 and IL-8 production in human lung fibroblasts via MAPK, PI3K-Akt, JAK and NF-κB signaling pathways. Int Immunopharmacol. 2018; 61: 119-25.
24. Xie HH, Shen H, Zhang L, Cui MY, Xia LP, Lu J. Elevated Serum Interleukin-34 Level in Patients with Systemic Lupus Erythematosus Is Associated with Disease Activity. Sci Rep. 2018; 8: 3462.
25. González-Sánchez HM, Baek JH, Weinmann-Menke J, Ajay AK, Charles JF, Noda M, et al. IL-34 and protein-tyrosine phosphatase receptor type-zeta-dependent mechanisms limit arthritis in mice. Lab Invest. 2022; 102: 846-58.
26. Li XL, Ménoret S, Bezie S, Caron L, Chabannes D, Hill M, et al. Mechanism and localization of CD8 regulatory T cells in a heart transplant model of tolerance. J Immunol. 2010; 185: 823-33.
27. El-Banna HS, El Khouly RM, Gado SE. Elevated serum interleukin-34 level in juvenile systemic lupus erythematosus and disease activity. Clin Rheumatol. 2020; 39: 1627-32.
28. Xi R, Fan Q, Yan X, Zhang H, Xie H, Gu G, et al. Increased Serum Interleukin-34 Levels Are Related to the Presence and Severity of Cardiac Dysfunction in Patients With Ischemic Cardiomyopathy. Front Physiol. 2018; 9: 904.
29. Preisser L, Miot C, Le Guillou-Guillemette H, Beaumont E, Foucher ED, Garo E, et al. IL-34 and macrophage colony-stimulating factor are overexpressed in hepatitis C virus fibrosis and induce profibrotic macrophages that promote collagen synthesis by hepatic stellate cells. Hepatology. 2014; 60: 1879-90.
30. Fan Q, Yan X, Zhang H, Lu L, Zhang Q, Wang F, et al. IL-34 is associated with the presence and severity of renal dysfunction and coronary artery disease in patients with heart failure. Sci Rep. 2016; 6: 39324.
31. Li Z, Jin D, Wu Y, Zhang K, Hu P, Cao X, et al. Increased serum interleukin-34 in patients with coronary artery disease. J Int Med Res. 2012; 40: 1866-70.
32. Zorena K, Jachimowicz-Duda O, Wąż P. The cut-off value for interleukin 34 as an additional potential inflammatory biomarker for the prediction of the risk of diabetic complications. Biomarkers. 2016; 21: 276-82.

GMJ 2024;35:382-386

DOI: http://dx.doi.org/10.12996/gmj.2024.4085

Evaluation of Ligamentum Mucosum in Anterior Cruciate Ligament Injuries

Ön Çapraz Bağ Yaralanmalarında Ligamentum Mukozumun Değerlendirilmesi

Mehmet Ali Tokgöz[1], Ethem Burak Oklaz[1], Muhammet Baybars Ataoğlu[1], Muhammed Şakir Calta[1], Anıl Köktürk[2], Ulunay Kanatlı[1]

[1]Department of Orthopaedics and Traumatology, Gazi University Faculty of Medicine, Ankara, Türkiye
[2]Clinic of Orthopaedics and Traumatology, Antalya City Hospital, Antalya, Türkiye

ABSTRACT

Objective: Over the past few years, histopathological studies have demonstrated that the ligamentum mucosum (LM) contains neural and vascular structures. These findings suggest that LM can be used for proprioception and revascularization in the repair of anterior cruciate ligament (ACL). The aim of this study was to evaluate the LM structure in knees with ACL injuries.

Methods: The data of patients who underwent knee arthroscopy at our clinic between 2017 and 2022 were retrospectively analyzed. Three groups were included in the study; acute ACL tears (n=89), chronic ACL tears (n=111) and intact ACLs (n=101). The arthroscopic video records of all patients were evaluated retrospectively. LM was defined in three different forms: (1) Intact, (2) ruptured, and (3) non-presence.

Results: The non-presence of the LM was significantly more common in chronic ACL tears compared to the other groups (p=0.021), while the presence of the LM (either intact or ruptured) was similar between acute ACL tears and intact ACLs. In acute tears, the number of intact LM was significantly lower than that of intact ACLs (p<0.001). However, it was significantly greater than that of chronic tears (p=0.001).

Conclusion: According to the present study, the likelihood of intact LM in chronic ACL tears is quite low. In this regard, we suggest that performing surgery in the acute phase of ACL injury will increase the chances of using the LM as a neurovascular source. In addition, because of the possible effect of the LM on proprioception, we recommend preserving the structure during knee arthroscopy procedures if a healthy LM is present.

Keywords: Ligamentum mucosum, anterior cruciate ligament injury, acute, chronic, knee arthroscopy

ÖZ

Amaç: Son yıllarda ligamentum mukozum (LM) üzerine yapılan histopatolojik çalışmalar, bu yapının nöral ve vasküler bileşenler içerdiğini ortaya koymuş ve LM'nin ön çapraz bağ (ÖÇB) onarımında propriyosepsiyon ve revaskülarizasyon amacıyla kullanılabileceği ifade edilmiştir. Sunulan çalışmanın amacı ÖÇB hasarı olan dizlerde LM varlığının değerlendirilmesidir.

Yöntemler: 2017-2022 yılları arasında kliniğimizce diz artroskopisi ameliyatı yapılan hastaların verileri retrospektif olarak incelenmiştir. Hastalar üç gruba ayrılarak incelenmiştir; akut ÖÇB yırtıkları (n=89), kronik ÖÇB yırtıkları (n=111) ve sağlam ÖÇB (n=101). Tüm hastaların artroskopik video kayıtları retrospektif olarak değerlendirilmiş ve LM, gruplarda üç farklı formda tanımlanmıştır: (1) Sağlam, (2) yırtık ve (3) LM yoktur.

Bulgular: LM yokluğu, kronik ÖÇB yırtıklarında diğer gruplara kıyasla anlamlı derecede daha yaygındı (p=0,021). Ayrıca, LM varlığı (sağlam ya da yırtık) akut ÖÇB yırtıkları ile sağlam ÖÇB'ler arasında benzerdi. Akut yırtıklarda, sağlam LM bulunma oranı, sağlam ÖÇB'lere göre anlamlı derecede daha azdı (p<0,001) iken kronik yırtıklara göre anlamlı derecede daha fazlaydı (p=0,001).

Sonuç: Sunulan çalışmadan elde edilen verilere göre kronik ÖÇB yırtıklarında sağlam LM görülme olasılığı oldukça düşüktür. Bu bağlamda, ÖÇB yaralanmalarında cerrahinin erken evrede yapılmasının, LM'nin nörovasküler bir kaynak olarak kullanılma şansını artıracağına inanmaktayız. Ayrıca, LM'nin propriyosepsiyon üzerindeki olası etkisi nedeniyle, diz artroskopisi sırasında sağlıklı bir LM varlığında yapının korunmasını önermekteyiz.

Anahtar Sözcükler: Ligamentum mukosum, ön çapraz bağ yaralanması, akut, kronik, diz artroskopisi

Address for Correspondence/Yazışma Adresi: Ethem Burak Oklaz, MD, Department of Orthopaedics and Traumatology, Gazi University Faculty of Medicine, Ankara, Türkiye
E-mail / E-posta: burakoklaz@gmail.com
ORCID ID: orcid.org/0000-0001-6241-8523

Received/Geliş Tarihi: 18.12.2023
Accepted/Kabul Tarihi: 25.06.2024

INTRODUCTION

The ligamentum mucosum (LM) is a structure located anterior to the anterior cruciate ligament (ACL) between the intercondylar notch of the femur and Hoffa's fat pad (1). LM, also known as the infrapatellar plica, was once thought to be a remnant of embryonic development (2,3). However, recent histological studies have indicated that the LM, similar to other ligaments in the knee, has an elastic structure and is composed of dense and regular connective tissue consisting mainly of type 1 collagen (4-8). Recent studies have revealed the presence of neurovascular tissue components within the structure of the LM. The presence of neural tissue components suggests that the LM may have a role in proprioception, similar to that of the ACL (7,9-11). The LM may also have a well-developed vascular structure, especially in the distal part of the ligament (11,12). Based on these properties, studies have suggested that LM could be used as a potential donor of vascular and neural tissue for ACL repair (12). To the best of our knowledge, clinical studies on the LM have only investigated its association with anterior knee pain and cartilage damage (11,13-15). Recent research on the relationship between LM and ACL injuries has increased, with a better understanding of the neurovascular structure of the LM. However, no clinical studies have been conducted on this subject. The aim of presented study was to evaluate the structure of the LM in knees with ACL injuries. Our hypothesis was that the presence of an intact LM in knees with chronic ACL injuries would likely be reduced by damage and subsequent degeneration.

MATERIALS AND METHODS

Retrospective evaluation was conducted on the arthroscopic video recordings of patients who underwent arthroscopic surgery at the current center between 2017 and 2022. The data of 435 patients were collected prospectively. Patients with inflammatory arthritis, tumors, patellofemoral malalignment, a history of previous knee surgery, or tears that were not in the acute or chronic phase of ACL injury (more than 6 weeks and less than 27 weeks) were excluded from the study. The groups included in the study were selected from the remaining 301 patients. Demographic data, including age and gender, were analyzed. The arthroscopy records of the patients were reviewed to determine the presence of ACL injury. The time period between the injury and surgery was assessed. If the time period was less than 6 weeks, the injury was considered acute; if the time period was more than 27 weeks, it was considered chronic (16). According to this classification, patients were divided into three groups: acute ACL tears (89 patients), chronic ACL tears (111 patients), and intact ACLs (101 patients) (85 meniscal injuries and 16 osteochondral defects).

During the arthroscopy, an experienced orthopaedic surgeon examined the intercondylar notch and Hoffa's fat pad, which are the attachment sites of the ligament, to assess the structure of the LM. If there was continuity in the ligament, it was considered to be intact (Figure 1a). If there was no continuity but fragments of the ligament were present, the ligament was considered ruptured (Figure 1b). If no ligament fragments were observed, they were considered non-presence (Figure 1c).

The arthroscopic surgery video recordings were evaluated by two knee surgeons with at least 10 years of experience. To investigate intraobserver reliability, the same observer re-evaluated all video records at intervals of more than 2 weeks from the initial evaluation. To evaluate interobserver reliability, another observer similarly evaluated all the video records randomly. The study was approved by the Gazi University Ethics Committee (approval number: 15, date: 09.01.2023), and written informed consent was obtained from all patients.

Statistical Analysis

The statistical analyses were performed using IBM SPSS Statistics for Windows, version 26.0 (IBM Corp., Armonk, N.Y., USA). Categorical variables were described as numbers and percentages, whereas continuous variables were presented as mean ± standard deviation-median (minimum-maximum value). The normality of continuous variables was assessed using visual methods (histograms and probability plots) and analytical methods (Kolmogorov-Smirnov and Shapiro-Wilk tests). One-way analysis of variance and least significant difference tests were used to compare age among 3 independent groups. The chi-square test was used to compare categorical variables between the independent groups. Interobserver and intraobserver reliability were determined using Cohen's kappa (κ).

RESULTS

A retrospective review was conducted for a total of 301 patients who were included in the study. Of these patients, 186 were male and 115 were female, with a mean age of 31.26±11.90 years and a median age of 31 years (range, 11-65 years) at the time of surgery. There were no statistically significant differences between the groups in

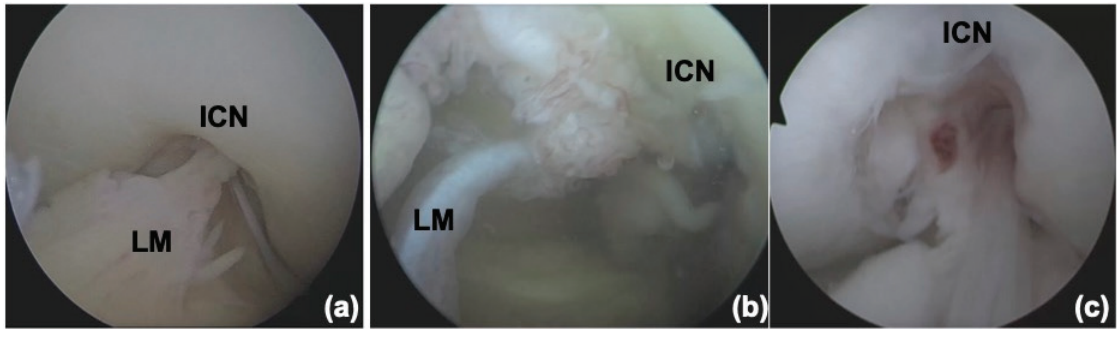

Figure 1. Arthroscopic imaging of the knee: The LM is intact and extends in front of the anterior cruciate ligament (a), ruptured LM fragments (b) and LM is not in presence (c).

ICN: Intercondylar notch, LM: Ligamentum mucosum.

terms of mean age or gender (p=0.489 and p=0.150, respectively) (Table 1). The mean time from injury to surgery was 4 weeks for acute ACL tears, 65 weeks for chronic ACL, and 42 weeks for intact ACLs.

When the groups were evaluated separately; in acute ACL tears, the prevalence of patients with intact and ruptured LM was similar and significantly higher than that of patients without LM (p<0.001). In chronic tears, the prevalence of intact and ruptured LM was similar, but the prevalence of no LM was significantly higher in this group (p=0.03). In intact ACLs, the majority of patients had intact LM (p<0.001) (Table 2).

When comparing the groups, it was found that intact LM was significantly more common in the intact ACL group than in the other groups (p<0.001). In acute ACL tears, intact LM was significantly lower compared to intact ACLs (p<0.001). However, it was significantly higher compared to chronic tears (p=0.001). While ruptured LM was most frequently observed in acute tears, they were least common in intact ACLs. There were significantly more patients without LM in the chronic tear group than in the other groups (p=0.021). The presence of LM (intact or ruptured) was found to be similar between in acute tears and intact ACLs (Table 2).

Intra- and interobserver Cohen's kappa values were assessed and found to demonstrate excellent agreement, with an interobserver kappa value of 0.856±0.036 and an intraobserver kappa value of 0.891±0.026.

DISCUSSION

The present study revealed two significant findings: First, the presence of an intact LM was significantly lower in knees with chronic ACL than in knees with acute injury and intact ACLs. Second, knees with acute ACL injuries had a similar percentage of LM presence as knees without ACL injuries. However, there is a significantly greater probability of damage to the LM in knees with acute ACL injury. We conclude that early surgical planning in patients with ACL injuries can increase the likelihood of using LM as a source for neurovascular purposes.

We believe that there may be two reasons for the higher incidence of LM rupture in knees with ACL injuries, particularly acute tears. First, Abreu et al. (6) showed that patients with ACL injuries have a higher prevalence of Hoffa fat pad pathology, which is due to the instability of the knee structure. By the similar mechanism LM attached to the Hoffa fat pad may also be at risk of damage due to instability in the knee. The second reason may be that the LM, which runs anteriorly and parallel to the ACL, can be torn by the same trauma that damages the ACL (17-19). It is possible that the damaged LM may degenerate over time. Amiel et al. (20) have shown that the ACL in the knee can degenerate after a tear. We are convinced that the LM, which has a ligamentous structure similar to that of the ACL, may also degenerate when injured. In conducted study, we also observed that patients in the acute phase had a high rate of LM rupture, whereas patients in the chronic phase had a high rate of LM absence instead of rupture.

The prevalence of LM has been studied using different methods, such as magnetic resonance imaging (MRI), cadaver dissection, and arthroscopic examination. A study conducted on cadavers to determine the prevalence of LM during early human life revealed that LM was present in all 70 knees examined (21). In another study that analyzed 51 cadaver knee joints, LM was observed in 66.7% of the specimens (7). In an arthroscopic study of 200 patients, it was found that 85% of them had LM (22). An MRI-based study revealed that this structure was present in 78.3% of knees (23). Degeneration is typically the cause of the observed decrease in LM incidence. The estimated prevalence of LM in young adults ranges between 65% and 80%. However, in the elderly population, this prevalence decreases to 37% (6,22,24). In the present study, the prevalence of LM (61%) was slightly lower than that in the general population in

Table 1. Comparison of demographic characteristics in 3 groups

	Group 1, (n=89)	Group 2, (n=111)	Group 3, (n=101)	p
	Mean ± SD	**Mean ± SD**	**Mean ± SD**	
Age	32.31±12.75	29.15±7.31	32.64±9.18	0.489
	n (%)	**n (%)**	**n (%)**	
Gender				0.150
Male	58 (65.2%)	80 (72.1%)	60 (59.4%)	
Female	31 (34.8%)	31 (27.9%)	41 (40.6%)	

Significant at 0.05 level; One-Way ANOVA for age, chi-square test for categorical data. SD: Standard deviation.

Table 2. The relationship between the ligamentum mucosum and groups

	Acute ACL tears	Chronic ACL tears	Intact ACLs
	n (%)	**n (%)**	**n (%)**
LM			
Intact	35 (39.4%)	25 (22.5%)	71 (70.3%)
Rupture	36 (40.4%)	29 (26.1%)	11 (10.9%)
Non-presence	18 (20.2%)	57 (51.4%)	19 (18.8%)

LM: Ligamentum mucosum, ACL: Anterior cruciate ligament.

the literature. We believe that the significant percentage (67%) of our study group comprised knees with ACL injuries.

In recent years, histological studies have provided a detailed understanding of the neurovascular structure of LM (7,11,21,25). It has been suggested that the LM may play a role in proprioception similar to that of the ACL due to its neural tissue. Furthermore, similar to ACL remnant tissue, the LM could be used to enhance proprioception in ACL reconstruction (7,11,25). In addition to neural tissue, the presence and location of vascular elements are also notable. The most hypovascular area of the ACL is the anterior part of its distal attachment (26). Gonera et al. (25) proposed that the LM, due to its vascular tissue, especially in the distal part, could be sutured to the ACL during repair procedures to provide vascular support. The blood supply and revascularisation process have a crucial role in the viability of the graft (27). Claes et al. (28) suggest that new blood vessels developing from the LM and infrapatellar fat pad could be involved in graft revascularization. As a consequence, suturing the LM to the ACL graft could provide a more effective vascularization process and increase the success rate of the reconstruction. Further anatomical and mechanical studies on the abovementioned methods are needed.

Study Limitations

The current study had several limitations, including its retrospective design, even if the data were collected prospectively. Hypotheses about the role of neural tissue in the LM in proprioception and its potential use in ACL revascularization owing to its vascular structure have been suggested based on histopathological studies. Although the literature suggests that suturing the LM to the ACL may be an effective surgical technique, no research has compared the healing time of the ACL and the improvement in proprioception between patients who have undergone this method and those who have not. Another limitation of the present study was that knees without ACL damage, rather than completely healthy knees, were included in the control group. Therefore, further clinical research is needed to better understand the role of the LM in ACL repair.

CONCLUSION

The present study concluded that the probability of an intact LM in chronic ACL tears was relatively low. Therefore, we suggest that early surgical intervention for ACL injuries could increase the chances of using the LM as a source of neurovascular supply. In addition, because of the possible effect of the LM on proprioception, we recommend preserving the structure during knee arthroscopy procedures if a healthy LM is present.

Ethics

Ethics Committee Approval: The study was approved by the Gazi University Ethics Committee (approval number: 15, date: 09.01.2023).

Informed Consent: Written informed consent was obtained from all patients.

Authorship Contributions

Concept: M.A.T., E.B.O., Design: M.Ş.C., Supervision: M.B.A., U.K., Resources: A.K., U.K., Materials: A.K., Data Collection or Processing: E.B.O., M.B.A., Analysis or Interpretation: M.A.T., M.B.A., Literature Search: E.B.O., Writing: E.B.O., M.Ş.C., Critical Review: U.K., A.K.

Conflict of Interest: No conflict of interest was declared by the authors.

Financial Disclosure: The authors declared that this study received no financial support.

REFERENCES

1. Gallagher J, Tierney P, Murray P, O'Brien M. The infrapatellar fat pad: anatomy and clinical correlations. Knee Surg Sports Traumatol Arthrosc. 2005; 13: 268-72.
2. Ogata S, Uhthoff HK. The development of synovial plicae in human knee joints: an embryologic study. Arthroscopy. 1990; 6: 315-21.
3. Cothran RL, McGuire PM, Helms CA, Major NM, Attarian DE. MR imaging of infrapatellar plica injury. AJR Am J Roentgenol. 2003; 180: 1443-7.
4. Boot-Handford RP, Tuckwell DS. Fibrillar collagen: the key to vertebrate evolution? A tale of molecular incest. Bioessays. 2003; 25: 142-51.
5. Duthon VB, Barea C, Abrassart S, Fasel JH, Fritschy D, Ménétrey J. Anatomy of the anterior cruciate ligament. Knee Surg Sports Traumatol Arthrosc. 2006; 14: 204-13.
6. Abreu MR, Chung CB, Trudell D, Resnick D. Hoffa's fat pad injuries and their relationship with anterior cruciate ligament tears: new observations based on MR imaging in patients and MR imaging and anatomic correlation in cadavers. Skeletal Radiol. 2008; 37: 301-6.
7. Gonera B, Kurtys K, Wysiadecki G, Podgórski M, Olewnik ŁH. The ligamentum mucosum: A new classification. Clin Anat. 2023; 36: 242-9.
8. Kim SJ, Choe WS. Pathological infrapatellar plica: a report of two cases and literature review. Arthroscopy. 1996; 12: 236-9.
9. Relph N, Herrington L, Tyson S. The effects of ACL injury on knee proprioception: a meta-analysis. Physiotherapy. 2014; 100: 187-95.
10. Mir SM, Talebian S, Naseri N, Hadian MR. Assessment of Knee Proprioception in the Anterior Cruciate Ligament Injury Risk Position in Healthy Subjects: A Cross-sectional Study. J Phys Ther Sci. 2014; 26: 1515-8.
11. Norris M, Corbo G, Banga K, Johnson M, Sandig M, Smallman T, et al. The biomechanical and morphological characteristics of the ligamentum mucosum and its potential role in anterior knee pain. Knee. 2018; 25: 1134-41.
12. Gonera B, Wysiadecki G, Kurtys K, Brzeziński P, Borowski A, Olewnik Ł. Immunohistochemical analysis of the ligamentum mucosum is the key to understand its clinical usefulness. Ann Anat. 2023; 249: 152106.
13. Ozcan M, Copuroğlu C, Ciftdemir M, Turan FN, Calpur OU. Does an abnormal infrapatellar plica increase the risk of chondral damage in the knee. Knee Surg Sports Traumatol Arthrosc. 2011; 19: 218-21.
14. Boyd CR, Eakin C, Matheson GO. Infrapatellar plica as a cause of anterior knee pain. Clin J Sport Med. 2005; 15: 98-103.
15. Demirag B, Ozturk C, Karakayali M. Symptomatic infrapatellar plica. Knee Surg Sports Traumatol Arthrosc. 2006; 14: 156-60.
16. Flint JH, Wade AM, Giuliani J, Rue JP. Defining the terms acute and chronic in orthopaedic sports injuries: a systematic review. Am J Sports Med. 2014; 42: 235-41.
17. Kiapour AM, Murray MM. Basic science of anterior cruciate ligament injury and repair. Bone Joint Res. 2014; 3: 20-31.
18. Kobayashi H, Kanamura T, Koshida S, Miyashita K, Okado T, Shimizu T, et al. Mechanisms of the anterior cruciate ligament injury in sports

activities: a twenty-year clinical research of 1,700 athletes. J Sports Sci Med. 2010; 9: 669-75.

19. Ishibashi Y, Adachi N, Koga H, Kondo E, Kuroda R, Mae T, et al. Japanese Orthopaedic Association (JOA) clinical practice guidelines on the management of anterior cruciate ligament injury - Secondary publication. J Orthop Sci. 2020; 25: 6-45.
20. Amiel D, Ishizue KK, Harwood FL, Kitabayashi L, Akeson WH. Injury of the anterior cruciate ligament: the role of collagenase in ligament degeneration. J Orthop Res. 1989; 7: 486-93.
21. Gonera B, Borowski A, Zielinska N, Palac W, Paulsen F, Olewnik Ł. Embryological approach to the morphology of the ligamentum mucosum of the human knee joint. Ann Anat. 2022; 244: 151983.
22. Kim SJ, Min BH, Kim HK. Arthroscopic anatomy of the infrapatellar plica. Arthroscopy. 1996; 12: 561-4.
23. Lee YH, Song HT, Kim S, Kim SJ, Suh JS. Infrapatellar plica of the knee: revisited with MR arthrographies undertaken in the knee flexion position mimicking operative arthroscopic posture. Eur J Radiol. 2012; 81: 2783-7.
24. Apostolopoulos AP, McConnell B, Manta A, Zafiropoulos G. The incidence of infrapatellar plicae in the elderly Welsh population. Folia Morphol (Warsz). 2012; 71: 194-7.
25. Petersen W, Tillmann B. Structure and vascularization of the cruciate ligaments of the human knee joint. Anat Embryol (Berl). 1999; 200: 325-34.
26. Petersen W, Tillmann B. Structure and vascularization of the cruciate ligaments of the human knee joint. Anat Embryol (Berl). 1999; 200: 325-34.
27. Yao S, Fu BS, Yung PS. Graft healing after anterior cruciate ligament reconstruction (ACLR) Asia Pac J Sports Med Arthrosc Rehabil Technol. 2021; 25: 8-15.
28. Claes S, Verdonk P, Forsyth R, Bellemans J. The "ligamentization" process in anterior cruciate ligament reconstruction: what happens to the human graft? A systematic review of the literature. Am J Sports Med. 2011; 39: 2476-83.

Original Investigation | Özgün Araştırma

GMJ 2024;35:387-392

DOI: http://dx.doi.org/10.12996/gmj.2024.4128

The Effect of Hysteroscopy on Fertility in Women with Unexplained Infertility

Açıklanamayan İnfertilitesi Olan Kadınlarda Histeroskopinin Fertilite Üzerine Etkisi

Rıza Dur, Betül Ahat, Ayşe Yalçınkaya Yılmaz, Cem Yağmur Özdemir, Mine Kanat Pektaş

Department of Obstetrics and Gynecology, Afyonkarahisar Health Sciences University Faculty of Medicine, Afyonkarahisar, Türkiye

ABSTRACT

Objective: This study aimed to investigate how undergoing hysteroscopy affects the reproductive rates of women with unexplained infertility.

Methods: A total of 145 women who were aged between 20 and 40 years, who had been diagnosed with unexplained infertility and who underwent hysteroscopy at the study center between 1 January 2021 and 1 January 2022 were enrolled in this study. All patients who underwent hysteroscopy were put to an 18-month-long follow-up period.

Results: The clinical pregnancy rate was 43.4%, whereas the live birth rate was 38.6% in this cohort. Average time to pregnancy took 5.6±1.8 months (range: 2-9 months). The mode of conception was unassisted in 28 pregnancies (44.4%) whereas the mode of conception was ovarian stimulation combined with intrauterine insemination in 23 pregnancies (36.5%) and in vitro fertilization in 12 pregnancies (19.1%). The patients who were able to conceive after hysteroscopy had significantly younger age, lower gravidity, and parity than those who failed to conceive (p=0.008, p=0.005 and p=0.001, respectively). The patients who successfully gave birth to living newborns after hysteroscopy had significantly younger age, lower gravidity, and parity than those who failed to deliver (p=0.040, p=0.003 and p=0.001, respectively). Septum resection was significantly more frequent and adhesiolysis was significantly less frequent in patients who were able to give birth to living newborns after hysteroscopy (p=0.038 and p=0.014, respectively).

Conclusion: Hysteroscopy appears to have a positive impact on live birth rates in women with unexplained infertility.

Keywords: Dysfunctional uterine bleeding, hysteroscopy, infertility, pregnancy

ÖZ

Amaç: Bu çalışmada açıklanamayan infertilitesi olan kadınlarda histeroskopi yapılmasının üreme oranlarını nasıl etkilediğinin araştırılması amaçlanmıştır.

Yöntemler: Çalışmaya 1 Ocak 2021 ile 1 Ocak 2022 tarihleri arasında, çalışma merkezinde açıklanamayan infertilite tanısı almış ve histeroskopi uygulanmış 20-40 yaş aralığındaki toplam 145 kadın dahil edildi. Histeroskopi uygulanan tüm hastalar 18 aylık takip edildi.

Bulgular: Bu kohorttaki klinik gebelik oranı %43,4 iken canlı doğum oranı %38,6 idi. Gebeliğe kadar geçen süre ortalama 5,6±1,8 ay idi (aralığı: 2-9 ay). Gebeliklerin 28'i (%44,4) spontan iken, 23 gebelik (%36,5) over stimülasyonu ve intrauterin inseminasyon kombinasyonuyla ve 12 gebelik (%19,1) ise in vitro fertilizasyon ile oluşmuştur. Histeroskopi sonrası gebe kalabilen hastaların yaşı, gebe kalamayanlara göre anlamlı derecede daha gençti, gebelik ve pariteleri daha düşüktü (sırasıyla; p=0,008, p=0,005 ve p=0,001). Histeroskopi sonrası canlı doğum yapabilen hastaların yaşları, doğum yapamayanlara göre anlamlı derecede daha genç, gebelik sayıları ve pariteleri daha düşüktü (sırasıyla; p=0,040, p=0,003 ve p=0,001). Histeroskopi sonrası canlı doğum yapabilen hastalarda septum rezeksiyonu anlamlı derecede daha sık, adezyolizis ise anlamlı derecede daha az sıklıkta görüldü (sırasıyla; p=0,038 ve p=0,014).

Sonuç: Histeroskopinin, açıklanamayan infertilitesi olan kadınlarda canlı doğum oranları üzerinde olumlu bir etkisi olduğu görülmektedir.

Anahtar Sözcükler: Disfonksiyonel uterin kanama, gebelik, histereskopi, infertilite

Address for Correspondence/Yazışma Adresi: Rıza Dur, MD, Department of Obstetrics and Gynecology, Afyonkarahisar Health Sciences University Faculty of Medicine, Afyonkarahisar, Türkiye
E-mail / E-posta: durriza@hotmail.com
ORCID ID: orcid.org/0000-0002-9225-9030

Received/Geliş Tarihi: 01.02.2024
Accepted/Kabul Tarihi: 13.03.2024

INTRODUCTION

Infertility has been described as the inability to conceive after 12 months of regular unprotected sexual intercourse (1). There is an identifiable cause of infertility in about 85% of the affected couples. Ovulatory disorders, male factor, and tubal-uterine involvement account for the identifiable causes of infertility (2). For the remaining 15% of the couples, unexplained infertility is diagnosed in the absence of any identifiable cause (3).

The treatment of unexplained infertility is based on increasing the chance of conception per cycle (4). The first choice is ovarian stimulation, which increases the number of available oocytes and thus enhances the conception rate. To provide a more precise timing of conception, ovarian stimulation can be combined with intrauterine insemination (IUI). Lastly, in vitro fertilization (IVF) can be performed to allow the fusion of oocytes and sperms (4,5).

It has been emphasized that the term "unexplained infertility" shrinks as the causes related with infertility become identified (3). For instance, endometrial receptivity, oxidative stress, and genetic factors might participate in the pathogenesis of infertility for the couples who have no identifiable cause despite undergoing routine infertility workup (6-8).

Hysteroscopy is an endoscopic procedure that has become the gold standard for the assessment of the cervical canal and uterine cavity (9). It has been reported that carrying out hysteroscopy before assisted reproduction treatment contributes to the success of this treatment (10). That is, hysteroscopy can improve reproductive outcomes by eliminating intrauterine pathologies and regulating implantation (11). Since couples with unexplained infertility should be offered a safe and cost-effective approach based on prognostic evaluation, it is prudent to include hysteroscopy in their work-up (12). However, routine use of hysteroscopy is not recommended in case of unexplained infertility (13).

The present study aimed to investigate how undergoing hysteroscopy affects the reproductive rates of women with unexplained infertility.

MATERIALS AND METHODS

This prospective cohort study was approved by the Ethics Committee of Afyonkarahisar Health Sciences University where it was undertaken (approval number: 2023/12/497, date: 01.12.2023). Each participant was informed about the study, and written informed consent was obtained from all participants.

A total of 145 women with unexplained infertility who underwent hysteroscopy at the study center between 1 January 2021 and 1 January 2022 were enrolled into this study. The inclusion criteria were being aged between 20 and 40 years and diagnosed with unexplained infertility. The diagnosis of unexplained infertility was made after known factors for infertility. were ruled out. Ovulation was verified with follicular monitoring by transvaginal ultrasonography and serial measurements of serum estradiol and/or mid-luteal progesterone ≥5 ng/mL within regular and uninduced menstrual cycles. Tubal patency was demonstrated by hysterosalpingography and/or pelvic laparoscopy. Male factors were designated according to the spermiogram parameters declared by the World Health Organization (14).

Women aged younger than 20 years and older than 40 years, the women with known cause of infertility such as ovulatory dysfunction and tubal obstruction, women who had partners with male factors, women who were diagnosed with endometrial hyperplasia or cancer after hysteroscopy, and women who abandoned the idea of conceiving were excluded.

All participants had pelvic examination and transvaginal ultrasonography with 7.5 MHz probe (Voluson E8, GE Healthcare, Chicago, IL, USA). Body mass index (BMI) was calculated by dividing body weight (kg) by the square of height (m^2).

Hysteroscopy Procedures

All hysteroscopy procedures were conducted between the 7th and 11th days of the menstrual cycle. Paracervical block was provided by 10 mL of 1% lidocaine in every procedure. A rigid 4 mm continuous flow BETTOCCHI® hysteroscope with 30° direction of view was inserted into the uterus through the cervical canal and uterine cavity was expanded by irrigation with 0.9% saline solution (Karl Storz Endoscopy, Utrecht, Netherlands). After introducing the hysteroscope via the internal cervical ostium, the uterine cavity was visualized carefully.

Whenever intrauterine pathology was detected, general anesthesia was administered, and operative hysteroscopy was performed. Before operative hysteroscopy, cervical dilatation up to 10 mm was achieved by using Hegar dilators. The intrauterine pressure was standardized to 150 mmHg during surgery by continuous infusion of 5% glucose solution through an automated pump. Monopolar instruments were used to remove the polyps, while an electroresectoscope was adopted to correct the uterine septum. After the resectoscope was positioned to confirm the location, size, and range of the septum, needle electrode was activated to cut the septum, and abdominal ultrasonography was used to monitor the safety of the surgery. Isthmocele repair was performed by a resectoscope with bipolar electrode loop (26 Fr., 4 mm, 0°). On the other hand, adhesiolysis was conducted using cold scissors with an irrigation/suction device. Hysteroscopy-related complications occurred in none of these patients.

All patients who underwent hysteroscopy were put to an 18-month-long follow up period after the procedure. Data related with demographic characteristics, infertility type and duration, hysteroscopy indications, operative procedures, histopathological findings, and reproductive and perinatal outcomes were acquired from medical records. Clinical pregnancy was defined in case fetal heartbeat was detected by ultrasonography.

Ovulation Induction and Intrauterine Insemination

Ovulation induction was carried out by administering clomiphene citrate, letrozole or recombinant follicle stimulating hormone (FSH). Clomiphene citrate was begun on 3rd day of the menstrual cycle and given at a dose of 50-150 mg/day for five days. Letrozole was started at a dose of 2.5-5 mg/day on 3rd day of the menstrual cycle and continued for 5 days. Recombinant FSH was administered according to the low-dose step-up protocol, beginning with doses of 37.5 to 75 IU/day. When transvaginal ultrasonography visualized that follicle size reached ≥18 mm, recombinant human chorionic gonadotropin

(HCG) was applied at a dose of 250 µg intramuscularly. It was made sure that there was only one dominant follicle at the day of HCG trigger. The following HCG trigger, IUI was performed after 24 or 36 hours. Semen samples for IUI were collected via masturbation and prepared with swim up method. After IUI was conducted by an elastic cannula, luteal phase support was provided by prescribing progesterone capsules of 200 mg vaginally. Luteal phase support was maintained by progesterone until 13th day of IUI when serum beta HCG levels were measured.

In Vitro Fertilization

A short-stimulation protocol was adopted, starting with the subcutaneous injection of gonadotropin releasing hormone agonist. Then, ovarian stimulation was provided with the administration of recombinant FSH, starting either on day 4 at 150 IU when the women were ≤37 years old or on day 2 with 225 or 300 IU if the women were older than 38 years. This dose was adjusted by transvaginal ultrasonography findings and serum estradiol concentrations during ovarian stimulation. When the desired follicle growth was achieved, HCG was injected at a dose of 10000 IU subcutaneously, followed by oocyte pickup 36 hours later.

Freshly ejaculated semen was liquefied and diluted 1:1 with N-2-hydroxyethylpiperazine-N'-2-ethanesulfonic acid (HEPES)-buffered Earle's medium supplemented with 0.5% human serum albumin. The diluted sample was pipetted on top of a 1 mL layer of 70% Percoll or a 1-mL layer of 70% PureSperm in a 12 mL tube and was processed by centrifuge (800 x g, 10 minutes). The supernatant was removed, and the sperm pellet (0.1-0.5 mL) was resuspended in 5 mL of HEPES-buffered Earle's medium. This suspension was washed twice, first in HEPES-buffered medium and a second time in universal IVF medium. The spermatozoa were kept at 37° C in a CO_2 incubator until IVF was achieved.

The retrieved oocyte-cumulus complexes (OCCs) were pooled and washed in HEPES-buffered Earle's medium and then randomly transferred into groups of two to six OCCs to droplets of 25 µL of universal IVF medium under mineral oil and then put into an incubator (37 °C, 5% CO_2).

The OCCs were then cultured individually in 25 µL droplets of universal IVF medium. Each oocyte was inseminated with 75000-150000 motile spermatozoa, 2-6 hours after oocyte retrieval. Fertilization was scored 16-18 hours after insemination. The surrounding cumulus cells were removed mechanically by repeated pipetting of the OCCs, and the oocytes were transferred to new 25 µL droplets of universal IVF medium. Embryo transfer occurred 3 days after oocyte retrieval. Transfer of one or two embryos was based on the regulations of the Turkish Ministry of Health. Women younger than 35 years of age and who were undergoing their first or second embryo transfer could only have a single embryo transfer. A maximum of two embryos could be transferred to women older than 35 years or who were undergoing second embryo transfer. Luteal phase support was maintained by progesterone until 13th day of embryo transfer when serum beta HCG levels were measured.

Statistical Analysis

The data collected were analyzed using the Statistical Package for Social Sciences version 22.0 (SPSS IBM, Armonk, NY, USA). Continuous variables were expressed as mean ± standard deviation, whereas categorical variables were denoted as numbers or percentages, where appropriate. Student's t-test and the chi-square test were used for comparisons. Two-tailed p values <0.05 were accepted as statistically significant.

RESULTS

Sixty-three clinical pregnancies were conceived by 145 women with unexplained infertility, and 56 pregnancies resulted in live births during the follow-up period. The clinical pregnancy rate was 43.4%, whereas the live birth rate was 38.6% in this cohort. Average time to pregnancy took 5.6±1.8 months (range: 2-9 months). The mode of conception was unassisted in 28 pregnancies (44.4%) whereas ovarian stimulation combined with IUI was performed to conceive 23 pregnancies (36.5%) and IVF was used to conceive 12 pregnancies (19.1%). Five miscarriages (7.9%), 1 ectopic pregnancy (1.6%) and 1 intrauterine demise (1.6%) occurred in this study cohort while there were 4 twin pregnancies (6.3%).

Table 1 presents the demographic and clinical characteristics of patients with unexplained infertility with respect to clinical pregnancy. The patients who were able to conceive after hysteroscopy had significantly younger age, lower gravidity, and parity than the patients who failed to conceive after hysteroscopy (p=0.008, p=0.005 and p=0.001 respectively). The patients who were able to conceive and the patients who failed to conceive were statistically similar with respect to BMI, duration, and type of infertility, and hysteroscopy indication (p>0.05 for all). In addition, the patients who succeeded to conceive and the patients who failed to conceive were statistically similar in aspect of hysteroscopy type, operative procedures, and histopathological findings (p>0.05 for all) (Table 2).

Table 3 demonstrates the demographic and clinical characteristics of patients with unexplained infertility with respect to live birth. Patients who were able to give birth to living newborns after hysteroscopy

Table 1. Demographic and clinical characteristics of the patients with respect to pregnancy

	Clinical pregnancy, (n=63)	No clinical pregnancy, (n=82)	p
Age (years)	27.9±4.7	30.3±5.9	0.008*
Gravidity	0.72±0.49	1.17±0.94	0.005*
Parity	0.43±0.24	0.76±0.56	0.001*
Body mass index (kg/m^2)	26.76±4.62	26.48±4.46	0.710
Duration of infertility (years)	4.0±2.7	4.6±3.0	0.196
Primary infertility	40 (63.5%)	43 (52.4%)	0.182
Secondary infertility	23 (36.5%)	39 (47.6%)	0.244
Hysteroscopy indication			
Uterine septum	26 (41.3%)	31 (37.8%)	0.634
Abnormal uterine bleeding	21 (33.3%)	33 (40.2%)	0.636
Uterine septum + abnormal bleeding	10 (15.9%)	14 (17.1%)	0.762
Dysmorphic uterus	6 (9.5%)	4 (4.9%)	0.764

*p<0.05 was accepted to be statistically significant.

had significantly younger age, lower gravidity, and parity than patients who failed to deliver living neonates after hysteroscopy (p=0.040, p=0.003 and p=0.001 respectively). The patients who succeeded in delivering living newborns and those who failed to give birth to living neonates were statistically similar with respect to BMI, duration, and type of infertility, and hysteroscopy indication (p>0.05 for all). Moreover, septum resection was significantly more frequent and adhesiolysis was significantly less frequent in patients who were able to give birth to living newborns after hysteroscopy (p=0.038 and p=0.014 respectively). The patients who succeeded in delivering living neonates and those who failed to give birth to living newborns were statistically similar in terms of hysteroscopy type and histopathological findings (Table 4).

Table 2. Hysteroscopy findings of the patients with respect to pregnancy

	Clinical pregnancy, (n=63)	No clinical pregnancy (n=82)	p
Diagnostic hysteroscopy	28 (44.4%)	31 (37.8%)	0.420
Operative hysteroscopy	35 (55.6%)	51 (62.2%)	0.496
Operative procedure			
Septum resection	10 (28.6%)	21 (41.2%)	0.667
Polyp resection	17 (48.5%)	19 (37.3%)	0.663
Isthmocele repair	5 (14.3%)	7 (13.7%)	0.465
Adhesiolysis	3 (8.6%)	4 (7.8%)	0.462
Histopathological findings			
Endometrial polyp	17 (48.5%)	19 (37.3%)	0.753
Proliferative endometrium	11 (31.5%)	18 (35.3%)	0.751
Secretory endometrium	5 (14.3%)	10 (19.6%)	0.308
Chronic endometritis	2 (5.7%)	4 (7.8%)	0.305

Table 3. Demographic and clinical characteristics of the patients with respect to live birth

	Live birth, (n=56)	No live birth, (n=89)	p
Age (years)	28.1±4.8	30.0±5.8	0.040*
Gravidity	0.71±0.46	1.14±0.92	0.003*
Parity	0.41±0.21	0.74±0.55	0.001*
Body mass index (kg/m^2)	26.77±4.79	26.49±4.36	0.717
Duration of infertility (years)	4.1±2.7	4.5±3.0	0.520
Primary infertility	37 (66.1%)	46 (51.7%)	0.088
Secondary infertility	19 (33.9%)	43 (48.3%)	0.125
Hysteroscopy indication			
Uterine septum	25 (44.6%)	32 (36.0%)	0.748
Abnormal uterine bleeding	19 (33.9%)	35 (39.3%)	0.744
Uterine septum + Abnormal bleeding	8 (14.3%)	16 (18.0%)	0.457
Dysmorphic uterus	4 (7.1%)	6 (6.7%)	0.452

*p<0.05 was accepted to be statistically significant.

DISCUSSION

The present study yields a clinical pregnancy rate of 43.4% and a live birth rate of 38.6% after hysteroscopy in couples with unexplained infertility. In addition, mode of conception was unassisted in 44.4% of pregnancies. Patients who were able to conceive after hysteroscopy were significantly younger, had lower gravidity, and had parity than those who failed to conceive. Patients who successfully gave birth to living newborns after hysteroscopy were significantly younger, had lower gravidity, and had parity than those who failed to deliver. Septum resection was significantly more frequent and adhesiolysis was significantly less frequent in patients who were able to give birth to living newborns after hysteroscopy.

Hysteroscopy is the gold standard for both the assessment and management of intrauterine pathologies (15). Yet, controversy remains regarding the adoption of hysteroscopy as a primary tool for the initial work-up of infertility (15-18). As an example, the American Society for Reproductive Medicine describes hysteroscopy as a relatively expensive and invasive procedure (16). In parallel, the National Institute for Health and Clinical Excellence has declared that hysteroscopy should not be performed during the primary workup for infertility (17). On the contrary, the Italian Society of Gynecological Endoscopy has highlighted hysteroscopy as a component of the initial screening for infertility (18). Specifically, the European Society of Human Reproduction and Endocrinology does not recommend the use of hysteroscopy for the detection and correction of intrauterine abnormalities that have not been observed by routine imaging in women with unexplained infertility (13,19).

The current treatment of unexplained infertility consists of expectant management, ovarian stimulation combined with IUI and IVF options (19). It has been reported that performing diagnostic hysteroscopy before embryo transfer does not improve pregnancy rates (20). However, a prospective study detected cervical, uterine, and endometrial abnormalities by hysteroscopy in 86% of women with unexplained infertility (21). Similarly, another study found uterine abnormalities in 26.3% of these women by saline infusion

Table 4. Hysteroscopy findings of the patients with respect to live birth

	Live birth, (n=56)	No live birth, (n=89)	p
Diagnostic hysteroscopy	25 (44.6%)	34 (38.2%)	0.442
Operative hysteroscopy	31 (55.4%)	55 (61.8%)	0.552
Operative procedure			
Septum resection	15 (48.4%)	13 (23.6%)	0.038*
Polyp resection	13 (41.9%)	26 (47.3%)	0.126
Isthmocele repair	3 (9.7%)	9 (16.4%)	0.158
Adhesiolysis	0 (0.0%)	7 (12.7%)	0.014*
Histopathological findings			
Endometrial polyp	13 (48.5%)	26 (47.2%)	0.255
Proliferative endometrium	12 (31.5%)	11 (20.0%)	0.257
Secretory endometrium	5 (14.3%)	14 (25.5%)	0.572
Chronic endometritis	1 (5.7%)	4 (7.3%)	0.626

*p<0.05 was accepted to be statistically significant.

sonography (22). Therefore, this study was designed to determine how undergoing hysteroscopy contributes to the reproductive rates of women with unexplained infertility.

The age of the couple is a crucial factor in fecundity rates, and especially the female age is a significant predictor of the clinical pregnancy rate in couples with unexplained infertility (1,3). As the female age exceeds 35 years, the number and quality of oocytes decrease rapidly. A major reason for this decline is the accumulation of metabolites within the ovarian microenvironment, which can lead to genetic mutations and telomere shortening (1,23). Similarly, the patients who were able to conceive and deliver living newborns after hysteroscopy had significantly younger age, and, thus, lower gravidity and parity than the remaining patients in this study.

A meta-analysis of 10 randomized controlled trials reported that live birth altered between 9% and 28% in couples receiving ovarian stimulation, 11% and 33% in couples undergoing IUI, 15% and 37% in couples having ovarian stimulation combined with IUI, and 14% to 47% in couples undergoing IVF due to unexplained infertility when the live birth rate was 17% in unassisted couples (24). In a study assessing young women with unexplained infertility and diminished ovarian reserve, the live birth rate was 11.3% for women receiving IUI and 22.6% for women having IVF treatment (25). A randomized controlled trial was conducted to designate the optimal treatment for unexplained infertility by evaluating long-term reproductive outcomes. The live birth rate was 67.8% during this one-year-long trial of 286 couples with unexplained infertility, and the overall live birth rate reached to 80.9% after the trial. The live birth rate was 64.3% in unassisted couples, whereas the live birth rate was 5.3% in couples undergoing IUI and 36.4% in couples having IVF treatment (26).

As for the present study, the clinical pregnancy rate was 43.4% while live birth rate was 38.6% in a cohort of 145 women with unexplained infertility. The mode of conception was unassisted in 44.4% of the pregnancies, whereas the mode of conception was ovarian stimulation combined with IUI in 36.5 of the pregnancies and IVF in 19.1% of the pregnancies. Compared with the literature, the discrepancies in the clinical pregnancy and live birth rates in this study could be attributed to heterogeneity in the cohort size and characteristics.

A uterine septum is a congenital uterine malformation that divides the uterine cavity into two by a longitudinal wall-like tissue and maintains the typically normal exterior contour of the uterus (27). The septate uterus itself is not considered as a reason for infertility, but it might interfere with the natural conception. On the other hand, the uterine septum is related with unfavorable pregnancy outcomes (27-30). Hysteroscopy provides definitive diagnosis and treatment for this most common uterine anomaly (28).

A meta-analysis of 7 studies emphasizes that hysteroscopic septum resection lowers the miscarriage rate (27). Another meta-analysis of 55 studies indicated that hysteroscopic resection significantly reduces the risk of miscarriage in patients with a septate uterus. Yet, hysteroscopic metroplasty exerts no significant effect on clinical pregnancy, live birth, or preterm delivery rates (28). A recent meta-analysis concluded that hysteroscopic septum resection significantly increases the rate of live births and decreases the rate of miscarriage in patients with recurrent pregnancy loss or primary infertility. However, the same efficiency of hysteroscopic resection does not take effect in patients with secondary infertility (29). Another recent meta-analysis specified the adverse effects of the uterine septum on reproductive and perinatal outcomes and showed that hysteroscopic treatment improves miscarriage rates (30).

Complying with literature, the patients who succeeded to conceive and the patients who failed to conceive were statistically similar with respect to hysteroscopic procedures in this study. Correspondingly, septum resection was significantly more frequent in patients who gave birth to living newborns after undergoing hysteroscopy.

Intrauterine adhesion refers to the presence of synechiae that can end up with the partial or total disruption of the uterine cavity and eventual impairment in the uterine shape. Infectious and/or traumatic damage to the basal layer of the endometrium results in intrauterine adhesion, which is occasionally associated with Asherman syndrome (31). The success rate of hysteroscopy has been found to be 95% in a cohort of 638 women diagnosed with Asherman syndrome (32). Therefore, it has been hypothesized that hysteroscopy optimizes fertility outcomes by accurately diagnosing intrauterine adhesions and their obliteration (33). In contrast, the prevalence of hysteroscopic adhesiolysis was significantly lower in women who successfully delivered living neonates after hysteroscopy. This contradictory finding can be due to the relatively higher recurrence risk of intrauterine adhesions and the association between intrauterine adhesions and poor reproductive outcomes (33,34).

CONCLUSION

Consequently, the findings of the present study suggest that hysteroscopy has a positive impact on the live birth rate of women diagnosed with unexplained infertility. However, these findings

Should be interpreted carefully because their power is limited by the relatively small cohort size and the variations in the sociodemographic and clinical features of the participants. Further research is warranted to clarify the role of hysteroscopy in the reproductive success of women with unexplained infertility.

Ethics

Ethics Committee Approval: This prospective cohort study was approved by the Ethics Committee of Afyonkarahisar Health Sciences University where it was undertaken (approval number: 2023/12/497, date: 01.12.2023).

Informed Consent: Each participant was informed about the study, and written informed consent was obtained from all participants.

Authorship Contributions

Concept: R.D., B.A., A.Y.Y., C.Y.Ö., M.K.P., Design: R.D., B.A., A.Y.Y., C.Y.Ö., M.K.P., Supervision: R.D., M.K.P., Resources: C.Y.Ö., Materials: R.D., B.A., A.Y.Y., Data Collection or Processing: R.D., B.A., A.Y.Y., Analysis or Interpretation: R.D., B.A., A.Y.Y., M.K.P., Literature Search: R.D., C.Y.Ö., Writing: R.D., M.K.P., Critical Review: M.K.P.

Conflict of Interest: No conflict of interest was declared by the authors.

Financial Disclosure: The authors declared that this study received no financial support.

REFERENCES

1. Carson SA, Kallen AN. Diagnosis and Management of Infertility: A Review. JAMA. 2021; 326: 65-76.
2. Phillips K, Olanrewaju RA, Omole F. Infertility: Evaluation and Management. Am Fam Physician. 2023; 107: 623-30.
3. Mol BW, Hart RJ. Unexplained Infertility. Semin Reprod Med. 2020; 38: 1-2.
4. Wang R, van Eekelen R, Mochtar MH, Mol F, van Wely M. Treatment Strategies for Unexplained Infertility. Semin Reprod Med. 2020; 38: 48-54.
5. Man JK, Parker AE, Broughton S, Ikhlaq H, Das M. Should IUI replace IVF as first-line treatment for unexplained infertility? A literature review. BMC Womens Health. 2023; 23: 557.
6. Santamaria X, Simón C. Endometrial Factor in Unexplained Infertility and Recurrent Implantation Failure. Semin Reprod Med. 2021; 39: 227-32.
7. Didziokaite G, Biliute G, Gudaite J, Kvedariene V. Oxidative Stress as a Potential Underlying Cause of Minimal and Mild Endometriosis-Related Infertility. Int J Mol Sci. 2023; 24: 3809.
8. Homer HA. The Role of Oocyte Quality in Explaining "Unexplained" Infertility. Semin Reprod Med. 2020; 38: 21-8.
9. Stamenov GS, Vitale SG, Della Corte L, Vilos GA, Parvanov DA, Nikolova DN, et al. Hysteroscopy and female infertility: a fresh look to a busy corner. Hum Fertil (Camb). 2022; 25: 430-46.
10. Chiofalo B, Palmara V, Vilos GA, Pacheco LA, Lasmar RB, Shawki O, et al. Reproductive outcomes of infertile women undergoing "see and treat" office hysteroscopy: a retrospective observational study. Minim Invasive Ther Allied Technol. 2021; 30: 147-53.
11. Bosteels J, van Wessel S, Weyers S, Broekmans FJ, D'Hooghe TM, Bongers MY, et al. Hysteroscopy for treating subfertility associated with suspected major uterine cavity abnormalities. Cochrane Database Syst Rev. 2018; 12: CD009461.
12. Wang R, Danhof NA, Tjon-Kon-Fat RI, Eijkemans MJ, Bossuyt PM, Mochtar MH, et al. Interventions for unexplained infertility: a systematic review and network meta-analysis. Cochrane Database Syst Rev. 2019; 9: CD012692.
13. Kamath MS, Rikken JFW, Bosteels J. Does Laparoscopy and Hysteroscopy Have a Place in the Diagnosis of Unexplained Infertility? Semin Reprod Med. 2020; 38: 29-35.
14. Björndahl L, Kirkman Brown J; other Editorial Board Members of the WHO Laboratory Manual for the Examination and Processing of Human Semen. The sixth edition of the WHO Laboratory Manual for the Examination and Processing of Human Semen: ensuring quality and standardization in basic examination of human ejaculates. Fertil Steril. 2022; 117: 246-51.
15. Genovese F, Di Guardo F, Monteleone MM, D'Urso V, Colaleo FM, Leanza V, et al. Hysteroscopy as An Investigational Operative Procedure in Primary and Secondary Infertility: A Systematic Review. Int J Fertil Steril. 2021; 15: 80-7.
16. Practice Committee of the American Society for Reproductive Medicine. Electronic address: ASRM@asrm.org; Practice Committee of the American Society for Reproductive Medicine. Uterine septum: a guideline. Fertil Steril 2016; 106: 530-40.
17. Di Spiezio Sardo A, Di Carlo C, Minozzi S, Spinelli M, Pistotti V, Alviggi C, et al. Efficacy of hysteroscopy in improving reproductive outcomes of infertile couples: a systematic review and meta-analysis. Hum Reprod Update. 2016; 22: 479-96.
18. Campo R, Santangelo F, Gordts S, Di Cesare C, Van Kerrebroeck H, De Angelis MC, et al. Outpatient hysteroscopy. Facts Views Vis Obgyn. 2018; 10: 115-22.
19. Guideline Group on Unexplained Infertility; Romualdi D, Ata B, Bhattacharya S, Bosch E, Costello M, et al. Evidence-based guideline: unexplained infertility†. Hum Reprod. 2023; 38: 1881-90.
20. Eserol F, Göksever Çelik H, Aytan AN, Çelik A, Çelik E, Buyru F, et al. The effect of diagnostic hysteroscopy performed before fresh and frozen-thawed embryo transfer in IVF cycles on reproductive outcomes. J Turk Ger Gynecol Assoc. 2021; 22: 206-11.
21. Makled AK, Farghali MM, Shenouda DS. Role of hysteroscopy and endometrial biopsy in women with unexplained infertility. Arch Gynecol Obstet. 2014; 289: 187-92.
22. Izhar R, Husain S, Tahir S, Husain S. Incidence of intrauterine abnormalities in Pakistani women with unexplained infertility diagnosed via saline infusion sonography. J Ultrason. 2018; 18: 186-92.
23. Guan H, Tang H, Pan L, Song H, Tang L. Pregnancy predictors in unexplained infertility after intrauterine insemination. J Gynecol Obstet Hum Reprod. 2021; 50: 102071.
24. Wang R, Danhof NA, Tjon-Kon-Fat RI, Eijkemans MJ, Bossuyt PM, Mochtar MH, et al. Interventions for unexplained infertility: a systematic review and network meta-analysis. Cochrane Database Syst Rev. 2019; 9: CD012692.
25. Wu Y, Liu H, Liu J. The Livebirth Rate Per In Vitro Fertilization Cycle Is Higher Than The Cumulative Live Birth Rates of Intrauterine Insemination for Patients of Poseidon Group 3 With Unexplained Infertility. Front Endocrinol (Lausanne). 2021; 12: 768975.
26. Vaughan DA, Goldman MB, Koniares KG, Nesbit CB, Toth TL, Fung JL, et al. Long-term reproductive outcomes in patients with unexplained infertility: follow-up of the Fast Track and Standard Treatment Trial participants. Fertil Steril. 2022; 117: 193-01.
27. Krishnan M, Narice BF, Ola B, Metwally M. Does hysteroscopic resection of uterine septum improve reproductive outcomes: a systematic review and meta-analysis. Arch Gynecol Obstet. 2021; 303: 1131-42.
28. Carrera M, Pérez Millan F, Alcázar JL, Alonso L, Caballero M, Carugno J, et al. Effect of Hysteroscopic Metroplasty on Reproductive Outcomes in Women with Septate Uterus: Systematic Review and Meta-Analysis. J Minim Invasive Gynecol. 2022; 29: 465-75.
29. Jiang Y, Wang L, Wang B, Shen H, Wu J, He J, et al. Reproductive outcomes of natural pregnancy after hysteroscopic septum resection in patients with a septate uterus: a systematic review and meta-analysis. Am J Obstet Gynecol MFM. 2023; 5: 100762.
30. Noventa M, Spagnol G, Marchetti M, Saccardi C, Bonaldo G, Laganà AS, et al. Uterine Septum with or without Hysteroscopic Metroplasty: Impact on Fertility and Obstetrical Outcomes-A Systematic Review and Meta-Analysis of Observational Research. J Clin Med. 2022; 11: 3290.
31. Lee WL, Liu CH, Cheng M, Chang WH, Liu WM, Wang PH. Focus on the Primary Prevention of Intrauterine Adhesions: Current Concept and Vision. Int J Mol Sci. 2021; 22: 5175. -
32. Di Spiezio Sardo A, Di Guardo F, Santangelo F, Cianci S, Giampaolino P. Commentary on "Assessment of Risk Factors of Intrauterine Adhesions in Patients with Induced Abortion and the Curative Effect of Hysteroscopic Surgery". J Invest Surg. 2019; 32: 90-2.
33. Hanstede MM, van der Meij E, Goedemans L, Emanuel MH. Results of centralized Asherman surgery, 2003-2013. Fertil Steril. 2015; 104: 1561-8.
34. Ghahiry AA, Refaei Aliabadi E, Taherian AA, Najafian A, Ghasemi M. Effectiveness of hysteroscopic repair of uterine lesions in reproductive outcome. Int J Fertil Steril. 2014; 8: 129-34.

Original Investigation | Özgün Araştırma

GMJ 2024;35:393-400

DOI: http://dx.doi.org/10.12996/gmj.2024.4167

Synergistic Effects of Thymoquinone and Carob Powder versus Dexamethasone in the Model of Asthma in Pregnant Rats: New Insights into their Therapeutic Effects

Gebe Sıçanlarda Astım Modelinde Timokinon ve Harnup Tozunun Deksametazonla Karşılaştırıldığında Sinerjik Etkileri: Terapötik Etkilerine İlişkin Yeni Görüşler

Ameerah Fadhil Ahmed[1], Şule Coşkun Cevher[2], Emine Gülceri Güleç Peker[3], Barbaros Balabanlı[2], Meral Ebegil[4]

[1]College Medical Laboratory Techniques, University of Alyarmok, Kirkuk, Iraq
[2]Department of Biology, Gazi University Faculty of Sciences, Ankara, Türkiye
[3]Department of Nursing, Giresun University Faculty of Healthy Sciences, Giresun, Türkiye
[4]Department of Statistics, Gazi University Faculty of Sciences, Ankara, Türkiye

ABSTRACT

Objective: When asthma and pregnancy coexist, the mother may be severely affected. One of the main reasons for this situation is that it is positively correlated with especially increased oxidative stress due to the co-occurrence of asthma and pregnancy. Even pregnancy alone increases oxidative stress in the body, and with the addition of asthma, an increased chain of events is added. In this sense, diet and nutrition styles can be considered as factors that regulate both events in a controlled way. Increasing anti-oxidant intake in the diet can play a leading role in eliminating the increased Reactive oxygen species; thus, this negative effect in asthma and pregnancy can be alleviated. Studies on the protective role of antioxidants in asthma are limited, but not few. The aim of this study was to reveal the strength of the effects of thymoquinone (TQ) and carob powder administration, which are known to have two different strong antioxidant effects during pregnancy, on the oxidative event in the mother with the diet management strategies.

Methods: In this study, it was tried to improve the asthmatic pregnant rat and to determine the direction of oxidant-antioxidant balance with a holistic antioxidant complex Female rats were divided into 3 groups: asthmatic pregnant group (1) sensitized via an intraperitoneal injection of ovalbumin (OVA) with alum on days 0 and 14 and exposed to aerosolized OVA 3 days over the subsequent 1 week then coupled with male rats to get pregnant; asthmatic pregnant with TQ and carob (CS) group (2) sensitized as above then administered each of TQ and CS on the last 5 days of pregnancy; and asthmatic pregnant with dexamethasone group (3) sensitized as above then received dexamethasone by intraperitoneal injection on last 5 days of pregnancy.

ÖZ

Amaç: Gebelikte astım varlığı, artan oksidatif stres nedeniyle hem anne hem de fetüs için risk oluşturabilir. Bu durumun en önemli nedenlerinden biri, özellikle astım ve gebeliğin birlikte görülmesi nedeniyle artan oksidatif stresle pozitif ilişkili olmasıdır. Tek başına gebelik bile vücutta oksidatif stresi artırır, buna ek olarak astımın eklenmesiyle olaylar zinciri daha da artar. Bu anlamda beslenme tarzları her iki olayı da kontrollü bir şekilde düzenleyen bir faktör olarak düşünülebilir. Diyette antioksidan alımının artırılması, artan reaktif oksijen türlerinin ortadan kaldırılmasında öncü rol oynayabilir; böylece astım ve gebelikteki bu olumsuz etki hafifletilebilir. Antioksidanların astımda koruyucu rolüne ilişkin çalışmalar sınırlıdır. Bu çalışmanın amacı, gebelik döneminde iki farklı güçlü antioksidan etkisi olduğu bilinen timokinon (TQ) ve harnup tozu uygulamasının diyet yönetimi stratejisi ile annedeki oksidatif olay üzerindeki etkilerinin gücünü ortaya koymaktır.

Yöntemler: Bu çalışmada, astımlı gebe sıçanlarda bütünsel bir antioksidan kompleks ile oksidan-antioksidan dengenin yönü belirlenmeye ve iyileştirilmeye çalışılmıştır. Dişi sıçanlar üç gruba ayrılmıştır: Astımlı gebe grup (1), 0. ve 14. günlerde alüminyum içeren ovalbümin (OVA) ile intraperitoneal enjeksiyon yoluyla duyarlılaştırıldı ve sonraki 1 hafta boyunca 3 gün boyunca aerosolize edilmiş OVA'ya maruz bırakıldı ve ardından gebe kalmak için erkek sıçanlarla birleştirildi; TQ ve harnup (CS) grubu (2) ile gebe kalan astımlı hastalara yukarıda belirtilen şekilde duyarlılık kazandırıldı ve daha sonra gebeliğin son 5 gününde TQ ve CS'nin her biri uygulandı; ve yukarıda belirtilen şekilde duyarlılaştırılan deksametazon grubu (3) ile astımlı gebelere gebeliğin son 5 gününde intraperitoneal enjeksiyon yoluyla deksametazon verildi.

Address for Correspondence/Yazışma Adresi: Şule Coşkun Cevher, PhD, Department of Biology, Gazi University Faculty of Sciences, Ankara, Türkiye
E-mail / E-posta: sule@gazi.edu.tr
ORCID ID: orcid.org/0000-0001-6204-2845

Received/Geliş Tarihi: 19.03.2024
Accepted/Kabul Tarihi: 01.08.2024

ABSTRACT

Results: The co-administration of TQ and CS decreased malondialdehyde levels, increased nitric oxide, ascorbic acid, and glutathione levels in lung tissue. In addition, the levels of some proinflammatory cytokines were decreased in the serum. The cumulative protective effects of TQ and CS were successful in reducing inflammation in the lungs.

Conclusion: The administration of TQ and CS may be considered as a candidate for a new herbal blend or adjuvant for asthmatic pregnant, given the side effects of cortisol.

Keywords: Asthmatic pregnant, carob, thymoquinone, oxidative stress, inflammation

ÖZ

Bulgular: TQ ve CS'nin birlikte uygulanması akciğer dokusunda malondialdehit seviyelerini azalttı ve nitrik oksit, askorbik asit ve glutatyon seviyelerini artırdı. Ayrıca, serumda bazı proenflamatuvar sitokinlerin seviyesi azalmıştır. TQ ve CS'nin kümülatif koruyucu etkisi akciğerdeki enflamasyonu azaltmada başarılı olmuştur.

Sonuç: Kortizolün yan etkileri göz önüne alındığında, TQ ve CS'nin uygulanması astımlı gebelerde yeni bir bitkisel karışım veya adjuvan adayı olarak düşünülebilir.

Anahtar Sözcükler: Astımlı gebe, harnup, timokinon, oksidatif stres, enflamasyon

INTRODUCTION

Asthma is a common disease that affects children and adults, particularly pregnant women. Maternal asthma brings not only the mother herself but also the morbidity and mortality associated with the fetus (1). Therefore, being both asthmatic and pregnant at the same time puts a huge burden on both the mother and the newborn (2).

Asthma is a fairly a disease with a high prevalence in the community and involves a complex interaction of various factors, such as inflammation, bronchial hyperresponsiveness, and airflow obstruction. The predominant character leading to clinical symptoms is contraction and inflammation of the smooth muscle, resulting in narrowing and airway obstruction. Numerous triggers, such as irritants and drugs, may cause bronchoconstriction in some patients. Airway inflammation may lead to blood vessel proliferation, mucus hypersecretion, subepithelial fibrosis, inflammatory cell infiltration, and smooth muscle hyperplasia (3,4). In asthma, many inflammatory cells (mast cells, neutrophils, macrophages, etc.) are related in the airway inflammation pathogenesis (5). Reactive oxygen species (ROS) are released as a result of cell metabolism. ROS stimulate histamine release and mucus secretion by contracting airway smooth muscles (6). All these reactions lead to increased inflammation. Both increased oxidants due to the open airways to the outside environment and the presence of airway inflammatory cell-derived ROS cause high levels of oxidative stress in the lung (7). An article on asthma susceptibility in mice found elevated levels of certain cytokines both in the lungs and systemically, particularly differences in T helper 2 (TH2) and TH17 cytokine levels (8).

Strong anti-inflammatory drugs, such as inhaled corticosteroids and anti-leukotrienes, are the basis for the treatment of asthma symptoms in the long term. Although these drugs are beneficial for the treatment of asthma, they have several side effects. Recently, traditional and herbal approaches have attracted attention in every field and constitute an important part of health systems worldwide (9). One of them, Nigella sativa has been known as an alternative treatment for asthma and other inflammatory diseases. Nigella sativa, which is traditionally used as a food and in the treatment of asthma, bronchitis, eczema, and inflammation, has various important biological effects (anti-inflammatory, anti-tumor, antioxidant) (10). Most of these biological properties have been associated with TQ, the primarily metabolite of Nigella sativa essential oil. TQ inhibits cycloxyoxygenase and lipoxygenase inflammation, decreases the ratio of TH2 cytokines and eosinophils. TQ is an inhibitor of asthma and inhibits eosinophil infiltration and decreases allergic airway inflammation. However, the mechanism of action of TQ during asthma treatment has not been fully elucidated (11-13).

CS (carob), which is grown extensively in the Mediterranean region, has a vital role and attracts attention in the food and medicine industries for economic and environmental reasons (Battle and Tous). Carob seed is a rich source of flavonoids such as gallotannin, ellagitannin, and proanthocyanidin. These phytochemicals have free radical-scavenging activities and are used against many diseases because of their pharmacological properties (14). Carob powder is a rich source of Niacin, B6, vitamins C, D, E, folic acid, and other valuable fatty acids (15). Therefore, it can be suggested that the protective effects against lipid peroxidation caused by ROS in tissues and the prevention of the depletion of the antioxidant enzyme; SOD, CAT, and glutathione (GSH) are attributed mostly to its chemical content. Plant flavonoids have also been reported to alleviate gingival inflammation via the suppression of nuclear NF-κβ translocation and myeloperoxidase activity, which may explain the reported inhibition of the pro-inflammatory mediators (15,16).

During pregnancy, there is a superimposed increased oxidative stress burden brought on by both pregnancy and asthma. The protective effects of exogenous antioxidants against oxidative stress are important in pregnancy with asthma. In this sense, herbal approaches attract attention today. Despite the increased oxidative stress resulting from asthma complications and asthma exacerbations during pregnancy, it has been reported that an increase in antioxidant supplements alleviates these effects (16).

To date, there is only one histologic and immuno-histological study which was done our laboratory related to the cumulative effect of TQ and CS in pregnant asthmatic rats (2). In this new study, our hypothesis is whether TQ and CS will have a positive effect on oxidative events and some indicator cytokines in pregnant rats with asthma and will show a potential synergistic effect.

MATERIALS AND METHODS

Experimental Design

The experimental design was carried out as described in our previous study (2). The experimental procedures were confirmed by Ethics Committee of Gazi University for Animal Experiments (approval number: G.Ü.ET-16.035, date: 21.03.2016). The experimental groups were designed as shown in Table 1.

Sensitization and inhalational exposure: All animals were sensitized according to the methods of Moura et al. (17) and Yang et al. (18) and the experimental timeline is shown in Figure 1.

Sample collection: Ketamine and xylazine were intramuscularly injected (IM) to anesthetize the rats. Lung samples from all rats were dissected after sacrificed by high dose of anesthetics, washed thoroughly with saline and kept in liquid nitrogen until they were held in the laboratory and then kept at -30 °C. Blood samples were collected in clot activator tubes then they centrifuged in 3000 rpm for 5 min. and the serums were kept at -30 °C.

Biochemical Analyses

Determination of MDA, NOx, AA, and GSH levels: Malondialdehyde (MDA) levels in both serum and tissue were measured by the method of Casini et al. (19). In this method, MDA reacts with thiobarbituric acid. The NOx levels in tissue were measured spectrophotometrically by the Griess reaction at 540 nm (20). Roe and Kuther's method modified by Berger et al. (21) was used for measuring ascorbic acid (AA) level in both tissue and serum. A modified Ellman method for GSH spectrophotometrically determination in tissue was used (22). Plasma RSH was determined using the spectrophotometric method (23).

Measurement of some cytokine levels: Some serum levels were measured with commercial kit [serum interleukin-1 beta (IL-1β) & tumor necrosis factor-alpha (TNF-α) DIAsource, BE and serum IL-13 Sunredbio, CHN].

Table 1. Experimental group design

Group 1 (n=6)	Asthmatic pregnant
Group 2 (n=6)	Asthmatic pregnant with TQ and CS treated
Group 3 (n=6)	Asthmatic pregnant with dexamethasone treated

TQ: Thymoquinone, CS: Carob.

Statistical Analysis

Data were given as means ± standard deviations, and the differences between groups were made using ANOVA post-hoc Tukey using the SPSS software package (IBM, USA) $p<0.05$ was considered statistically significant.

RESULTS

In this study, the in the dexamethasone treatment group, the MDA levels increased the most. MDA levels decreased in treated group with TQ and CS (group 2) ($p<0.05$) (Table 2). On the other hand, serum MDA levels decreased in TQ + CS treatment group (Table 4). Application of TQ + CS were decreased serum MDA levels. The lung tissue increased in combination of TQ and CS (Table 2, $p<0.05$).

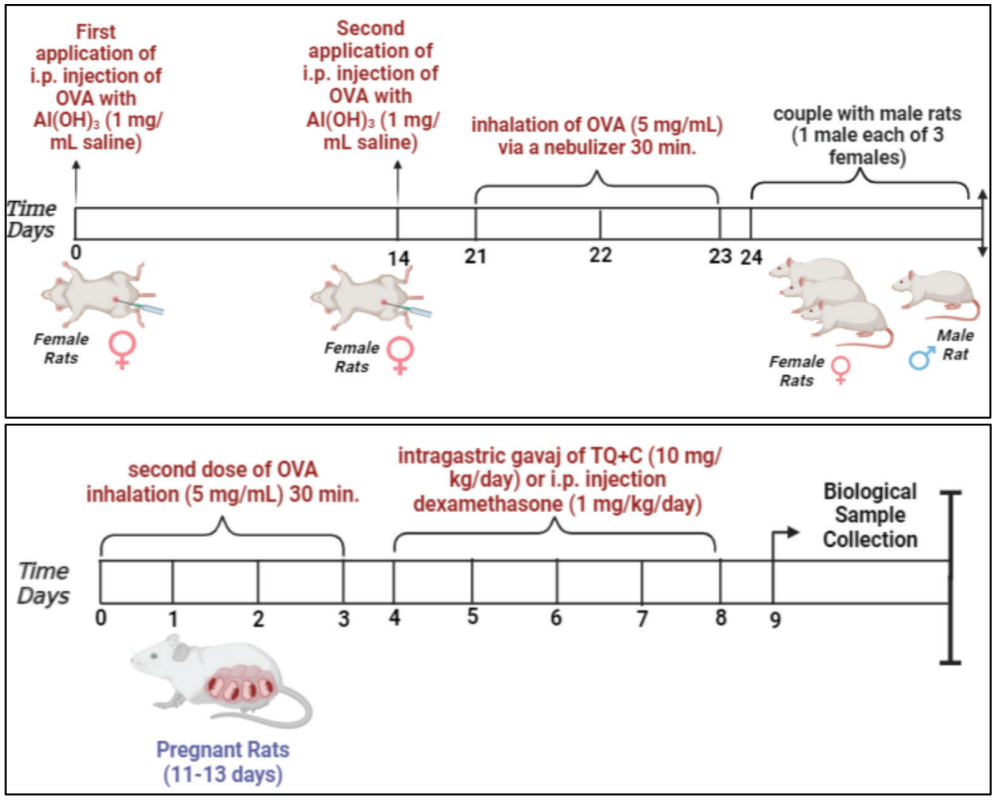

Figure 1. Experimental timeline. To develop a model of asthma, female rats were first treated OVA for 14 days (i.p. injection). At the end of 14 days, a second OVA treatment was performed (i.p. injection). On days 21, 22, and 23, OVA was administered by inhalation. Female rats in an asthma model were created with OVA, were mated with male rats. Pregnant rats aged 1-13 days were given OVA by inhalation for 3 days, and the asthma model was repeated. TQ + CS treatment was administered pregnant rats for 5 days. Tissue serum and plasma of the rats sacrificed at the end of the treatment were separated and subjected to biochemical analysis.

TQ: Thymoquinone, CS: Carob, OVA: Ovalbumin.

In our study, application of dexamethasone increased lung tissue GSH levels (p<0.05) (Table 2). The tissue levels of AA increased after the dual administration of TQ + CS (with parallel lung tissue NO levels) (p<0.05) (Table 2).

TQ and CS administration did not show any change in serum TNF-α levels (Table 3). TNF-α levels in dexamethasone group was in increasing trend when compared to both (p>0.05) (Table 3). Our findings showed that dual TQ + CS administration significantly decreased both IL-1β and IL-13 levels in asthmatic rat serum. The WBC differential content in the serum was shown in Table 5. The eosinophil percentage was significantly decreased in the treatment group compared with the other groups (p<0.05).

DISCUSSION

Asthma and pregnancy remain a worrying issue today, as both the mother and the fetus struggle to cope with the heavy burden of these conditions. Both being pregnant and having asthma are known as conditions in which the oxidative stress load is higher than normal in women.

Antioxidants are one of the best solutions that come to mind in terms of supporting against increased oxidative stress in pregnancy. Asthma is a serious condition manifested by asthma exacerbations in pregnant women. Asthma exacerbation rates are known to increase and trigger with pregnancy, and this rate is not negligible (24). In the treatment of asthma, corticosteroids are used cautiously because they do not pose a risk to both the mother and the fetus, but they are still hesitant by the patients even at the minimum dose. Natural methods are also often preferred to prevent the onset of asthma symptoms and exacerbations, ensure optimal lung function, and manage risk factors for poor asthma outcomes and comorbidities. Taking advantage of plants is one of them.

Asthma occurs when chronic inflammation in the airway remodeling (25). The respiratory response in IgE-mediated asthma involves mast cell degranulation and histamine and leukotriene mediators. Sensitization with ovalbumin (OVA) is known to stimulate and

Table 2. Biochemical results in the lung tissues of pregnant rats

Groups	MDA levels (nmol/g tissue)	NO levels (nmol/g tissue)	GSH levels (µmol/g tissue)	AA levels (µg/g tissue)
Asthmatic pregnant (I)	14.81±1.18	19.80±3.09	0.88±0.18	16.71±0.83
Asthmatic pregnant with TQ + CS (II)	13.87±1.56*	36.36±1.27*	1.01±0.23	20.59±0.91*
Asthmatic pregnant with dexamethasone (III)	17.56±0.30	18.40±1.65	3.99±0.77a	14.64±0.85

Each value is the mean ± standard deviation of 6 animals per group. *p<0.05 when compared to group 1 and 3, ap<0.05 when compared to group 1 and 2. TQ: Thymoquinone, CS: Carob, GSH: Glutathione, AA: Ascorbic acid.

Table 3. TNF-α, IL-1β and IL-13 levels in the serum of pregnant rats

Groups	TNF-α levels, (pg/mL)	IL-1β levels, (pg/mL)	IL-13 levels, (pg/mL)
Asthmatic pregnant (I)	1.95±0.66	51.99±2.02	58.39±0.84
Asthmatic pregnant with TQ + CS (II)	1.86±1.18	34.59±2.33*	46.98±0.15*
Asthmatic pregnant with dexamethasone (III)	3.58±1.77	53.24±1.85	55.52±0.08

Each value is the mean ± standard deviation of 6 animals per group. *p<0.05 when compared to groups 1 and 3. TQ: Thymoquinone, CS: Carob, GSH: Glutathione, AA: Ascorbic acid.

Table 4. Biochemical results in the serum of pregnant rats

Groups	MDA levels, (nmol/mL serum)	RSH levels, (nmol/mL serum)	AA levels, (nmol/mL serum)
Asthmatic pregnant (I)	5.16±1.26	357.26±97.85	2.03±0.23
Asthmatic pregnant with TQ + CS (II)	2.24±0.34*	467.93±82.23	1.90±0.19
Asthmatic pregnant with dexamethasone (III)	2.53±0.53*	407.31±59.27	3.30±0.21

Each value is the mean ± standard deviation of 6 animals per group. *p<0.05 when compared to group 1. TQ: Thymoquinone, CS: Carob, GSH: Glutathione, AA: Ascorbic acid, MDA: Malondialdehyde.

Table 5. Differential WBC count in the serum of pregnant rats

Groups	Monocytes percentage, (%)	Lymphocytes percentage, (%)	Neutrophils percentage, (%)	Eosinophils percentage, (%)
Asthmatic pregnant (1)	4.83±1.77	71±6.32	18.5±6.10	5.50±3.20
Asthmatic pregnant with TQ + CS (2)	3.50±1.89	68±11.87	25.83±10.67	2±1*
Asthmatic pregnant with dexamethasone (3)	4.67±2.42	42.33±19.73a	45.67±11.91a	5±1.91

*p<0.05 when compared to 1 and 3 groups. ap<0.05 when compared to 1 and 2 groups.
TQ: Thymoquinone, CS: Carob, WBC: White blood cell

increase inflammatory cell infiltration and airway responsiveness (26). Tissue lung MDA level increased in control group. Our findings were consistent with those of a previous study (27). MDA is a common indicator of lipid peroxidation. You et al. (28) showed that superoxide anion and hydrogen peroxide released in large amounts from activated inflammatory cells in the pulmonary alveoli lead to an increase in MDA and maintain inflammation. In consistent with above studies in our study, we found increased lipid peroxidation accompanied by OVA exposure in lung tissue.

Biochemical results content of the lung tissue and serum: Carob pod treatment (aqueous extract) might mitigate lipid peroxidation in brain and heart. It is also thought to play a role in protecting against cardiovascular and neuronal diseases (29,30). Otherwise, the anti-inflammatory activities of thymoquinone (TQ) support the effect of it on lung inflammation (31). The effects of Nigella sativa on inflammation, asthma, and the immune system have been reported (10). Although it is thought that TQ shows its effects through its antioxidant properties in Th1 and Th2 cells, its mechanism of action is not fully understood (32). It shows that TQ and CS, which have a strong antioxidant potential, reduced the harmful effects of ROS. In our study, the in dexamethasone treatment group, the MDA levels increased the most. MDA levels decreased in treated group with TQ and CS (group 2) ($p<0.05$) (Table 2). On the other hand, serum MDA levels decreased in TQ + CS treatment group (Table 4). Application of TQ + CS were decreased serum MDA levels. This decrease may be due to the antioxidative properties of TQ and CS. It is thought that TQ and CS treatment, which are used as potential antioxidants during asthma attacks, reduces oxidative biomarkers and thus may improve asthma.

Nitric oxide (NO) is a messenger molecule produced by several NO synthases, and it plays an important role as a neurotransmitter, vasodilator, and bronchodilator in the lungs. It can promote the inflammatory response in asthma (33). The lung tissue increased in combination of TQ and CS (Table 2, $p<0.05$). However, previous studies have shown that TQ decreases NO levels (34,35). We suggest that vitamin C-rich CS leads to an increase in NO levels. d'Uscio et al. (36) pointed out that long-term treatment with vitamin C increases NO synthesis activities and vascular tetrahydrobiopterin levels, which supports our result.

GSH is a vital for antioxidant defense system and airway cells activities (37). In our study, application of dexamethasone increased lung tissue GSH levels ($p<0.05$) (Table 2). Dexamethasone is used in the treatment of asthma and is a member of the glucocorticoid drug class. Glucocorticoids are very effective in treating asthma, and they have various effects on the inflammatory response, such as reducing antigen-induced infiltration of eosinophils and cytokine production (38). Long-term use leads to side effects such as oxidative injury, nuclear DNA damage, and mitochondrial dysfunction (39). Thus, alternative treatment methods are required. Our finding showed similarities to Ismael and Shaffie's results (40). They found that fish oil and fish oil + dexamethasone alleviated OVA-induced modifies in lung function tests. GSH levels in group 2 also increased however insignificant ($p>0.05$). Abd El Aziz et al. (41) reported that TQ improved LPS-induced GSH reduction. This is a remarkable study of the dual effects of TQ and CS in an experimental asthmatic model, and there is no literature finding about the effectiveness of CS in the lung tissue of asthmatic rats. It is believed that the antioxidant properties of carob are due to its polyphenolic and other metabolites.

AA (vitamin C) alleviates the harmful effects of ROS (42). In this study, the tissue levels of AA increased after the dual administration of TQ + CS (with parallel lung tissue NO levels) ($p<0.05$) (Table 2). The enormous vitamin C content in carob powder probably mediated the increased AA levels in lung tissue in group 2 (15). Similarly, oral TQ administration has been shown to increase the levels of antioxidants such as vitamin C (43). When all these findings are evaluated together, it is thought that the increased AA levels detected in the lung tissue of group 2 are due to exogenously administered TQ + CS. On the other hand, whether the AA level in the serum was not statistically different between the TQ and CS applied group and the control group, it was in an increasing trend in the TQ + CS group of AA level. Some mammals, such as humans and rats, cannot manufacture AA in their bodies, so they must take food containing AA. Hence, it can be thought that there is an interaction between AA and GSH. Our results showed that when dexamethasone administration was compared with TQ and CS, application, there was an inverse relationship between AA and GSH.

Cytokine levels in serum: Scott et al. (44) examined female fetuses with moderate asthmatic mothers such as placental expression of TNF-α and some interleukins and found increased cytokine levels compared to control. When asthma and pregnancy coexist, an associated increased inflammation in maternal and placental circulation is considered (45,46). In inflammatory diseases, such as asthma, the levels of cytokines such as TGF-β, TNF-α, IL-6, IL-8, and IL-10, change and contribute negatively to the progression of the disease (47). Osei-Kumah et al. (48) suggested that some cytokine concentrations were increased but the others were not during pregnancy. In another study, they found some serum levels to be unchanged, such as interleukin, GMCSF, Interferon gamma, and TNF-α, in obese pregnant women (47). Our study differs from these studies in that it is an experimental animal study, but this is in parallel with the fact that they have similar metabolic pathways. Considering this context, increased cytokine levels were detected in pregnant rats with asthma. The co-administration of TQ and carob provides a significant decrease in serum cytokine levels, and inflammatory processes turned it into a positive direction. Inflammation plays an essential role in asthma pathophysiology. This includes the interaction of various cell types and mediators with the airway, which reveals the characteristic features of the disease. Mediators of airway smooth muscle have been suggested to be important in asthma (49). One of these mediators is TNF-α stimulates histamine (50), and human mast cells participate in a positive autocrine cycle that increases cytokine secretion (51). Increased levels of TNF-α in the airways of asthmatic patients suggest that TNF-α is involved in the inflammatory process in asthma (52,53). There is evidence that TNF-α expression is increased in the airways in asthma (53). El Gazzar et al. (54) reported that TQ reduced Th-2 and inflammatory cell infiltration in the lung, thereby alleviating pulmonary inflammation TQ blocks the production of TNF-α by targeting nuclear transactivation of nuclear factor-kappa, thus exerting a positive effect in reducing airway inflammation (54). Tekeoglu et al. (55) showed in a rheumatoid arthritis model with chronic inflammation that TQ inhibited TNF-α production. Surprisingly in our study, TQ and CS administration did not show any change in serum TNF-α levels (Table 3). According to

TNF-α results, other cytokines (IL-1β and IL-13) take a greater role in the inflammation process and may be due to the application doses of TQ + CS and short-term treatment administration. TNF-α levels in dexamethasone group was in increasing trend when compared to both ($p>0.05$) (Table 3). Low doses of dexamethasone used to treat asthma may cause these increases. Our findings showed that dual TQ + CS administration significantly decreased both IL-1β and IL-13 levels in asthmatic rat serum. The imbalance between oxidant and antioxidant metabolites is thought to be involved in the pathogenesis of chronic obstructive pulmonary disease (56). Abd El Aziz et al. (41) conducted that while LPS-induced lung injury by stimulate IL-1β production; TQ (8 mg/g) decreased it on airway-induced hypersensitivity mice. Another study revealed that, TQ decreased IL-4, IL-5 and IL-13 in airway (12). In addition, it has been reported that carob extract is non-toxic, does not have serious side effects and contains zinc and phenolic components that have antioxidant activity (57,58). Zinc can suppress oxidation by binding to sulfhydryl groups in proteins, and it can activate the binding site of copper and iron in lipid, protein, and DNA (59). Another metabolite that protects biomolecules against ROS damage or formation is zinc. Zinc deficiency in biological membranes increases oxidative damage and impairs their functions (57,60). These studies prove that TQ and CS can inhibit inflammatory pathway cytokines.

Differential WBC content: The pathophysiology of asthma occurs a variety of changes at the cellular level as a result of the activity of eosinophils, mast cells, neutrophils, and T-lymphocytes (5). The WBC differential content in the serum was shown in Table 5. The eosinophil percentage was significantly decreased in the treatment group compared with the other groups ($p<0.05$).

CONCLUSION

Our findings lead us to consider that, dual applying of TQ and CS plays a critical role in reducing lipid peroxidation and consequently inflammation in pregnant asthmatic rats. Thus, we believe that the administration of dual TQ and CS can be used as a potential adjuvant in clinical practice, especially at the time of an attack in pregnant women with asthma.

Acknowledgements: We wish to thank projects of scientific investigation (BAP) of Gazi University for their constant interest and valuable advice on this project (05/2016-22).

Ethics

Ethics Committee Approval: The experimental procedures were confirmed by Ethics Committee of Gazi University for Animal Experiments (approval number: G.Ü.ET-16.035, date: 21.03.2016).

Informed Consent: Patient approval has not been obtained as it is performed on animals.

Authorship Contributions

Concept: Ş.C.C., Design: Ş.C.C., B.B., Supervision: Ş.C.C., Resources: Ş.C.C., Materials: Ş.C.C., A.F.A., Data Collection or Processing: A.F.A., M.E., E.G.G.P., Analysis or Interpretation: A.F.A., M.E., E.G.G.P., Literature Search: A.F.A., E.G.G.P., Writing: A.F.A., Ş.C.C., Critical Review: Ş.C.C., B.B., Other: Ş.C.C.,

Conflict of Interest: No conflict of interest was declared by the authors.

Financial Disclosure: This work was partially supported by the Gazi University Scientific Research Projects Coordination Unit through a research grant no: 05/2016-22.

REFERENCES

1. Meakin AS, Saif Z, Jones AR, Aviles PFV, Clifton VL. Review: Placental adaptations to the presence of maternal asthma during pregnancy. Placenta. 2017; 54: 17-23.
2. Ahmed AF, Cevher SC. The preventive effect of thymoquinone and Ceratonia siliqua L. in experimental asthmatic pregnant rats: histologically and immunohistochemically evaluation. Hittite Journal of Science and Engineering. 2019; 6: 215-22.
3. Barnes PJ. Immunology of asthma and chronic obstructive pulmonary disease. Nat Rev Immunol. 2008; 8: 183-92.
4. Holgate ST. Pathogenesis of asthma. Clin Exp Allergy. 2008; 38: 872-97.
5. Wang G, Liu Y, Yang M, Liu S, Ma L, Gong S, et al. Effects of beta-arrestin 2 on cytokine production of CD4+ T lymphocytes of mice with allergic asthma. Indian J Exp Biol. 2011; 49: 585-93.
6. Adler KB, Holden-Stauffer WJ, Repine JE. Oxygen metabolites stimulate release of high-molecular-weight glycoconjugates by cell and organ cultures of rodent respiratory epithelium via an arachidonic acid-dependent mechanism. J Clin Invest. 1990; 85: 75-85.
7. Wood LG, Gibson PG, Garg ML. Biomarkers of lipid peroxidation, airway inflammation and asthma. Eur Respir J. 2003;21:177-86.
8. Manners S, Alam R, Schwartz DA, Gorska MM. A mouse model links asthma susceptibility to prenatal exposure to diesel exhaust. J Allergy Clin Immunol. 2014; 134: 63-72.
9. Gohil KJ, Patel JA, Gajjar AK. Pharmacological Review on Centella asiatica: A Potential Herbal Cure-all. Indian J Pharm Sci. 2010; 72: 546-56.
10. Ali BH, Blunden G. Pharmacological and toxicological properties of Nigella sativa. Phytother Res. 2003; 17: 299-305.
11. Malik S, Ahmad S, Chaudhary I. Nigellimine N-oxide-a new isoquinoline alkaloid from the seeds of Nigella sativa. Heterocycles (Sendai). 1985; 23: 953-5.
12. El Gazzar M, El Mezayen R, Marecki JC, Nicolls MR, Canastar A, Dreskin SC. Anti-inflammatory effect of thymoquinone in a mouse model of allergic lung inflammation. Int Immunopharmacol. 2006; 6: 1135-42.
13. Ammar el-SM, Gameil NM, Shawky NM, Nader MA. Comparative evaluation of anti-inflammatory properties of thymoquinone and curcumin using an asthmatic murine model. Int Immunopharmacol. 2011; 11: 2232-6.
14. Luthria DL. Significance of sample preparation in developing analytical methodologies for accurate estimation of bioactive compounds in functional foods. Journal of the Science of Food and Agriculture. 2006; 86: 2266-72.
15. Youssef MKE, El-Manfaloty MM, Ali HM. Assessment of proximate chemical composition, nutritional status, fatty acid composition and phenolic compounds of carob (Ceratonia siliqua L.). Food and Public Health. 2013; 3: 304-8.
16. Grieger JA, Wood LG, Clifton VL. Improving asthma during pregnancy with dietary antioxidants: the current evidence. Nutrients. 2013; 5: 3212-34.
17. Moura CT, Bezerra FC, de Moraes IM, Magalhães PJ, Capaz FR. Increased responsiveness to 5-hydroxytryptamine after antigenic challenge is inhibited by nifedipine and niflumic acid in rat trachea in vitro. Clin Exp Pharmacol Physiol. 2005; 32: 1119-23.

18. Yang EJ, Lee JS, Song BB, Yun CY, Kim DH, Kim IS. Anti-inflammatory effects of ethanolic extract from Lagerstroemia indica on airway inflammation in mice. J Ethnopharmacol. 2011; 136: 422-7.
19. Casini AF, Ferrali M, Pompella A, Maellaro E, Comporti M. Lipid peroxidation and cellular damage in extrahepatic tissues of bromobenzene-intoxicated mice. Am J Pathol. 1986; 123: 520-31.
20. Miranda KM, Espey MG, Wink DA. A rapid, simple spectrophotometric method for simultaneous detection of nitrate and nitrite. Nitric Oxide. 2001; 5: 62-71.
21. Berger J, Shepard D, Morrow F, Taylor A. Relationship between dietary intake and tissue levels of reduced and total vitamin C in the nonscorbutic guinea pig. J Nutr. 1989; 119: 734-40.
22. Aykaç G, Uysal M, Yalçin AS, Koçak-Toker N, Sivas A, Oz H. The effect of chronic ethanol ingestion on hepatic lipid peroxide, glutathione, glutathione peroxidase and glutathione transferase in rats. Toxicology. 1985; 36: 71-6.
23. Xie QM, Wu X, Wu HM, Deng YM, Zhang SJ, Zhu JP, et al. Oral administration of allergen extracts from Dermatophagoides farinae desensitizes specific allergen-induced inflammation and airway hyperresponsiveness in rats. Int Immunopharmacol. 2008; 8: 1639-45.
24. Schatz M, Dombrowski MP, Wise R, Thom EA, Landon M, Mabie W, et al. Asthma morbidity during pregnancy can be predicted by severity classification. J Allergy Clin Immunol. 2003; 112: 283-8.
25. Bergeron C, Boulet LP. Structural changes in airway diseases: characteristics, mechanisms, consequences, and pharmacologic modulation. Chest. 2006; 129: 1068-87.
26. Elwood W, Lötvall JO, Barnes PJ, Chung KF. Characterization of allergen-induced bronchial hyperresponsiveness and airway inflammation in actively sensitized brown-Norway rats. J Allergy Clin Immunol. 1991; 88: 951-60.
27. Zemmouri H, Sekiou O, Ammar S, El Feki A, Bouaziz M, Messarah M, et al. Urtica dioica attenuates ovalbumin-induced inflammation and lipid peroxidation of lung tissues in rat asthma model. Pharm Biol. 2017; 55: 1561-8.
28. You H, Chen S, Mao L, Li B, Yuan Y, Li R, et al. The adjuvant effect induced by di-(2-ethylhexyl) phthalate (DEHP) is mediated through oxidative stress in a mouse model of asthma. Food Chem Toxicol. 2014; 71: 272-81.
29. Sebai H, Souli A, Chehimi L, Rtibi K, Mohamed A, El-Benna J, et al. In vitro and in vivo antioxidant properties of Tunisian carob (Ceratonia siliqua L.). J Med Plants Res. 2013; 7: 85-90.
30. Abdel-Rahman M, Bauomy AA, Salem FEH, Ahmed Khalifa M. Carob extract attenuates brain and lung injury in rats exposed to waterpipe smoke. Egyptian Journal of Basic and Applied Sciences. 2018; 5: 31-40.
31. Hajhashemi V, Ghannadi A, Jafarabadi H. Black cumin seed essential oil, as a potent analgesic and antiinflammatory drug. Phytother Res. 2004; 18: 195-9.
32. Keyhanmanesh R, Boskabady MH, Khamneh S, Doostar Y. Effect of thymoquinone on the lung pathology and cytokine levels of ovalbumin-sensitized guinea pigs. Pharmacol Rep. 2010; 62: 910-6.
33. Ricciardolo FL, Nijkamp FP, Folkerts G. Nitric oxide synthase (NOS) as therapeutic target for asthma and chronic obstructive pulmonary disease. Curr Drug Targets. 2006; 7: 721-35.
34. Kanter M. Thymoquinone attenuates lung injury induced by chronic toluene exposure in rats. Toxicol Ind Health. 2011; 27: 387-95.
35. El-Mahmoudy A, Matsuyama H, Borgan MA, Shimizu Y, El-Sayed MG, Minamoto N, et al. Thymoquinone suppresses expression of inducible nitric oxide synthase in rat macrophages. Int Immunopharmacol. 2002; 2: 1603-11.
36. d'Uscio LV, Milstien S, Richardson D, Smith L, Katusic ZS. Long-term vitamin C treatment increases vascular tetrahydrobiopterin levels and nitric oxide synthase activity. Circ Res. 2003; 92: 88-95.
37. Fitzpatrick AM, Teague WG, Burwell L, Brown MS, Brown LA; NIH/NHLBI Severe Asthma Research Program. Glutathione oxidation is associated with airway macrophage functional impairment in children with severe asthma. Pediatr Res. 2011; 69: 154-9.
38. Xu L, Olivenstein R, Martin JG, Powell WS. Inhaled budesonide inhibits OVA-induced airway narrowing, inflammation, and cys-LT synthesis in BN rats. J Appl Physiol (1985). 2000; 89: 1852-8.
39. Gvozdjáková A, Kucharská J, Bartkovjaková M, Gazdíková K, Gazdík FE. Coenzyme Q10 supplementation reduces corticosteroids dosage in patients with bronchial asthma. Biofactors. 2005; 25: 235-40.
40. Salama A, Zaki H, Elshenawy S, Denshary E, Ismaiel IE, Sh NM. Effects of fish oil and dexamethasone in experimentally-induced bronchial asthma. Australian journal of basic and applied sciences. 2012; 6: 497-506.
41. Abd El Aziz AE, El Sayed NS, Mahran LG. Anti-asthmatic and anti-allergic effects of thymoquinone on airway-induced hypersensitivity in experimental animals. Journal of Applied Pharmaceutical Science. 2011; 109-17.
42. Güleç Peker EG, Coşkun Ş, Özer Ç, Barbaros Balabanli K, Gönül B. The effect of ascorbic acid supplementation on brain oxidative events in experimental diabetes. Medicinal chemistry research. 2010; 19: 364-74.
43. Sankaranarayanan C, Pari L. Thymoquinone ameliorates chemical induced oxidative stress and β-cell damage in experimental hyperglycemic rats. Chem Biol Interact. 2011; 190: 148-54.
44. Scott NM, Hodyl NA, Murphy VE, Osei-Kumah A, Wyper H, Hodgson DM, et al. Placental cytokine expression covaries with maternal asthma severity and fetal sex. J Immunol. 2009; 182: 1411-20.
45. Murphy VE, Gibson PG, Smith R, Clifton VL. Asthma during pregnancy: mechanisms and treatment implications. Eur Respir J. 2005; 25: 731-50.
46. Goldstein JA, Gallagher K, Beck C, Kumar R, Gernand AD. Maternal-Fetal Inflammation in the Placenta and the Developmental Origins of Health and Disease. Front Immunol. 2020; 11: 531543.
47. Bhaumik S, Lockett J, Saif Z, Lai A, Salomon C, Whitehead JP, et al. The impact of obesity and uncontrolled asthma during pregnancy on metabolic and inflammatory pathways. J Asthma. 2023; 60: 1141-52.
48. Osei-Kumah A, Smith R, Clifton VL. Maternal and cord plasma cytokine and chemokine profile in pregnancies complicated by asthma. Cytokine. 2008; 43: 187-93.
49. Brightling CE, Bradding P, Symon FA, Holgate ST, Wardlaw AJ, Pavord ID. Mast-cell infiltration of airway smooth muscle in asthma. N Engl J Med. 2002; 346: 1699-705.
50. van Overveld FJ, Jorens PG, Rampart M, de Backer W, Vermeire PA. Tumour necrosis factor stimulates human skin mast cells to release histamine and tryptase. Clin Exp Allergy. 1991; 21: 711-4.
51. Coward WR, Okayama Y, Sagara H, Wilson SJ, Holgate ST, Church MK. NF-kappa B and TNF-alpha: a positive autocrine loop in human lung mast cells? J Immunol. 2002; 169: 5287-93.
52. Ying S, Robinson DS, Varney V, Meng Q, Tsicopoulos A, Moqbel R, et al. TNF alpha mRNA expression in allergic inflammation. Clin Exp Allergy. 1991; 21: 745-50.
53. Bradding P, Roberts JA, Britten KM, Montefort S, Djukanovic R, Mueller R, et al. Interleukin-4, -5, and -6 and tumor necrosis factor-alpha in normal and asthmatic airways: evidence for the human mast cell as a source of these cytokines. Am J Respir Cell Mol Biol. 1994; 10: 471-80.

54. El Gazzar MA, El Mezayen R, Nicolls MR, Dreskin SC. Thymoquinone attenuates proinflammatory responses in lipopolysaccharide-activated mast cells by modulating NF-kappaB nuclear transactivation. Biochim Biophys Acta. 2007; 1770: 556-64.
55. Tekeoglu I, Dogan A, Ediz L, Budancamanak M, Demirel A. Effects of thymoquinone (volatile oil of black cumin) on rheumatoid arthritis in rat models. Phytother Res. 2007; 21: 895-7.
56. MacNee W. Accelerated lung aging: a novel pathogenic mechanism of chronic obstructive pulmonary disease (COPD). Biochem Soc Trans. 2009; 37: 819-23.
57. Ebuehi OA, Akande GA. Effect of zinc deficiency on memory, oxidative stress and blood chemistry in rats. International Journal of Biological and Chemical Sciences. 2002; 2: 74-82.
58. Gulay MS, Yildiz-Gulay O, Ata A, Balic A, Demirtas A. Toxicological evaluation of carob (Ceratonia silique) bean extracts in male New Zealand White rabbits. Journal of Animal and Veterinary Advances. 2012; 11: 1853-7.
59. Zago MP, Oteiza PI. The antioxidant properties of zinc: interactions with iron and antioxidants. Free Radic Biol Med. 2001; 31: 266-74.
60. Takeda A, Tamano H, Tochigi M, Oku N. Zinc homeostasis in the hippocampus of zinc-deficient young adult rats. Neurochem Int. 2005; 46: 221-5.

Original Investigation | Özgün Araştırma

GMJ 2024;35:401-406

DOI: http://dx.doi.org/10.12996/gmj.2024.4178

Effects of Aerobic Exercise on Leukocyte-Mediated Liver Destruction in a Rat Model of Metabolic Syndrome

Metabolik Sendromlu Sıçan Modelinde Aerobik Egzersizin Lökosit Aracılı Karaciğer Tahribatı Üzerindeki Etkileri

Fatmanur Er[1], Leyla Çimen[2], Ceren Suveren[3], Canan Yılmaz[4], Nurten Türközkan*

[1]Department of Action and Training, Atatürk University Faculty of Sports Sciences, Erzurum, Türkiye
[2]Department of Medical Biochemistry, Faculty of Medicine, Gaziantep Islam Science and Technology University, Gaziantep, Türkiye
[3]Department of Training Sciences, Gazi University Faculty of Sports Sciences, Ankara, Türkiye
[4]Department of Biochemistry, Faculty of Medicine, Gazi University, Ankara, Türkiye
*Retired

ABSTRACT

Objective: In this study, the levels of malondialdehyde (MDA), myeloperoxidase (MPO), and 3-nitrotyrosine (3-NT), which are known as oxidative/nitrosative stress markers, were investigated in the liver tissues of rats with metabolic syndrome model induced by a high fructose diet, and the possible protective effects of aerobic exercise in fructose-fed rats were determined.

Methods: Rats were divided into four groups: control, fructose, exercise, and fructose plus exercise. Metabolic syndrome was induced in rats using 20% (w/v) fructose solution in tap water, and exercise was administered every day at the same hour for an experimental period of 8 weeks in total, 30 min a day, five days a week. After eight weeks, systolic blood pressure (SBP), serum lipid, glucose, insulin, MDA MPO, and 3-NT levels were quantified.

Results: The metabolic syndrome model was successfully demonstrated by fructose administration. Compared with the C group, F caused a significant increase in SBP, serum insulin, and triglyceride levels and liver MDA, MPO, and 3-NT levels. Exercise counteracted and healed the changes in SBP, serum insulin, triglyceride, and liver MDA, MPO, and 3-NT levels in fructose-fed rats ($p<0.05$).

Conclusion: These results indicate that high fructose consumption causes metabolic syndrome in rats, and aerobic exercise has beneficial effects on the components of metabolic syndrome. Exercise not only reduces the known risk factors of the disease, but also protects the liver while preventing oxidative and nitrosative damage caused by the MPO-H_2O_2 system in the liver, which increases with the effect of

ÖZ

Amaç: Bu çalışmada, yüksek fruktozlu diyetle metabolik sendrom modeli oluşturulan sıçanların karaciğer dokularında oksidatif/nitrosatif stres belirteçleri olarak bilinen malondialdehit (MDA), miyeloperoksidaz (MPO) ve 3-nitrotirozin (3-NT) düzeyleri araştırılmış ve fruktozla beslenen sıçanlarda aerobik egzersizin olası koruyucu etkileri belirlenmiştir.

Yöntemler: Sıçanlar dört gruba ayrıldı: kontrol, fruktoz, egzersiz ve fruktoz artı egzersiz. Sıçanlarda metabolik sendrom musluk suyunda %20 (ağırlık/hacim) fruktoz çözeltisi kullanılarak oluşturuldu ve egzersiz, toplamda 8 haftalık deneysel bir süre boyunca her gün aynı saatte, haftada beş gün, günde 30 dakika uygulandı. Sekiz hafta sonra sistolik kan basıncı (SBP), serum lipid, glikoz, insülin, MDA, MPO ve 3-NT düzeyleri ölçüldü.

Bulgular: Metabolik sendrom modeli fruktoz uygulamasıyla başarılı bir şekilde gösterildi. Fruktoz grubu kontrol grubuyla karşılaştırıldığında, SBP, serum insülin ve trigliserit düzeylerinde ve karaciğer MDA, MPO ve 3-NT düzeylerinde önemli bir artışa neden oldu. Egzersiz, fruktozla beslenen sıçanlarda SBP, serum insülin, trigliserit ve karaciğer MDA, MPO ve 3-NT düzeylerindeki değişiklikleri dengeledi ve iyileştirdi ($p<0,05$).

Sonuç: Bu çalışma yüksek fruktoz tüketiminin sıçanlarda metabolik sendroma neden olduğunu ve aerobik egzersizin metabolik sendromun bileşenleri üzerinde yararlı etkileri olduğunu göstermektedir. Egzersiz sadece hastalığın bilinen risk faktörlerini azaltmakla kalmaz, aynı zamanda karaciğeri korurken karaciğerde fruktozun etkisiyle artan ve alkolsüz yağlı karaciğer hastalığının oluşumu için gerekli olan MPO-

Address for Correspondence/Yazışma Adresi: Fatmanur Er, MD, Department of Action and Training, Atatürk University Faculty of Sports Sciences, Erzurum, Türkiye
E-mail / E-posta: fatmanur.er@atauni.edu.tr
ORCID ID: orcid.org/0000-0002-9203-4974

Received/Geliş Tarihi: 29.03.2024
Accepted/Kabul Tarihi: 28.08.2024

fructose and is necessary for the formation of non-alcoholic fatty liver disease.

Keywords: Metabolic syndrome, non-alcoholic fatty liver disease, malondialdehyde, myeloperoxidase, 3-nitrotyrosine

H_2O_2 sisteminin neden olduğu oksidatif ve nitrozatif hasarı önlediği söylenebilir.

Anahtar Sözcükler: Metabolik sendrom, non-alkolik yağlı karaciğer hastalığı, malondialdehit, miyeloperoksidaz, 3-nitrotirozin

INTRODUCTION

Metabolic syndrome, also known as syndrome X, is a disease characterized by abdominal obesity, hypertension, hypertriglyceridemia, and insulin resistance. Metabolic syndrome is not a single disease; it is a significant risk factor for other conditions, such as cardiovascular disease, obesity, and type II diabetes. In addition, the critical risk factor for non-alcoholic fatty liver disease (NAFLD) is metabolic syndrome. One of the essential causes of metabolic syndrome is excessive intake of F and high fructose corn syrup (1-3). Humans and animals that are administered fructose develop the criteria of metabolic syndrome. There is much evidence that excess fructose intake has defective effects on liver function (3-5). Fructose consumption is considered a risk factor in metabolic syndrome as a lipogenic compound and accumulates in the liver; the critical marker of NAFLD is hepatic triglyceride accumulation (6,7).

NAFLD is known for hepatic and systemic insulin resistance and dyslipidemia. Accumulating evidence supports that NAFLD is often referred to as a hepatic manifestation of metabolic syndrome. The first step in NAFLD is hepatic steatosis, which can then progress to steatohepatitis, hepatic fibrosis, and cirrhosis (6,8-10). It has been reported that insulin resistance may be a significant risk factor, and it leads to defects in fatty acid accumulation. As a result of high amounts of lipid in hepatocytes, steatosis and inflammation may be observed in the liver (11,12). Although the pathogenesis of NAFLD is not well understood, it has been suggested that inflammatory mediators play a central role in inflammation and fibrosis (13). On the other hand, neutrophils are the critical and first type of immune cells that respond to liver inflammatory changes. It has been reported that neutrophils are implicated in metabolic dysregulation, inflammation, and fibrosis of NAFLD development (14).

Myeloperoxidase (MPO) is a heme peroxidase found in leukocytes. It is stored in cytoplasmic granules and, due to phagocytic activation, is released into the extracellular compartment. It has been reported that MPO is defined-as an early marker of inflammation and oxidative stress. There is a relationship between chronic inflammation, insulin resistance, and increased MPO activity (15-18). To date, it has been reported that there is no safe and effective pharmacotherapy for the treatment of NAFLD (7). Investigators recommend lifestyle modification such as dietary modification and regular physical activity, for the management of NAFLD. It has been reported that physical exercise may be effective against NAFDL through insulin resistance, reduces excess delivery synthesis to the liver, and increases fatty acid oxidation (19-21).

It has been reported that physical exercise may be effective on NAFLD through various pathways. It improves peripheral insulin resistance, reduces the excess delivery of fatty acids and glucose for free acids synthesis to the liver, and increases fatty acid oxidation (19-21). Little is known about the role of leucocyte sequestration in fructose-induced metabolic syndrome model in both mechanisms of MPO-mediated tyrosine nitration and lipid peroxidation in NAFLD. In addition, we did not find evidence that regular exercise improves MPO-mediated tissue damage in NAFLD in rat' fructose-induced metabolic syndrome model. Therefore, our study to evaluate the effect of regular aerobic exercise on leukocyte-mediated liver tissue damage in metabolic syndrome-induced NAFLD.

MATERIALS AND METHODS

Adult Sprague-Dawley male rats were purchased from the Gazi University Laboratory Animals Raising and Experimental Research Center. Ethical approval was received from Gazi University Animal Experiments Local Ethics Committee (approval number: E-66332047-604.01.02-786048, date: 01.11.2023). Four groups were created with six experimental animals in each group. During the eight weeks, animals that were fed a standard rat diet, were housed on a 12:12 h light: Dark cycle and free access to food and drinking.

Control (C): Untreated normal control group.

Fructose (F): This group, until the end of the eighth weeks, were fed fresh, prepared 20% fructose in tap water. There were also no restrictions on drinking water either (22,23).

Exercise (E): Running exercise was administered to the animals every day using a treadmill at the same hour for a study period of 8 weeks, 30 min a day, five days a week (24).

Fructose + exercise (F + E): Animals in this group, during the study, both fructose was given and treadmill running exercise was applied (24).

All rats' weights were recorded weekly, and systolic blood pressures (SBP) were measured with the tail-cuff sphygmomanometer method at the beginning of the study, at the end of week 4, and at the end of week 8 (24). At the end of eight weeks, the animals were sacrificed under ketamine-xylazine anesthesia. Intracardiac blood samples were collected, serum was separated, and rat liver tissue were taken and stored at -80 °C until analysis.

Biochemical Measurement

Serum glucose and triglyceride concentrations were measured using standard enzymatic methods with AU5800 clinical chemistry autoanalyzer (Beckman Coulter, USA). Serum insulin concentrations were measured by using an ELISA kit (Millipore, Billerica, MA). Insulin resistance calculated by Homeostasis Model Assessment of Insulin Resistance Index [(HOMA-IR):Fasting insulin (mU/L)*fasting glucose (mmol/L)/22.5]. Liver tissue MPO activity was determined by Schierwagen et al. (25) method. The liver MDA amount was measured with the HPLC method (26). For 3-nitrotyrosine (3-NT) measurements in the liver, tissue homogenates were prepared according to the method described by Kamisaki et al. (27). Liver tissue 3-NT levels were detected on HPLC with a UV detector set at 274 nm as (28).

Statistical Analysis

All statistical analyses were performed using "IBM SPSS Statistics 24" statistical package software (SPSS Inc., Chicago, IL). The Kolmogorov-Smirnov test was used to determine whether continuous variable distributions were normal. Since study groups did not show a normal distribution were used Kruskal-Wallis analysis and Comparisons between groups were performed using the Mann-Whitney U test. More than two measurements in a single group the Friedman Variance analysis is used to determine changes over time. Probability values of less than 0.05 were accepted as significant.

RESULTS

The body weights and SBP are given in Table 1. The body weights of F group were higher compared with the E and F + E groups (p<0.05, p=0.004; p=0.032). The SBF value of the F group was higher than that of the C group (p<0.05, p=0.004). Furthermore, the SBF of the F group was higher compared with the E and the F + E groups (p<0.05, p=0.001; p=0.014).

Biochemical parameters, triglyceride, glucose, insulin and HOMA-IR values are given in Table 2. The serum triglyceride levels of the F group were significantly higher compared with the C, E and F + E groups (p<0.05, p=0.045; p=0.008; p=0.004). Compared with the F group, the serum glucose and insulin levels and HOMA-IR indexes were significantly higher compared with the C and E groups (p<0.05, p=0.004; p=0.008). In addition, as shown in Table 2, a statistically significantly higher in the HOMA-IR values of the F group was compared with the F + E group levels (p<0.05, p=0.004); however, C and E groups were significantly lower compared with the F + E group (p<0.05, p=0.002; p=0.004).

The liver MDA, MPO, and 3-NT levels of the four groups were indicated in Table 3. Compared with the F group, the MDA, MPO, and 3-NT levels in the F group were higher compared with the C and E groups (p<0.05, p=0.001). The MDA levels of the F + E group was higher compared with the C group (p<0.05, p=0.020). As can be seen in Table 3, 3-NT levels were detected clearly in the liver tissue of animals exposed to fructose, whereas 3-NT was not detected in the liver tissue of control and exercise animals.

DISCUSSION

In our study, hypertension, hypertriglyceridemia, insulin resistance, and blood insulin values, which are accepted as metabolic syndrome criteria, increased in rats after fructose administration. Thus, the metabolic syndrome model was successfully realized. In addition to being associated with cardiovascular diseases and type II diabetes, metabolic syndrome has been considered an essential risk factor for NAFLD in recent years (9,11). However, the sedentary life of our age increases the frequency of metabolic syndrome and its hepatic component, NAFLD, day by day.

Table 1. Body weights and systolic blood pressures of groups

Group	Body weight (g)		Systolic blood pressure (mmHg)		
	Beginning	End	Beginning	4th week	8th week
Control	208.66±8.213	251.83±8.232*	128.33±3.204	124.30±7.437	121.81±6.635
Fructose	217.4±8.734	279.2±20.166*	126.6±6.066	139.75±3.869	176.57±4.280*[a]
Exercise	215.2±4.266	234.6±3.646*[b]	124.2±4.658	118.26±6.753[b]	117.13±5.907[b]
Fructose + exercise	200.83±4.266[b]	240.5±3.646*[b]	121.83±7.277	122.62±6.593	133.17±8.443[#]

[a]p<0.05 compare with the control group, [b]p<0.05 compere with the fructose group, [c]p<0.05 compare with the exercise group, [d]p<0.05 compare with the fructose plus exercise group, [*]p<0.05 systolic blood pressures compared with initial values, [#]p<0.05 systolic blood pressures compared with 4th week values.

Table 2. Biochemical parameters of groups

Group	Glucose (mmol/L)	Triglyceride, (mg/dL)	Insulin, (mU/L)	HOMA-IR
Control	9,293±0.172	35.66±5,278	4,518±0.561	1.86±0.215
Fructose	13.41±1,064[a]	62.74±7,483[a]	12.36±1,236[a]	7.34±0.618[a]
Exercise	9.46±0.478[b]	35.64±4,375[b]	4.71±0.723[b]	1.97±0.287[b]
Fructose + exercise	10.62±1,040	34.16±7,359[b]	8.25±1,459	3.94±1,045[a,b,c]

[a]p<0.05 compare with the control group, [b]p<0.05 compere with the fructose group, [c]p<0.05 compare with the exercise group, [d]p<0.05 compare with the fructose plus exercise group, HOMA-IR: Homeostasis Model Assessment of Insulin Resistance.

Table 3. Biochemical parameters of groups

Group	MDA, nmol/g tissue	MPO, U/min/g tissue	3-NT, nmol/g tissue
Control	0.03±0.002	7.1±0.296	Not detectable
Fructose	1.22±0.081a	19.03±0.280a	4.01±0.067
Exercise	0.03±0.003b	7.26±0.233b	Not detectable
Fructose + exercise	0.52±0.085a	11.9±0.352	1.94±0.100

[a]p<0.05 compare with the control group, [b]p<0.05 compere with the fructose group, [c]p<0.05 compare with the exercise group, [d]p<0.05 compare with the fructose plus exercise group, MDA: Malondialdehyde, MPO: Myeloperoxidase, 3-NT: 3-nitrotyrosine.

NAFLD is a liver disease characterized by excessive fat storage in liver cells. In some cases, NAFLD is a pathological condition that progresses from steatosis to steatohepatitis, fibrosis, and end-stage liver disease (cirrhosis). Triglycerides accumulated in the liver cause hepatocyte stress, resulting in inflammation and cell death (7,12). Chemokines and cytokines released from dying cells activate immune cells such as neutrophils and macrophages. Inactivated neutrophils trigger a respiratory burst event, and free oxygen radicals that cause liver tissue destruction are formed (29,30). Although there are many factors in the development of NAFLD, oxidative stress and insulin resistance are considered the main problems. Although there have been various studies on the pathogenesis of NAFLD, it is still among the subjects that still need to be fully elucidated. The first step in the pathogenesis is the formation of steatosis, followed by the addition of inflammation. The neutrophil count has been reported to be important in the development and progression of NAFLD, and it has been suggested that these cells are essential markers of chronic inflammation. A relationship exists between NAFLD, insulin resistance, and neutrophil count (31,32).

In this study, to determine the oxidative/nitrosative stress that may be caused by a fructose diet, the levels of MDA, MPO, which is an indicator of lipid peroxidation, and 3-NT, which is a marker of protein nitration, and the effect of exercise on these parameters in liver tissue were investigated.

MPO is a cytoplasmic heme peroxidase found in neutrophil granules. The enzyme released into the extracellular compartment during phagocytic activation has been accepted as the earliest marker of inflammation and oxidative stress (15-18). Researchers have emphasized a close relationship between ROS production by MPO and inflammation and tissue destruction observed in chronic inflammatory diseases (29,33). Rensen et al. (33) revealed that the number of neutrophils increased in NAFLD and MPO activity and expression in the detected inflammation. Our study observed a significant increase in MPO activity in fructose-mediated metabolic syndrome rat livers. Our results follow those of other investigators working on this subject (29,33).

In various pathologies, measuring MDA in biological samples is a reliable indicator of radical production (34). It is known that fructose administration generally produces a prooxidant environment and renders cell membranes vulnerable to peroxidative damage. Lipid peroxidation is a critical process for atherogenesis, and the development of hypertension, and the products formed from that place may also contribute to tissue damage through direct cytotoxic effects (35). It has been reported that MDA levels, an indicator of lipid peroxidation, are significantly increased in various tissues of rodents administered a high fructose diet (34,36,37). Our model observed that the amount of MDA, a lipid peroxidation product, increased in parallel with an increase in hepatic MPO by a fructose diet. da Fonseca et al. (38) found lipid peroxidation increased in the plasma of patients diagnosed with metabolic syndrome due to an increase in MPO. Hendriks and Bunder reported that fatty acids are enzymatically subjected to lipid peroxidation. Enzymes such as MPO and lipoxygenase are responsible for this and the increase in MDA in the tissue. Thus, they stated that lipids lose their properties and cause liver tissue destruction in NAFLD (30).

In this study, 3-NT levels, which is an indicator of protein nitration in tissues, were examined, and it was observed that 3NT, a marker of nitrosative damage in tissues, could not be detected in the liver tissue of the control group. In contrast, it showed a significant increase after fructose administration. 3NT occurs as a result of the nitration of protein-bound and free tyrosine residues with reactive peroxynitrite and causes protein modifications (39). Nitrosative modifications of proteins cause fragmentation, increased crosslinking, and aggregation and may lead to irreversible loss of function in enzyme and receptor proteins due to nitration (40). As in our results, it was determined by immunohistochemical methods that 3-NT staining was significantly increased in various tissues of rodents administered a fructose diet in previous studies (40-42). In a survey by Ahsan (39), he emphasized that 3NT is formed by catalysis of a class of peroxidases using H_2O_2 and nitrite as substrates and may be an essential marker in tissue destruction. It has been reported that activated macrophages form superoxide and NO, then the two combine to form peroxynitrite, and this peroxynitrite nitrifies the amino acid tyrosine to form 3NT (43).

3-NT is a peroxynitrite-mediated pathological marker. Again, Rensen et al. (33) demonstrated the presence of hypocrisy-modified proteins in the liver of patients with NAFLD and showed that this was mediated through the MPO-H_2O_2 system and ultimately led to nitrite accumulation in the tissue.

All of these results support our findings. The main aim of our study was to administer fructose only to one group of rats. In contrast, in a fructose-mediated metabolic syndrome model, the other group received exercise training with fructose for eight weeks to examine its effect on MPO-mediated oxidative and nitrosative stress in the liver.

In a previous study, we applied the same exercise in a metabolic syndrome model that we created under the same conditions and observed that fructose-mediated increased hypertension decreased, blood triglyceride and insulin levels decreased, and insulin resistance, which is very important in NAFLD, was regulated (44). In this study, in our fructose-mediated metabolic syndrome model, it was observed that the increased liver MPO activity after treatment running exercise decreased significantly compared to the values in the fructose group, even if it did not decrease to the level of the control group. In the literature, researchers have reported that physical exercise prevents hepatic stethocin development and does this by stimulating lipid oxidation and inhibiting lipid synthesis (20). In another similar study, researchers emphasized that regular moderate aerobic exercise increases the killing capacity of neutrophils and makes the organism resistant to infection. In contrast, long periods of heavy exercise may significantly reduce neutrophil activation and decrease the resistance of organisms to infections (45).

As seen from all these results, the treatment running aerobic exercise we applied in our study was appropriate regarding dose and period. On the one hand, it prevented the oxidative and nitrosative damage caused by the MPO-H_2O_2 system, which increases with the effect of fructose in the liver and is vital for forming NAFLD. On the other hand, it protects cell resistance mechanisms against infections by keeping this system balanced.

Study Limitations

Finally, there are some limitations to this study. First, It may not be possible for the animal models used to create complex models such as MetS to fully resemble human physiology. The second limitation is that the duration sufficient in animal models for the MetS model may not fully reflect the chronic processes seen in humans. In addition, another limitation of the study is that practices such as diet and exercise applied to animals may affect the validity as they create an environment different from the animals' natural environment.

CONCLUSION

More human and animal studies with larger sample sizes and longer follow-up periods are needed to compare the long-term effects of exercise therapy in patients with MetS.

Ethics

Ethics Committee Approval: Adult Sprague-Dawley male rats were purchased from the Gazi University Laboratory Animals Raising and Experimental Research Center. Ethical approval was received from Gazi University Animal Experiments Local Ethics Committee (approval number: E-66332047-604.01.02-786048, date: 01.11.2023).

Informed Consent: Patient approval has not been obtained as it is performed on animals.

Authorship Contributions

Concept: F.E., L.Ç., C.S., C.Y., N.T., Design: F.E., C.Y., N.T., Supervision: F.E., L.Ç., C.S., C.Y., N.T., Resources: F.E., C.Y., Materials: F.E., C.Y., N.T., Data Collection or Processing: F.E., C.Y., N.T., Analysis or Interpretation: F.E., L.Ç., C.S., C.Y., N.T., Literature Search: F.E., C.Y., Writing: F.E., N.T., Critical Review: F.E., L.Ç., C.S., C.Y., N.T.

Conflict of Interest: No conflict of interest was declared by the authors.

Financial Disclosure: The authors declared that this study received no financial support.

REFERENCES

1. Saklayen MG. The Global Epidemic of the Metabolic Syndrome. Curr Hypertens Rep. 2018; 20: 12.
2. Wainwright P, Byrne CD. Bidirectional Relationships and Disconnects between NAFLD and Features of the Metabolic Syndrome. Int J Mol Sci. 2016; 17: 367.
3. Stanhope KL, Goran MI, Bosy-Westphal A, King JC, Schmidt LA, Schwarz JM, et al. Pathways and mechanisms linking dietary components to cardiometabolic disease: thinking beyond calories. Obes Rev. 2018; 19: 1205-35.
4. Hannou SA, Haslam DE, McKeown NM, Herman MA. Fructose metabolism and metabolic disease. J Clin Invest. 2018; 128: 545-55.
5. Softic S, Cohen DE, Kahn CR. Role of Dietary Fructose and Hepatic De Novo Lipogenesis in Fatty Liver Disease. Dig Dis Sci. 2016; 61: 1282-93.
6. Alex S, Boss A, Heerschap A, Kersten S. Exercise training improves liver steatosis in mice. Nutr Metab (Lond). 2015; 12: 29.
7. Reddy AJ, George ES, Roberts SK, Tierney AC. Effect of dietary intervention, with or without co-interventions, on inflammatory markers in patients with nonalcoholic fatty liver disease: a systematic literature review. Nutr Rev. 2019; 77: 765-86.
8. Saremi L, Lotfıpanah S, Mohammadi M, Hosseinzadeh H, Hosseini-Khah Z, Johari B, et al. Association between PPARGC1A single nucleotide polymorphisms and increased risk of nonalcoholic fatty liver disease among Iranian patients with type 2 diabetes mellitus. Turk J Med Sci. 2019; 49: 1089-94.
9. Pierantonelli I, Svegliati-Baroni G. Nonalcoholic Fatty Liver Disease: Basic Pathogenetic Mechanisms in the Progression From NAFLD to NASH. Transplantation. 2019; 103: e1-13.
10. Satapathy SK, Sanyal AJ. Epidemiology and Natural History of Nonalcoholic Fatty Liver Disease. Semin Liver Dis. 2015; 35: 221-35.
11. Saadeh S. Nonalcoholic Fatty liver disease and obesity. Nutr Clin Pract. 2007; 22: 1-10.
12. Lim JW, Dillon J, Miller M. Proteomic and genomic studies of non-alcoholic fatty liver disease--clues in the pathogenesis. World J Gastroenterol. 2014; 20: 8325-40.
13. Gao B, Tsukamoto H. Inflammation in Alcoholic and Nonalcoholic Fatty Liver Disease: Friend or Foe? Gastroenterology. 2016; 150: 1704-9.
14. Ou R, Liu J, Lv M, Wang J, Wang J, Zhu L, et al. Neutrophil depletion improves diet-induced non-alcoholic fatty liver disease in mice. Endocrine. 2017; 57: 72-82.
15. Arnhold J. The Dual Role of Myeloperoxidase in Immune Response. Int J Mol Sci. 2020; 21: 8057.
16. Zaki M, Basha W, Reyad H, Mohamed R, Hassan N, Kholousi S. Association between Myeloperoxidase Levels and Risk of Insulin Resistance in Egyptian Obese Women. Open Access Maced J Med Sci. 2018; 6: 629-33.
17. Garagiola ML, Tarán M, Scribano MP, Balceda A, García E, Fonseca I et al. Myeloperoxidase as an indicator of oxidative stress in metabolic syndrome. Revista Argentina de Cardiología 2016; 84: 514.
18. Ndrepepa G. Myeloperoxidase - A bridge linking inflammation and oxidative stress with cardiovascular disease. Clin Chim Acta. 2019; 493: 36-51.
19. Ahmed IA, Mikail MA, Mustafa MR, Ibrahim M, Othman R. Lifestyle interventions for non-alcoholic fatty liver disease. Saudi J Biol Sci. 2019; 26: 1519-24.
20. Lavoie JM, Gauthier MS. Regulation of fat metabolism in the liver: link to non-alcoholic hepatic steatosis and impact of physical exercise. Cell Mol Life Sci. 2006; 63: 1393-409.
21. van der Windt DJ, Sud V, Zhang H, Tsung A, Huang H. The Effects of Physical Exercise on Fatty Liver Disease. Gene Expr. 2018; 18: 89-101.
22. de Moura RF, Ribeiro C, de Oliveira JA, Stevanato E, de Mello MA. Metabolic syndrome signs in Wistar rats submitted to different high-fructose ingestion protocols. Br J Nutr. 2009; 101: 1178-84.
23. Nakagawa T, Hu H, Zharikov S, Tuttle KR, Short RA, Glushakova O, et al. A causal role for uric acid in fructose-induced metabolic syndrome. Am J Physiol Renal Physiol. 2006; 290: F625-31.
24. Sebai M, Lu S, Xiang L, Hester RL. Improved functional vasodilation in obese Zucker rats following exercise training. Am J Physiol Heart Circ Physiol. 2011; 301: H1090-6.
25. Schierwagen C, Bylund-Fellenius AC, Lundberg C. Improved method for quantification of tissue PMN accumulation measured by myeloperoxidase activity. J Pharmacol Methods. 1990; 23: 179-86.
26. Tukozkan N, Erdamar H, Seven I. Measurement of total malondialdehyde in plasma and tissues by high-performance liquid chromatography and thiobarbituric acid assay. Firat Med J. 2006;11: 88.
27. Kamisaki Y, Wada K, Nakamoto K, Kishimoto Y, Kitano M, Itoh T. Sensitive determination of nitrotyrosine in human plasma by

isocratic high-performance liquid chromatography. J Chromatogr B Biomed Sci Appl. 1996; 685: 343-7.

28. Türközkan N, Ozan G, Bircan FS, Şahin N. Effect of Taurine on Liver Xanthine Oxidase Activity and 3-Nitrotyrosine Level in Endotoxemia. Gazi Medical Journal. 2011; 22: 14-7.
29. Hwang S, Yun H, Moon S, Cho YE, Gao B. Role of Neutrophils in the Pathogenesis of Nonalcoholic Steatohepatitis. Front Endocrinol (Lausanne). 2021; 12: 751802.
30. Hendrikx T, Binder CJ. Oxidation-Specific Epitopes in Non-Alcoholic Fatty Liver Disease. Front Endocrinol (Lausanne). 2020; 11: 607011.
31. Mendez-Sanchez N, Cruz-Ramon VC, Ramirez-Perez OL, Hwang JP, Barranco-Fragoso B, Cordova-Gallardo J. New Aspects of Lipotoxicity in Nonalcoholic Steatohepatitis. Int J Mol Sci. 2018; 19: 2034.
32. Hotamisligil GS. Inflammation and metabolic disorders. Nature. 2006; 444: 860-7.
33. Rensen SS, Slaats Y, Nijhuis J, Jans A, Bieghs V, Driessen A, et al. Increased hepatic myeloperoxidase activity in obese subjects with nonalcoholic steatohepatitis. Am J Pathol. 2009; 175: 1473-82.
34. Polizio AH, Gonzales S, Muñoz MC, Peña C, Tomaro ML. Behaviour of the anti-oxidant defence system and heme oxygenase-1 protein expression in fructose-hypertensive rats. Clin Exp Pharmacol Physiol. 2006; 33: 734-9.
35. Bhagya D, Prema L, Rajamohan T. Therapeutic effects of tender coconut water on oxidative stress in fructose fed insulin resistant hypertensive rats. Asian Pac J Trop Med. 2012; 5: 270-6.
36. Nandhini AT, Thirunavukkarasu V, Ravichandran MK, Anuradha CV. Effect of taurine on biomarkers of oxidative stress in tissues of fructose-fed insulin-resistant rats. Singapore Med J. 2005; 46: 82-7.
37. Crescenzo R, Bianco F, Falcone I, Coppola P, Liverini G, Iossa S. Increased hepatic de novo lipogenesis and mitochondrial efficiency in a model of obesity induced by diets rich in fructose. Eur J Nutr. 2013; 52: 537-45.
38. da Fonseca LJ, Nunes-Souza V, Guedes Gda S, Schettino-Silva G, Mota-Gomes MA, Rabelo LA. Oxidative status imbalance in patients with metabolic syndrome: role of the myeloperoxidase/hydrogen peroxide axis. Oxid Med Cell Longev. 2014; 2014: 898501.
39. Ahsan H. 3-Nitrotyrosine: A biomarker of nitrogen free radical species modified proteins in systemic autoimmunogenic conditions. Hum Immunol. 2013; 74: 1392-9.
40. Pooranaperundevi M, Sumiyabanu MS, Viswanathan P, Sundarapandiyan R, Anuradha CV. Insulin resistance induced by a high-fructose diet potentiates thioacetamide hepatotoxicity. Singapore Med J. 2010; 51: 389-98.
41. Kannappan S, Palanisamy N, Anuradha CV. Suppression of hepatic oxidative events and regulation of eNOS expression in the liver by naringenin in fructose-administered rats. Eur J Pharmacol. 2010; 645: 177-84.
42. Rajasekar P, Viswanathan P, Anuradha CV. Beneficial impact of L-carnitine in liver: a study in a rat model of syndrome X. Amino Acids. 2008; 35: 475-83.
43. Pfeiffer S, Lass A, Schmidt K, Mayer B. Protein tyrosine nitration in cytokine-activated murine macrophages. Involvement of a peroxidase/nitrite pathway rather than peroxynitrite. J Biol Chem. 2001; 276: 34051-8.
44. Er F, Zorba E, Günay M, Koz M, Yılmaz C, Paşaoğlu ÖT, et al. Effect of Exercise and Quercetin in Rats with Metabolic Syndrome Induced with Fructose. Metab Syndr Relat Disord. 2022; 20: 57-66.
45. Smith JA, Telford RD, Mason IB, Weidemann MJ. Exercise, training and neutrophil microbicidal activity. Int J Sports Med. 1990; 11: 179-87.

Original Investigation | Özgün Araştırma

GMJ 2024;35:407-415

DOI: http://dx.doi.org/10.12996/gmj.2024.4191

Comparison and Evaluation of the Effectiveness of Traditional Neuroanatomy Teaching in Medical Education with Virtual-Reality Application Based On 3D Virtual

Tıp Eğitiminde Geleneksel Nöroanatomi Öğretiminin Etkinliğinin 3 Boyutlu Sanal Gerçekliğe Dayalı Uygulama ile Karşılaştırılması ve Değerlendirilmesi

Ece Alim[1-3], Özlem Coşkun[4], Tuncay Veysel Peker[1]

[1]Department of Anatomy, Gazi University Faculty of Medicine, Ankara, Türkiye
[2]College of Arts and Sciences, Florida Gulf Coast University, Florida, United States of America
[3]Neuroscience and Neurotechnology Center of Excellence NÖROM, Ankara, Türkiye
[4]Department of Medical Education and Informatics, Gazi University Faculty of Medicine, Ankara, Türkiye

ABSTRACT

Objective: Learning neuroanatomical structures is difficult in traditional medical education. Knowledge and visual materials in neuroanatomy books or atlases are static and limited to two dimensions. The limitations of cadaver and plastic models have been overcome by developing three-dimensional (3D) anatomical models using digital visualization technologies. Medical students are better able to understand the spatial topography of a large number of neuroanatomical structures that are condensed into a small region when they use 3D visualization technologies, such as virtual reality (VR) and augmented reality. In our study, which will provide a new window to classical neuroanatomy education, we aimed to evaluate how much 3D neuroanatomical models based on VR applications affect the success and motivation of medical school students enrolled in neuroanatomy courses.

Methods: For this purpose, four exams were given to second-year medical faculty students before the classical theoretical course, after the theoretical course, after VR training and application, and six months later to evaluate the long-term effects of the training.

Results: The success averages were assessed on a scale of 10; the average score was 3.38 for students who participated in the evaluation after traditional theoretical training and 4.55 for the VR training group. In the long-term evaluation after six months, the average score was found to be higher in the VR training group.

Conclusion: Our study contributes to the literature by demonstrating the positive long-term effects of VR-based neuroanatomy training on memory.

Keywords: Neuroanatomy, medical education, virtual reality, augmented reality, anatomic models, long-term effects

ÖZ

Amaç: Geleneksel tıp eğitiminde nöroanatomik yapıları öğrenmek zordur. Nöroanatomi kitaplarında veya atlaslarında bulunan bilgi ve görsel materyaller statik olup iki boyutla sınırlıdır. Kadavra ve plastik modellerin kısıtlılığı, dijital görselleştirme teknolojileri kullanılarak üç boyutlu (3D) anatomik modellerin geliştirilmesiyle çözülmüştür. Tıp öğrencileri, sanal gerçeklik (VR) ve artırılmış gerçeklik gibi 3D görselleştirme teknolojilerinden yararlandıklarında, küçük bir bölgeye yoğunlaştırılmış birçok nöroanatomik yapıların uzamsal topografisini daha iyi anlayabilirler. Klasik nöroanatomi eğitimine yeni bir pencere açacak olan çalışmamızda, VR uygulamasına dayalı 3D nöroanatomik modellerin, tıp fakültesi öğrencilerinin nöroanatomi derslerindeki başarı ve motivasyonunu ne kadar etkilediğini değerlendirmeyi amaçladık.

Yöntemler: Bu amaçla, ikinci sınıf tıp fakültesi öğrencilerine klasik teorik ders öncesinde, teorik ders sonrasında, VR eğitimi ve uygulaması sonrasında ve eğitimin uzun vadeli etkilerini değerlendirmek için altı ay sonra olmak üzere toplam dört sınav yapıldı.

Bulgular: Başarı ortalamaları 10 üzerinden değerlendirilmiştir; geleneksel teorik eğitim sonrası değerlendirmeye katılan öğrenciler için ortalama puan 3,38, VR eğitimi grubunda ise 4,55 olmuştur. Altı ay sonraki uzun vadeli değerlendirmede, VR eğitimi grubunun ortalama puanı daha yüksek bulunmuştur.

Sonuç: Çalışmamız, VR tabanlı nöroanatomi eğitiminin hafıza üzerindeki olumlu uzun vadeli etkilerini göstererek literatüre katkı sağlayacaktır.

Anahtar Sözcükler: Nöroanatom, tıp eğitimi, sanal gerçeklik, artırılmış gerçeklik, anatomik modeller, uzun vadeli etkiler

Address for Correspondence/Yazışma Adresi: Ece Alim, MD, Department of Anatomy, Gazi University Faculty of Medicine, Ankara, Türkiye
E-mail / E-posta: ece.alim06@gmail.com
ORCID ID: orcid.org/0000-0002-4686-0677

Received/Geliş Tarihi: 18.04.2024
Accepted/Kabul Tarihi: 01.08.2024

INTRODUCTION

Due to the increasing effect of technological development, 21st-century anatomy education has undergone dynamic changes compared to traditional anatomy education in the 19th and 20th centuries. On the other hand, the increase in the number of students applying to medical schools and changes in the anatomy curriculum (1) have caused a decrease in the time allocated to anatomy (2-4). This situation results in a decline in the anatomy knowledge of young doctors (5).

Neuroanatomy is one of the most difficult anatomy subjects for medical students to learn and for young doctors to apply their basic neurological knowledge in the clinic. The challenges of neurology are explained by poor anatomical knowledge and limited patient contact. One of the most effective ways to reduce negrophobia is to teach neuroanatomy and neurophysiology successfully (6).

Neuroanatomy, as a component of the anatomy curriculum, has been impacted by the overall decline of the entire anatomy curriculum. Moreover, it stands out as one of the most disliked and challenging sections for students in the entire anatomy curriculum (7). There are two important reasons for this: Firstly, the central and peripheral nervous systems are more complex than other anatomical systems, and second, the neuroanatomy models, atlases, or computer software provided by educational institutions are insufficient and fail to meet expectations.

Detailed examinations of the central and peripheral nervous systems in cadavers create limitations for educators in undergraduate and graduate education in neuroanatomy. For example, it is almost impossible to demonstrate anatomical structures, such as cranial nerve nuclei and descending-ascending pathways, contained within the brain stem, which measure approximately 7.5 cm in length. Additionally, fixed cadaver tissue is not robust and exhibits toxic properties due to fixation solutions (8-11). Furthermore, computed tomography and magnetic resonance imaging images taken from patients still lack the detail required to adequately display these structures.

The innovative approach in neuroanatomy education predominantly revolves around three-dimensional (3D) modeling on computers, virtual reality (VR), and augmented reality (AR). Although the history of 3D anatomical modeling, which forms the foundation of VR and AR, can be traced back to ancient times, the first modern computer graphic models were created in 1979 by Dietrichs and Walberg (12), focusing on the cat's fastigial nucleus. 3D anatomical models are effective learning tools for two reasons: their capacity to elucidate complex neuroanatomical structures in a simple and comprehensible manner, and individuals' inherent motivation to study and understand these structures (13). The preparation of 3D anatomical models based on digital visualization formats has addressed the limitations of cadaver and plastic models and is poised to replace them in the coming years. The utilization of 3D visualization technologies such as VR and AR aids in comprehending the spatial topography of numerous neuroanatomical structures concentrated within a confined area.

Our recent literature reviews indicate that the use of VR and AR applications for 3D imaging of the nervous system has risen to 18 and 20 publications, respectively, since 2006 (14,15). Undoubtedly, the decrease in equipment costs (computers, glasses, software) has played a significant role in this (16).

Although classical physical brain anatomy models or those obtained from 3D printers allow examination in 3D spatial terms, they limit interaction with the model (17). We now have scientific evidence strongly recommending the use of VR applications in teaching and learning processes. Additionally, they have been shown to significantly enhance students' imagination, creativity, and learning (16,18).

The best method for teaching neuroanatomy remains an unresolved issue. Consequently, research on this subject persists and will continue in the coming years (7). Neuroanatomy education is more receptive to innovations as a balancing factor compared to the anatomy of other organ systems.

In our retrospective studies, it is evident that providing infrastructure for cadaver dissection, which held significant importance in anatomy education in the 20th century, and maintaining expertise in this field incurs high costs. Consequently, there has been a decline in medical students' utilization of cadaver dissection as a means of familiarizing themselves with anatomy (19,20).

There is a limited number of articles on the use of VR to teach neuroanatomy and its educational contributions (21). In addition, research on the effectiveness of such systems and their acceptance by students has remained at an individual or limited level. The findings obtained mostly consist of studies focusing on student satisfaction. Furthermore, there are very few studies measuring short-term and long-term learning success, as well as the efficacy of the devices used in education. In this study, we developed an original VR brain model and examined its effects on long-term learning, recall, satisfaction, and motivation. In the future, we plan to transform this model into a web-based application that can be accessible to users worldwide.

MATERIALS AND METHODS

Participants

Our study is an intervention study planned to implement a new education model and measure its effectiveness. The application was carried out with 170 volunteers: 102 female (60%) and 68 male (40%) students from Gazi University Faculty of Medicine, term 2 students. Participants signed a consent form indicating their voluntary participation. Additionally, approval was obtained from the Ethics Commission of Gazi University for this study (approval number: E-77082166-604.01.02-275165, date: 27.01.2022). There were no stereographic visual disturbances reported by the students.

Materials and VR Model Preparation Steps

3D digital models were prepared to depict anatomical structures in the central nervous system (including superficial and deep structures), cranial nerves, vestibular structures, and the brainstem in detail. For this purpose, we utilized a 3D digital modeling and animation program called Cinema 4D (Maxon Computer, Friedrichsdorf, Germany). These innovative models were meticulously crafted. Initially, we encountered difficulty in finding existing models and 3D visuals that provided detailed representations of the cranial nerve nuclei and ascending and descending pathways in the brainstem in the literature and visual scans we conducted. Therefore, we developed

a unique brainstem VR model. These structures are closely aligned with the topics covered in the neuroanatomy curriculum.

Subsequently, we transferred the models to a VR editor program called ROT (Infotron, Ankara, Türkiye) and integrated them with anatomical information to enhance interactivity. ROT is a unity-based VR editing program capable of seamlessly importing models in .fbx format and textures in .png format. Once the models and anatomical information were integrated and made interactive, they became readily available for use. The program is fully compatible with "HTC Vive Pro" and "Oculus Quest II," enabling users to navigate the virtual environment and interact with the models using handheld controllers. Furthermore, ROT offers additional features such as segmenting models and annotating them with text via handheld controllers to enhance student engagement during virtual presentations.

Traditional 2D Lecture and 3D-VR Training

Within the scope of the study, one lecture was conducted for the students in the amphitheater using a familiar PowerPoint presentation, projected onto the screen from a computer. The presentation was designed by anatomists with an interest in clinical anatomy teaching. This course was delivered in the format of a traditional 2D lecture lasting 40 minutes. Following this, the use of 3D imaging glasses and handheld controllers was explained to the students, and subsequently, a VR-supported training session was conducted. The students wore glasses to interact with the models prepared using the VR program. This VR practice session also lasted 40 minutes, mirroring the duration of the traditional 2D lesson. An assessment was conducted by evaluating the students' performance on the subject and gathering their feedback in a focus group.

Study Design of the Quantitative Measurements with the Contents of the Pre-Lecture, Post-Lecture, and Post-VR and Long-Term Exams

To assess students' understanding of the subject matter, a total of 10 questions focused on the three parts of the brainstem were administered to the participating students. Three questions included visuals obtained from models of the brain module, while seven were multiple-choice questions. The questions presented in the model required the students to fill in the blanks. An example of such a test is provided in Table 1. These questions were developed and agreed upon by the anatomists responsible for both theoretical and practical training. The students did not see the questions before the examination.

The first exam was conducted before the lesson, without providing any explanation of the subject matter to the students. Subsequently, a theoretical lecture on the topic was delivered. Following the lesson, a second exam, consisting of different questions but covering the same content, was administered to the students who had attended the theoretical lecture.

After the theoretical lecture, 60 volunteers from among these students underwent the VR application during which the structures learned in the theoretical lesson were demonstrated using the brain module. At the conclusion of this session, a third test, which featured different questions on the same content, was administered.

Six months after the conclusion of the neurological sciences committee, another exam, with content identical to the previous ones but featuring different questions, was administered to the same participants. The purpose of the final test was to assess the retention of the learned information.

In our literature review, we found no studies that measured the short- and long-term success and retention of knowledge in neuroanatomy lessons using VR. Thus, our study represents the first of its kind in the world.

Statistical Analysis

All statistical analyses and calculations were conducted using the SPSS statistical program (version 21.0, SPSS Inc., Chicago, IL, USA). The normal distribution of the obtained numerical data was assessed using the Shapiro-Wilk test. Non-parametric tests were employed if $p<0.05$, while parametric tests were applied if $p>0.05$. Subsequently, comparisons between groups were performed. Statistical significance was determined by considering values with $p\leq0.05$.

RESULTS

Demographic Data

One hundred seventy students volunteered to participate in this study. As no student reported any abnormality in stereoscopic vision, all volunteers were randomized to either the 3D or 2D teaching groups. One hundred seventy medical students (100%) attended the pre-test (first test) before the theoretical lecture, with 168 (98.8%) attending the 2D, PowerPoint-based theoretical lecture and second test. Sixty students (35.2%) underwent 3D-VR training and subsequently attended the third test. Six months later, 162 students participated in a fourth exam to assess the long-term effects of the training. Demographic details were available for all students, with the gender distribution consisting of 102 females (60%) and 68 males (40%). The average age of the students was 19.8 years (range: 19-22 years). All students had completed two semesters of medical school; they were in their third semester when the first three tests were administered and the fourth semester was when the fourth test was administered.

Examination Results of Four Tests with Ten Questions

The class average of the 10-question first test, which was given to 170 second-year students immediately before the lecture, was 1.92 out of 10. The average score for female students, who make up 60% of the class, was 2 out of 10, while the average for male students, comprising 40% of the class, was found to be 1.82 out of 10.

The group average of the second exam, administered to 168 students who listened to the 2D theoretical lecture in the lecture hall, was 3.38 out of 10. The average score for female students was 3.51 out of 10, and for male students, it was 3.16 out of 10.

For the third exam, the group average after the 3D-VR training and application, with 60 voluntary participants out of 170, was 4.55 out of 10. The average score for female students was 4.5 out of 10, and for male students, it was 4.62 out of 10.

Six months after the completion of the neurological sciences committee, the group average of the fourth exam, administered to

Table 1. A sample of tests containing multiple choice questions on theoretical and applied anatomy of the brain stem

1. Which of the following correctly represents the parts of the brain stem? I. Midbrain II. Internal capsule III. Pons IV. Medulla oblongata V. Cerebellum	a) I, II, III, IV b) II, III, V c) ***I, III, IV*** d) I, III, IV, V e) II, IV, V
2.Which of the following has the highest number of dopaminergic neurons?	a) Area pretectalis b) Tectum mesencephali c) Tegmentum mesencephali d) ***Substantia nigra*** e) Nucleus ruber
3.Which nucleus is located between the substantia nigra and aquaduct of midbrain?	a) Nucleus of the oculomotor nerve b) Nucleus of the trochlear nerve c) ***Red nucleus*** d) Pontine nuclei e) Edinger-Westphal nucleus
4.Which center plays a role in the reflex movements of the head, neck and eyes against sudden auditory, somatic, and visual stimuli?	a) The inferior colliculus b) ***Superior colliculus*** c) Pretectal area d) Tectum of midbrain e) Substantia nigra
5.Which of the information about medulla oblongata is false?	a) It is the most caudal part of the brain stem. b) Connected to the cerebellum with the inferior cerebellar peduncle. c) The last 4 cranial nerves leave the brain stem from the medulla oblongata. d) ***The basilar artery sits on the basilar groove on its anterior surface*** e) It is separated from the pons with bulbopontin groove.
6. Which cranial nerve gets out from the bulbopontin groove?	a) IX. cranial nerve b) X. cranial nerve c) V. cranial nerve d) ***VI. cranial nerve*** e) XI. cranial nerve
7. Which of the statements about the pons is false?	a) It is adjacent to the cerebellum through the 4th ventricle b) It is adjacent to the clivus through the cisterna pontis c) It is separated from the bulbus by the sulcus bulbopontinus d) ***Inferior cerebellar pedincle is connected with the cerebellum*** e) The basilar artery sits on the basilar groove on its anterior surface
8. Write the name of the indicated structure. **<u>Oculomotor nerve</u>**	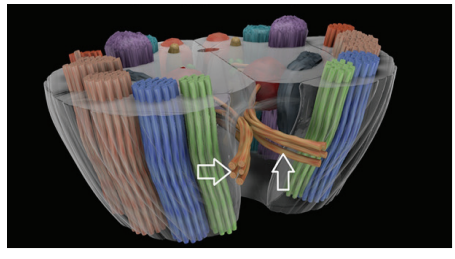

Table 1. Continued

9. Write the name of the indicated structure. **Inferior colliculus**	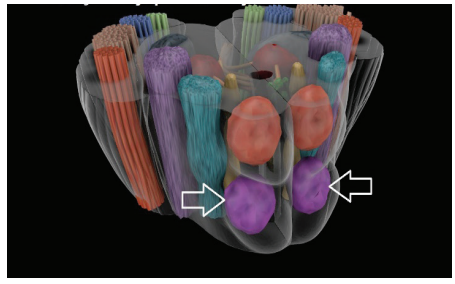
10. Write the name of the indicated structure. **Medial lemniscus**	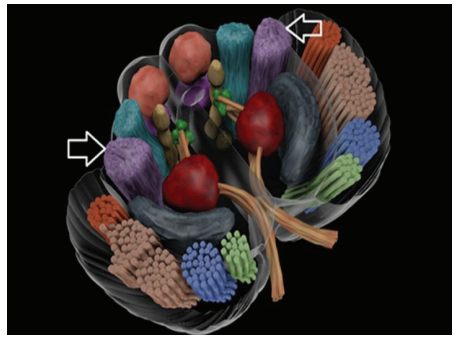

Correct answers in bold italic font.

162 students out of 170, was 4.61 out of 10. The average score for female students was 4.73 out of 10, and for male students, it was 3.85 out of 10.

Statistical Evaluation of Results

The class average of the 10-question first test, administered to 170 second-year students immediately before the lecture, was 1.92 out of 10. Among the students, females, who constitute 60% of the class, achieved an average score of 2 out of 10, while males, comprising 40% of the class, attained an average score of 1.82 out of 10.

Although the number of students participating in the exams varied, 60 students who took the third exam participated in all other exams. To assess statistical significance, the success rates of the 60 students who participated in all four exams were evaluated internally. Additionally, the success rates of the 170 students who took the first exam, the 168 students who took the second exam, and the 162 students who took the fourth exam were evaluated independently within their respective groups.

The figure below (Figure 1) illustrates the results of four exams taken by 60 second-year students from Gazi University Faculty of Medicine, who were taught about the brain stem in an anatomy lecture and subsequently underwent a 3D-VR application related to the subject. Among the 60 students who took each exam, the average score for the first exam was 1.767 (p=0.0005), for the second exam was 3.267 (p=0.0148), for the third exam was 4.550 (p=0.0078), and for the fourth exam was 4.867 (p=0.0595). Accordingly, a statistically significant difference was observed between the first and second exams, the second and third exams, the first and third exams, and the first and fourth exams. However, although there was a difference between the third and fourth examinations, the difference was not statistically significant.

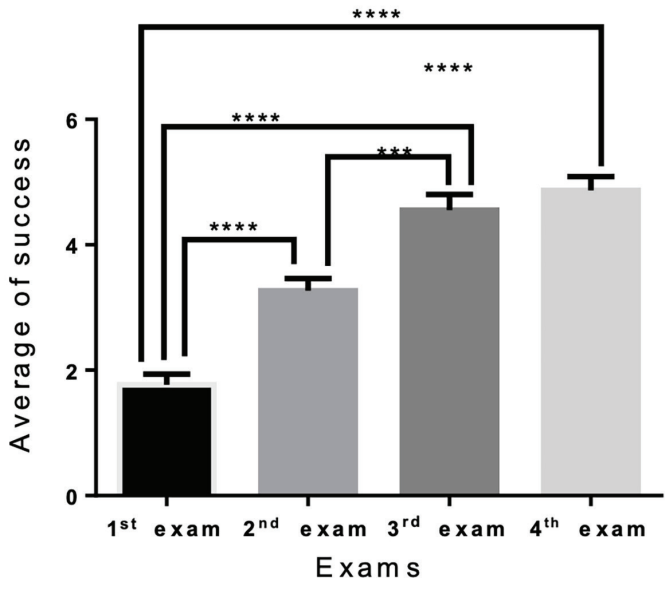

Figure 1. The graph shows the average success rate of the students who participated in the 1st, 2nd, 3rd, and 4th exams.

****p<0.0005; ****p<0.001 difference between groups.*

When evaluating the success in the exams according to gender among the 60 students who participated in all four exams, a statistically significant difference was observed in the results of the second exam. Although the average success rate of the girls was higher than that of the boys in the first, second, and fourth exams (Figure 2), the difference was not statistically significant (p≤0.05).

When comparing the exam results of the 36 female students and 24 male students out of the 60 students who took all the exams, it was

observed that the average success rate increased progressively in consecutive exams. There was no statistical significance between the third and fourth examinations in both groups (p=0.18 for females; p=0.14 for males) (Figure 3).

When conducting a statistical evaluation among the 170 students who took the first exam, the 168 students who took the second exam, and the 162 students who took the fourth exam, statistical significance was found between the first and second exams, the second and fourth exams, and the first and fourth exams (Figure 4) (p<0.001, p<0.001, p<0.001, respectively).

The purpose of our research was not to evaluate the examination performance of students but rather to assess the influence of different anatomy instruction techniques on students. You can watch the video we prepared by holding your smartphone's camera to the QR code (Figure 5).

DISCUSSION

The rise in the utilization of educational technologies and tools over the last two decades has facilitated the emergence of digital education (17,22). Today, applications such as electronic resources, game-based learning, and VR are being extensively utilized for learning and acquiring professiona practice skills.

The use of tablets and smartphones in neuroanatomy education has facilitated the comprehension of complex deep brain structures (17,23). However, these technologies only offer two dimensional (2D) views, limiting students' ability to grasp the subject from a 3D perspective and fully understand the dimensions, volumes, and relationships of anatomical structures within the depths of the brain and brainstem.

Error-free 3D brain models, developed for academic purposes and accredited by experts in the subject, can be easily integrated into a VR environment. This allows detailed examination of numerous structures in the normal human brain that are not visible to the naked eye. The only disadvantage of this method is its inability to replicate the textural stimuli experienced during cadaver dissection. However, wearable technologies developed using today's advancements have addressed tactile feedback issues.

Moreover, VR technologies enable students to interact with such technology in reproducible and controllable environmen (17,24). This technology enables students to experience learning content through various sensory inputs, including sight, sound, and touch, thereby immersing them in the virtual environment (25). Additionally, its repeatability allows students to enhance their learning in the classroom beyond the predetermined study program (17,26).

Examination of the literature on 3D visualization of the nervous system revealed a significant increase in interest. In 2011, only 4 articles on VR and AR emphasized this topic, a number that increased to 18 and 10 by today. This trend highlights VR's advantageous position among new technologies for viewing and manipulating neuroanatomical structures with interactivity. It signifies a significant shift in how people learn about neuroanatomy, with the cadaver-based learning method being increasingly replaced by technology between 2011 and 2018. Additionally, eight studies utilizing educational technologies such as VR and AR have been documented to explore the use of 3D in neuroanatomy (13). Some of these methods include local VR-based stereo-imaging techniques for learning about the ventricular system and neurovascular structures (27), skull (28,29), brain structures, and cranial nerves (28).

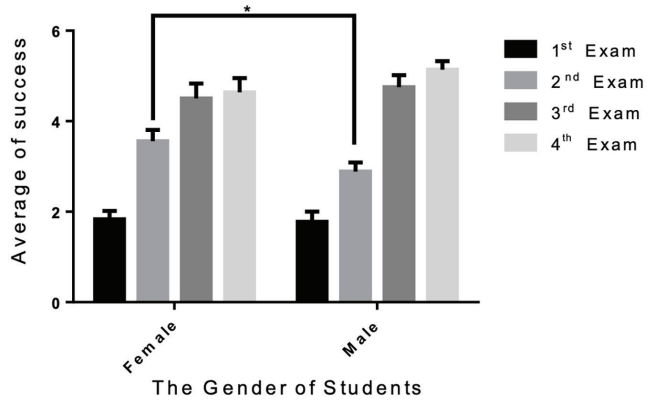

Figure 2. The graph shows the average success rate of the students who participated in all 4 exams by gender.

**p≤0.05 difference between groups.*

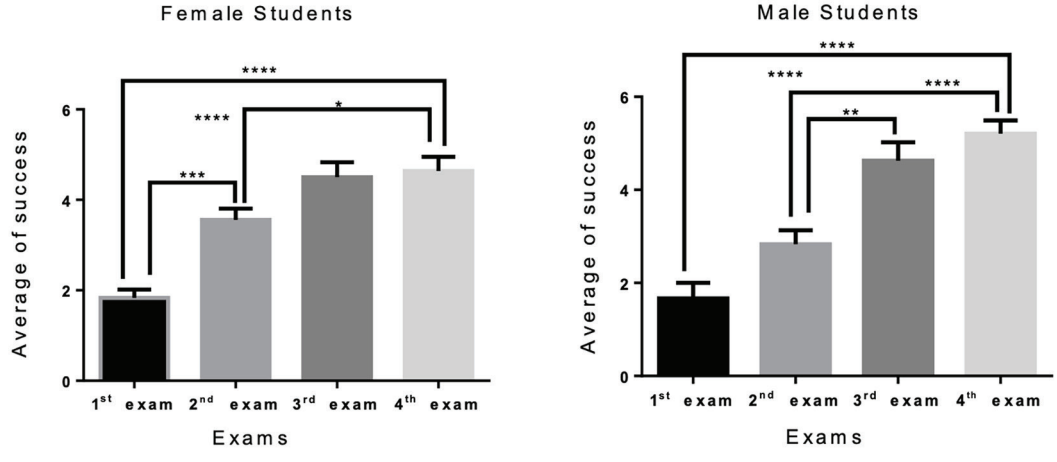

Figure 3. The graph shows the average success rate of female students on the left and male students on the right who took the 1st, 2nd, 3rd, and 4th exams.

**p≤0.05, **p≤0.01, ***p≤0.001, ****p<0.001 difference between groups.*

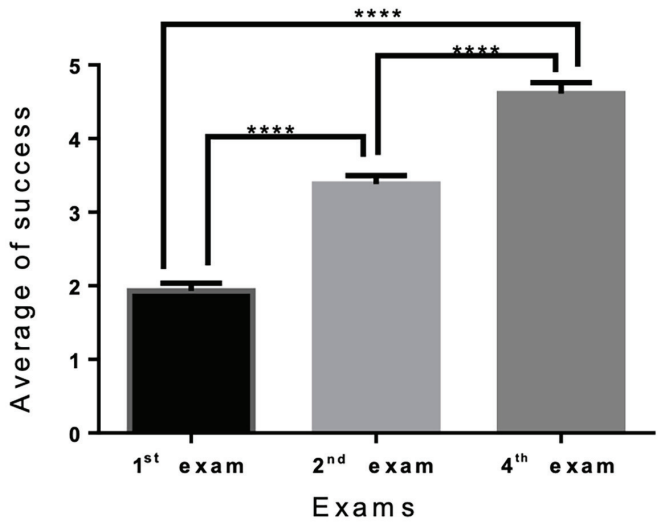

Figure 4. The graph shows the average success rate of the students who took the 1st, 2nd, and 4th exams.

*****p<0.001 difference between groups.*

Our observations indicate that although the number of these studies has increased, they remain insufficient. Furthermore, these studies have predominantly focused on superficial brain structures to demonstrate neuroanatomical structures to students. However, it would be intriguing to develop and utilize VR and AR applications for 3D visualization of deep brain structures in neuroanatomy education (13). In a study conducted by Estevez et al. (30) in 2010, they emphasized that physical models that allow for high levels of manipulation of deep brain structures yield positive result.

The brain module developed in this study aims to address the shortcomings identified by the limited number of studies on this subject. An important innovation introduced by our brain module is its ability to enlarge the brain stem, along with its deep structures, by 10-15 times, enabling interaction with the student. This feature represents the world first.

In our study, we evaluated the results of tests conducted to assess the understanding and retention of superficial and deep brain stem structures by a group of 60 students who participated in neuroanatomy training activities. According to the results obtained, the average score on the first test, administered before the traditional 2D theory course, was 1.767. After completing the traditional 2D theory course, the average score on the second test was 3.267. Following the 3D-VR training and application, the average score on the third test for this group was 4.55. Six months after the training and practices, the group's average score on the fourth test was 4.867. Comparatively, the average score of 102 students who did not receive 3D-VR training or application was found to be 4.46. These results indicate that VR, either alone or in combination with classical methods, can be beneficial for learning deep neuroanatomical structures.

The learning style is widely recognized as a crucial element of the learning process. Experimenting with different teaching techniques and recognizing students' individual learning preferences will aid in determining the ideal length for efficient study sessions and enhance academic performance. Ogut et al. (31) conducted a study on anatomy teaching techniques to investigate the impact of four distinct learning styles on student education. They utilized "Kolb's Learning Style Inventory" model for their analysis. Their findings confirmed that learning style affects both the length of study and the scores achieved in theoretical anatomy courses (31). Engaging in practical exercises to apply knowledge strengthens the learning process. Consistent practice aids in solidifying information, thereby facilitating students' ability to remember and utilize their knowledge across diverse situations. Maintaining a positive attitude fosters a growth mindset, which motivates students to tackle challenges and learn from mistakes. This mindset improves their capacity to acquire new knowledge and adapt to various subjects.

Ferrer-Torregrosa et al. (32) and Kugelmann et al. (33) reported that 62% of the students surveyed expressed interest in using AR

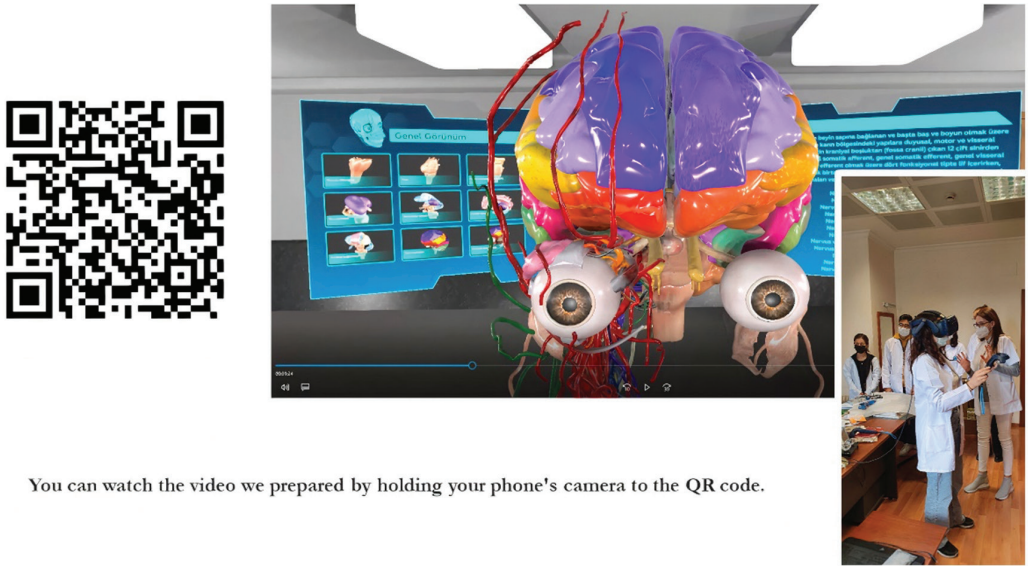

Figure 5. VR Brain Module QR code.

VR: Virtual reality.

for anatomy work. However, Kugelmann et al. (33) did not provide statistical analysis on the subject. This suggests that the effects of VR and AR application tools on student motivation in both general anatomy and neuroanatomy education have not been fully explored. A comprehensive examination of the literature on motivation reveals four important motivational concepts (34). These are attention, relevance, gratification, encouragement, and sustainability, respectively. In our study, students who experienced VR provided feedback indicating that the subject matter became ingrained in their memory, facilitated their learning, and heightened their interest and motivation. Additionally, we conducted statistical and comparative analyses of the test results obtained from the target groups in our study.

Much of the research on medical education has emphasized the learning process of students, often overlooking their emotional experiences (35). Perhaps the primary reason for this is that traditional teaching has predominantly emphasized the cognitive and behavioral development of students for knowledge acquisition (36). However, although emotions associated with the events experienced by students facilitate the retention of learned material, the learning processes persist longer in students' memories (37). Negative emotions, such as boredom, anxiety, and frustration, can impede the storage and retrieval of information from memory when needed for a task (38). According to mixed education methodologies, Stepan et al. (27) reported that students exhibit higher motivation, participation, and understanding in lessons when virtual environments were utilized. Studies have demonstrated that the knowledge acquired for learning anatomy and neuroanatomy is often forgotten even just a few months after the completion of the course (4,39). The Neurosurgical atlas, prepared by anatomists, neurosurgeons, and 3D computer graphic artists, was published in an article in 2019. This article featured a series of interactive 3D VR models that provide a tour of the neurosurgical operating room as well as several critical aspects of cranial surgical anatomy (40). Both in this study and in our work, innovations in 3D and VR digital technology are thought to not only enable the creation of much more sophisticated and realistic educational resources compared to traditional 2D materials but also to support the advancement of medical education by starting with basic anatomy knowledge in the early years and further enhancing the quality of education. In this study, we compared traditional and VR applications in neuroanatomy education. Upon reviewing the literature, we found a lack of significant studies that incorporate statistical data and evaluate long-term information retention among students. Our study revealed a significant correlation between student motivation and success, particularly in the VR group. We observed that VR applications in neuroanatomy education, which utilize accredited models prepared by experts and error-free neuroanatomical structures, meet students' educational expectations. Comparing the exam results, which aimed to demonstrate the long-term effects of VR-supported education, with those of students who did not receive VR training, we concluded that Virtual Reality Application Based on 3D Virtual Neuroanatomic Models, an innovative approach in medical education, aids students in retaining the subject matter. Considering that cadaveric brain dissections were the gold standard in neuroanatomy education in the 19th and 20th centuries (41), it is unsurprising that VR and AR will likely play a central role in the field in the next decade.

Nevertheless, our study also has its limitations. VR glasses used in education can only accommodate one student at a time and may induce dizziness, nausea, or vomiting in users. Despite these drawbacks, the VR application offers significant advantages. Immersing learners in a virtual environment provides the sensation of being within the anatomical structure, enabling real-time exploration and interaction. Hence, there is a pressing need for new neuroanatomy curricula that integrate clinical aspects and emerging technologies, catering to students' intrinsic motivation, and facilitate both short-term and long-term learning.

CONCLUSION

Neuroscience, or neuroanatomy, stands as the most daunting subject among anatomy courses in medical faculties. Complexity often leads students to dread neurological sciences in their career planning, potentially exacerbating public health challenges for an aging population grappling with neurological diseases. Our study, leveraging today's 3D technology in anatomy education, has the potential to elevate classical neuroanatomy education to new heights, contributing significantly to medical education. In addition, by demonstrating the long-term positive effects of VR training on memory, our study fills a crucial gap in the literature.

Ethics

Ethics Committee Approval: Additionally, approval was obtained from the Ethics Commission of Gazi University for this study (approval number: E-77082166-604.01.02-275165, date: 27.01.2022).

Informed Consent: Participants signed a consent form indicating their voluntary participation.

Authorship Contributions

Concept: E.A., Ö.C., T.V.P., Design: E.A., Ö.C., T.V.P., Supervision: Ö.C., T.V.P., Resources: E.A., T.V.P., Materials: E.A., T.V.P., Data Collection or Processing: E.A., T.V.P., Analysis or Interpretation: E.A., Ö.C., T.V.P., Literature Search: E.A., T.V.P., Writing: E.A., T.V.P., Critical Review: Ö.C., T.V.P.

Conflict of Interest: No conflict of interest was declared by the authors.

Financial Disclosure: The authors declared that this study received no financial support.

REFERENCES

1. Frenk J, Chen L, Bhutta ZA, Cohen J, Crisp N, Evans T, et al. Health professionals for a new century: transforming education to strengthen health systems in an interdependent world. Lancet. 2010; 376: 1923-58.
2. Drake RL, McBride JM, Lachman N, Pawlina W. Medical education in the anatomical sciences: the winds of change continue to blow. Anat Sci Educ. 2009; 2: 253-9.
3. Louw G, Eizenberg N, Carmichael SW. The place of anatomy in medical education: AMEE Guide no 41. Med Teach. 2009; 31: 373-86.
4. Bergman EM, van der Vleuten CP, Scherpbier AJ. Why don't they know enough about anatomy? A narrative review. Med Teach. 2011; 33: 403-9.

5. Farey JE, Bui DT, Townsend D, Sureshkumar P, Carr S, Roberts C. Predictors of confidence in anatomy knowledge for work as a junior doctor: a national survey of Australian medical students. BMC Med Educ. 2018; 18: 174.
6. Szirmai I. Neurofóbia [Neurophobia]. Ideggyogy Sz. 2012; 65: 221-8.
7. Arantes M, Arantes J, Ferreira MA. Tools and resources for neuroanatomy education: a systematic review. BMC Med Educ. 2018; 18: 94.
8. Lim KH, Loo ZY, Goldie SJ, Adams JW, McMenamin PG. Use of 3D printed models in medical education: A randomized control trial comparing 3D prints versus cadaveric materials for learning external cardiac anatomy. Anat Sci Educ. 2016; 9: 213-21.
9. Naftulin JS, Kimchi EY, Cash SS. Streamlined, Inexpensive 3D Printing of the Brain and Skull. PLoS One. 2015; 10: e0136198.
10. Vaccarezza M, Papa V. 3D printing: a valuable resource in human anatomy education. Anat Sci Int. 2015; 90: 64-5.
11. McMenamin PG, Quayle MR, McHenry CR, Adams JW. The production of anatomical teaching resources using three-dimensional (3D) printing technology. Anat Sci Educ. 2014; 7: 479-86.
12. Dietrichs E, Walberg F. The cerebellar corticonuclear and nucleocortical projections in the cat as studied with anterograde and retrograde transport of horseradish peroxidase. I. The paramedian lobule. Anat Embryol (Berl). 1979; 158: 13-39.
13. Sotgiu MA, Mazzarello V, Bandiera P, Madeddu R, Montella A, Moxham B. Neuroanatomy, the Achille's Heel of Medical Students. A Systematic Analysis of Educational Strategies for the Teaching of Neuroanatomy. Anat Sci Educ. 2020; 13: 107-16.
14. Adnan S, Xiao J. A scoping review on the trends of digital anatomy education. Clin Anat. 2023; 36: 471-91.
15. Newman HJ, Meyer AJ, Wilkinson TJ, Pather N, Carr SE. Technology enhanced neuroanatomy teaching techniques: A focused BEME systematic review of current evidence: BEME Guide No. 75. Med Teach. 2022; 44: 1069-80.
16. Mendez-Lopez M, Juan MC, Molla R, Fidalgo C. Evaluation of an Augmented Reality Application for Learning Neuroanatomy in Psychology. Anat Sci Educ. 2022; 15: 535-51.
17. Obrero-Gaitán E, Nieto-Escamez FA, Zagalaz-Anula N, Cortés-Pérez I. An Innovative Approach for Online Neuroanatomy and Neurorrehabilitation Teaching Based on 3D Virtual Anatomical Models Using Leap Motion Controller During COVID-19 Pandemic. Front Psychol. 2021; 12: 590196.
18. Herrera G, Jordan R, Veraa L. Abstract concept and imagination teaching through Virtual Reality in people with Autism Spectrum Disorders. Technol Disabil. 2006; 18: 173-80.
19. Gartner LP. Anatomical sciences in the allopathic medical school curriculum in the United States between 1967-2001. Clin Anat. 2003; 16: 434-9.
20. Korf HW, Wicht H, Snipes RL, Timmermans JP, Paulsen F, Rune G, et al. The dissection course - necessary and indispensable for teaching anatomy to medical students. Ann Anat. 2008; 190: 16-22.
21. Javan R, Davidson D, Javan A. Nerves of Steel: a Low-Cost Method for 3D Printing the Cranial Nerves. J Digit Imaging. 2017; 30: 576-83.
22. Martinengo L, Yeo NJY, Markandran KD, Olsson M, Kyaw BM, Car LT. Digital health professions education on chronic wound management: A systematic review. Int J Nurs Stud. 2020; 104: 103512.
23. Wainman B, Wolak L, Pukas G, Zheng E, Norman GR. The superiority of three-dimensional physical models to two-dimensional computer presentations in anatomy learning. Med Educ. 2018; 52: 1138-46.
24. Bennett JA, Saunders CP. A Virtual Tour of the Cell: Impact of Virtual Reality on Student Learning and Engagement in the STEM Classroom. J Microbiol Biol Educ. 2019; 20: 20.2.37.
25. Pothier DD, Hughes C, Dillon W, Ranalli PJ, Rutka JA. The use of real-time image stabilization and augmented reality eyewear in the treatment of oscillopsia. Otolaryngol Head Neck Surg. 2012; 146: 966-71.
26. Zhao J, Xu X, Jiang H, Ding Y. The effectiveness of virtual reality-based technology on anatomy teaching: a meta-analysis of randomized controlled studies. BMC Med Educ. 2020; 20: 127.
27. Stepan K, Zeiger J, Hanchuk S, Del Signore A, Shrivastava R, Govindaraj S, et al. Immersive virtual reality as a teaching tool for neuroanatomy. Int Forum Allergy Rhinol. 2017; 7: 1006-13.
28. Kockro RA, Amaxopoulou C, Killeen T, Wagner W, Reisch R, Schwandt E, et al. Stereoscopic neuroanatomy lectures using a three-dimensional virtual reality environment. Ann Anat. 2015; 201: 91-8.
29. Goodarzi A, Monti S, Lee D, Girgis F. Effect of Stereoscopic Anaglyphic 3-Dimensional Video Didactics on Learning Neuroanatomy. World Neurosurg. 2017; 107: 35-9.
30. Estevez ME, Lindgren KA, Bergethon PR. A novel three-dimensional tool for teaching human neuroanatomy. Anat Sci Educ. 2010; 3: 309-17.
31. Ogut E, Senol Y, Yildirim FB. Do learning styles affect study duration and academic success? Eur J Anat. 2017; 21: 235-40.
32. Ferrer-Torregrosa J, Torralba J, Jimenez MA, García S, Barcia JM. ARBOOK: Development and Assessment of a Tool Based on Augmented Reality for Anatomy. J Sci Educ Technol. 2015; 24: 119-24.
33. Kugelmann D, Stratmann L, Nühlen N, Bork F, Hoffmann S, Samarbarksh G, et al. An Augmented Reality magic mirror as additive teaching device for gross anatomy. Ann Anat. 2018; 215: 71-7.
34. Keller JM. Motivational design for learning and performance: The ARCS model approach. Springer Science & Business Media, 2009.
35. Frenzel AC, Becker-Kurz B, Pekrun R, Goetz T, Lüdtke O. Emotion transmission in the classroom revisited: A reciprocal effects model of teacher and student enjoyment. J Educ Psychol. 2018; 110: 628-39.
36. Barajas M, Gannaway GJ. Implementing E-learning in the traditional higher education institutions. High Educ Eur. 2007; 32: 111-9.
37. Pell MD, Monetta L, Paulmann S, Kotz SA. Recognizing Emotions in a Foreign Language. J Nonverbal Behav. 2009; 33: 107-20.
38. Gesú F, Seminara Á. Neurodidáctica y la implicación de emociones en el aprendizaje - Dialnet . Dialnet. 2012: 5-39.
39. Billings-Gagliardi S, Mazor KM. Effects of review on medical students' recall of different types of neuroanatomical content. Acad Med. 2009; 84: S34-7.
40. Tomlinson SB, Hendricks BK, Cohen-Gadol A. Immersive Three-Dimensional Modeling and Virtual Reality for Enhanced Visualization of Operative Neurosurgical Anatomy. World Neurosurg. 2019; 131: 313-20.
41. Ghosh SK. Human cadaveric dissection: a historical account from ancient Greece to the modern era. Anat Cell Biol. 2015; 48: 153-69.

GMJ 2024;35:416-421

DOI: http://dx.doi.org/10.12996/gmj.2024.4205

The Relationship Between Serum miRNAs and Surgical Prognostic Factors in Gastric Cancers

Mide Kanserlerinde Serum miRNA Düzeyleri ile Cerrahi Prognostik Faktörler Arasındaki İlişki

Çağrı Büyükkasap[1], Engin Küçükdiler[2], Mahir Nasirov[3], Niyazi Samet Yılmaz[4], Hasan Dağlı[5], İlke Önen[6], Furkan Aydoğdu[7], Aydın Yavuz[1], Hüseyin Göbüt[1], Asiye Uğraş Dikmen[8], Kürşat Dikmen[1], Hasan Bostancı[1], Özlem Gülbahar[9], Abdulkadir Bedirli[1]

[1]Department of General Surgery, Gazi University Faculty of Medicine, Ankara, Türkiye
[2]Aydın State Hospital, Aydın, Türkiye
[3]Caspian International Hospital, Baku, Azerbaijan
[4]Polatlı Duatepe State Hospital, Ankara, Türkiye
[5]Department of Medical Biochemistry, Kahramanmaraş Sütçü İmam University Faculty of Medicine, Kahramanmaraş, Türkiye
[6]Department of Medical Biology, Gazi University Faculty of Medicine, Ankara, Türkiye
[7]Bandırma Training and Research Hospital, Balıkesir, Türkiye
[8]Department of Public Health, Gazi University Faculty of Medicine, Ankara, Türkiye
[9]Department of Medical Biochemistry, Gazi University Faculty of Medicine, Ankara, Türkiye

ABSTRACT

Objective: There is a continued need for biomarkers for patients with gastric cancer that can aid in diagnosis, treatment follow-up, and relapse detection. The objective of this study was to investigate the role of serum microRNA (miRNAs) in diagnosing gastric cancer and their relationship with prognostic factors that impact the choice of surgical approach.

Methods: We compared the serum miRNA expression levels of 35 patients who underwent gastrectomy and D2 lymph node dissection for gastric adenocarcinoma between 2015-2018 with those of 33 controls. We also evaluated the relationship between serum miRNA expression levels and pathological prognostic factors.

Results: The serum levels of miR-17-5p, miR-21-5p, miR-27a-3p, miR-146a-5p, miR-148a-3p, and miR-203a-3p were significantly higher in gastric cancer patients. In early gastric cancer patients, serum levels of miR-21-5p, miR-27a-3p, miR-106b-5p, miR-146a-5p, and miR-148a-3p levels were significantly higher. Furthermore, serum levels of miR-106b-5p and miR-146a-5p were associated with tumor localization [area under the curve (AUC): 0.773, 0.797; p=0.049, 0.036], while serum levels of miR-27a-3p and miR-148a-5p were associated with the T-stage of the tumor (AUC: 0.748, 0.729; p=0.036, 0.049).

Conclusion: Serum levels of miR-17-5p, miR-21-5p, miR-27a-3p, and miR-203a-3p were found to be diagnostic biomarkers in gastric

ÖZ

Amaç: Gastrik kanser hastalarında tanı, tedavi takibi ve nüks tespitinde yardımcı olabilecek biyobelirteçlere olan ihtiyaç devam etmektedir. Bu çalışmanın amacı, mide kanserinin teşhisinde serum mikroRNA'larının (miRNA) rolünü ve cerrahi yaklaşım seçimini etkileyen prognostik faktörlerle ilişkilerini araştırmaktır.

Yöntemler: 2015-2018 yılları arasında gastrik adenokanser nedeniyle gastrektomi ve D2 lenf nodu diseksiyonu uygulanan 35 hastanın serum miRNA ekspresyon seviyelerini 33 kontrolle karşılaştırıldı. Ayrıca serum miRNA ekspresyon seviyeleri ile patolojik prognostik faktörler arasındaki ilişkiy değerlendirildi.

Bulgular: Gastrik kanser hastalarında miR-17-5p, miR-21-5p, miR-27a-3p, miR-146a-5p, miR-148a-3p ve miR-203a-3p'nin serum seviyeleri anlamlı derecede daha yüksekti. Erken gastrik kanser hastalarında, miR-21-5p, miR-27a-3p, miR-106b-5p, miR-146a-5p ve miR-148a-3p serum seviyeleri önemli ölçüde daha yüksekti. Ayrıca miR-106b-5p ve miR-146a-5p serum seviyeleri tümör lokalizasyonuyla ilişkilendirildi [eğri altındaki alan (AUC): 0,773, 0,797; p=0,049, 0,036], miR-27a-3p ve miR-148a-5p serum seviyeleri ise tümörün T-evresiyle ilişkilendirildi (AUC: 0,748, 0,729; p=0,036, 0,049).

Sonuç: miR-17-5p, miR-21-5p, miR-27a-3p ve miR-203a-3p'nin serum düzeylerinin gastrik kanserlerde tanısal biyobelirteçler olduğu bulundu. Serum miR-106b-5p ve miR-146a-5p'nin ifade düzeylerinin tümör

Address for Correspondence/Yazışma Adresi: Çağrı Büyükkasap, MD, Department of General Surgery, Gazi University Faculty of Medicine, Ankara, Türkiye
E-mail / E-posta: cagribk@gmail.com
ORCID ID: orcid.org/0000-0002-9141-4289

Received/Geliş Tarihi: 05.05.2024
Accepted/Kabul Tarihi: 16.07.2024

ABSTRACT

cancers. The expression levels of serum miR-106b-5p and miR-146a-5p were found to be related to tumor location, whereas the expression levels of serum miR-27a-3p and miR-148a-5p were found to be related to the T-stage of the tumor. These findings can impact the surgical approach for gastric cancer patients.

Keywords: Gastric cancer, microRNA, prognosis

ÖZ

lokasyonuyla ilişkili olduğu, serum miR-27a-3p ve miR-148a-5p'nin ifade düzeylerinin ise tümörün T-evresiyle ilişkili olduğu bulundu. Bu bulgular mide kanseri hastalarına yönelik cerrahi yaklaşımı etkileyebilir.

Anahtar Sözcükler: Gastrik kanser, mikroRNA, prognoz

INTRODUCTION

Gastric cancers remain a significant type of cancer worldwide. According to the data of the year 2020, it is ranked fifth in the world in terms of incidence and fourth in terms of cancer-related deaths (1). Although mortality rates from gastric cancer have decreased over time, most gastric cancer patients receive a diagnosis at advanced stages due to insufficient clinical symptoms and delayed presentation.

Gastroscopy and biopsy remain the gold standard for diagnosing gastric cancer. However, unwanted results can occur due to low sensitivity, high cost, and dependency on the individual (2). Non-invasive serological markers, such as serum pepsinogen, gastrin-17, cancer embryonic antigen (CEA), and carbohydrate antigen (CA19-9), which are used in the diagnosis and prognosis of gastric cancer, have low sensitivity and specificity (3,4). Hence, there is a need for valuable biomarkers that can be utilized for diagnosis, monitoring treatment, and detecting recurrence.

In recent years, microRNA (miRNAs) have been shown to function as tumor suppressors or oncogenes in various cancer types, including gastric cancer (5,6). After their roles in cancer pathogenesis, progression, and migration were proven, they have been considered potential biomarkers for diagnosis and prognosis. During this process, studies on the use of circulating miRNAs as diagnostic and prognostic biomarkers have increased due to their stability compared to tissue miRNAs, ease of non-invasive collection, and ability to repeat measurements. It has been shown that the serum levels of some miRNA species can be useful biomarkers for diagnosis, prognosis, and treatment monitoring in most cancer types, including gastric cancer. Prognostic factors in gastric cancer include age, gender, tumor location, invasion depth, number of metastatic lymph nodes, and TNM stage, and these factors can affect decisions about surgical treatment (7,8). However, limited studies have shown the relationship between serum miRNA levels and these prognostic factors (9,10). The purpose of this study was to investigate the role of serum miRNAs in diagnosing gastric cancer and their correlation with prognostic factors that influence the choice of surgical approach.

MATERIALS AND METHODS

Between September, 2015 and December, 2018, serum samples were collected from 35 patients who underwent gastrectomy and D2 lymph node dissection for histologically confirmed gastric adenocarcinoma. Patients who received neoadjuvant chemotherapy or radiotherapy, had distant metastases, and had peritoneal carcinomatosis were excluded from the study. Patients were divided into gastric cancer group (GCG) and control group (CG). Based on the AJCC/UICC TNM classification 8th edition, the clinical stage of gastric adenocarcinoma was determined (11). Patients' demographic and clinicopathological characteristics were prospectively collected. Thirty-three healthy participants served as controls. This study was funded by the Gazi University Department of Projects of Scientific Inquiry and was approved by the Institutional Review Board of the Gazi University Faculty of Medicine Ethics Committee (approval number: 666, date: 24.09.2018). Informed consent was obtained from all patients and healthy volunteers who participated in the study.

Collection of Samples, RNA Extraction, and qRT-PCR

Peripheral venous blood was collected (18 cc) together with blood samples taken preoperative from each patient and healthy volunteer. The samples were centrifuged, and serum samples were stored at -80 °C. Subsequently, total RNA was isolated from serum samples using Qiagen miRNeasy following the manufacturer's guide. Complementary DNA reactions were prepared using a Qiagen miScript II Kit. Afterwards, preamplification reaction and RT-PCR mix were prepared using a Qiagen miScript microfluidics PreAMP Kit, Qiagen, miScript Microfluidic PCR kit, respectively. Expression of miR-17-5p, miR-21-5p, miR-27a-3p, miR-101-3p, miR-106b-5p, miR-146a-5p, miR-148a-3p, miR-200a-3p, miR-203a-3p by quantitative RT-PCR (qRT-PCR) with Biomark according to the instructions of the manufacturer (Fluidigm, South San Francisco, CA). The expression cel-mir-39 was used as the internal control. The cycle threshold (CT) value is defined as the number of PCR cycles at which the fluorescent signal crosses the threshold (Figure 1). The difference in CT values between the internal control and each miRNA was presented as -ΔCT. ΔΔCT is the difference of ΔCT values between serum samples. $2^{\Delta\Delta CT}$ represents the exponential value of ΔCT, which means fold change in expression.

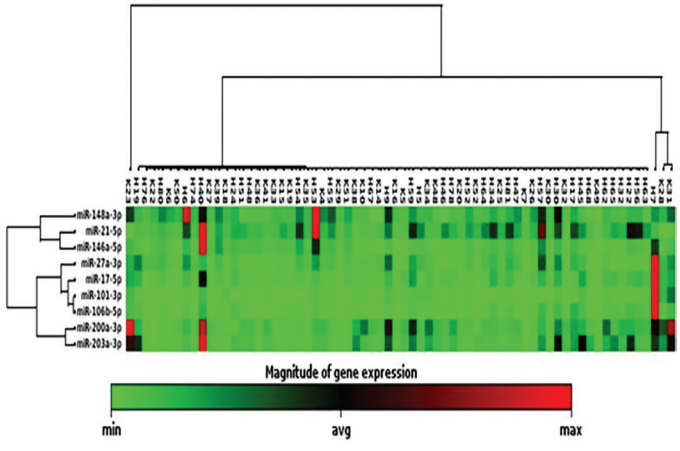

Figure 1. Distribution of miRNA expression levels.
miRNAs: microRNA, min: Minimum, max: Maximum, avg: Average.

Statistical Analysis

Raw data from the RT-PCR device (Biomark HD, Fluidigm, USA) were loaded into the "Qiagen miScript miRNA PCR Array Data Analysis" software to compare with the CG. Values were standardized using "Global mean normalization" (12). Data comparing patient and CGs were used. ΔCT and $2^{-\Delta CT}$ values for each group were calculated using IBM SPSS Statistics v.22. Demographic qualitative variables are presented as numbers and percentages, and the chi-square test was used for comparisons between the two groups. Quantitative variables were presented as median and interquartile range (IQR; 25-75 percentiles). Non-parametric tests were used according to the analysis of visual and operational normal distribution compliance. Mann-Whitney U test was used for comparisons between the two groups. The relationship between serum miRNA expression levels determined by the $2^{-\Delta CT}$ method and prognostic factors was evaluated by receiver operating characteristic (ROC) analysis. The variable considered as the primary endpoint in the ROC analysis was taken as a dichotomous variable, and the area under the curve (AUC), sensitivity, and specificity were calculated. When the calculated form of type-1 error, p-value, is <0.05, it was considered significant.

RESULTS

Serum miRNA expression levels were determined for a total of 68 subjects, including 35 patients and 33 controls. There were no significant difference in terms of gender, smoking history, family history, and blood groups between the GCG and CG groups. Age was statistically different between the two groups (p<0.005). Pathological features of GCG are presented in Table 1.

All miRNAs in the GCG showed higher serum expression levels than in CG. The serum expression levels of miR-17-5p, miR-21-5p, miR-27a-3p, miR-146a-5p, miR-148-3p, and miR-203a-3p were significantly higher in the GCG than in the CG (p=0.031; 0.001; 0.011; 0.04; 0.019; 0.041, respectively). Although the expression of miR-106b-5p was 3.44 times higher in the GCG than in the CG, the increase was not statistically significant (p=0.074) (Table 2) (Figure 2a).

Compared with the CG, significant increases were observed in the serum expression levels of miR-21-5p, miR-27a-3p, miR-106b-5p, miR-146a-5p, and miR-148-3p in patients with early gastric cancer (p=0.001; 0.003; 0.05; 0.011; 0.002, respectively) (Table 2) (Figure 2b).

In patients with tumor located in the cardia, significant increases were observed in the serum expression levels of miR-17-5p, miR-21-5p, miR-27a-3p, miR-106b-5p, miR-146a-5p, miR-148-3p, and miR-203a-3p compared with CG (p=0.002; 0.001; 0.001; 0.001; 0.001; 0.001; 0.021, respectively). Although serum expression levels of miR-200a-3p were 2.67 times higher in patients with tumor located in cardia compared to the CG, this increase was not statistically significant (p=0.236) (Table 2).

In patients with tumor located outside the cardia, increases in serum expression levels of miR-21-5p and miR-27a-3p were statistically significant when compared with CG (p=0.001 and p=0.03, respectively). Despite the 2.16-fold increase in miR-17-5p expression, 2.93-fold increase in miR-106b-5p expression, and 2.31-fold increase in miR-203a-3p expression in patients with non-cardia localization, these increases were not statistically significant (p=0.059; 0.122; 0.07, respectively) (Table 2).

Compared with the CG, significant increases were observed in the serum expression levels of miR-17-5p, miR-21-5p, miR-27a-3p, miR-106b-5p, and miR-203a-3p in patients with diffuse type gastric cancer (p=0.005; 0.001; 0.003; 0.007; 0.038, respectively) (Table 2).

In patients with intestinal type gastric cancer, significant increases were observed in the serum expression levels of miR-17-5p, miR-21-5p, miR-27a-3p, miR-146a-5p, and miR-148a-3p (p=0.005; 0.001; 0.019; 0.016; 0.008, respectively). Although serum expression levels of miR-106b-5p and miR-203a-3p were 3.61 and 2.33 times higher, respectively, in patients with intestinal type gastric cancer than in the CG, this difference was not statistically significant (p=0.058 and p=0.091, respectively) (Table 2).

Table 1. Pathologic characteristics of gastric cancer group

Characteristics	Values
Tumor size (cm), median (IQR[a])	4.0 (0.9-10.0)
Tumor localization, n (%)	
Cardiac	5 (14.3%)
Non-cardiac	30 (85.7%)
Gastrectomy type, n (%)	
Total gastrectomy	23 (65.7%)
Proximal gastrectomy	2 (5.7%)
Distal gastrectomy	10 (28.6%)
Differentiation type, n (%)	
Low grade differentiated	19 (54.3%)
Well differentiated	16 (45.7%)
Lauren classification, n (%)	
Intestinal type	26 (74.3%)
Diffuse type	9 (25.7%)
Borrmann classification, n (%)	
Type 1-2	7 (20%)
Type 3-4	28 (80%)
2 median (IQR[a])	41 (31-57)
Metastatic lymph nodes, median (IQR[a])	5 (0-9)
pT, n (%)	
pT1	7 (20.0%)
PT2	1 (2.9%)
pT3	12 (34.3%)
pT4	15 (42.9%)
pN, n (%)	
pN0	9 (25.7%)
pN1	7 (20.0%)
pN2	2 (5.7%)
pN3	17 (48.6%)
Angiolymphatic invasion, n (%)	28 (80.0%)
Staging, n (%)	
Stage 1-2	17 (48.6%)
Stage 3	18 (51.4%)

[a]Interquartile range.

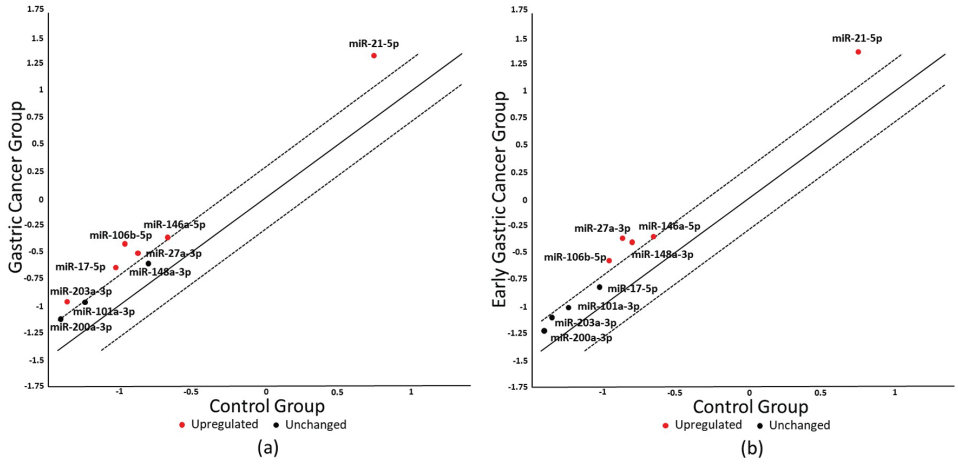

Figure 2. (a) Graphical distribution of fold change ratios of serum miRNA expression levels compared to the control group (b) Graphical distribution of fold change ratios of serum miRNA expression levels compared to the control group in early gastric cancer patients.

miRNAs: microRNA

Table 2. Comparison of serum miRNA expression levels between groups

	Gastric cancer vs. control groups		Early gastric cancer: control group		Cardiac carcinoma and control groups		Non-cardiac carcinoma vs. control group		Diffuse-type carcinoma vs. control group		İntestinal type carcinoma vs. control group	
miRNA	**FC***	**p**	**FC***	**p**	**FC***	**p**	**FC***	**p**	**FC***	**p**	**FC***	**p**
miR-17-5p	2.393	**0.031**	1,59	0.163	4.413	**0.002**	**2.161**	0.059	2.458	**0.005**	2.371	**0.041**
miR-21-5p	3.82	**0.001**	4.248	**0.001**	10.114	**0.001**	3.248	**0.001**	3.087	**0.001**	4.112	**0.001**
miR-27a-3p	2.358	**0.011**	3.182	**0.003**	5.733	**0.001**	2.034	**0.03**	2.558	**0.003**	2.293	**0.019**
miR-101-3p	1.857	0.44	1.647	0.863	1.72	0.862	1.881	0.415	1.669	0.925	1.927	0.361
miR-106b-5p	**3.443**	0.074	2.468	**0.05**	9.017	**0.001**	**2.932**	0.122	2.986	**0.007**	**3.617**	0.058
miR-146a-5p	2.037	**0.04**	2.067	**0.011**	8.066	**0.001**	1.619	0.085	1.242	0.978	2.417	**0.016**
miR-148a-3p	1.569	**0.019**	2.398	**0.002**	3.355	**0.001**	1.383	0.056	1.05	0.577	1.803	**0.008**
miR-200a-3p	1.914	0.468	1.493	0.78	**2.671**	0.236	1.811	0.69	1.883	0.51	1.925	0.582
miR-203a-3p	2.479	**0.041**	1.738	0.486	3.776	**0.021**	**2.311**	0.07	2.951	**0.038**	**2.333**	0.091

*FC: Fold change, miRNA: MicroRNA.

Evaluation of the Relationship between Serum miRNA Expression Levels and Prognostic Factors

The relationship between serum miRNA expression levels determined by the $2^{-\Delta CT}$ method and prognostic factors was evaluated by ROC analysis. The serum expression levels of miR-106b-5p and miR-146a-5p were found to be associated with tumor location (AUC: 0.773; 0.797; p=0.049; 0.036, respectively) (Table 3) (Figure 3a, b). The serum expression levels of miR-27a-3p and miR-148-5p were found to be associated with the T-stage of the tumor (AUC: 0.748; 0.729; p=0.036; 0.049, respectively) (Table 3) (Figure 3c, d).

DISCUSSION

Due to the low sensitivity and specificity of current non-invasive biomarkers for diagnosing and prognosing gastric cancer, there is a need for more useful biomarkers. It has been shown that the serum expression levels of some miRNA species can be a useful biomarker for the diagnosis and prognosis of gastric cancer (13). However, studies on their relationship with the location and T-stage, which can affect surgical management are limited. The aim of this study was to evaluate the relationship between serum miRNA levels and pathological features that affect the diagnosis, surgical management, and prognosis of gastric cancer.

Previous studies have shown that the serum expression levels of the miRNAs evaluated in our study can be used as diagnostic biomarkers for gastric cancer (10,14-17). Consistent with the literature, our study showed that miR-17-5p, miR-21-5p, miR-27a-3p, miR-146a-5p, miR-148a-5p, and miR-203a-3p serum expression levels can be used as diagnostic biomarkers for gastric cancer. In addition, the statistically significant differences in the serum expression levels of miR-21-5p, miR-27a-3p, miR-106b-5p, miR-146a-5p, and miR-148a-5p in early-stage gastric cancer patients compared to the CG indicate that these miRNAs can also be used for diagnosis in early-stage gastric cancer patients.

Table 3. Evaluation of the relationship between serum miRNA expression levels and prognostic factors

	Lymph node metastasis		Differentiation		Localization		T-stage		Tumor size		Angiolymphatic invasion		Stage		c-erb-B2	
	AUC*	p	AUC*	p	AUC*	p	AUC*	p	AUC*	p	AUC*	p	AUC*	p	AUC*	p
miR-17-5p	0.397	0.365	0.563	0.527	0.600	0.480	0.616	0.326	0.460	0.689	0.510	0.934	0.598	0.322	0.470	0.867
miR-21-5p	0.415	0.450	0.430	0.484	0.700	0.157	0.625	0.289	0.425	0.453	0.520	0.869	0.618	0.235	0.545	0.802
miR-27a-3p	0.494	0.955	0.523	0.816	0.640	0.322	**0.748**	**0.036**	0.560	0.549	0.518	0.885	0.621	0.222	0.682	0.316
miR-101-3p	0.476	0.836	0.550	0.617	0.543	0.759	0.600	0.398	0.587	0.386	0.584	0.496	0.578	0.428	0.477	0.900
miR-106b-5p	0.385	0.308	0.537	0.714	**0.773**	**0.049**	0.514	0.906	0.453	0.641	0.469	0.805	0.637	0.166	0.515	0.933
miR-146a-5p	0.532	0.777	0.553	0.594	**0.797**	**0.036**	0.662	0.169	0.563	0.527	0.589	0.470	0.492	0.934	0.530	0.867
miR-148a-3p	0.412	0.439	0.375	0.211	0.610	0.437	**0.729**	**0.049**	0.397	0.301	0.472	0.821	0.658	0.109	0.758	0.155

*AUC: Area under the curve.

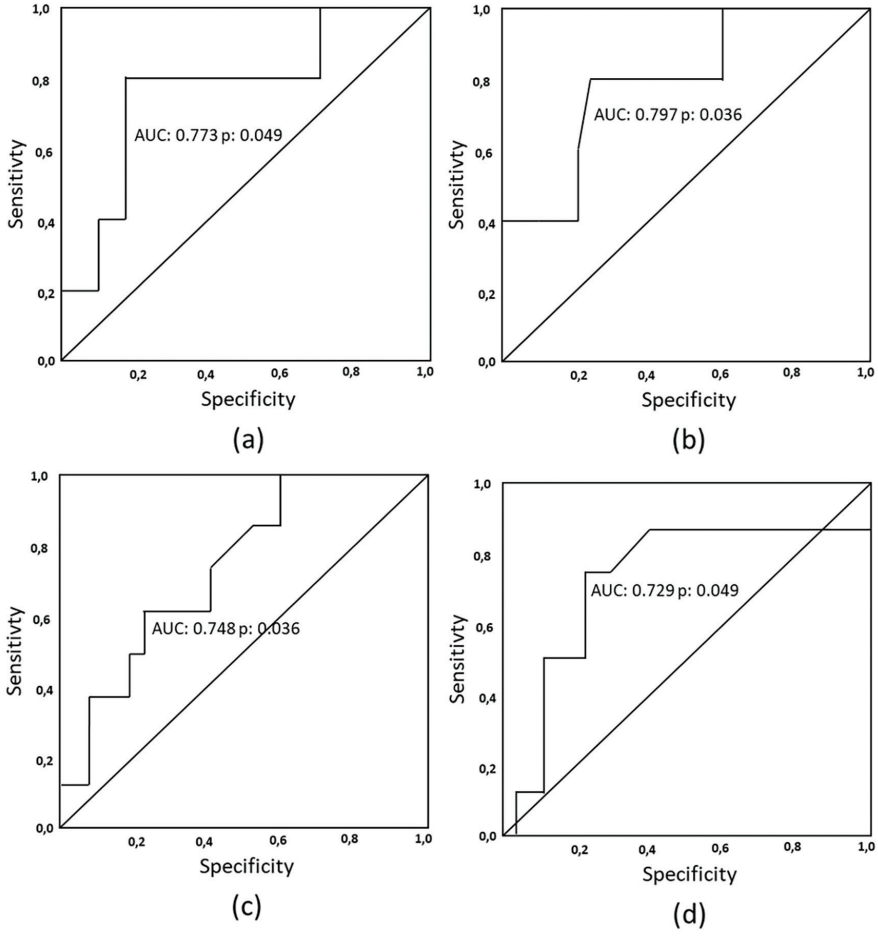

Figure 3. (a) ROC analysis of miR-106b-5p serum expression level in tumor localization discrimination, (b) ROC analysis of miR-146a-5p serum expression level in tumor localization discrimination, (c) ROC Analysis of miR-27a-3p serum expression level in T-extension discrimination, (d) ROC analysis of miR-148a-5p serum expression level in T-extension discrimination.

ROC: Receiver operating characteristic.

Study Limitations

Previous limited studies have indicated that serum miR-27a-3p expression levels could be a prognostic biomarker for gastric cancer (10,17). However, these studies have focused on lymph node metastasis and TNM staging rather than the T-stage of the tumor. In addition to these studies, our study showed that miR-27a-3p and miR-148a-5p serum expression levels are related to T -stage and can be prognostic biomarkers. Furthermore, we believe that miR-106b-5p and miR-146a-5p are potential prognostic biomarkers because of their significant variations in serum expression levels in gastric cardia cancers based on tumor location, another important prognostic factor.

CONCLUSION

Serum miRNA expression levels can play an important role in addressing the need for non-invasive biomarkers for evaluating prognostic factors that can affect surgical management and the diagnosis of gastric cancers. Our study showed that serum miR-17-5p, miR-21-5p, miR-27a-3p, miR-146a-5p, miR-148a-5p, and miR-203a-3p expression levels are diagnostic biomarkers for gastric cancer. Additionally, we observed that miR-21-5p, miR-27a-3p, miR-106b-5p, miR-146a-5p, and miR-148a-5p serum expression levels are diagnostic for early-stage gastric cancers. The relationship of serum miR-106b-5p and miR-146a-5p expression levels with tumor location and serum miR-27a-3p and miR-148a-5p expression levels with the T-stage of the tumor can prevent radical surgical interventions in patients with near-normal serum expression levels of these miRNAs during the preoperative period. However, further comprehensive studies are required to confirm our hypothesis.

Ethics

Ethics Committee Approval: This study was funded by the Gazi University Department of Projects of Scientific Inquiry and was approved by the Institutional Review Board of the Gazi University Faculty of Medicine Ethics Committee (approval number: 666, date: 24.09.2018).

Informed Consent: Informed consent was obtained from all patients and healthy volunteers who participated in the study.

Authorship Contributions

Concept: Ç.B., Design: Ç.B., H.D., A.U.D., Supervision: Ö.G., A.B., Resources: Ç.B., A.B., Material: Ç.B., E.K., M.N., A.Y., H.G., H.B., Data Collection or Processing: Ç.B., E.K., M.N., A.Y., H.G., H.B., Analysis or Interpretation: N.S.Y., H.D., İ.Ö., Ö.G., Literature Search: Ç.B., F.A., K.D., Writing: Ç.B., Critical Review: Ö.G., A.B.

Conflict of Interest: No conflict of interest was declared by the authors.

Financial Disclosure: This study was funded by the Gazi University Department of Projects of Scientific Inquiry.

REFERENCES

1. Sung H, Ferlay J, Siegel RL, Laversanne M, Soerjomataram I, Jemal A, et al. Global Cancer Statistics 2020: GLOBOCAN Estimates of Incidence and Mortality Worldwide for 36 Cancers in 185 Countries. CA Cancer J Clin. 2021; 71: 209-49.
2. Abad MRA, Shimamura Y, Fujiyoshi Y, Seewald S, Inoue H. Endocytoscopy: technology and clinical application in upper gastrointestinal tract. Transl Gastroenterol Hepatol. 2020; 5: 28.
3. Zhang A, Zou X, Yang S, Yang H, Ma Z, Li J. Effect of NETs/COX-2 pathway on immune microenvironment and metastasis in gastric cancer. Front Immunol. 2023; 14: 1177604.
4. Zhu XD, Zhang LX, Luo PQ, Zhu H, Wei ZJ, Xu AM. Prognostic significance of post-preoperative tumor markers increments in patients with non-metastatic gastric cancer. J Cancer Res Clin Oncol. 2023; 149: 12191-201.
5. Chen Y, Shen Y, Lin P, Tong D, Zhao Y, Allesina S, et al. Gene regulatory network stabilized by pervasive weak repressions: microRNA functions revealed by the May-Wigner theory. Natl Sci Rev. 2019; 6: 1176-88.
6. Qin Y, Liang R, Lu P, Lai L, Zhu X. Depicting the Implication of miR-378a in Cancers. Technol Cancer Res Treat. 2022; 21: 15330338221134385.
7. Wu D, Lu J, Xue Z, Zhong Q, Xu BB, Zheng HL, et al. Evaluation of dynamic recurrence risk for locally advanced gastric cancer in the clinical setting of adjuvant chemotherapy: a real-world study with IPTW-based conditional recurrence analysis. BMC Cancer. 2023; 23: 964.
8. Kulig P, Pach R, Majewska O, Kulig J. Clinicopathological Prognostic Factors Determining Outcomes of Treatment in Gastric Cancer Surgery. In Vivo. 2022; 36: 2927-35.
9. Jiang X, Wang W, Yang Y, Du L, Yang X, Wang L, et al. Identification of circulating microRNA signatures as potential noninvasive biomarkers for prediction and prognosis of lymph node metastasis in gastric cancer. Oncotarget. 2017; 8: 65132-42.
10. Kim SY, Jeon TY, Choi CI, Kim DH, Kim DH, Kim GH, et al. Validation of circulating miRNA biomarkers for predicting lymph node metastasis in gastric cancer. J Mol Diagn. 2013; 15: 661-9.
11. Amin MB, Greene FL, Edge SB, Compton CC, Gershenwald JE, Brookland RK, et al. The Eighth Edition AJCC Cancer Staging Manual: Continuing to build a bridge from a population-based to a more "personalized" approach to cancer staging. CA Cancer J Clin. 2017; 67: 93-9.
12. Kozomara A, Griffiths-Jones S. miRBase: annotating high confidence microRNAs using deep sequencing data. Nucleic Acids Res. 2014; 42: D68-73.
13. Schwarzenbach H, Nishida N, Calin GA, Pantel K. Clinical relevance of circulating cell-free microRNAs in cancer. Nat Rev Clin Oncol. 2014; 11: 145-56.
14. Cholewinski G, Garczorz W, Francuz T, Owczarek AJ, Kimsa-Furdzik M, Blaszczynska M, et al. Expression of let-7a, miR-106b and miR-29b is changed in human gastric cancer. J Physiol Pharmacol. 2022; 73.
15. Sierzega M, Kaczor M, Kolodziejczyk P, Kulig J, Sanak M, Richter P. Evaluation of serum microRNA biomarkers for gastric cancer based on blood and tissue pools profiling: the importance of miR-21 and miR-331. Br J Cancer. 2017; 117: 266-73.
16. Park JL, Kim M, Song KS, Kim SY, Kim YS. Cell-Free miR-27a, a Potential Diagnostic and Prognostic Biomarker for Gastric Cancer. Genomics Inform. 2015; 13: 70-5.
17. Juzėnas S, Saltenienė V, Kupcinskas J, Link A, Kiudelis G, Jonaitis L, et al. Analysis of Deregulated microRNAs and Their Target Genes in Gastric Cancer. PLoS One. 2015; 10: e0132327.

Original Investigation | Özgün Araştırma

GMJ 2024;35:422-432

DOI: http://dx.doi.org/10.12996/gmj.2024.4241

Molecular and Clinical Overview of Type 1 Neurofibromatosis: Single Center Study and Mini Review on NF1-Associated Vasculopathy and Juvenile Myelomonocytic Leukemia

Tip 1 Nörofibromatozise Moleküler ve Klinik Genel Bakış: NF1 ile İlişkili Vaskülopati ve Jüvenil Miyelomonositik Lösemi Üzerine Tek Merkez Çalışması ve Kısa Gözden Geçirme

Şule Altıner[1,2], Alper Han Çebi[3]

[1]Department of Medical Genetics, University of Health Sciences Türkiye, Trabzon Kanuni Training and Research Hospital, Trabzon, Türkiye
[2]Department of Medical Genetics, Ankara University Faculty of Medicine, Ankara, Türkiye
[3]Department of Medical Genetics, Karadeniz Technical University Faculty of Medicine, Trabzon, Türkiye

ABSTRACT

Objective: Neurofibromatosis type 1 (NF1) is a genetic disorder presenting primary with variable patterns of skin pigmentation, neurofibromas and iris Lisch nodules. In addition, likely pathogenic/pathogenic mutations of the *NF1* gene predispose to multiple tumors. Juvenile myelomonocytic leukemia (JMML) is also associated with NF1. Molecular diagnosis is important in patients with an atypical presentation, as well as in children who have not yet developed sufficient characteristic features or for providing prenatal diagnosis. The purpose of this study was to define *NF1* gene mutations in the northeastern part of Türkiye and to contribute to the mutational spectrum of NF1. In addition, rare findings, such as cerebral vasculopathy and JMML, were discussed over the phenotypic findings.

Methods: In this study, *NF1* gene sequence analysis was performed using next-generation sequencing in 32 unrelated Turkish patients with a prediagnosis of NF1.

Results: Disease-causing variants were found in 68.75% (n=22/32) of the patients, whereas two of them were novel. Our study was also important in the aspect of vasculopathy regarding the frequency which was 9.1% of in a relatively small patient group. Another aspect was the distinct distribution of malignant tumors. In contrast to central nervous system malignancies, which are the most common malignancies apart from malignant peripheral nerve sheath tumors in the literature, JMML was the most common in our study.

Conclusion: The aim of this study is to draw attention to rare symptoms, such as vasculopathy and JMML, in NF1 in a small cohort. Although

ÖZ

Amaç: Nörofibromatozis tip 1 (NF1), sıklıkla değişken deri pigmentasyonları, nörofibromlar ve iris Lisch nodülleri bulguları gösteren genetik bir hastalıktır. Ayrıca *NF1* genindeki olası patojenik/patojenik mutasyonlar tümör gelişimine zemin hazırlarlar. Juvenil miyelomonositik lösemi (JMML) de NF1 ile ilişkilidir. Atipik prezentasyonlu hastalarda ve yeterli karakteristik bulguları ortaya çıkmamış çocuklarda veya prenatal tanının sağlanmasında moleküler tanı önemlidir. Bu çalışmanın amacı Türkiye'nin kuzeydoğusundaki *NF1* gen mutasyonlarını tanımlamak ve NF1'in mutasyon spektrumuna katkıda bulunmaktır. Ayrıca NF1'in serebral vaskülopati ve JMML gibi nadir görülen bulguları da fenotipik bulgular üzerinden tartışılmıştır.

Yöntemler: Bu çalışmada NF1 ön tanısı ile, aralarında akrabalık olmayan 32 Türk hastada yeni nesil dizileme tekniği ile *NF1* geni dizi analizi yapıldı.

Bulgular: Hastaların %68,75'inde (n=22/32) hastalığa neden olan varyant saptanırken, bunlardan ikisi novel idi. Çalışmamız aynı zamanda nispeten küçük bir hasta grubunda %9,1 oranında görülen vaskülopati açısından da önemliydi. Diğer bir önemli sonuç ise malign tümörlerin dağılımı idi. Literatürde malign periferik sinir kılıfı tümörleri dışında en sık görülen maligniteler santral sinir sistemi maligniteleri iken bizim çalışmamızda en sık JMML görüldü.

Sonuç: Bu çalışmanın amacı küçük bir kohortta NF1'de vaskülopati ve JMML gibi nadir görülen bulgulara dikkat çekmektir. JMML nadir görülen bir çocukluk çağı kanseri olmasına rağmen RASopatilere

Address for Correspondence/Yazışma Adresi: Şule Altıner, MD, Department of Medical Genetics, University of Health Sciences Türkiye, Trabzon Kanuni Training and Research Hospital, Trabzon; Ankara University Faculty of Medicine, Ankara, Türkiye
E-mail / E-posta: bicers@ankara.edu.tr
ORCID ID: orcid.org/0000-0001-5789-8630

Received/Geliş Tarihi: 18.06.2024
Accepted/Kabul Tarihi: 03.07.2024

ABSTRACT

JMML is a rare childhood cancer, it is accompanied by RASopathies. It is important to investigate this association because JMLL treatment approaches change in the presence of germline mutations.

Keywords: Neurofibromatosis type 1, NF1, cerebrovascular stenosis, leukemia, JMML

ÖZ

eşlik eder. JMLL ile RASopati ilişkisinin araştırılması oldukça önemlidir çünkü germ hattı mutasyonlarının varlığında JMML tedavi yaklaşımları değişmektedir.

Anahtar Sözcükler: Nörofibromatozis tip 1, NF1, serebrovasküler stenoz, lösemi, JMML

INTRODUCTION

Neurofibromatosis type 1 (NF1) is one of the most frequent human genetic disorders. The incidence of NF1 is 1 per 2000 and 3000 births worldwide (1,2). Heterozygous pathogenic variants of the *NF1* gene cause this disease (3,4). The most common symptoms are variable skin pigmentation, multiple benign neurofibromas and iris Lisch nodules. Plexiform neurofibromas, malignant peripheral nerve sheath tumors, optic nerve and other central nervous system gliomas, vasculopathy, scoliosis, tibial dysplasia, and learning disabilities are less common but serious manifestations of NF1 (3).

The diagnosis of NF1 can be made in an individual who does not have a parent diagnosed with NF1 if two or more of the following are present according to revised diagnostic criteria for NF1: Six or more café-au-lait macules (CALMs) (>5 mm in greatest diameter in prepubertal individuals and >15 mm in greatest diameter in postpubertal individuals), freckling in the axillary or inguinal region [at least one of the two pigmentary findings (CALMs or freckling) should be bilateral], two or more neurofibromas of any type or one plexiform neurofibroma, optic pathway glioma, two or more iris Lisch nodules identified by slit lamp examination or two or more choroidal abnormalities defined as bright, patchy nodules imaged by optical coherence tomography/near-infrared reflectance imaging, a distinctive osseous lesion such as sphenoid dysplasia, anterolateral bowing of the tibia, or pseudarthrosis of a long bone, a heterozygous pathogenic NF1 variant with a variant allele fraction of 50% in apparently normal tissue such as white blood cells. In addition, a child of a parent who meets the diagnostic criteria specified above merits a diagnosis of NF1 in the presence of one or more of the criteria are present (5). The majority of patients have only mild manifestations of NF1, but symptoms increase with age. Because many features of NF1 increase in frequency with age, most patients without a family history meet the criteria by the age of eight (3,5). Findings that are common and can be determined objectively by many physicians are included in the diagnostic criteria. However, there are many findings other than those specified in the diagnostic criteria. Of these findings, juvenile myelomonocytic leukemia (JMML) and vasculopathy are critical findings for patient management. Therefore, it is important to examine patients for symptoms in all systems that may accompany NF1, apart from the diagnostic criteria (1).

NF1 is characterized by extreme clinical variability both among patients and within families (3,6). Modifier genes and/or environmental factors are possible reasons for this variability (7).

The average life expectancy is reduced in patients with NF1 compared to general population, and vasculopathy and malignant peripheral nerve sheath tumors are the most important causes of early death (3).

The diagnosis of NF1 is established by "revised diagnostic criteria for NF1". Molecular genetic testing is necessary in patients with an atypical presentation or in children who have not developed the most characteristic features to provide prenatal diagnosis (3).

The *NF1* gene comprises 60 exons and spans 350 kb of genomic DNA (3). More than 2500 mutations have been reported in the *NF1* gene in the human gene mutation database. Although diverse mutations are observed, most cause loss-of-function of the gene product and protein truncation (8). Among these, 5% were deletions encompassing the entire *NF1* locus (9). Almost half of all affected individuals have NF1 because of *de novo* mutations. Many genetic changes are unique to a particular family (3).

NF1 encodes neurofibromin, which is expressed in many tissues, but highly in neurons, non-myelinating Schwann cells, oligodendroglia cells, and dorsal root ganglia (10). Neurofibromin is an Ras GTPase-activating protein (GAP), which down regulates ras protein activity. Therefore, GAP acts as a tumor suppressor by controlling cellular proliferation. Several mutations diminish GAP activity, stimulate cellular proliferation, indicating the importance of RAS regulation in NF1 (4,6). Due to its effects on Ras-MAPK signaling via GAP, NF1 has been considered in RASopathy syndromes (4). In this study, patient data for which the diagnosis of NF1 was confirmed via mutation analysis were discussed. The aim of this study was to identify *NF1* gene mutations in northeastern Türkiye and to contribute to the mutational spectrum of NF1. In addition, rare findings, such as cerebral vasculopathy and JMML, were discussed over the phenotypic findings.

MATERIALS AND METHODS

Patients

A total of 32 patients with a pre-diagnosis of NF1 who were consulted to the medical genetics departments of the University of Health Sciences Türkiye, Trabzon Kanuni Training and Research Hospital and Karadeniz Technical University Faculty of Medicine, from 2017 to 2019, were taken to the study. All patients were born in northeast Türkiye. In addition, they were descended from families in the same region. This study was approved by the Institutional Ethics Committee by University of Health Sciences Türkiye, Trabzon Kanuni Training and Research Hospital (approval number: 2019/22, date: 25.04.2019). Informed written consent was obtained from the patient's parents. Each patient underwent a detailed evaluation by a medical geneticist. Prenatal and birth histories as well as family history were recorded, and pedigree analysis besides detailed physical examination, was performed. Dysmorphic features were evaluated in detail and noted. Cranial magnetic resonance imaging (MRI) was offered to all patients, but only pathological findings

were mentioned in the neurologic finding section of Table 2. On the other hand, MR angiography was planned in cases with any clinical suspicion of cranial vascular pathology.

Peripheral blood samples were collected from the patients and their parents, if possible. Patient DNA were extracted by QIAcube® automated DNA isolation system (Qiagen) according to the manufacturer's instructions.

All coding exons, including flanking intron regions, of the *NF1* gene were amplified by polymerase chain reaction. After library enrichment (MiSeq Reagent Kit v2, MS-102-2003) and quality control, the samples were sequenced using the MiSeq platform (Illumina, San Diego, California, United States). Raw reads were quality-trimmed with Trimmomatic and mapped to the reference human genome (hg19) with using Burrows-Wheeler Alignment Tool. Duplicates were removed using SAMTools and realignment across indels and base quality recalibration were performed with GATK.

Sanger sequencing was used to confirm low-quality variants, insertions/deletions, and splice site alterations on Applied Biosystems 3130 Genetic Analyzer. In addition, Sanger sequencing was used for segregation analysis.

Statistical Analysis

Descriptive study. Statistical analysis were not performed.

Data analysis and variant classification: The sequence was analyzed from both forward and reverse *stands* and compared with the *NF1* reference sequence NM_001042492.3 (https://www.ncbi.nlm.nih.gov/nuccore/NM_001042492). Reads were analyzed using the Integrative Genomics Viewer program, and read alignment was done according to the hg19/GRCh37 human reference genome. A minimum of 100x coverage was accepted read depth. Variants with a frequency higher than 0.5% were filtered out.

The identified variants were queried by browsing the HGMD (8), ClinVar (11) databases. Common variants were excluded by minor allele frequency (MAF >1) score by using 1000 Genomes Project (http://www.1000genomes.org/), gnomAD (https://gnomad.broadinstitute.org/) and NCBI dbSNP (database of Single Nucleotide Poylmorphisms https://www.ncbi.nlm.nih.gov/snp/) database. In silico prediction algorithms [PolyPhen2 (12), SIFT (13), MutationTaster software (14), and conservation scores (PlyloP 100)] (https://ccg.epfl.ch/mga/hg19/phylop/phylop.html) were used to interpret novel variants. The American College of Medical Genetics and Genomics and the Association for Molecular Pathology 2015 guidelines were used for the final variant classification (15).

RESULTS

NF1 gene sequence analysis was performed in 32 unrelated patients (18 males-14 female age: 1-47 years) in this study. Of them, a disease-causing variant was found in 22 and (68.75%) (Table 1). Twenty-two discrete mutations were detected. One mutation was observed twice (c.1019_1020delCT, p. Ser340CysfsTer12), whereas one patient harbored two pathogenic variants (c.1185+1G>T, IVS10+1G>T; c.8059_8060delAG, p. Ser2687CysfsTer5, which both were *de novo* but, cis/trans location could not be determined).

No mutational hotspot region was detected. Two mutations were novel (2/22), 13 were single nucleotide variants (13/22), eight were deletions (8/22) and one was insertion (1/22). Most variants were single nucleotide change mutations that cause disease by creating frameshift or premature stop codons. Concisely, the mechanism underlying this disease was the altered coding that led to truncated neurofibromin in the majority of mutations.

Family study could be performed for 20 of the patients, and eight mutations were found to be inherited (five paternal vs. 3 maternal), whereas 12 were *de novo*. No family history was noted for cases with *de novo* mutations. Mosaicism was not detected in the DNA extracted from the peripheral blood specimens of the patients and parents.

Fifteen out of 22 patients with pathogenic variant and 3 out of 10 patients without pathogenic variant fulfilled the diagnostic criteria. The diagnostic utility of NGS was 83% (15/18) for patients who fulfilled the NIH criteria in this study. The ages of seven patients who had molecular diagnosis without meeting the NIH criteria were 1-6 and none of them had a family history and harbored *de novo* mutations (cases: 5, 8, 11, 13, 15, 17 and 22).

The medical history and clinical findings of patients with molecular diagnosis is as follows (Table 2). Eight out of 22 patients had a parent who meets the diagnostic criteria. All patients had skin manifestations. The most common skin finding was CALMs. Although all patients had CALMs, in seven patients they were not sufficient to be a diagnostic criterion (case 5, 8, 11, 13, 15, 17, 22). The second was freckling (13/22) and the third was neurofibroma (9/22). Lisch nodules were detected in nine patients. Macrocephaly, which was detected in 13 patients, was also common in our cohort. The presence of focal areas of signal intensity (FASI) were the most common brain MRI findings (10/22). The other findings were scoliosis (2/22), short stature (2/22), learning disability (3/22), developmental delay (1/22), dural ectasia (1/22), and hydrocephalus (1/22). Cranial vascular pathology was detected in two patients (case 9 and 11) (Figures 1, 2), who had also intellectual disability and epilepsy. Malignancies were found in four patients. One patient had high-grade glioma, one had optic glioma, and two had JMML. Because of the wide distribution of mutations on the *NF1* gene, genotype-phenotype correlation could not be established.

DISCUSSION

NF1 mutation analysis is difficult due to the large size of the gene, presence of pseudogenes, and lack of mutation hotspots (16). In addition, approximately in 5% of patients have NF1 resulting from whole gene deletions (17). Current laboratory methodologies should be combined to detect mutations (18). RNA analysis is more sensitive than DNA methods with a detection rate of 95.8% (19). On the other hand, NGS was involved in diagnosis, providing a less costly method than Sanger sequencing and faster turnaround. Deletion/duplication analysis of the *NF1* and *SPRED1* gene sequence analysis should be performed in undiagnosed cases (16,18). Besides, alternative diagnoses, including, but not limited to, Legius syndrome, Noonan syndrome with multiple lentigines, and constitutional mismatch repair deficiency syndrome should be considered (5).

Table 1. List of detected disease-causing variants

Case no	Nucleotide change	Amino acid change	Location	Coding impact	Variant type	Reference	Inheritance	Pathogenicity (ACMG criteria)
1	c.479G>T	p. Arg160Met	Exon 4	Missense variant	SNV	HGMD	*De novo*	Pathogenic
2	c.1019_1020delCT	p. Ser340CysfsTer12	Exon 9	Frameshift variant	Deletion	ClinVar, HGMD	*De novo*	Pathogenic
3	c.1019_1020delCT	p. Ser340CysfsTer12	Exon 9	Frameshift variant	Deletion	ClinVar, HGMD	Maternal	Pathogenic
4	c.1393_1394delAG	p. Leu466TyrfsTer3	Exon 13	Frameshift variant	Deletion	ClinVar	*De novo*	Pathogenic
5	c.1722-3C>A		Intron 15	Splicing variant	SNV	ClinVar	*De novo*	Likely pathogenic
6	c.1885G>A	p. Gly629Arg	Exon 17	Missense variant	SNV	ClinVar, HGMD	NA	Pathogenic
7	c.2325G>C	p. Glu775Asp	Exon 19	Splicing variant	SNV	ClinVar, HGMD	*De novo*	Pathogenic
8	c.2466dupA	p. Gly823ArgfsTer8	Exon 21	Frameshift variant	Insertion	Novel	*De novo*	Pathogenic
9	c.3445A>G	p. Met1149Val	Exon 26	Missense variant	SNV	ClinVar, HGMD	*De novo*	Pathogenic
10	c.3457_3460delCTCA	p. Leu1153MetfsTer4	Exon 26	Frameshift variant	Deletion	ClinVar	Paternal	Pathogenic
11	c.3525_3526delAA	p. Arg1176SerfsTer18	Exon 27	Frameshift variant	Deletion	ClinVar, HGMD	*De novo*	Pathogenic
12	c.3826C>T	p. Arg1276Ter	Exon 28	Non-sense variant	SNV	ClinVar, HGMD	NA	Pathogenic
13	c.3897delA	p. Lys1299AsnfsTer10	Exon 29	Frameshift variant	Deletion	ClinVar, HGMD	*De novo*	Pathogenic
14	c.3916C>T	p. Arg1306Ter	Exon 29	Non-sense variant	SNV	ClinVar, HGMD	Paternal	Pathogenic
15	c.4084C>T	p. Arg1362Ter	Exon 30	Frameshift variant	SNV	ClinVar, HGMD	*De novo*	Pathogenic
16	c.4769T>G	p. Leu1590Ter	Exon 36	Non-sense variant	SNV	ClinVar, HGMD	Paternal	Pathogenic
17	c.4931A>G	p. Asp1644Gly	Exon 37	Missense variant	SNV	ClinVar, HGMD	*De novo*	Pathogenic
18	c.5347_5350delTATT	p. Tyr1783MetfsTer10	Exon 38	Frameshift variant	Deletion	ClinVar	Maternal	Pathogenic
19	c.5489G>T	p. Arg1830Leu	Exon 38	Missense variant	SNV	ClinVar, HGMD	Paternal	Pathogenic
20	c.5902C>T	p. Arg1968Ter	Exon 40	Non-sense variant	SNV	ClinVar, HGMD	Maternal	Pathogenic
21	c.6854_6855delAC	p. Tyr2285Ter	Exon 46	Non-sense variant	deletion	Novel	Paternal	Pathogenic
22	c.1185+1G>T // c.8059_8060delAG	IVS10+1G>T // p. Ser2687CysfsTer5	Intron 10 // exon 55	Splicing variant // frameshift variant	SNV // deletion	ClinVar, HGMD // ClinVar, HGMD	*De novo*	Pathogenic // pathogenic

ACMG: American College of Medical Genetics, HGMD: Human gene mutation database, SNV: Single nucleotide variant.

Table 2. Medical history and clinical findings of patients with molecular diagnosis. Table was designed according to revised diagnostic criteria for NF1 Legius et al. (5)

Case no	Age/ sex	A parent who meets the diagnostic criteria	Café-au-lait macules*	Freckling**	Neurofibromas***	Optic pathway glioma	Lisch nodules or choroidal abnormalities¶	Distinctive osseous lesion₮	Other	Neurologic	Neoplasia other than optic pathway glioma
1	8/M	-	+	+	-	+	-	-	Macrocephaly	Learning disability, presence of FASI detected by brain MRI	-
2	9/F	-	+	+	+	-	-	-	Macrocephaly	Presence of FASI detected by brain MRI	-
3	38/F	+	+	+	-	-	Lisch nodules	-	Macrocephaly	-	-
4	40/F	-	+	+	-	-	Lisch nodules	-	-	Learning disability	-
5	6/F	-	-#	-	-	-	-	-	Macrocephaly	Presence of FASI detected by brain MRI	-
6	47/F	-	+	-	+	-	Lisch nodules	-	Osteopenia	-	-
7	14/M	-	+	+	+	-	Lisch nodules	-	Macrocephaly, short stature	Presence of FASI detected by brain MRI	-
8	2/F	-	-#	+	-	-	-	-	Macrocephaly	Presence of FASI detected by brain MRI, hydrocephalus	High grade glioma
9	11/M	-	+	+	+	-	Lisch nodules	-	-	Intellectual disability, severe stenosis, and poor filling from the distal m1 segment of the right medial cerebral artery, epilepsy	-
10	30/F	+	+	+	+	-	Lisch nodules	-	Short stature	-	-
11	3/M	-	-#	-	-	-	-	-	Macrocephaly	Intellectual disability, prominent sulcus of right frontoparietal region, cortical atrophy and thinning in the right middle cerebral artery branches were observed in T2-weighted MRI, epilepsy	-

Table 2. Continued

Case no	Age/ sex	A parent who meets the diagnostic criteria	Café-au-lait macules*	Freckling**	Neurofibromas***	Optic pathway glioma	Lisch nodules or choroidal abnormalities¶	Distinctive osseous lesion₮	Other	Neurologic	Neoplasia other than optic pathway glioma
12	36/M	-	+	+	+	-	Lisch nodules	-	-	-	-
13	2/M	-	-#	-	-	-	-	-	Macrocephaly, juvenile xanthogranuloma	-	-
14	21/F	+	+	+	+	-	Lisch nodules	-	-	Learning disability	-
15	1/M	-	-#	-	-	-	-	-	Macrocephaly	-	Juvenile myelomonocytic leukemia
16	2/F	+	+	-	-	-	-	-	Juvenile xanthogranuloma	Presence of FASI detected by brain MRI	-
17	6/M	-	-#	-	-	-	-	-	Macrocephaly	-	-
18	3/M	+	+	-	-	-	-	-	Scoliosis	Presence of FASI detected by brain MRI, dural ectasia	-
19	2/M	+	+	+	-	-	-	-	Macrocephaly	Developmental delay, presence of FASI detected by brain MRI	-
20	33/M	+	+	+	+	-	Lisch nodules	-	Macrocephaly	-	-
21	14/M	+	+	+	+	-	-	-	Macrocephaly, scoliosis	Presence of FASI detected by brain MRI	-
22	3/M	-	-#	-	-	-	-	-	-	Presence of FASI detected by brain MRI	Juvenile myelomonocytic leukemia

*Six or more café-au-lait macules over 5 mm in greatest diameter in prepubertal individuals and over 15 mm in greatest diameter in postpubertal individuals. At least one of the two pigmentary findings (café-au-lait macules or freckling) should be bilateral. -# Although patients had café-au-lait macules, none was sufficient to be a diagnostic criterion. **Freckling in the axillary or inguinal region. At least one of the two pigmentary findings (café-au-lait macules or freckling) should be bilateral. ***Two or more neurofibromas of any type or one plexiform neurofibroma. ¶Two or more iris Lisch nodules identified by slit lamp examination or two or more choroidal abnormalities. ₮Such as sphenoid dysplasia, b anterolateral bowing of the tibia, or pseudarthrosis of a long bone.
FASI: Focal areas of signal intensity, MRI: Magnetic resonance imaging, M: Male, F: Female.

A Turkish population study from Ulusal et al. (20) and Bildirici et al. (21) suggested that NGS and multiplex ligation-dependent probe amplification (MLPA) methods are practical and helpful tools for genetic diagnosis of NF1. Sharifi et al. (22) used a multi-step process of NGS, MLPA, and array-comparative genomic hybridization in the analysis of NF1 patients.

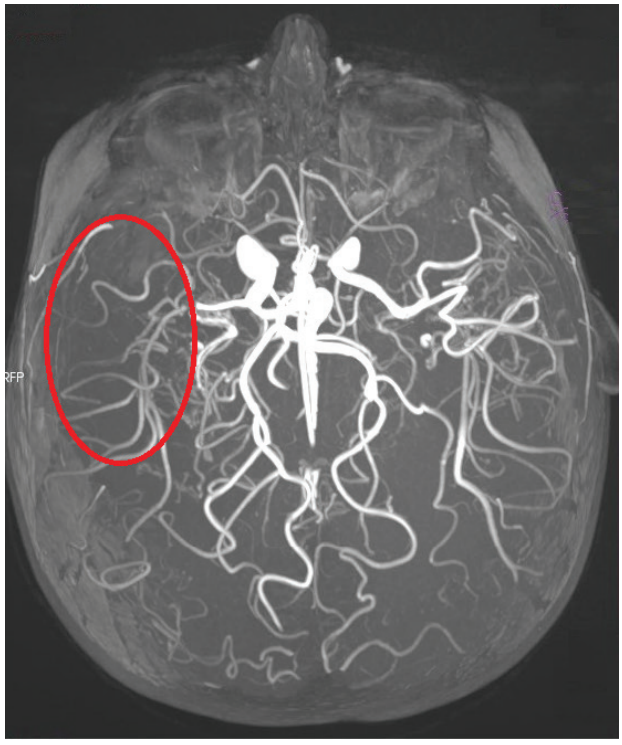

Figure 1. Cranial magnetic resonance imaging of case 9. Severe stenosis from the distal of the right middle cerebral artery M1 segment in 3D image and poor filling compared to its symmetry.

Although three patients fulfilled the revised diagnostic criteria for NF1, no pathogenic variant was detected in our study: 4-year-old male with eight CALMs >5 mm, axillary freckling, two Lisch nodules, and optic glioma; 15-year-old male with multiple CALMs >15 mm, axillary freckling, three neurofibromas, three Lisch nodules, family history of NF1; 27-year-old female with multiple CALMs >15 mm, axillary freckling, multiple neurofibromas, two Lisch nodules, scoliosis. Extensive genetic tests should be performed to detect possible deletions, deep intronic or non-coding region mutations.

All patients who harbor a pathogenic mutation and do not fulfill the revised diagnostic criteria are between 1-6 years of age (cases: 5, 8, 11, 13, 15, 17, 22). NF1 mutation analysis was performed in these patients' variable set of clinical features (CALMs, freckling, juvenile xanthogranuloma, macrocephaly, JMML, presence of FASI detected by MRI). Further clinical and genetic evaluation is recommended if the patient's diagnostic criteria do not meet NF1, despite NF1 pathogenic variants. Two cases met the diagnostic criteria after serial observations and follow-up (case 8 and 11). Further genetic analysis is planned for the remaining patients to verify whether the variant is germline, somatic, or mosaic. Cases 15 and 22 did not continue follow-up at our center. Since both patients did not have a parent who met the diagnostic criteria with NF1, further genetic analysis from a second tissue such as buccal must be performed.

In this study, disease-causing variants in the *NF1* gene were identified at a rate of about 68.75% with NGS, which is consistent with the sequencing method analysis in different studies (23,24). Our study emphasizes the benefits of NGS, which is very suitable in terms of producing rapid results economically and we suggest that it can be used as a first-step test.

According to family studies, 60% (12/20) of patients had the disorder caused by *de novo* mutations, which is also compatible with literature (3).

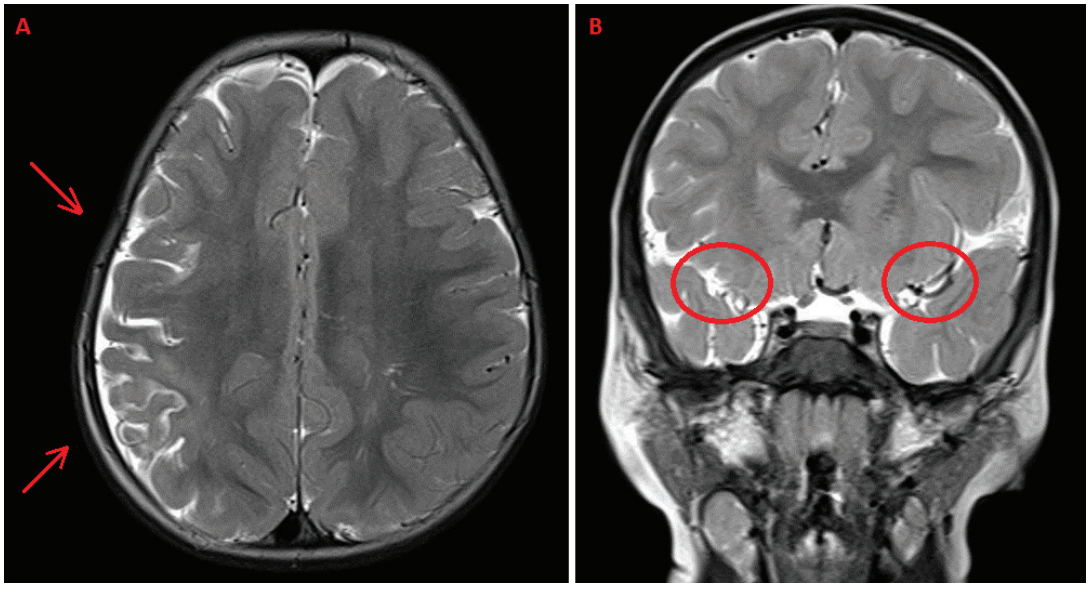

Figure 2. Cranial imaging of case 11. (A) Cortical atrophy and prominent sulcus of right frontoparietal region in axial T2-weighted magnetic resonance imaging (MRI). (B) Thinning in the right middle cerebral artery branches were observed in coronal T2-weighted MRI.

Table 3. List of in silico analysis of putative novel variants

Case no	Nucleotide change	Amino acid change	Splice distance	Coding impact	Mutation taster	PhyloP100
8	c.2466dupA	p. Gly823ArgfsTer8	58	Frameshift variant	Disease causing (prob:1)	5.708
21	c.6854_6855delAC	p. Tyr2285Ter	36	Non-sense variant	Disease causing (prob:1)	8.618

Two variants were considered as novel pathogenic according to population data, predictive impact, and segregation analysis (Supplementary Figure 1). The distribution according to their coding impacts was frameshift and non-sense. These variants were evaluated by comprehensive in silico analysis (Table 3). Evolutionary sequence homology and splice distance were shown for all novel variants. These variants were detected in cases 8 and 21. Case 8 was a two-year-old female. She was consulted by our department after being diagnosed with high-grade glioma. She had three CALMs >5 mm in greatest diameter, bilateral axillary freckling, macrocephaly, presence of FASI detected by brain MRI, and hydrocephalus. Neither of the parents was diagnosed with NF1. CALMs were increased in number and size during serial observations and follow up and she met revised diagnostic criteria for NF1. Case 21 was fourteen-year-old male who had ten CALMs >15 mm in greatest diameter, bilateral freckling in the axillary and inguinal regions, and multiple neurofibromas in his trunk. He also had macrocephaly, scoliosis, presence of FASI detected on brain MRI. His father was also diagnosed with NF1.

Genotype-phenotype correlation is not easy to discuss because of the high clinical variability in NF1. No clear genotype-phenotype correlation has been recognized in NF1 so far, apart from four alterations: Whole NF1 deletion associated with severe phenotype with facial dysmorphism, cognitive deficits, early onset of multiple cutaneous neurofibromas, and cardiovascular anomalies. In addition, patients have a higher lifetime risk of developing malignant peripheral nerve sheath tumors. A 3-bp in-frame deletion of c.2970-2972delAAT is associated with typical pigmentary features of NF1 but with few cutaneous or surface plexiform neurofibromas (2). Missense variants affecting *NF1* codon Arg1809 in exon 29 (exon 38 of NM_001042492.3) are associated with multiple café au lait spots in the absence of cutaneous neurofibromas or clinically apparent plexiform neurofibromas (25). Missense variants affecting codons 844-848 are associated with a more severe phenotype and higher risk of developing malignancies (2). These mutations were not detected in our cohort, and no genotype-phenotype correlation could be made within detected mutations.

Patients with NF1 are known to have a predisposition for various benign and malignant tumors. Neurofibromas are the most prevalent benign tumors. Nervous system malignancies are the most common malignant tumors, occurring more frequently than in the general population in patients with NF1. In addition, gastrointestinal stromal tumors, pheochromocytomas, and JMML are known to associate with NF1(26,27). Although the heterozygous state of NF1 is known to cause abnormal cell growth, tumor predisposition in NF1-associated malignancies is largely explained by the loss of heterozygosis (10).

Malignancies were found in four patients in our study. One patient had high-grade glioma, one had optic glioma, and two had JMML. Our study was interesting regarding the distribution of malignant tumors. Although central nervous malignancies are the most common malignancies apart from malignant peripheral nerve sheath tumors in the literature, leukemia was also common in our study with a rate of 9.1% (2/22). Leukemia is an interesting subtitle in NF1 because of its irrelevance to the nervous system. *NF1* gene has tumor suppressor role in early myelopoiesis (28). Somatic second hits of NF1 were also shown in patients with NF1 and myeloid disorders (29,30). In addition, NF1 knockout mouse embryos showed aberrant growth in myeloid hematopoietic cells, which were hypersensitive to granulocyte-macrophage colony-stimulating factor (31). Elucidating the underlying cause of JMML is important to determine treatment strategies. The management of patients with germline mutations differs from patients with only somatic mutations (32). Although the association of JMML in NF1 is not common, it is important to keep JMML in mind in NF1 as it determines treatment strategies. JMML and juvenile xanthogranulomas frequently co-exist in NF1. Observing juvenile xanthogranulomas in children with NF1 may raise awareness to actively search for other alarming signs of JMML (33). Chronic myelomonocytic leukemia was detected in 9% of patients with NF1 in the Great Britain cohort (34). Myeloid malignancies (1 acute lymphocytic leukemia, 1 JMML, 1 acute myeloid leukemia) were detected at a rate of 15.7% in an NF1 cohort from southern Türkiye (35). Interestingly no JMML was not observed in a large Finnish cohort of pediatric malignancies in NF1 (26). JMML incidence is <1 according to large series (36,37). Our hospital is not a regional center for pediatric hematological malignancies; however, the high frequency might be a bias due to the small sample size.

Cranial vascular pathology was detected in two patients (9.1% 2/22) in our study. Vascular abnormality-incidence that is associated with NF1 is increasing. NF1 vasculopathy can cause pseudoaneurysm, aneurysm, arteriovenous malformations, stenosis, and occlusion. Vasculopathy of the major arteries can have serious consequences. Cerebrovascular lesions can also be seen in NF1 patients; arteriovenous malformations, pseudoaneurysm, aneurysm, vascular stenosis, occlusion, and Moyamoya disease have been reported (3). Neurofibromin is expressed in blood vessel endothelial and smooth muscle cells, and vascular abnormalities in NF1 might be caused by the modification of neurofibromin function in these cells (38).

The frequency of vasculopathy is not known, due to both insufficient extensive studies and the presence of asymptomatic patients. Rea et al. (39) found the prevalence of cerebrovascular lesion to be 6% over 266 patients with NF1 who underwent cranial MRI. Rosser et al. (40) reported 2.5% of 316 and Cairns and North (41) reported 5% of 144 NF1 patients with a cerebrovascular lesion, which was detected on cranial MRI. D'Arco et al. (42) studied the usefulness of cranial MRA in patients with NF1. They found intracranial stenosis in 7.4% of 125 patients with NF1 who underwent both MRI and MRA. The higher prevalence in D'Arco et al. (42) might be due to the use of cranial MRA in addition to MRI.

The prevalence of vascular pathology was 9.1% (2/22) in our study. The patients were three- and 11-year-old males with intellectual disability and epilepsy (case 9, 11). Other causes of vasculopathy were excluded from these patients. Although case 9 fulfilled the

diagnostic criteria, case 11 was diagnosed after follow-up. The higher prevalence of vascular pathology (9.1%) compared with the current literature (2.5-7.4%) might be a bias due to the small sample size. Seizure and ID were interpreted to be secondary to vasculopathy. Both proteins are known to accompany NF1 (3,43). Intellectual disability is seen 6-7% of patients with NF1 (43). The etiology of ID in our study might be due to cerebral atrophy secondary to stenosis. In addition, seizures might be a result of cerebral ischemia.

Sobata et al. (44) grouped NF1 cerebrovascular lesions into three as stenotic, aneurysmal, and both stenotic and aneurysmal. Stenotic lesions are known to occur in younger patients (41,42). The patients had stenosis in our study, which is consistent with the literature.

Although lesions in other arteries have been reported (39-42,44), only middle cerebral artery was affected in both patients in our study. This result was probably due to the small sample size in our study and not using cranial MRA in all cases.

Some cerebrovascular lesions progress and eventually require surgical and medical treatment. Early medical/surgical intervention was suggested to prevent complications (39). Cerebrovascular lesions can be detected in asymptomatic patients, but some do not progress. Asymptomatic patients represent a clinical dilemma (41). Further comprehensive studies are necessary to gain more experience in the cerebrovascular pathology of NF1.

Study Limitations

It is important to acknowledge the limitations of the current study. Sample size is small in the current study. Further studies that include larger cohort is necessary.

CONCLUSION

We report three years of data on the molecular and clinical findings of NF1 in patients from northeast Türkiye. This study will contribute to the characteristics of patients with NF1. Among the detected mutations, two were novel. Further definition of the mutations will contribute to a better understanding of disease pathogenesis and manifestations. Rare features were detected as well as classic features of NF1. This study is also important for showing importance of NF1 vasculopathy. Although it can be detected in asymptomatic patients, NF1 vasculopathy can cause serious complications. Medical and/or surgical procedures are needed in some cases. Keeping this in mind could enable timely therapy. Our study shows that genetic analysis improved follow-up and counseling.

Ethics

Ethics Committee Approval: This study was approved by the Institutional Ethics Committee by University of Health Sciences Türkiye, Trabzon Kanuni Training and Research Hospital (approval number: 2019/22, date: 25.04.2019).

Informed Consent: Informed written consent was obtained from the patient's parents.

Authorship Contributions: Concept: Ş.A., Design: Ş.A., A.H.Ç., Supervision: Ş.A., A.H.Ç., Resources: Ş.A., A.H.Ç., Material: Ş.A., A.H.Ç., Data Collection or Processing: Ş.A., A.H.Ç., Analysis or Interpretation: Ş.A., A.H.Ç., Literature Search: Ş.A., A.H.Ç., Writing: Ş.A., Critical Review: Ş.A., A.H.Ç.

Conflict of Interest: No conflict of interest was declared by the authors.
Financial Disclosure: The authors declared that this study received no financial support.

REFERENCES

1. Peduto C, Zanobio M, Nigro V, Perrotta S, Piluso G, Santoro C. Neurofibromatosis Type 1: Pediatric Aspects and Review of Genotype-Phenotype Correlations. Cancers (Basel). 2023; 15: 1217.
2. Tsipi M, Poulou M, Fylaktou I, Kosma K, Tsoutsou E, Pons MR, et al. Phenotypic expression of a spectrum of Neurofibromatosis Type 1 (NF1) mutations identified through NGS and MLPA. J Neurol Sci. 2018; 395: 95-105.
3. Jett K, Friedman JM. Clinical and genetic aspects of neurofibromatosis 1. Genet Med. 2010; 12: 1-11.
4. Ratner N, Miller SJ. A RASopathy gene commonly mutated in cancer: the neurofibromatosis type 1 tumour suppressor. Nat Rev Cancer. 2015; 15: 290-301.
5. Legius E, Messiaen L, Wolkenstein P, Pancza P, Avery RA, Berman Y, et al. Revised diagnostic criteria for neurofibromatosis type 1 and Legius syndrome: an international consensus recommendation. Genet Med. 2021; 23: 1506-13.
6. Shen MH, Harper PS, Upadhyaya M. Molecular genetics of neurofibromatosis type 1 (NF1). J Med Genet. 1996; 33: 2-17.
7. Palma Milla C, Lezana Rosales JM, López Montiel J, Andrés Garrido LD, Sánchez Linares C, Carmona Tamajón S, et al. Neurofibromatosis type I: mutation spectrum of NF1 in spanish patients. Ann Hum Genet. 2018; 82: 425-36.
8. Stenson PD, Mort M, Ball EV, Shaw K, Phillips A, Cooper DN. The Human Gene Mutation Database: building a comprehensive mutation repository for clinical and molecular genetics, diagnostic testing and personalized genomic medicine. Hum Genet. 2014; 133: 1-9.
9. Mautner VF, Kluwe L, Friedrich RE, Roehl AC, Bammert S, Högel J, et al. Clinical characterisation of 29 neurofibromatosis type-1 patients with molecularly ascertained 1.4 Mb type-1 NF1 deletions. J Med Genet. 2010; 47: 623-30.
10. Yohay KH. The genetic and molecular pathogenesis of NF1 and NF2. Semin Pediatr Neurol. 2006; 13: 21-6.
11. Landrum MJ, Lee JM, Benson M, Brown GR, Chao C, Chitipiralla S, et al. ClinVar: improving access to variant interpretations and supporting evidence. Nucleic Acids Res. 2018; 46: D1062-7.
12. Adzhubei I, Jordan DM, Sunyaev SR. Predicting functional effect of human missense mutations using PolyPhen-2. Curr Protoc Hum Genet. 2013; Chapter 7: Unit7.20.
13. Kumar P, Henikoff S, Ng PC. Predicting the effects of coding non-synonymous variants on protein function using the SIFT algorithm. Nat Protoc. 2009; 4: 1073-81.
14. Schwarz JM, Cooper DN, Schuelke M, Seelow D. MutationTaster2: mutation prediction for the deep-sequencing age. Nat Methods. 2014; 11: 361-2.
15. Richards S, Aziz N, Bale S, Bick D, Das S, Gastier-Foster J, et al. Standards and guidelines for the interpretation of sequence variants: a joint consensus recommendation of the American College of Medical Genetics and Genomics and the Association for Molecular Pathology. Genet Med. 2015; 17: 405-24.

16. Valero MC, Martín Y, Hernández-Imaz E, Marina Hernández A, Meleán G, Valero AM, et al. A highly sensitive genetic protocol to detect NF1 mutations. J Mol Diagn. 2011; 13: 113-22.
17. Pasmant E, Sabbagh A, Spurlock G, Laurendeau I, Grillo E, Hamel MJ, et al. NF1 microdeletions in neurofibromatosis type 1: from genotype to phenotype. Hum Mutat. 2010; 31: E1506-18.
18. Sabbagh A, Pasmant E, Imbard A, Luscan A, Soares M, Blanché H, et al. NF1 molecular characterization and neurofibromatosis type I genotype-phenotype correlation: the French experience. Hum Mutat. 2013; 34: 1510-8.
19. Evans DG, Bowers N, Burkitt-Wright E, Miles E, Garg S, Scott-Kitching V, et al. Comprehensive RNA Analysis of the NF1 Gene in Classically Affected NF1 Affected Individuals Meeting NIH Criteria has High Sensitivity and Mutation Negative Testing is Reassuring in Isolated Cases With Pigmentary Features Only. EBioMedicine. 2016; 7: 212-20.
20. Ulusal SD, Gürkan H, Atlı E, Özal SA, Çiftdemir M, Tozkır H, et al. Genetic Analyses of the NF1 Gene in Turkish Neurofibromatosis Type I Patients and Definition of three Novel Variants. Balkan J Med Genet. 2017; 20: 13-20.
21. Bildirici Y, Kocaaga A, Karademir-Arslan CN, Yimenicioglu S. Evaluation of Molecular and Clinical Findings in Children With Neurofibromatosis Type 1: Identification of 15 Novel Variants. Pediatr Neurol. 2023; 149: 69-74.
22. Sharifi S, Kalaycı T, Palanduz Ş, Öztürk Ş, Cefle K. Clinical Characteristics and Mutation Spectrum of Neurofibromatosis Type 1 in 27 Turkish Families. Balkan Med J. 2021; 38: 365-73.
23. Bahsi T, Saat H. Neurofibromatosis Type 1 Molecular Diagnosis in Turkish Patients. GMJ. 2020; 31: 406-9.
24. Terzi YK, Oğuzkan-Balcı S, Anlar B, Varan A, Ersoy-Evans S, Sharafi P, et al. Clinical findings and mutation analysis of NF1 patients in Turkey. Meta Gene. 2918; 15: 80-3.
25. Pinna V, Lanari V, Daniele P, Consoli F, Agolini E, Margiotti K, et al. p.Arg1809Cys substitution in neurofibromin is associated with a distinctive NF1 phenotype without neurofibromas. Eur J Hum Genet. 2015; 23: 1068-71.
26. Peltonen S, Kallionpää RA, Rantanen M, Uusitalo E, Lähteenmäki PM, Pöyhönen M, et al. Pediatric malignancies in neurofibromatosis type 1: A population-based cohort study. Int J Cancer. 2019; 145: 2926-32.
27. Rosenbaum T, Wimmer K. Neurofibromatosis type 1 (NF1) and associated tumors. Klin Padiatr. 2014; 226: 309-15.
28. Miles DK, Freedman MH, Stephens K, Pallavicini M, Sievers EL, Weaver M, et al. Patterns of hematopoietic lineage involvement in children with neurofibromatosis type 1 and malignant myeloid disorders. Blood. 1996; 88: 4314-20.
29. Ramamoorthy S, Lebrecht D, Schanze D, Schanze I, Wieland I, Andrieux G, et al. Biallelic inactivation of the NF1 tumour suppressor gene in juvenile myelomonocytic leukaemia: Genetic evidence of driver function and implications for diagnostic workup. Br J Haematol. 2024; 204: 595-605.
30. Shannon KM, O'Connell P, Martin GA, Paderanga D, Olson K, Dinndorf P, et al. Loss of the normal NF1 allele from the bone marrow of children with type 1 neurofibromatosis and malignant myeloid disorders. N Engl J Med. 1994; 330: 597-601.
31. Bollag G, Clapp DW, Shih S, Adler F, Zhang YY, Thompson P, et al. Loss of NF1 results in activation of the Ras signaling pathway and leads to aberrant growth in haematopoietic cells. Nat Genet. 1996; 12: 144-8.
32. Wintering A, Dvorak CC, Stieglitz E, Loh ML. Juvenile myelomonocytic leukemia in the molecular era: a clinician's guide to diagnosis, risk stratification, and treatment. Blood Adv. 2021; 5: 4783-93.
33. Carton C, Evans DG, Blanco I, Friedrich RE, Ferner RE, Farschtschi S, et al. ERN GENTURIS tumour surveillance guidelines for individuals with neurofibromatosis type 1. EClinicalMedicine. 2023; 56: 101818.
34. Stiller CA, Chessells JM, Fitchett M. Neurofibromatosis and childhood leukaemia/lymphoma: a population-based UKCCSG study. Br J Cancer. 1994; 70: 969-72.
35. İncecik F, Altunbaşak Ş, Hergüner MÖ, Bayram İ, Küpeli S, Demirbilek H. Oncologic manifestations in children with neurofibromatosis type 1 in Turkey. Turk J Pediatr. 2013; 55: 266-70.
36. Matsui I, Tanimura M, Kobayashi N, Sawada T, Nagahara N, Akatsuka J. Neurofibromatosis type 1 and childhood cancer. Cancer. 1993; 72: 2746-54.
37. Varan A, Şen H, Aydın B, Yalçın B, Kutluk T, Akyüz C. Neurofibromatosis type 1 and malignancy in childhood. Clin Genet. 2016; 89: 341-5.
38. Hamilton SJ, Friedman JM. Insights into the pathogenesis of neurofibromatosis 1 vasculopathy. Clin Genet. 2000; 58: 341-4.
39. Rea D, Brandsema JF, Armstrong D, Parkin PC, deVeber G, MacGregor D, et al. Cerebral arteriopathy in children with neurofibromatosis type 1. Pediatrics. 2009; 124: e476-83.
40. Rosser TL, Vezina G, Packer RJ. Cerebrovascular abnormalities in a population of children with neurofibromatosis type 1. Neurology. 2005; 64: 553-5.
41. Cairns AG, North KN. Cerebrovascular dysplasia in neurofibromatosis type 1. J Neurol Neurosurg Psychiatry. 2008; 79: 1165-70.
42. D'Arco F, D'Amico A, Caranci F, Di Paolo N, Melis D, Brunetti A. Cerebrovascular stenosis in neurofibromatosis type 1 and utility of magnetic resonance angiography: our experience and literature review. Radiol Med. 2014; 119: 415-21.
43. Lehtonen A, Howie E, Trump D, Huson SM. Behaviour in children with neurofibromatosis type 1: cognition, executive function, attention, emotion, and social competence. Dev Med Child Neurol. 2013; 55: 111-25.
44. Sobata E, Ohkuma H, Suzuki S. Cerebrovascular disorders associated with von Recklinghausen's neurofibromatosis: a case report. Neurosurgery. 1988; 22: 544-9.

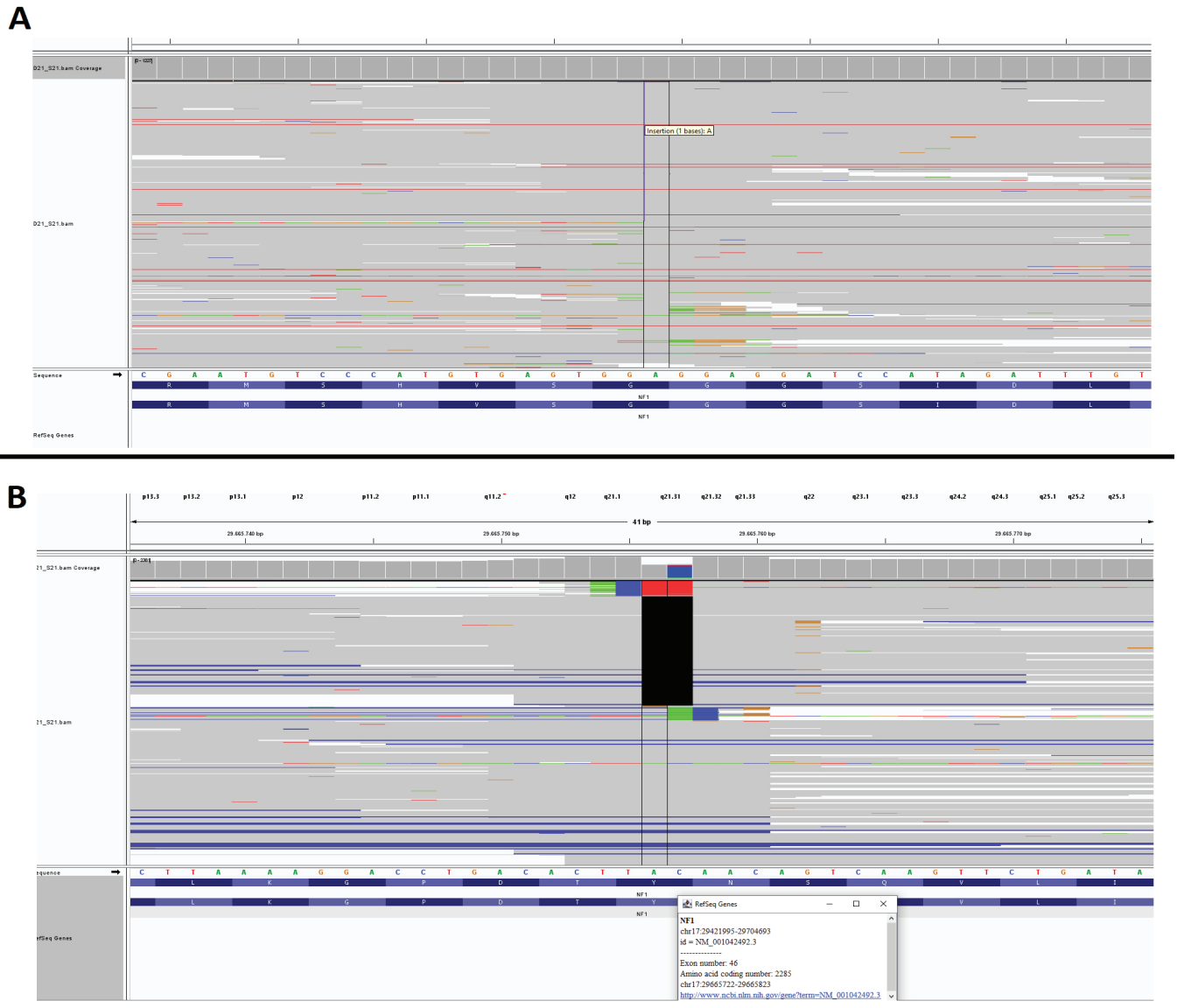

Supplementary Figure 1. Integrative genomics viewer images of novel mutations. (A) c.2466dupA, (B) c.6854_6855delAC.

GMJ 2024;35:433-437

DOI: http://dx.doi.org/10.12996/gmj.2024.4281

Long-Term Results of Cabergoline Add-on Long-Acting Somatostatin Analogue Therapy in Acromegaly Patients

Akromegali Hastalarında Uzun Etkili Somatostatin Analog Tedavisine Eklenen Kabergolin Tedavisinin Uzun Dönem Sonuçları

Mehmet Muhittin Yalçın[1], Gizem Bedir Keser[2], Meriç Coşkun[1], Afruz Babayeva[1], Emrah Çeltikçi[3], Mehmet Arda İnan[4], Emetullah Cindil[5], Aylar Poyraz[4], Ethem Turgay Cerit[1], Alev Eroğlu Altınova[1], Müjde Aktürk[1], Füsun Baloş Törüner[1], Mehmet Ayhan Karakoç[1], İlhan Yetkin[1]

[1]Department of Endocrinology and Metabolism, Gazi University Faculty of Medicine, Ankara, Türkiye
[2]Department of Internal Medicine, Gazi University Faculty of Medicine, Ankara, Türkiye
[3]Department of Neurosurgery, Gazi University Faculty of Medicine, Ankara, Türkiye
[4]Department of Pathology, Gazi University Faculty of Medicine, Ankara, Türkiye
[5]Department of Radiology, Gazi University Faculty of Medicine, Ankara, Türkiye

ABSTRACT

Objective: To investigate the efficacy of the dopamine agonist cabergoline in uncontrolled acromegaly despite long-acting somatostatin analog (SSA).

Methods: Thirty-five patients with acromegaly who were followed up in the department of endocrinology and metabolism of our university were analyzed. Thirty-five patients with acromegaly who did not respond adequately to postoperative SSA and in whom cabergoline was added to the treatment were analyzed. Patients were retrospectively evaluated in terms of age, gender, insulin-like growth factor-1 (IGF-1) values before and after cabergoline, disease duration, treatment dose, adenoma size, growth hormone level, and prolactin staining on pathologic examination.

Results: Seventeen (48.6%) patients were female. The median age was 46.0 (41-53) years, and the median disease age was 10 (3-43) years. Twenty-eight (80.0%) were macroadenomas, 7 (20.0%) were microadenomas, and prolactin staining was observed in 10 (27.8%) cases. The IGF-1 level was 443 (346-628) ng/mL before cabergoline treatment and 27.4% decrease in IGF-1 was observed after treatment ($p<0.001$). There was no correlation between IGF-1 decrease and cabergoline dose. The change in IGF-1 was not correlated with tumor size and age but was correlated with pre-cabergoline IGF-1 level ($r=0.364$, $p=0.03$). 8 (22.9%) patients went into remission with cabergoline treatment. There was no difference in age, gender, tumor size, or pre-treatment IGF-1 levels between those who went into

ÖZ

Amaç: Uzun etkili somatostatin analoğuna (SSA) rağmen kontrol altına alınamayan akromegalide dopamin agonisti kabergolinin etkinliğini araştırmaktır.

Yöntemler: Üniversitemiz endokrinoloji ve metabolizma bölümünde takip edilen 35 akromegali hastası analiz edildi. Postoperatif dönemde kullandıkları SSA'ya yeterli yanıt vermeyen ve tedaviye kabergolin eklenen 35 akromegali hastası analiz edildi. Hastalar yaş, cinsiyet, kabergolin öncesi ve sonrası insülin benzeri büyüme faktörü-1 (IGF-1) değerleri, hastalık süresi, tedavi dozu, adenom boyutu, büyüme hormonu düzeyi ve patolojik incelemede prolaktin boyanması açısından retrospektif olarak değerlendirildi.

Bulgular: On yedi (%48,6) hasta kadındı. Ortanca yaş 46,0 (41-53) yıl ve ortanca hastalık yaşı 10 (3-43) yıldı. Hastaların 28'i (%80,0) makroadenom, 7'si (%20,0) mikroadenomdu ve 10 (%27,8) olguda prolaktin boyanması gözlendi. Kabergolin tedavisi öncesi IGF-1 düzeyi 443 (346-628) ng/mL iken tedavi sonrası IGF-1'de %27,4 azalma gözlendi ($p<0,001$). IGF-1 azalması ile kabergolin dozu arasında korelasyon yoktu. IGF-1'deki değişim tümör boyutu ve yaş ile korele değildi ancak kabergolin öncesi IGF-1 düzeyi ile korele idi ($r=0,364$, $p=0,03$). 8 (%22,9) hasta kabergolin tedavisi ile remisyona girmişti. Kabergolin tedavisi ile remisyona girenler ve girmeyenler arasında yaş, cinsiyet, tümör boyutu veya tedavi öncesi IGF-1 düzeyleri açısından fark yoktu. Bu 8 hasta incelendiğinde, takip süresi boyunca kabergolin tedavisine devam edildiği; bir hastada SSA tedavisi kesilerek, üç hastada SSA dozu

Address for Correspondence/Yazışma Adresi: Mehmet Muhittin Yalçın, MD, Department of Endocrinology and Metabolism, Gazi University Faculty of Medicine, Ankara, Türkiye
E-mail / E-posta: yalcin.muhittin@gmail.com
ORCID ID: orcid.org/0000-0002-1041-6881

Received/Geliş Tarihi: 31.08.2024
Accepted/Kabul Tarihi: 11.09.2024

ABSTRACT

remission with cabergoline treatment and those who did not. When these 8 patients were analyzed, it was observed that cabergoline treatment was continued throughout the follow-up period; remission was maintained in one patient by discontinuing SSA treatment, in three patients by decreasing the SSA dose, in two patients without treatment change, and in two patients by changing the SSA preparation.

Conclusion: Cabergoline is used in the treatment of acromegaly due to its antiproliferative and proapoptotic effects on pituitary adenoma cells. The efficacy of cabergoline added to SSA treatment is controversial in the literature. In our study, remission was achieved in 22.9% and IGF-1 reduction was observed in 27.4% with cabergoline treatment in patients with inadequate response to SSA treatment. Cabergoline added to SSA is an effective treatment in terms of IGF-1 control. This effect may continue in the long-term.

Keywords: Acromegaly, cabergoline, somatostatin analog

ÖZ

azaltılarak, iki hastada tedavi değişikliği yapılmadan ve iki hastada SSA preparatı değiştirilerek remisyonun korunduğu gözlendi.

Sonuç: Kabergolin hipofiz adenom hücreleri üzerindeki antiproliferatif ve proapoptotik etkileri nedeniyle akromegali tedavisinde kullanılmaktadır. SSA tedavisine eklenen kabergolinin etkinliği literatürde tartışmalıdır. Çalışmamızda SSA tedavisine yetersiz yanıt veren hastalarda kabergolin tedavisi ile %22,9 oranında remisyon sağlanmış ve %27,4 oranında IGF-1 azalması gözlenmiştir. SSA'ya eklenen kabergolin IGF-1 kontrolü açısından etkili bir tedavidir. Bu etki uzun dönemde de devam edebilir.

Anahtar Sözcükler: Akromegali, kabergolin, somatostatin analoğu

INTRODUCTION

Acromegaly is a chronic disease caused by excessive secretion of growth hormone (GH), usually by a pituitary tumor. It is a disease that affects men and women equally, with a prevalence of 40 to 130 per million.

Although transsphenoidal surgery is the preferred first-line treatment for acromegaly (1), 20% of patients with microadenomas and 40-60% of patients with macroadenomas cannot be cured only by surgery and require adjuvant medical therapy (2). Pharmacological treatments; including long-acting somatostatin analogs (SSA), dopamine agonists, and GH receptor antagonists, have gained importance in providing biochemical and symptomatic control of the disease (3).

SSAs are considered the first choice for the medical treatment of acromegaly and can normalize insulin-like growth factor-1 (IGF-1) levels in approximately 50% of patients (4). However, IGF-1 normalization is not achieved in at least 35% of patients, suggesting resistance to SSAs (2). In addition, in some patients, drug compliance may be poor because of side effects or injection-related difficulties (5).

Pegvisomant (PEG), which acts as a GH receptor antagonist, either alone or when added to SSA, normalizes IGF-1 levels in approximately 97% of patients but does not cause tumor shrinkage (1). Regular monitoring of liver enzyme levels, intermittent changes in injection sites, and skin examination for lipohypertrophy or rashes are important in patients treated with this drug (6). The need for daily injections and its high cost limit the use of PEG (7,8).

Cabergoline is an ergot-derived dopamine D2 receptor agonist that can be used for the medical treatment of acromegaly. The antiproliferative and proapoptotic effects on pituitary tumor cells have been observed in various studies. Cabergoline can be used alone or as an add-on therapy in patients who are partially resistant to SSA or who are not fully controlled with maximum dose PEG. It has been shown to normalize plasma IGF-1 levels in up to 39% of patients with acromegaly during monotherapy. In addition, the convenience of oral administration, better compliance, and lower economic costs compared with SSA and PEG make cabergoline an attractive option for acromegalic patients who often need long-lasting medical therapy to achieve disease control (9).

As data on the beneficial effects of adding cabergoline to the medical regimen in acromegalic patients uncontrolled with long-acting SSAs are still limited (1); the aim of this study was to examine the efficacy of dopamine agonist cabergoline treatment in uncontrolled acromegaly despite the long-acting SSA and to observe the long-term results of this treatment.

MATERIALS AND METHODS

Permission was received for our research from Gazi University Faculty of Medicine Ethics Committee (approval number: 597, date: 28.06.2021). Among the patients with acromegaly who were followed up in the Gazi University Faculty of Medicine, Department of Endocrinology and Metabolism between January 1, 2005, and February 1, 2020; thirty-five cases, in which cabergoline was added to the treatment because of insufficient response to SSA were analyzed retrospectively. The patients were evaluated in terms of age, gender, IGF-1 values before and after cabergoline treatment, disease duration, treatment dose, adenoma size, GH level, and prolactin staining on pathological examination. Since the normal value range for IGF-1 level is a parameter that changes with age, the ratio of "patient's IGF-1 value/upper limit of normal for age-specific IGF-1" was used in the statistical calculation. In the evaluation after cabergoline treatment, control IGF-1 measurements at the 3rd month after treatment were used.

Patients who did not use SSA and were followed up only with cabergoline, those who underwent simultaneous SSA dose changes with the addition of cabergoline, those who added PEG concurrently with cabergoline, and those who did not have follow-up data were excluded from the study.

Statistical Analysis

In our study, statistical analyses will be performed using SPSS for Windows Version 22' program. Frequencies for the variables in the categorized data type (qualitative) and the mean ± standard deviation, if suitable for the normal distribution, for the variables in the numerical data type (quantitative) and median (minimum-maximum) values if not suitable for the normal distribution, were specified. Whether the variables fit the normal distribution or not was evaluated with the Kolmogorov-Smirnov test. Parametric tests (Independent sample t-test) were used for variables that matched

the normal distribution, and non-parametric tests (chi-square, Mann-Whitney U test) were used for those that did not. The Spearman correlation test was used for the correlation between continuous variables. The statistical significance value of this study was accepted as p≤0.05.

RESULTS

Seventeen (48.6%) patients were women. The median age was 46.0 (41-53) years, and the disease age was 10 (3-43) years. The follow-up period for cabergoline treatment was 6.0 (1-15) years. There were macroadenomas in 28 (80.0%) patients, microadenomas in 7 (20.0%) patients, and prolactin staining in addition to GH was observed in pathological samples from 10 (28.5%) patients. 20 (57.1%) patients had a history of gamma-knife therapy before cabergoline treatment. The maximum cabergoline dose was 1.50 mg/week (1-5 mg/week) (Table 1).

The median IGF-1 level was 443 ng/mL before cabergoline treatment, it was 308 ng/mL after cabergoline. A 27.4% decrease in IGF-1 levels was observed after cabergoline treatment (p<0.001). Although the upper limit of normal ratio for IGF-1/IGF-1 before cabergoline was 1.53 (1.10-5.30), it was found to be 1.16 (0.20-3.60) after cabergoline (Table 2).

Although the change in IGF-1 levels was positively correlated with pre-cabergoline IGF-1 level (P=0.364, p=0.03), no correlation was found between tumor size, age, and cabergoline dose.

Eight (22.9%) patients achieved normal IGF-1 levels following cabergoline treatment. No difference was observed between patients with normal IGF-1 levels who received cabergoline treatment and those with high IGF-1 levels in terms of age, sex, tumor size, disease duration, duration of follow-up with cabergoline treatment, prolactin staining, and history of gamma-knife before cabergoline.

Table 1. General characteristics of patients

Age (year)*	46.0 (27-69)
Disease duration (year)*	10.0 (3-43)
Cabergolin treatment duration (year)*	6.0 (1-15)
Maximum CAB dose (mg/week)	1.5 (1-5)
Macroadenoma, n (%)	28 (80)
Prolactin staining percentage, (%)	
Positive	10 (28.5)
Negative	16 (45.8)
Unknown	9 (25.7)
Gamma knife therapy before CAB, n (%)	20 (57.1)

*Median (minimum-maximum). CAB: Cabergoline.

In 8 patients with normal IGF-1 levels after cabergoline treatment, the maximum cabergoline dose was 1.00 (1-2) mg/week, and the percent IGF-1 change was -47.41 (-81.92/-26.33) with cabergoline treatment. In this patient group, the upper limit of normal ratio for IGF-1/IGF-1 before cabergoline was 1.31 (1.10-1.67), whereas the upper limit of normal ratio for IGF-1/IGF-1 after cabergoline was 0.79 (0.20-1.00) was determined (p<0.01).

In 27 patients with high IGF-1 levels after cabergoline therapy, the maximum cabergoline dose was 2.00 (1-5) mg/week; upper limit of normal for pre-cabergoline IGF-1/IGF-1 was 1.65 (1.10-5.30); upper limit of normal for IGF-1/IGF-1 after cabergoline is 1.37 (1.02-3.60); The percent change in IGF-1 with cabergoline treatment was -18.02 (-75.65/21.01). There was a statistically significant difference between the two patient groups with normal IGF-1 and high IGF-1 levels after cabergoline treatment in terms of the maximum dose of cabergoline and the percentage of change in IGF-1 levels with cabergoline therapy (p=0.050; p=0.019) (Table 3).

A statistically significant difference was observed between the upper limit of normal for IGF-1/IGF-1 before cabergoline and the upper limit of normal for IGF-1/IGF-1 after cabergoline between these two groups (p=0.001; p<0.01) (Table 2).

After cabergoline therapy, cabergoline therapy was continued for a median follow-up of 4 years (1-8 years) in 8 patients with normal IGF-1 levels; It was observed that the normal IGF-1 level was maintained by discontinuing SSA treatment in one patient, decreasing the SSA dose in three, without changing the treatment in two, and changing the SSA preparation in two.

DISCUSSION

Long-term medical treatment is important for patients with acromegaly when an adequate response cannot be achieved with surgical treatment. Although SSA is preferred in the first line, SSA unresponsiveness can be observed even when the maximum dose is reached (10). Since the late 1990s, studies have been carried out to add cabergoline to SSA treatment.

In studies on cabergoline treatment added to SSA, IGF-1 normalization was found to be between 42% and 44% at 6-12 months follow-up (11,12). Studies have shown that this combination is most effective in patients with mildly elevated IGF-1 levels (13). In our study, the upper limit of the normal ratio for IGF-1/IGF-1 was 1.31 (1.10-1.67) times in patients with normal IGF-1 levels under cabergoline treatment, whereas this ratio was 1.65 (1.10-5.30) times in patients with high IGF-1 levels. In light of this information, we believe that cabergoline treatment may be more effective in patients with mild to moderate IGF-1 levels in the postoperative period. There are also data in this direction in the literature (9).

In longer (18-24 months) follow-up periods, normalization of IGF-1 levels were observed at rates ranging from 37% to 40% (1,14). Abs et al. (15) treated 64 patients with acromegaly for 40 months and

Table 2. IGF and IGF-1/IGF-1 ULN before and after CAB

	Before CAB	After CAB	p
IGF-1 (ng/mL)*	443.0 (265-1607)	308.0 (52-1091)	<0.01
IGF-1/IGF-1 ULN*	1.5 (1.1-5.3)	1.2 (0.2-3.6)	<0.01

*Median (minimum-maximum). IGF-1: Insulin-like growth factor 1, ULN: Upper limit of normal, CAB: Cabergoline.

Table 3. Clinical and laboratory parameters between normal and high IGF-1 levels after CAB

	Normal IGF-1 after CAB, (n=8)	High IGF-1 after CAB, (n=27)	
Female, n (%)	6 (75)	11 (40.7)	0.12
Age (year)*	47.0 (34-64)	46.0 (27-69)	0.69
Disease duration (year)*	8.5 (3-43)	10.5 (4-36)	0.813
Follow-up period (year):	4.0 (1-8)	6.0 (1-15)	0.173
Macroadenoma, n (%)	7 (87.5)	21(77.8)	1.00
Prolactin staining percentagen (%)			
Positive	2 (25)	8 (29.6)	1.00
Negative	4 (50)	12 (44.4)	
Unknown	2 (25)	7 (26.0)	
Gamma Knife therapy before CAB, n (%)	4 (50)	16 (59.3)	0.70
Max CAB dose (mg/week)	1.0 (1.0-2.0)	2.0 (1.0-5.0)	0.05
IGF-1 before CAB*	335 (265- 418)	500 (272-1607)	**<0.001**
IGF-1 after CAB*	177 (52-230)	353 (262-1091)	**<0.001**
IGF-1/IGF-1 ULN before CAB	1.31 (1.10-1.67)	1.65 (1.10-5.30)	**<0.001**
IGF-1/IGF-1 ULN after CAB	0.79 (0.20-1.00)	1.37 (1.02-3.60)	**<0.001**
IGF decrease after CAB (%)	-47.4 (-81.9/-26.3)	-18.0 (-75.7/-21.0)	**0.02**

*Median (minimum-maximum). IGF-1: Insulin-like growth factor 1, CAB: Cabergoline, ULN: Upper limit of normal.

found that IGF-1 reached normal levels in 39% of the patients after cabergoline use (at doses ranging from 1.0-3.5 mg per week). In our study, there was 30.5% decrease in IGF levels after CAB therapy in patients already on SSA treatment after 6.0 (1-15) years follow-up period. 22.9% of patients achieved normal IGF levels with CAB therapy.

One of our patients with normal IGF-1 levels after cabergoline treatment was discontinued from SSA treatment and was followed up only under cabergoline treatment. In 3 patients, the current SSA dose could be reduced. In 2 patients, we continue to follow-up with normal IGF-1 levels under cabergoline treatment without SSA dose change during the 4 and 8-year follow-up periods. In 2 patients, while they were followed up at normal IGF-1 level with cabergoline during the 2-year follow-up period, we observed that the IGF-1 level returned to normal levels by making changes in the SSA preparation due to the increasing trend of IGF-1 level after 2 years. Based on the present data, it can be concluded that the normal IGF-1 level obtained under cabergoline treatment can be maintained over the long term.

Study Limitations

Our study has some limitations. First, this was a retrospective designed study. The small sample size prevented us from drawing definite conclusions. Since the patients were normoprolactinemic, the correlation between cabergoline treatment and prolactin levels could not be evaluated.

CONCLUSION

In our study, in patients who did not respond adequately to SSA treatment, normalization of IGF-1 level was reached in 22.9% and IGF-1 reduction was observed in 27.4% with cabergoline treatment. Cabergoline added to SSA may be an effective treatment for the control of acromegaly in patients with moderately high IGF-1 levels. We believe that this effect may continue in the long term.

Ethics

Ethics Committee Approval: Permission was received for our research from Gazi University Faculty of Medicine Ethics Committee (approval number: 597, date: 28.06.2021).

Informed Consent: Retrospective study.

Authorship Contributions

Concept: M.E.Y., G.B.K., M.C., A.B., E.Ç., M.A.İ., E.C., A.P., E.T.C., A.E.A., M.A., F.B.T., M.A.K., İ.Y., Design: M.E.Y., G.B.K., M.C., A.B., E.Ç., M.A.İ., E.C., A.P., E.T.C., A.E.A., M.A., F.B.T., M.A.K., İ.Y., Supervision: M.E.Y., G.B.K., M.C., A.B., E.Ç., M.A.İ., E.C., A.P., E.T.C., A.E.A., M.A., F.B.T., M.A.K., İ.Y., Resources: M.E.Y., G.B.K., M.C., A.B., E.Ç., M.A.İ., E.C., A.P., E.T.C., A.E.A., M.A., F.B.T., M.A.K., İ.Y., Material: M.E.Y., G.B.K., M.C., A.B., E.Ç., M.A.İ., E.C., A.P., E.T.C., A.E.A., M.A., F.B.T., M.A.K., İ.Y., Data Collection or Processing: M.E.Y., G.B.K., M.C., A.B., E.Ç., M.A.İ., E.C., A.P., E.T.C., A.E.A., M.A., F.B.T., M.A.K., İ.Y., Analysis or Interpretation: M.E.Y., G.B.K., M.C., A.B., E.Ç., M.A.İ., E.C., A.P., E.T.C., A.E.A., M.A., F.B.T., M.A.K., İ.Y., Literature Search: M.E.Y., G.B.K., M.C., A.B., E.Ç., M.A.İ., E.C., A.P., E.T.C., A.E.A., M.A., F.B.T., M.A.K., İ.Y., Writing: M.E.Y., G.B.K., M.C., A.B., E.Ç., M.A.İ., E.C., A.P., E.T.C., A.E.A., M.A., F.B.T., M.A.K., İ.Y., Critical Review: M.E.Y., G.B.K., M.C., A.B., E.Ç., M.A.İ., E.C., A.P., E.T.C., A.E.A., M.A., F.B.T., M.A.K., İ.Y., Other: M.E.Y., G.B.K., M.C., A.B., E.Ç., M.A.İ., E.C., A.P., E.T.C., A.E.A., M.A., F.B.T., M.A.K., İ.Y.

Conflict of Interest: No conflict of interest was declared by the authors.
Financial Disclosure: The authors declared that this study received no financial support.

REFERENCES

1. Vilar L, Azevedo MF, Naves LA, Casulari LA, Albuquerque JL, Montenegro RM, et al. Role of the addition of cabergoline to the management of acromegalic patients resistant to longterm treatment with octreotide LAR. Pituitary. 2011; 14: 148-56.
2. Suda K, Inoshita N, Iguchi G, Fukuoka H, Takahashi M, Nishizawa H, et al. Efficacy of combined octreotide and cabergoline treatment in patients with acromegaly: a retrospective clinical study and review of the literature. Endocr J. 2013; 60: 507-15.
3. Ben-Shlomo A, Melmed S. Acromegaly. Endocrinol Metab Clin North Am. 2008; 37: 101-22.
4. Bernabeu I, Alvarez-Escolá C, Paniagua AE, Lucas T, Pavón I, Cabezas-Agrícola JM, et al. Pegvisomant and cabergoline combination therapy in acromegaly. Pituitary. 2013; 16: 101-8.
5. Cozzi R, Attanasio R, Barausse M, Dallabonzana D, Orlandi P, Da Re N, et al. Cabergoline in acromegaly: a renewed role for dopamine agonist treatment? Eur J Endocrinol. 1998; 139: 516-21.
6. Tritos NA, Biller BM. Pegvisomant: a growth hormone receptor antagonist used in the treatment of acromegaly. Pituitary. 2017; 20: 129-35.
7. Feenstra J, de Herder WW, ten Have SM, van den Beld AW, Feelders RA, et al. Combined therapy with somatostatin analogues and weekly pegvisomant in active acromegaly. Lancet. 2005; 365: 1644-6.
8. Moore DJ, Adi Y, Connock MJ, Bayliss S. Clinical effectiveness and cost-effectiveness of pegvisomant for the treatment of acromegaly: a systematic review and economic evaluation. BMC Endocr Disord. 2009; 9: 20.
9. Marazuela M, Ramos-Leví A, Sampedro-Núñez M, Bernabeu I. Cabergoline treatment in acromegaly: pros. Endocrine. 2014; 46: 215-9.
10. Colao A, Auriemma RS, Lombardi G, Pivonello R. Resistance to somatostatin analogs in acromegaly. Endocr Rev. 2011; 32: 247-71.
11. Cozzi R, Attanasio R, Lodrini S, Lasio G. Cabergoline addition to depot somatostatin analogues in resistant acromegalic patients: efficacy and lack of predictive value of prolactin status. Clin Endocrinol (Oxf). 2004; 61: 209-15.
12. Gatta B, Hau DH, Catargi B, Roger P, Tabarin A. Re-evaluation of the efficacy of the association of cabergoline to somatostatin analogues in acromegalic patients. Clin Endocrinol (Oxf). 2005; 63: 477-8.
13. Lim DS, Fleseriu M. The role of combination medical therapy in the treatment of acromegaly. Pituitary. 2017; 20: 136-48.
14. Mattar P, Alves Martins MR, Abucham J. Short- and long-term efficacy of combined cabergoline and octreotide treatment in controlling igf-I levels in acromegaly. Neuroendocrinology. 2010; 92: 120-7.
15. Abs R, Verhelst J, Maiter D, Van Acker K, Nobels F, Coolens JL, et al. Cabergoline in the treatment of acromegaly: a study in 64 patients. J Clin Endocrinol Metab. 1998; 83: 374-8.

Original Investigation | Özgün Araştırma

GMJ 2024;35:438-441

DOI: http://dx.doi.org/10.12996/gmj.2024.4293

Diagnostic Value of Sodium, White Blood Cell, Neutrophil Levels; White Blood Cell/ Sodium and Neutrophil/Sodium Ratios in Appendicitis in Pediatric Patients

Pediatrik Yaş Grubu Apandisit Hastalığında Sodyum, Beyaz Kan Hücresi, Nötrofil Düzeyleri; Beyaz Küre/Sodyum ve Nötrofil/Sodyum Oranlarının Tanısal Değeri

Cem Kaya, Gökhan Arkan, Fatma Nur Aracıer Uçaner, Leyla Nur Türker, Alparslan Kapısız, Ramazan Karabulut, Zafer Türkyılmaz, Kaan Sönmez

Department of Pediatric Surgery, Gazi University Faculty of Medicine, Ankara, Türkiye

ABSTRACT

Objective: Acute appendicitis is one of the most common causes of abdominal pain requiring surgical intervention in children. Although clinical and imaging modalities play a central role in disease diagnosis, laboratory markers, such as white blood cell (WBC) count, neutrophil count, and electrolyte disturbances, particularly sodium levels, have been explored as potential indicators of disease severity. This study aimed to evaluate the relationship between serum sodium levels, WBC and neutrophil counts, and their respective ratios with the diagnosis and severity of appendicitis.

Methods: This retrospective analysis included 176 pediatric patients who underwent appendectomy. Patients were divided into three groups based on pathological findings: Group 1 (non-appendicitis, n=59), group 2 (acute appendicitis, n=82), and group 3 (perforated appendicitis, n=35). WBC, neutrophil, and sodium levels were recorded. ANOVA and post-hoc Tukey's tests were used to assess differences between groups. A logistic regression model was employed to evaluate the combined ability of WBC, neutrophil, and sodium levels to distinguish group 1 from groups 2 and 3, and the model's performance was evaluated using the area under the ROC curve (AUC).

Results: Significant differences were observed between group 1 and groups 2 and 3 regarding WBC (p<0.001), neutrophil (p<0.001), and sodium levels (p<0.001). Group 3 had the highest WBC count (17,123±4,491 cells/µL) and the lowest sodium levels (132.5±1.4 mEq/L), whereas group 1 had the lowest WBC count (10,660±3,804 cells/µL) and the highest sodium levels (137.5±2.6 mEq/L). Logistic regression analysis of the combined WBC, neutrophil, and sodium values obtained an AUC of 0.703, indicating moderate diagnostic utility.

ÖZ

Amaç: Akut apandisit, çocuklarda cerrahi müdahale gerektiren en yaygın karın ağrısı nedenlerinden biridir. Tanıda klinik değerlendirme ve görüntüleme yöntemleri önemli rol oynasa da, beyaz kan hücresi (WBC) sayısı, nötrofil sayısı ve özellikle sodyum seviyeleri gibi laboratuvar belirteçleri hastalığın şiddetini gösterebilecek potansiyel işaretler olarak araştırılmıştır. Bu çalışmada, serum sodyum seviyeleri, WBC ve nötrofil sayıları ile bunların oranlarının apandisit tanısı ve şiddeti ile ilişkisi değerlendirilmektedir.

Yöntemler: Apandektomi geçiren 176 pediatrik hasta üzerinde retrospektif bir analiz yapılmıştır. Hastalar patolojik bulgulara göre üç gruba ayrıldı: Grup 1 (apandisit olmayan, n=59), grup 2 (akut apandisit, n=82) ve grup 3 (perfore apandisit, n=35). WBC sayısı, nötrofil sayısı ve sodyum seviyeleri kaydedildi. Gruplar arasındaki farkları değerlendirmek için tek yönlü ANOVA ve post-hoc Tukey testleri kullanıldı. Grup 1 ile grup 2 ve 3'ü ayırt etmek için WBC, nötrofil ve sodyum seviyelerinin birlikte değerlendirildiği lojistik regresyon modeli kullanıldı ve modelin performansı ROC eğrisi altındaki alan (AUC) ile değerlendirildi.

Bulgular: WBC (p<0,001), nötrofil (p<0,001) ve sodyum seviyeleri (p<0,001) açısından grup 1 ile grup 2 ve 3 arasında anlamlı farklar gözlendi. Grup 3, en yüksek WBC sayısına (17.123±4.491 hücre/µL) ve en düşük sodyum seviyesine (132.5±1.4 mEq/L) sahipken, grup 1 en düşük WBC sayısına (10.660±3.804 hücre/µL) ve en yüksek sodyum seviyesine (137.5±2.6 mEq/L) sahipti. WBC, nötrofil ve sodyum değerlerinin birlikte değerlendirildiği lojistik regresyon analizi, AUC'nin 0,703 olduğunu ve orta düzeyde tanısal fayda sağladığını gösterdi.

Address for Correspondence/Yazışma Adresi: Cem Kaya, MD, Department of Pediatric Surgery, Gazi University Faculty of Medicine, Ankara, Türkiye
E-mail / E-posta: drcemkaya61@gmail.com
ORCID ID: orcid.org/0000-0003-4265-4013

Received/Geliş Tarihi: 20.09.2024
Accepted/Kabul Tarihi: 30.09.2024

Conclusion: This study demonstrated that WBC count, neutrophil count, and sodium level, as well as their ratios, can aid in diagnosing appendicitis in pediatric patients. Although sodium levels were significantly lower in patients with appendicitis, no significant difference was found between acute and perforated appendicitis. The WBC/sodium and neutrophil/sodium ratios could be valuable in clinical practice, especially for distinguishing between appendicitis and non-appendicitis cases. Further research is warranted to explore their utility in larger populations.

Keywords: Acute appendicitis, sodium, white blood cell count, neutrophil, hyponatremia

Sonuç: Bu çalışma, WBC sayısı, nötrofil sayısı ve sodyum seviyeleri ile bu değerlerin oranlarının, pediatrik hastalarda apandisit tanısında yararlı olabileceğini göstermektedir. Sodyum seviyeleri apandisit vakalarında anlamlı derecede düşük olmasına rağmen, akut ve perfore apandisit arasında istatistiksel olarak anlamlı bir fark bulunamamıştır. WBC/sodyum ve nötrofil/sodyum oranları, özellikle apandisit ve apandisit olmayan vakaların ayırt edilmesinde klinik uygulamada değerli olabilir. Daha geniş popülasyonlarda bu belirteçlerin faydasını incelemek için daha fazla araştırmaya ihtiyaç vardır.

Anahtar Sözcükler: Akut apandisit, sodyum, beyaz küre sayısı, nötrofil, hiponatremi

INTRODUCTION

Acute appendicitis is one of the most common causes of abdominal pain requiring surgical intervention, particularly in pediatric and adult populations (1). Although modern diagnostic imaging techniques, such as ultrasound and computed tomography (CT), have improved the early detection of appendicitis, accurately assessing disease severity and predicting complications remains a challenge (2).

In recent years, electrolyte disturbances, particularly hyponatremia, have been proposed as potential markers of inflammation and systemic stress in various surgical conditions (3). Sodium, a key electrolyte for maintaining cellular homeostasis and fluid balance, is frequently affected in acute inflammatory processes. Disruption of this mechanism may reflect systemic inflammation and fluid shifts that occur in response to severe infections or tissue injury (4).

Several studies have highlighted the association between hyponatremia and severe appendicitis, suggesting that lower sodium levels are associated with higher rates of perforation, abscess formation, and postoperative complications (5). In particular, hyponatremia has been proposed as a surrogate marker for more advanced disease, potentially aiding clinicians in identifying patients at greater risk for poor outcomes (6,7).

Nevertheless, the clinical utility of hyponatremia as a prognostic marker in appendicitis remains controversial. While some studies support its association with complicated appendicitis, other studies have found no significant relationship between sodium levels and disease severity, emphasizing the need for further investigation (8,9). Given these conflicting findings, exploring the potential role of sodium disturbances in predicting appendicitis outcomes in a more comprehensive and systematic manner is crucial.

The aim of this study was to evaluate the relationship between serum sodium levels, WBC and neutrophil counts, WBC/sodium ratio, and appendicitis.

MATERIALS AND METHODS

This retrospective study, initiated after receiving approval from Gazi University Clinical Research Ethics Committee (approval number: 514, date: 27.06.2022), included 176 pediatric patients who underwent appendectomy due to appendicitis and underwent complete blood counts and biochemistry tests between 2019 and 2021. Patients were divided into three groups based on pathological findings: non-appendicitis (group 1), acute appendicitis (group 2), and perforated appendicitis (group 3). Patient data, including sex, age (in months), white blood cell count (WBC), neutrophil count, sodium levels, WBC/sodium ratio, neutrophil/sodium ratio, and pathological results, were collected from hospital records.

Blood samples were collected preoperatively from all patients. WBC and neutrophil counts were measured in units of cells per microliter (cells/μL) using an automated hematology analyzer. Sodium levels were measured in milliequivalents per liter (mEq/L) using standard electrolyte panels.

Statistical Analysis

Data were analyzed using SPSS Version 22.0 for Windows (IBM Corp, Armonk, NY). Continuous variables, such as WBC count, neutrophil count, sodium level, WBC/sodium ratio, and neutrophil/sodium ratio, were presented as mean ± standard deviation. Normality of data was assessed using the Shapiro-Wilk test. Because the data were normally distributed ($p>0.05$ for all variables), one-way analysis of variance was used to compare continuous variables between the pathology groups. A post-hoc analysis was performed using Tukey's test to identify specific group differences. Additionally, a logistic regression model was used to assess whether WBC, neutrophil, and sodium levels, when considered together, could distinguish between group 1 and groups 2 and 3. The model performance was evaluated using the area under the receiver operating characteristic curve (AUC). A p-value 0.05 was considered statistically significant.

RESULTS

A total of 176 pediatric patients were included in the study. The mean age of the patients was 135.6±47.8 months, with 43.2% (n=76) being female and 56.8% (n=100) being male. Based on the pathological results, 59 patients (33.5%) were classified as having non-appendicitis (group 1), 82 patients (46.6%) as having acute appendicitis (group 2), and 35 patients (19.9%) as having perforated appendicitis (group 3).

A significant difference was found in terms of WBC count between group 1 (non-appendicitis), group 2 (acute appendicitis), and group 3 (perforated appendicitis) ($p<0.001$). Group 3 had the highest WBC count (17,123±4,491 cells/μL), whereas group 1 had the lowest WBC count (10,660±3,804 cells/μL). No significant difference was found between group 2 (15,914±4,451 cells/μL) and group 3 (Table 1, Figure 1).

Similarly, significant differences were observed in terms of neutrophil counts between groups 1, 2 and 3 ($p<0.001$). Group 3 had the highest neutrophil count (14,581±4,054 cells/μL), whereas group 1 had the lowest (8,469±5,998 cells/μL). No significant difference was

Table 1. Patient characteristics and laboratory findings by groups

Variable	Group 1 (non-appendicitis)	Group 2 (acute appendicitis)	Group 3 (perforated appendicitis)	p
WBC (cells/µL)	10,660±3,804	15,914±4,451	17,123±4,491	<0.001
Neutrophil (cells/µL)	8,469±5,998	13,046±4,375	14,581±4,054	<0.001
Sodium (mEq/L)	137.5±2.6	137.0±2.3	132.5±1.4	<0.001
WBC/sodium ratio	7,767±2,804	11,500±3,471	12,929±3,434	<0.001
Neutrophil/sodium ratio	5,690±2,951	9,535±3,229	11,011±3,105	<0.001

WBC: White blood cell.

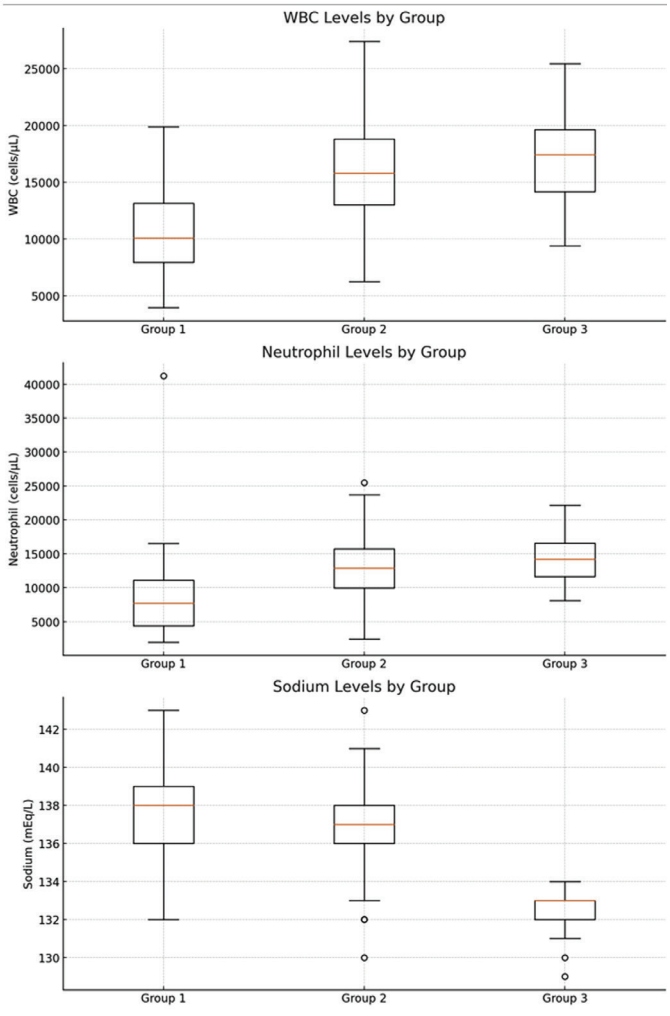

Figure 1. Box plot illustrating the distribution of white blood cell, neutrophil, and sodium levels by group.

WBC: White blood cell.

found between group 2 (13,046±4,375 cells/µL) and group 3 (Table 1, Figure 1).

Both group 2, 3 had significantly lower sodium levels than group 1 (p<0.001). Group 3 had the lowest sodium level (132.5±1.4 mEq/L), whereas group 1 had the highest (137.5±2.6 mEq/L). No significant difference was observed between group 2 (137.0±2.3 mEq/L) and group 3 (Table 1, Figure 1).

When we evaluated the WBC/sodium ratio, significant differences were found between groups 1, 2, and 3 (p<0.001). Group 3 had the highest WBC/sodium ratio (12,929±3,434), whereas group 1 had the lowest (7,767±2,804). No significant difference was found between group 2 (11,500±3,471) and group 3. Similarly, when we looked at the neutrophil/sodium ratio, group 3 had the highest neutrophil/sodium ratio (11,011±3,105), and group 1 had the lowest (5,690±2,951) (p<0.001). No significant difference was found between group 2 (9,535±3,229) and group 3 (Table 1).

When WBC, neutrophil, and sodium levels were evaluated together using a logistic regression model, the AUC was 0.703. This indicates a moderate ability to distinguish group 1 from groups 2 and 3 when these parameters are used in combination.

DISCUSSION

Acute appendicitis is one of the most common surgical causes of abdominal pain in children and often requires urgent surgical intervention. If untreated, appendicitis can lead to complications, such as perforation, peritonitis, and sepsis, which can significantly increase morbidity and mortality rates. Thus, early and accurate diagnosis is essential. However, diagnosing appendicitis in children is more challenging than in adults, as children may have difficulty expressing their symptoms clearly, and the clinical presentation can overlap with other pediatric conditions. In particular, younger children may present with non-specific symptoms, such as nausea, vomiting, anorexia, and diffuse abdominal pain, which can delay diagnosis and increase the risk of perforation. The diagnostic process often involves a combination of clinical evaluation, laboratory testing, and imaging. Clinical signs such as tenderness at McBurney's point, right lower-quadrant pain, and guarding may suggest appendicitis. Laboratory findings frequently include leukocytosis and elevated C-reactive protein although these markers are not always specific to appendicitis. Imaging studies, including ultrasonography (US) and CT, play a key role in diagnosis. However, because of concerns about radiation exposure, the use of CT in children is approached with caution, and US is often preferred as the first-line imaging modality (10-14).

Diagnosis of this condition remains a significant clinical challenge, especially in young children, because of its atypical presentation and overlap of symptoms with other gastrointestinal conditions. In response to this challenge, several diagnostic scoring systems have been developed, including the Alvarado score and Pediatric Appendicitis score. In addition, sodium levels can be used as a marker of appendicitis severity (15).

This study highlights the difficulty of diagnosing acute appendicitis in children and demonstrates that WBC, neutrophil, and sodium levels may serve as important biomarkers for assessing the severity of appendicitis. The results indicate that patients with non-perforated appendicitis (group 2) and perforated appendicitis (group 3) had significantly higher WBC and neutrophil counts compared to non-appendicitis patients (group 1). These findings are consistent with those of Nissen and Tröbs (16), who reported that elevated WBC and neutrophil counts support the diagnosis of appendicitis.

Hyponatremia has gained increasing attention as a potential biochemical marker of disease severity in the differential diagnosis of acute and complicated appendicitis. Numerous publications have increasingly been published in recent years supporting sodium as a significant differentiating biochemical marker (8,17,18). Although sodium levels were lower in complicated appendicitis, the findings of this study revealed no statistically significant difference between acute appendicitis and complicated appendicitis in terms of sodium levels. Nonetheless, a significant difference was found between patients with and without appendicitis. In our study, patients with perforated appendicitis (group 3) had the lowest sodium levels (132.5±1.4 mEq/L), which was significantly lower than those in the non-appandicitis group (group 1), who had the highest sodium levels (137.5±2.6 mEq/L).

CONCLUSION

Considering that the WBC/sodium and neutrophil/sodium ratios significantly differ in the diagnosis of appendicitis, it can be concluded that these ratios should be considered in clinical practice. Although the WBC/sodium and neutrophil/sodium ratios were higher in the perforated appendicitis group than in the acute appendicitis group, no statistically significant difference was found. In conclusion, the present study indicates that WBC, neutrophil, and sodium levels are important biomarkers for the diagnosis of appendicitis in children. Early diagnosis of acute appendicitis and the presence of conditions leading to perforation is critical to prevent complications.

Ethics

Ethics Committee Approval: The study protocol was approved by the Gazi University Clinical Research Ethics Committee (approval number: 514, date: 27.06.2022).

Informed Consent: Retrospective study.

Authorship Contributions

Concept: C.K., Design: G.A., Supervision: R.K., Z.T., Resources: K.S., Materials: A.K., Data Collection or Processing: F.N.A.U., L.N.T., Analysis or Interpretation: C.K., Literature Search: G.A., Writing: G.A., C.K., Critical Review: R.K., Z.T., K.S.

Conflict of Interest: No conflict of interest was declared by the authors.

Financial Disclosure: The authors declared that this study received no financial support.

REFERENCES

1. Huckins DS, Copeland K. Diagnostic accuracy of combined WBC, ANC and CRP in adult emergency department patients suspected of acute appendicitis. Am J Emerg Med. 2021; 44: 401-6.
2. Lee WH, O'Brien S, McKinnon E, Collin M, Dalziel SR, Craig SS, et al. Study of pediatric appendicitis scores and management strategies: A prospective observational feasibility study. Acad Emerg Med. 2024. doi: 10.1111/acem.14985.
3. Turhan VB, Ünsal A, Öztürk B, Öztürk D, Buluş H. Predictive value of serum sodium level in determining perforated appendicitis. Ulus Travma Acil Cerrahi Derg. 2022; 28: 290-5.
4. Rose BD, Post TW. Clinical Physiology of Acid-Base and Electrolyte Disorders. McGraw-Hill; 2001.
5. Pogorelić Z, Lukšić B, Ninčević S, Lukšić B, Polašek O. Hyponatremia as a predictor of perforated acute appendicitis in pediatric population: A prospective study. J Pediatr Surg. 2021; 56: 1816-21.
6. Cordova Sanchez A, Bhuta K, Shmorgon G, Angeloni N, Murphy R, Chaudhuri D. The association of hyponatremia and clinical outcomes in patients with acute myocardial infarction: a cross-sectional study. BMC Cardiovasc Disord. 2022; 22: 276.
7. Fratangelo L, Nguyen S, D'Amelio P. Hyponatremia and aging-related diseases: key player or innocent bystander? A systematic review. Syst Rev. 2023; 12: 84.
8. Anand S, Krishnan N, Birley JR, Tintor G, Bajpai M, Pogorelić Z. Hyponatremia-A New Diagnostic Marker for Complicated Acute Appendicitis in Children: A Systematic Review and Meta-Analysis. Children (Basel). 2022; 9: 1070.
9. Messias B, Cubas I, Oliveira C, Hashimoto F, Mocchetti E, Ichinose T, et al. Usefulness of serum sodium levels as a novel marker for predicting acute appendicitis severity: a retrospective cohort study. BMC Surg. 2023; 23: 312.
10. Bhatt M, Joseph L, Ducharme FM, Dougherty G, McGillivray D. Prospective validation of the pediatric appendicitis score in a Canadian pediatric emergency department. Acad Emerg Med. 2009; 16: 591-6.
11. Saucier A, Huang EY, Emeremni CA, Pershad J. Prospective evaluation of a clinical pathway for suspected appendicitis. Pediatrics. 2014; 133: e88-95.
12. Samuel M. Pediatric appendicitis score. J Pediatr Surg. 2002; 37: 877-81.
13. Kaiser S, Frenckner B, Jorulf HK. Suspected appendicitis in children: US and CT--a prospective randomized study. Radiology. 2002; 223: 633-8.
14. Dahabreh IJ, Adam GP, Halladay CW, Steele DW, Daiello LA, Wieland LS, et al. Diagnosis of Right Lower Quadrant Pain and Suspected Acute Appendicitis [Internet]. Rockville (MD): Agency for Healthcare Research and Quality (US); 2015.
15. Stiel C, Elrod J, Klinke M, Herrmann J, Junge CM, Ghadban T, et al. The Modified Heidelberg and the AI Appendicitis Score Are Superior to Current Scores in Predicting Appendicitis in Children: A Two-Center Cohort Study. Front Pediatr. 2020; 8: 592892.
16. Nissen M, Tröbs RB. The lymphocyte-to-monocyte ratio may distinguish complicated from non-complicated pediatric appendicitis: A retrospective study and literature review. Pediatr Neonatol. 2022; 63: 146-53.
17. Symeonidis NG, Pavlidis ET, Psarras KK, Stavrati K, Nikolaidou C, Marneri A, et al. Preoperative Hyponatremia Indicates Complicated Acute Appendicitis. Surg Res Pract. 2022; 2022: 1836754.
18. Walsh A, Lala S, Wells C, Upadhyay V. Hyponatremia an indicator of complicated appendicitis in children: Starship experience. ANZ J Surg. 2022; 92: 747-52.

GMJ 2024;35:442-444

DOI: http://dx.doi.org/10.12996/gmj.2023.3821

Chronic Pancreatitis with Unilateral Pleural Effusion: An Atypical Presentation

Tek Taraflı Plevral Efüzyonlu Kronik Pankreatit: Atipik Bir Sunum

Illani Binti Riza[1], Yap Yoon Chin[1], Lo Zhen Zhen[2]

[1]Jabatan Kecemasan dan Trauma, Hospital Queen Elizabeth, Kota Kinabalu, Malaysia
[2]Department of Emergency Medicine, Faculty of Medicine and Health Sciences, University Malaysia Sabah, Kota Kinabalu, Sabah, Malaysia

ABSTRACT

Pancreaticopleural fistula is a rare complication of acute or chronic pancreatitis. The most prevalent reasons for chest discomfort in this patient were pleural effusion, mediastinal or pleural pseudocyst. A 42-year-old man presented with left pleuritic chest pain and cough. A plain chest X-ray revealed two large suspicious opacities in the left lung. A contrast-enhanced computed tomography thorax and pancreas shows left pleural effusion and features suggestive of chronic pancreatitis. There was peripancreatic collection and pancreatic duct dilatation which communicated with the left pleura, causing left pleural effusion. Pleural fluid samples showed high pleural fluid amylase and albumin. Endoscopic retrograde cholangiopancreatography (ERCP) was done and the pancreatic duct was stented. Repeated ERCP a month later showed no leakage after stent insertion.

Keywords: Pancreaticopleural fistula, pleural effusion, chronic pancreatitis

ÖZ

Pankreatikoplevral fistül akut veya kronik pankreatitin nadir bir komplikasyonudur. Bu hastada göğüs rahatsızlığının en sık görülen nedenleri plevral efüzyon, mediastinal veya plevral psödokist idi. Kırk iki yaşında erkek hasta sol plöretik göğüs ağrısı ve öksürük şikayetiyle başvurdu. Düz göğüs röntgeninde sol akciğerde iki adet büyük şüpheli opaklık görüldü. Kontrastlı bilgisayarlı toraks ve pankreas tomografisinde sol plevral efüzyon ve kronik pankreatiti düşündüren özellikler görülmektedir. Peripankreatik kolleksiyon ve sol plevra ile iletişim kuran pankreas kanalında dilatasyon mevcuttu ve sol plevral efüzyona neden oldu. Plevral sıvı örneklerinde yüksek plevra sıvısı amilazı ve albumini saptandı. Endoskopik retrograd kolanjiyopankreatografi (ERCP) yapıldı ve pankreas kanalına stent takıldı. Bir ay sonra tekrarlanan ERCP'de stent takılmasından sonra herhangi bir sızıntı görülmedi.

Anahtar Sözcükler: Pankreatikoplevral fistül, plevral efüzyon, kronik pankreatit

INTRODUCTION

Pleural effusion due to a pancreaticopleural fistula is a very rare occurrence, accounting for fewer than 1% of all occurrences (1). It occurs in 3-7% of patients with pancreatitis (2). More uncommon than pancreatic ascites is pancreaticopleural fistula. It may manifest as a massive recurrent pleural effusion.

CASE REPORT

A 42-year-old man presented with left pleuritic chest pain and cough. A plain chest X-ray revealed two large suspicious opacities in the left lung. A contrast-enhanced computed tomography (CT) thorax and pancreas shows left pleural effusion and features suggestive of chronic pancreatitis. There was peripancreatic collection and pancreatic duct dilatation that communicated with the left pleura, causing left pleural effusion. Pleural fluid samples showed high pleural fluid amylase and albumin. Endoscopic retrograde cholangiopancreatography (ERCP) was done, pancreatic duct leak likely at the body/tail junction with a stricture at the head of the pancreas. The pancreatic duct was stented. Repeated ERCP a month later showed no leakage after stent insertion. Sputum acid-

Address for Correspondence/Yazışma Adresi: Lo Zhen Zhen, MD, Department of Emergency Medicine, Faculty of Medicine and Health Sciences, University Malaysia Sabah, Kota Kinabalu, Sabah, Malaysia
E-mail / E-posta: lozhenzhen@ums.edu.my
ORCID ID: orcid.org/S0000-0001-7960-1412

Received/Geliş Tarihi: 03.03.2023
Accepted/Kabul Tarihi: 24.05.2023

fast bacillus were negative, and blood culture revealed no growth. Tumor markers were negative.

The patient was then well enough to be discharged home with antibiotics and analgesics. During the patient's recent follow-up, ERCP was done and no contrast leak was observed with the previous stent *in situ*. Informed consent was obtained.

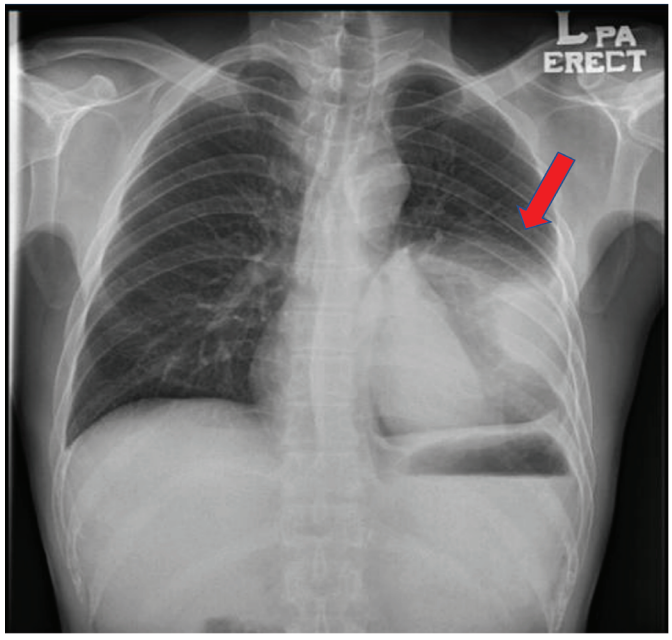

Figure 1. Left lung masses suspicious of extrapulmonary lesions with meniscal sign were noted on the arrival chest X-ray.

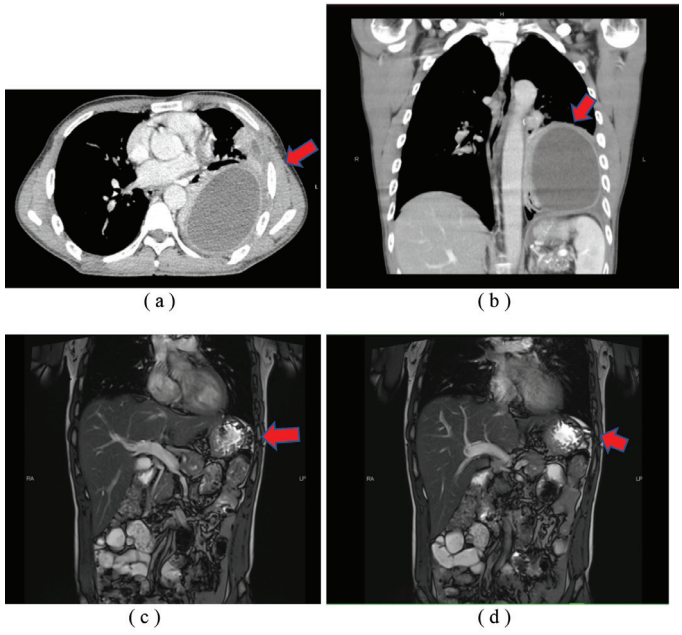

Figure 2. (a, b) are the contrast enhanced CT thorax showing large peripheral rim enhancement of fluid density in the left lower lobe pleural cavity, which extends anteriorly into the inferior lingula region with split pleural sign, which is suggestive of left lung empyema. (c, d) are MRCP suggestive of chronic pancreatitis, pancreatic tail thickening with filling defect seen within the pancreatic duct at the distal part of the body.

CT: Computed tomography, MRCP: Magnetic resonance cholangiopancreatography.

DISCUSSION

Pleural effusion is one of the rare complications of both acute and chronic pancreatitis. This condition can be caused by trans-diaphragm lymphatic blockage or pancreaticopleural fistula due to a leak and disruption of the pancreatic duct or pseudocyst. Pancreaticopleural fistulas can be formed if the disruption of the duct occurs posteriorly to the retroperitoneum region. The pancreatic enzyme can migrate superiorly to the mediastinum, causing rupture into the pleural cavity, and the formation of a connection (3). Chest symptoms caused by pleural effusion are often misleading. Abdominal symptoms like epigastric pain, may be absent (4).

Pancreaticopleural fistula is an uncommon consequence of chronic alcoholic pancreatitis, with an annual prevalence of 0.4-4.5 per cent in alcoholic patients (5). The serum amylase level is usually slightly raised, as in this patient, likely due to amylase reabsorption from the pleural surface and may indicate a pancreaticopleural fistula.

The first line of investigation is a chest X-ray. However, it only provides limited information. In this case, the abnormal finding of two heterogenous lung masses were identified in the chest X-ray that raised the suspicious of malignancy and empyema.

The gold standard investigation for pleural effusion investigation is CT thorax. It provides accurate delineation of the fistula, if present, as well as useful information on the location and extent of the pleural effusion (6,7). This patients CT contrasted thorax only reported as a left empyema with no fistula detected.

To diagnose pancreaticopleural fistula, CT or magnetic resonance cholangiopancreatography (MRCP) may be useful in certain situations. In 80% of the cases, ERCP leads to diagnosis, and in 59-74% of the cases, it reveals the fistulous tract (6,8,9). However, visualization of the fistulous tract is not always possible (8). In individuals with a more distal source of ductal disruption than the location of ductal obstruction, ERCP may not be able to detect a fistula.

In this patient, pancreatic duct leak was likely at the body/tail junction with a stricture at the head of the pancreas, and stenting was performed. However, no fistulous tract was found during the ERCP. This finding might be due to distal pancreatic ductal disruption. Subsequent MRCPs suggestive of chronic pancreatitis and strictures were found in the distal and proximal main pancreatic ducts. We were unable to diagnose pancreaticopleural fistula through MRCP. Post ERCP and stenting, the patient improved drastically and was discharged well.

When considering the clinical presentation of left pleural effusion with increased pleural fluid amylase, chronic pancreatitis, and pancreatic duct leak at the body/tail junction during ERCP with effective treatment response, it is highly suggestive of a pancreaticopleural fistula.

The use of early pleural fluid amylase testing can help to avoid a delay in diagnosis. Pleural effusion drainage, pancreatic secretion inhibition with medications, and possibly ERCP combined pancreatic duct stenting are the initial treatment.

Ethics

Informed Consent: It was obtained.

Authorship Contributions

Concept: Y.Y.C., L.Z.Z., Design: L.Z.Z., Data Collection or Processing: I.B.R., Analysis or Interpretation: Y.Y.C., Literature Search: I.B.R., Writing: I.B.R., Y.Y.C.

Conflict of Interest: No conflict of interest was declared by the authors.

Financial Disclosure: The author declared that this study received no financial support.

REFERENCES

1. Burgess NA, Moore HE, Williams JO, Lewis MH. A review of pancreatico-pleural fistula in pancreatitis and its management. HPB Surg. 1992; 5: 79-86.
2. Materne R, Vranckx P, Pauls C, Coche EE, Deprez P, Van Beers BE. Pancreaticopleural fistula: diagnosis with magnetic resonance pancreatography. Chest. 2000; 117: 912-4.
3. Browne GW, Pitchumoni CS. Pathophysiology of pulmonary complications of acute pancreatitis. World J Gastroenterol. 2006; 12: 7087-96.
4. Dhebri AR, Ferran N. Nonsurgical management of pancreaticopleural fistula. JOP. 2005; 6: 152-61.
5. Galluzzo A, Iannicelli E, Marignani M, Delle Fave G, David V. A pancreatico-pleural fistula diagnosed with magnetic resonance cholangiopancreatography. JOP. 2008; 9: 654-7.
6. Sut M, Gray R, Ramachandran M, Diamond T. Pancreaticopleural fistula: a rare complication of ERCP-induced pancreatitis. Ulster Med J. 2009; 78: 185-6.
7. Dhebri AR, Ferran N. Nonsurgical management of pancreaticopleural fistula. JOP. 2005; 6: 152-61.
8. Safadi BY, Marks JM. Pancreatic-pleural fistula: the role of ERCP in diagnosis and treatment. Gastrointest Endosc. 2000; 51: 213-5.
9. Rockey DC, Cello JP. Pancreaticopleural fistula. Report of 7 patients and review of the literature. Medicine (Baltimore). 1990; 69: 332-44.

GMJ 2024;35:445-448

DOI: http://dx.doi.org/10.12996/gmj.2023.4033

Coincidental or Connected: Synchronous Giant Gastric GIST and Malignant Colonic Polyp: A Case Report

Tesadüf veya Bağlantılı: Eşzamanlı Dev Gastrik GİST ve Malign Kolon Polipi: Bir Olgu Sunumu

Terukumar Chandrasekaran[1], Lim Li Yi[2], JJ Mah[2], RK Sriram[2], Nik Amin Sahid[3]

[1]Department of General Surgery, Faculty of Medicine, University Kebangsaan Malaysia, Kuala Lumpur, Malaysia
[2]Department of Surgery, Colorectal Surgery Unit, Queen Elizabeth Hospital, Kota Kinabalu, Malaysia
[3]Department of Surgical, Universitiy Malaysia Sabah, Faculty of Medicine & Health Sciences, Kota Kinabalu, Malaysia

ABSTRACT

Gastrointestinal stromal tumors (GIST) are rare mesenchymal neoplasms of the gastrointestinal tract, most commonly occurring in the stomach. The concurrence of GIST with another malignancy is an uncommon phenomenon, with few works of literature reported. We report a rare synchronous giant gastric GIST with a malignant colonic polyp. A 70-year-old woman presented with an upper abdominal mass. There were no changes in bowel habits. CEA level was normal. Contrasted computed tomography of the abdomen revealed a huge gastric mass with incidental findings of a suspicious mass in the sigmoid colon. Esophagogastroduodenoscopy revealed extrinsic compression with normal overlying mucosa, suggesting a submucosal mass. Colonoscopy revealed a large polypoidal mass in the sigmoid colon, and initial biopsy revealed tubulovillous adenoma with high-grade dysplasia. Wide local excision of the gastric tumor and table snare polypectomy were performed. The base of the polyp was also taken for biopsy. The patient had an uneventful recovery and was discharged home well. Postoperative histopathological examination showed gastric GIST and adenocarcinoma of the sigmoid polyp. The polyp base showed no malignancy. The patient was started on imatinib 400 mg once a day. GIST and colon malignant polyps are two distinct types of neoplasms that can occur synchronously. GIST tumours arise from the interstitial cells of Cajal and are characterized by mutations in *KIT/PDGFRA* genes. Conversely, malignant polyps are epithelial tumours that arise from the colonic mucosa classically because of alterations in the APC tumour suppressor gene, resulting in overactivation of the Wnt/β-catenin signaling pathway. Synchronous GISTs and malignant colon polyps are rare, and their molecular basis is distinct. However, it is crucial to consider the possibility of genetic predisposition in patients with such tumors. In a case of GIST, the surgeon should recognize the possibility of another tumor with a different histological origin. High clinical analysis needed during laparotomy for GIST to detect a

ÖZ

Gastrointestinal stromal tümörler (GİST), gastrointestinal sistemin nadir görülen mezenkimal neoplazmalarıdır ve en sık midede görülür. GİST'nin başka bir malignite ile birlikteliği nadir görülen bir olgudur ve literatürde çok az çalışma bildirilmiştir. Kötü huylu kolon polipi olan nadir bir senkron dev gastrik GIST bildiriyoruz. Üst karın bölgesinde kitle şikayetiyle 70 yaşında kadın hasta başvurdu. Barsak alışkanlıklarında değişiklik olmadı. CEA düzeyi normaldi. Karın bölgesinin kontrastlı bilgisayarlı tomografisi, sigmoid kolonda şüpheli bir kitleye rastlanan büyük bir gastrik kitleyi ortaya koydu. Özofagogastroduodenoskopide, normal üst mukoza ile birlikte ekstrinsik bası saptandı ve submukozal kitleyi düşündürdü. Kolonoskopide sigmoid kolonda büyük polipoidal kitle saptandı ve ilk biyopside yüksek dereceli displaziye sahip tübülovillöz adenom görüldü. Mide tümörünün geniş lokal eksizyonu ve table snare polipektomisi yapıldı. Polipin tabanından da biyopsi alındı. Hasta sorunsuz bir şekilde iyileşerek taburcu edildi. Ameliyat sonrası histopatolojik incelemede gastrik gist ve sigmoid polibin adenokarsinomu saptandı. Polip tabanında malignite saptanmadı. Hastaya günde bir kez 400 mg imatinib başlandı. GİST ve kolon malign polipleri eş zamanlı olarak ortaya çıkabilen iki ayrı neoplazm türüdür. GİST tümörleri Cajal'ın interstisyel hücrelerinden kaynaklanır ve *KIT/PDGFRA* genlerindeki mutasyonlarla karakterizedir. Buna karşılık, malign polipler, klasik olarak APC tümör baskılayıcı genindeki değişiklikler sonucu Wnt/β-katenin sinyal yolunun aşırı aktivasyonu sonucu kolon mukozasından kaynaklanan epitel tümörlerdir. Eş zamanlı GİST'ler ve malign kolon polipleri nadir görülür ve moleküler temelleri farklıdır. Ancak bu tür tümörlere sahip hastalarda genetik yatkınlık olasılığının da göz önünde bulundurulması önemlidir. GİST olgusunda cerrah, farklı histolojik kökenli başka bir tümörün olasılığını göz önünde bulundurmalıdır. GİST'te senkron tümör tespiti için laparotomi sırasında yüksek klinik analize ihtiyaç vardır. Nadir görülmesi ve literatürün sınırlı olması nedeniyle, cerrahların hasta

Address for Correspondence/Yazışma Adresi: Nik Amin Sahid, Department of Surgical, Universiti Malaysia Sabah, Faculty of Medicine & Health Sciences, Kota Kinabalu, Malaysia
E-mail / E-posta: nike_opo@ums.edu.my
ORCID ID: orcid.org/0000-0003-0199-7837

Received/Geliş Tarihi: 26.10.2023
Accepted/Kabul Tarihi: 14.03.2024

ABSTRACT

synchronous tumor. Due to its rare occurrence and limited literature further GIST with another synchronous tumor must be conducted to help surgeons optimize patient management.

Keywords: Gastrointestinal stromal tumor, malignant colonic polyp, synchronous tumor

ÖZ

yönetimini optimize etmesine yardımcı olmak için başka bir senkron tümörle birlikte daha fazla GİST yapılmalıdır.

Anahtar Sözcükler: Gastrointestinal stromal tümör, kötü huylu kolon polip, senkron tümör

INTRODUCTION

Gastrointestinal stromal tumor (GIST) is the most common mesenchymal-derived neoplasm arising from the gastrointestinal (GI) tract (1). It accounts for only 0.1-3% of all GI neoplasms (1). The incidence is 1.5 per 100,000 per year (1). This indicates the rarity of the tumor. It is peak incidence in the sixth and seventh decades (2). It originates from the interstitial call of Cajal, which is responsible for gut motility and can present anywhere along the GI tract. The most common site of origin is the stomach (60%), followed by the small intestine (30%) (1). Historically GIST is classified as leiomyomas or leiomyosarcoma as it represents similar histological appearance with smooth muscle neoplasm. However, recent studies now consider them as separate entities based on the identification of C-kit receptor or the PDGFR receptor mutation in GIST. GISTs have malignant potential, and their nature is difficult to predict (3). The coexistence of GIST with other primary GI malignancy with different histology origin has rarely been reported in the literature (3).

Malignant colonic polyp is defined as macroscopically benign appearing adenoma that harbors a focus of adenocarcinoma that invades beyond muscularis mucosae into submucosa (4,5). It accounts about 2-5% of all removed polyps (4). Large colon polyps (defined >2 cm) and polyps with high-grade dysplasia (HGD) carry a higher risk of carcinoma (4,6). It is accepted that most malignant neoplasms of the colon arise from the precursor adenomatous polyp. This adenoma-carcinoma sequence is a stepwise progression from normal epithelium to carcinoma, often with intervening dysplasia, that occurs as a result of multiple sequential genetic mutations. Colorectal adenocarcinoma is a significant clinical problem and the third most common neoplasm worldwide (5,7).

CASE REPORT

70-year-old women presented with abdominal discomfort for a year. Patients denied a history of abdominal pain, altered bowel habits, or any constitutional symptom. She had no family history associated with malignancy. On clinical examination noted upper abdominal mass. Her CEA level was normal. She is subjected to radiological and endoscopic workup to identify the origin of the mass.

Contrasted computed tomography (CT) of the abdomen revealed a large, enhancing and fungating homogenous mass gastric mass with an the sigmoid colon. The sigmoid mass could represent a metastasis or synchronous tumor (Figure 1a, b). Esophagogastroduodenoscopy revealed extrinsic compression with normal overlying mucosa, suggesting a submucosal mass. Colonoscopy revealed a large polypoidal mass in the sigmoid colon (>2 cm) (Figure 2), from which an initial biopsy revealed tubulovillous adenoma with HGD.

The patient is scheduled for surgery. The operative findings revealed a large tumor (15x20 cm) originating from the stomach (Figures 3, 4). There were no ascites, peritoneal, or liver nodules. Wide local excision of the gastric tumor and table snare polypectomy of the sigmoid polyp were performed (Figure 5). The base of the polyp was taken for biopsy. The patient had an uneventful recovery and was discharged home well. Histopathological examination of the resected specimens revealed gastric GIST and adenocarcinoma of the sigmoid polyp. The base of the polyp has no dysplasia or malignancy seen. The patient was started on imatinib.

DISCUSSION

GIST is the most common mesenchymal neoplasia of the GI tract, but one-third of cases are detected incidentally during investigations or therapeutic procedures for unrelated diseases (8,9). The incidence of GIST is generally small in size (8,10). GIST predominantly involves the stomach (60%), small intestine (30%), colon (7%), and rectum (7%) and it originates from the interstitial pacemaker cells of Cajal (2). The percentage of GIST with other neoplasm reported between

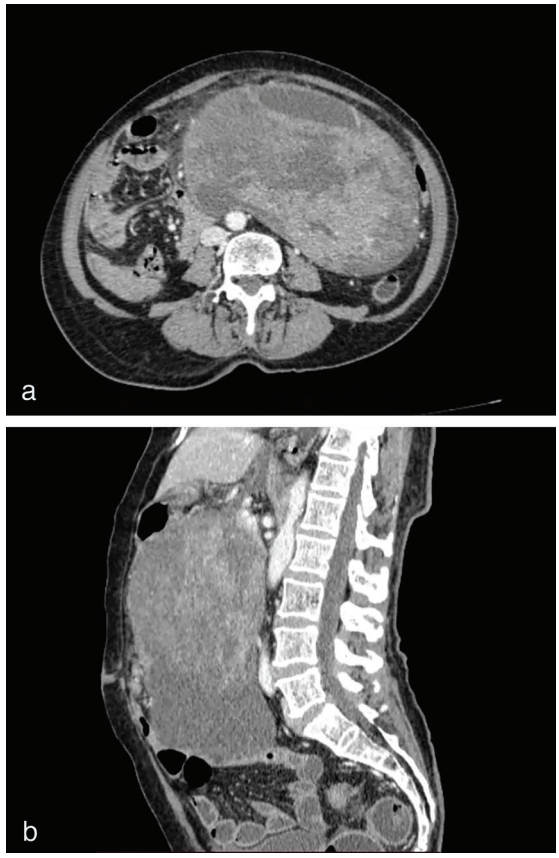

Figure 1. (a, b) CT features of a large heterogenously enhancing and hypervascularised intraperitoneal mass that appears to arise from the stomach (greater curvature) with a cystic component.

CT: Computed tomography.

3-33% (2). The most important markers of GIST are CD 117 (C-kit protein) and CD 34 (hematopoietic cell progenitor antigen). The vast majority of GIST cases are positive for CD 117 (95%), CD 34 (70-80%), smooth muscle actin (40%) PS 100 (5%) and desmin (2%) (9). CD117 immunoreceptors represent the gold standard for diagnosing GIST and the criteria required to initiate imatinib masylate therapy (9). Few syndromes have been reported in literature which associated GIST with other neoplasia such as the Von Recklinghausen's disease, the Carney triad (gastric GIST, lung chondoma and paraganglioma), and familial GIST (11). Outside this scope, it has not been confirmed whether the co-existence is incidental or a result of a related pathophysiological process. The most common secondary neoplasm in GIST cases is GI malignancy (2).

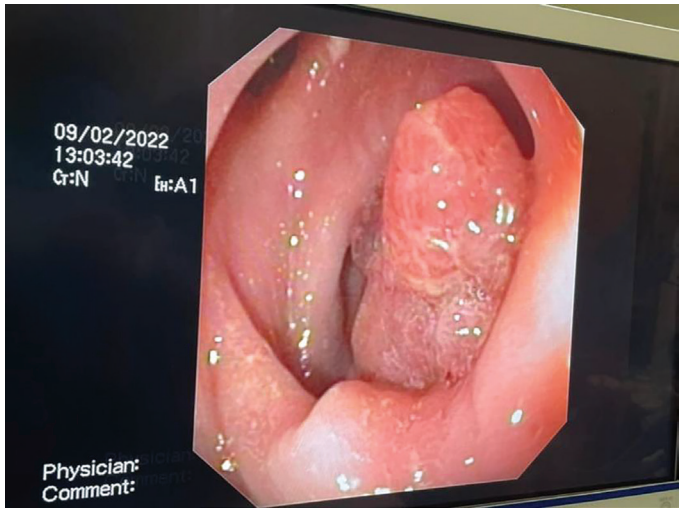

Figure 2. Endoscopic image of the sigmoid polyp.

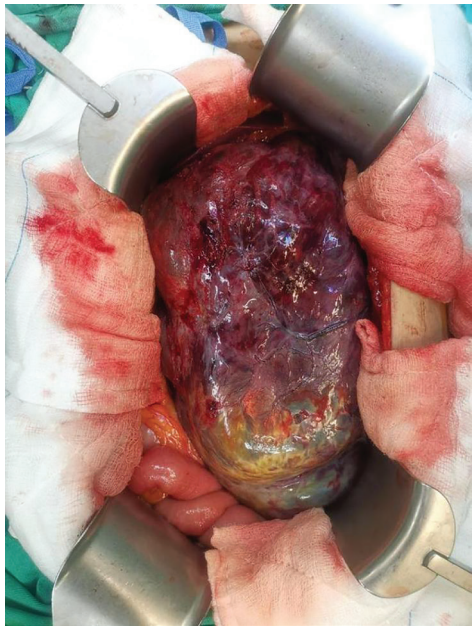

Figure 3. Intraoperative view of stomach GIST.
GIST: Gastrointestinal stromal tumors.

A study conducted by Kaur et al. (2) identified 101 patients with GIST and 14 (13.8%) of them had non-GIST-associated tumors. Nine of the 14 cases were female, median age 68 (10-79 years), and the stomach was the site of presentation of GIST for 8 cases (57.1%). Non-GIST tumor is more frequent in the stomach (adenocarcinoma) and colon/rectum (adenocarcinoma) each 4 cases. The other sites were breast (ductal carcinoma), kidney (clear cell carcinoma), prostate (adenocarcinoma), endometrium (adenocarcinoma), ovary (adenocarcinoma), and adrenal (neuroblastoma), with one case each. The tumors were synchronous in 7 cases. Agaimy et al. (11) analyzed 14 studies that mentioned the presence of GIST with other neoplasia and also their own records and found 444 patients with second tumors in a total of 4,777 patients with GIST (9.3%). The major type of other primary tumors are GI carcinomas (228-47%), with colorectal tumors being the most frequent site (109-22%), followed by stomach (95-19%). The other primaries reported by Agaimy et al. (11) were lymphoma/leukemia (7%), prostate carcinoma (9%), breast (7%), kidney (6%), lung (5%), female genital tract (5%) and carcinoid tumor (3%).

In a study by Liu et al. (12) in China, discovered 54 cases of incidental GIST occurred during surgery for 311 GI epithelial malignant tumors, accounting for 17.4%. Matli et al. (13) reported ileal GIST with ampulla adenocarcinoma. Ding et al. (8) reported a case of dual pathology in stomach: Synchronous poorly differentiated neuroendocrine carcinoma and GIST of the stomach.

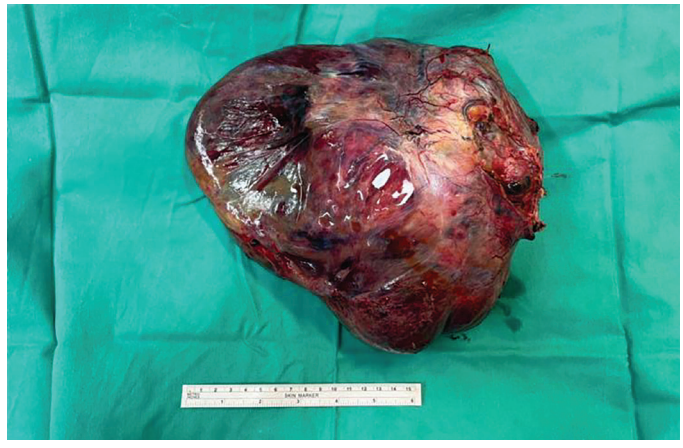

Figure 4. Wide local gastric tumor excision.

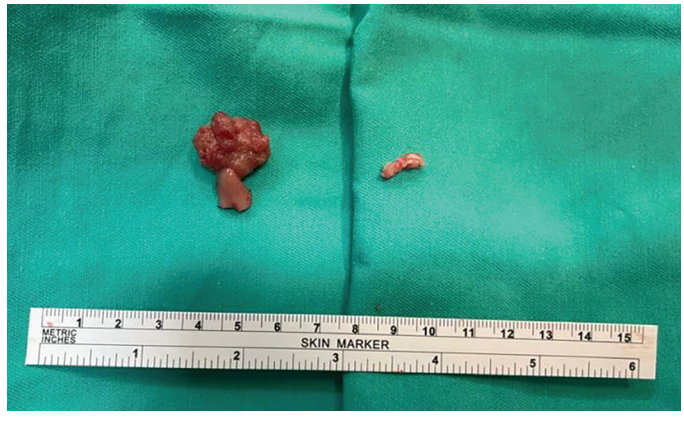

Figure 5. Snare polypectomy specimen.

Synchronous or metachronous occurrence of GIST with other neoplasia must always be considered during patient management. Here, we discuss a case of GIST, and colon malignant polyps are two distinct types of neoplasms that can occur synchronously. GIST tumors arise from the interstitial cells of Cajal and are characterized by mutations in *KIT/PDGFRA* genes. Conversely, malignant polyps are epithelial tumors that arise from the colonic mucosa classically because of alterations in the APC tumor suppressor gene, resulting in overactivation of the Wnt/β-catenin signaling pathway.

Some authors have postulated that they may share common carcinogenic pathways or genetic mutations with the proliferation of different cell lines (14). Further studies are required to analyze the molecular and genetic mechanisms of carcinogenesis.

An interesting matter in our write up here is the synchronous presentation of GIST in the stomach with a malignant colonic polyp. The coexistence of GIST with another histological tumor is uncommon (10,15). To our knowledge, there is no evidence to suggest a common factor in the tumorogenesis of these two pathologically distinct tumors.

CONCLUSION

The managing clinician and histopathologist should be aware of the occurrence of GIST combined with another neoplasm. Dual pathology may be misinterpreted as metastatic nodule or recurrence, which would change the management and patient outcomes. In cases of diagnostic dilemma, histopathological assessment is suggested. It may not always be possible to diagnose a coexisting tumor preoperatively. Surgeons should be aware of cases of GIST to recognize for coexisting pathology during intraoperative assessment and be prepared to modify the surgical plan accordingly. Due to its rarity and limited literature to date, further research on GIST with another synchronous tumor is required. A multidisciplinary approach to GIST management is suggested.

Ethics

Informed Consent: It was obtained.

Authorship Contributions

Concept: T.C., L.L.Y., J.J.M., R.K.S., Design: T.C., L.L.Y., J.J.M., R.K.S., N.A.S., Data Collection or Processing: T.C., L.L.Y., J.J.M., R.K.S., N.A.S., Analysis or Interpretation: T.C., L.L.Y., J.J.M., R.K.S., N.A.S., Literature Search: T.C., L.L.Y., J.J.M., R.K.S., N.A.S., Writing: T.C., L.L.Y., J.J.M., R.K.S., N.A.S.

Conflict of Interest: No conflict of interest was declared by the authors.

Financial Disclosure: The author declared that this study received no financial support.

REFERENCES

1. Al-Maghrabi H, Meliti A. Gastric gastrointestinal stromal tumor with osseous differentiation and stromal calcification: a case report and review of literature. SAGE Open Med Case Rep. 2017; 5: 2050313X17746310.
2. Kaur R, Bhalla S, Nundy S, Jain S. Synchronous gastric gastrointestinal stromal tumor (GIST) and other primary neoplasms of gastrointestinal tract: report of two cases. Ann Gastroenterol. 2013; 26: 356-9.
3. Nemes C, Rogojan L, Surdea-Blaga T, Seicean A, Dumitrascu DL, Ciuce C. Gastrointestinal stromal tumor (GIST) associated with synchronous colon adenocarcinoma - a case report. J Gastrointestin Liver Dis. 2012; 21: 101-3.
4. Lowe D, Saleem S, Arif MO, Sinha S, Brooks G. Role of Endoscopic Resection Versus Surgical Resection in Management of Malignant Colon Polyps: a National Cancer Database Analysis. J Gastrointest Surg. 2020; 24: 177-87.
5. Zammit AP, Panahi SE, Brown I, Hooper JD, Clark DA, Riddell AD. Management of high and low risk malignant polyps: a population-wide analysis. Colorectal Dis. 2023; 25: 66-74.
6. Mehta N, Abushahin A, Sadaps M, Alomari M, Vargo J, Patil D, et al. Recurrence with malignancy after endoscopic resection of large colon polyps with high-grade dysplasia: incidence and risk factors. Surg Endosc. 2021; 35: 2500-8.
7. Aarons CB, Shanmugan S, Bleier JI. Management of malignant colon polyps: current status and controversies. World J Gastroenterol. 2014; 20: 16178-83.
8. Ding J, Sun P, Cai XY, Fei SH, Wu J, Qi YK, et al. Synchronous poorly-differentiated neuroendocrine carcinoma and gastrointestinal stromal tumor of the stomach: a case report with immunohistochemical and molecular genetic analyses of KIT and PDGFRA. Int J Clin Exp Pathol. 2014; 7: 9076-80.
9. Efstathios P, Athanasios P, Papaconstantinou I, Alexandros P, Frangisca S, Sotirios G, et al. Coexistence of gastrointestinal stromal tumor (GIST) and colorectal adenocarcinoma: A case report. World J Surg Oncol. 2007; 5: 96.
10. Theodosopoulos T, Dellaportas D, Psychogiou V, Gennatas K, Kondi-Pafiti A, Gkiokas G, et al. Synchronous gastric adenocarcinoma and gastrointestinal stromal tumor (GIST) of the stomach: a case report. World J Surg Oncol. 2011; 9: 60.
11. Agaimy A, Wünsch PH, Sobin LH, Lasota J, Miettinen M. Occurrence of other malignancies in patients with gastrointestinal stromal tumors. Semin Diagn Pathol. 2006; 23: 120-9.
12. Liu YJ, Yang Z, Hao LS, Xia L, Jia QB, Wu XT. Synchronous incidental gastrointestinal stromal and epithelial malignant tumors. World J Gastroenterol. 2009; 15: 2027-31.
13. Matli VVK, Zibari GB, Wellman G, Ramadas P, Pandit S, Morris J. A rare synchrony of adenocarcinoma of the ampulla with an ileal gastrointestinal stromal tumor: A case report. World J Gastrointest Oncol. 2022; 14: 2253-65.
14. Shariq O, Odedra A, Alexopoulos AS, Gould S, Soobrah R. Synchronous occurrence of gastrointestinal stromal tumour and ovarian neoplasm in a patient presenting with acute cholecystitis. J Gastrointest Cancer. 2012; 43: 113-6.
15. Jafferbhoy S, Paterson H, Fineron P. Synchronous gist, colon and breast adenocarcinoma with double colonic polyp metastases. Int J Surg Case Rep. 2014; 5: 523-6.

GMJ 2024;35:449-451

DOI: http://dx.doi.org/10.12996/gmj.2024.4237

Transition of Thyroid Autoantibodies by Rituximab Treatment in Women with Rheumatoid Arthritis

Romatoid Artritli Kadınlarda Rituksimab Tedavisiyle Tiroid Otoantikorlarının Geçişi

Hüseyin Demirci[1], Ebru Aydoğan[2], Bilge Ceydilek[3]

[1]Clinic of Endocrinology and Metabolism, Ankara Etlik City Hospital, Ankara, Türkiye
[2]Department of Occupational Medicine, Hacettepe University Hospitals, Ankara, Türkiye
[3]Clinic of Endocrinology and Metabolism, Acıbadem International Hospital, Ankara, Türkiye

ABSTRACT

Rituximab was first used as a treatment for B-cell malign lymphoma, and it is currently used in the treatment of rheumatoid arthritis. On the other hand, an association between rheumatoid arthritis with another autoimmune disease Hashimoto's thyroiditis is a condition that can be expected. Thirty-four-year-old female patient with rheumatoid arthritis received disease-modifying agents in various combinations for 9 years. Due to unresponsiveness to treatment, the biological agent rituximab was initiated. The patient also had euthyroided Hashimoto's thyroiditis and nodular goiter for 15 years. At the time of the diagnosis of Hashimoto thyroiditis, anti-thyroid peroxidase (anti-TPO): 45 IU/mL (0-35), anti-thyroglobulin (anti-Tg) >3000 IU/mL (0-115) but after 4 cycles of treatment with rituximab anti-TPO: 7.38 U/mL (0-35), anti-Tg <10 U/mL (0-115). According to the literature; in patients treated with rituximab for thyroid MALT lymphoma, rheumatoid arthritis, and Grave's disease, few have been reported to have declined levels of thyroid autoantibodies. The levothyroxine replacement dose decreased in some of these patients. The decline in thyroid antibodies with the treatment of rituximab reveals the hope that Hashimoto's thyroiditis may be treatable. To understand the effect of rituximab treatment on the pathogenesis of Hashimoto's disease further studies involving a large series is required.

Keywords: Hashimoto's thyroiditis, autoimmune thyroiditis, rituximab

ÖZ

İlk olarak B-hücreli malign lenfoma tedavisi için kullanılan rituksimab, günümüzde romatoid artrit tedavisinde de kullanılmaktadır. Öte yandan, romatoid artritin bir başka otoimmün hastalık olan Hashimoto tiroiditi ile birlikteliği de beklenen bir durumdur. Otuz dört yaşında romatoid artritli kadın hasta, 9 yıl boyunca hastalık modifiye edici ajanlar çeşitli kombinasyonlarda kullanıldı. Tedaviye yanıtsızlık nedeniyle biyolojik ajan rituksimab başlandı. Hastada ayrıca 15 yıldır ötiroid Hashimoto tiroiditi ve nodüler guatr vardı. Hashimoto tiroiditi tanısı konulduğunda anti-tiroid peroksidaz (anti-TPO): 45 IU/mL (0-35), anti-tiroglobulin (anti-Tg) >3000 IU/mL (0-115) iken rituksimab ile 4 kür tedavi sonrası anti-TPO: 7,38 U/mL (0-35), anti-Tg<10 U/mL (0-115) idi. Literatüre göre; tiroid MALT lenfoma, romatoid artrit ve Graves hastalığı için rituksimab ile tedavi edilen hastaların çok azında tiroid otoantikor seviyelerinde düşüş bildirilmiştir. Bu hastaların bazılarında levotiroksin replasman dozu azalmıştır. Rituksimab tedavisi ile tiroid antikorlarının azalması, Hashimoto tiroiditinin tedavi edilebilir olabileceği umudunu ortaya koymaktadır. Rituksimab tedavisinin Hashimoto hastalığının patogenezi üzerindeki etkisini anlamak için geniş serileri içeren daha ileri çalışmalara ihtiyaç vardır.

Anahtar Sözcükler: Hashimoto tiroiditi, otoimmün tiroidit, rituksimab

Address for Correspondence/Yazışma Adresi: Hüseyin Demirci, MD, Clinic of Endocrinology and Metabolism, Ankara Etlik City Hospital, Ankara, Turkey
E-mail / E-posta: drhdemirci@gmail.com
ORCID ID: orcid.org/0000-0003-0737-2360

Received/Geliş Tarihi: 14.06.2024
Accepted/Kabul Tarihi: 29.07.2024

INTRODUCTION

Rituximab, a monoclonal antibody specific for CD20 positive B-lymphocytes, was first used to treat malign B-cell lymphomas (1). Nowadays, it is effective in the treatment of rheumatoid arthritis and is used in patients who are resistant to disease-modifying agents (2,3). On the other hand, an association of rheumatoid arthritis with another autoimmune disease Hashimoto's thyroiditis is a condition that can be expected. Thyroid autoantibody positivity was significantly higher in patients with rheumatoid arthritis than in those without autoimmune rheumatic disease (4,5). Lymphocytic infiltration is seen in the thyroid in Hashimoto's thyroiditis and can be seen in the synovium in rheumatoid arthritis. Here, we present a case of change in thyroid autoantibodies after rituximab use for the treatment of rheumatoid arthritis in patients with Hashimoto thyroiditis.

CASE REPORT

Informed consent was obtained from the patient. Thirty-four-year-old female patient diagnosed with seropositive rheumatoid arthritis is being followed for 11 years. At the time of diagnosis, there was bilateral arthritis in wrist joints and first and 3rd metacarpophalangeal joints, morning stiffness lasting about 4 hours, rheumatoid factor and anti-cyclic citrullinated peptide positivity, increase in sedimentation and C-reactive protein, and periarticular osteopenia on hand radiographs. Disease-modifying agents (DMARDs), methylprednisolone, hydroxychloroquine, sulfasalazine, leflunomide, and methotrexate were used in various combinations for 9 years. Two years ago, the patient was considered DMARD-resistant, and biological agents were considered suitable for treatment.

Because the patient had bilateral axillary lymphadenopathy 2 cm in size, to rule out the diagnosis of tuberculosis and lymphoma, lymph node biopsy was recommended, but the patient refused. Whereupon of biological agents, anti-tumor necrosis factor therapy was canceled, and rituximab was started to be given. Intravenous rituximab regimen of 1000 mg given twice at an interval of two weeks was repeated every 6 months. Four cycles of rituximab have been given to the patient so far. No side effects were observed during treatment. The DAS-28, which is used to assess disease activity score significantly decreased with rituximab treatment. Hydroxychloroquine 200 mg/day, methylprednisolone 2 mg/day, and methotrexate 15 mg/week were continued with rituximab therapy. There was nodular goiter and euthyroid Hashimoto's thyroiditis for nearly 15 years in the patient's medical history. Fifteen years ago, anti-thyroid peroxidase (anti-TPO): 45 IU/mL (0-35), anti-thyroglobulin (anti-Tg) >3000 IU/mL (0-115), thyroid-stimulating hormone (TSH): 0.9 mIU/L (0.4 to 4.6) (Table 1). In thyroid ultrasonography, the right lobe was 15x20x53 mm, the left lobe was 17x18x51 mm, and the parenchyma was minimally heterogeneous. There was a 20x18x8 mm solid nodule in the left lobe and fine needle aspiration biopsy was performed. There was no cytological atypia, which was consistent with Hashimoto thyroiditis. During the intervening 13 years, patients didn't go thyroid controls but rarely checked TSH levels were within the normal range, and patients didn't have levothyroxine replacement

Before starting treatment with rituximab anti-TPO: 42 U/mL (0-35), anti-Tg >2000 U/mL (0-115), TSH: 1.4 UI/mL (0.35-4.5), respectively (Table 1). In thyroid ultrasonography, the right lobe was 19x18x73 mm and the left lobe was 20x19x62 mm parenchyma was slightly heterogeneous, and there was a 12 mm solid nodule in the left lobe. After 4 cycles of rituximab treatment, anti-TPO: 7.38 U/mL (0-35), anti-TG <10 U/mL (0-115), TSH: 1.24 UI/mL (0.27 to 4.2) was detected (Table 1). Thyroid antibody levels at the last follow-up were rechecked and confirmed by the same laboratory.

When we compared thyroid ultrasonography just before the initiation of rituximab treatment and 4 cycles post-treatment, there were no changes in thyroid gland size, structure, parenchymal changes, or nodule size.

DISCUSSION

"May rituximab help to treat Hashimoto's thyroiditis due to the drop in the levels of thyroid autoantibodies?" questions come to mind. Hashimoto's thyroiditis is an autoimmune disease associated with lymphocytic infiltration of the thyroid gland and elevated thyroid autoantibody levels (6). Rheumatoid arthritis is an autoimmune disease associated with lymphocyte infiltration in the synovium of the joint space (7). Rituximab exerts its effect by binding to the CD20 antigen in B-cells and depleting B-lymphocytes. B-cell damage via direct apoptosis, complement-mediated cell lysis stimulation of Fc gamma receptor-mediated antibody-dependent cytotoxicity, and stopping the cell proliferation (8). Which of these mechanisms is more dominant is not yet known.

B-cells are important for the development of most of the autoimmune diseases. The activation of CD4 T-lymphocytes makes the beginning of the autoimmune pathways of Hashimoto's thyroiditis, then both CD4 lymphocytes and CD8 T-lymphocytes stimulate B-cells (9). It has been shown that B-cell depletion inhibits spontaneous autoimmune thyroiditis in NOD.H-2h4 mice (10).

Similarly, in the case of Raterman et al. (11), the patient with Hashimoto's thyroiditis using levothyroxine replacement after 1 cycle of rituximab treatment for rheumatoid arthritis developed thyrotoxicosis with immeasurably low thyroid autoantibody titers.

Levothyroxine replacement itself may cause a drop in anti-TPO levels (12). Kahara et al. (13) reported a case of 3 patients who developed thyroid MALT lymphoma on the basis that Hashimoto's thyroiditis

Table 1. Thyroid autoantibodies and thyroid-stimulating hormone levels

	At the time of diagnosis	Before starting rituximab	After four cycles of rituximab
TSH (mU/mL)	0.9 (0.4-4.6)	1.4 (0.35-4.5)	1.24 (0.27-4.2)
Anti-Tg (U/mL)	>3000 (0-115)	>2000 (0-115)	<10 (0-115)
Anti-TPO (U/mL)	45 (0-35)	42 (0-35)	7.38 (0-35)

Anti-TPO: Anti-thyroid peroxidase, TSH: Thyroid-stimulating hormone, Anti-Tg: Anti-thyroglobulin.

showed a significant decrease in the levels of both TSH and anti-TPO after rituximab treatment.

The first of these patients had rituximab treatment in association with high-dose chemotherapy, and the second one had rituximab treatment in association with high-dose steroids, and these agents have been shown to reduce the levels of thyroid autoantibodies (14). The third patient in this case had radiotherapy due to nasopharynx carcinoma 1 year before rituximab treatment. Just before initiating rituximab therapy, the third patient was subclinical hypothyroid and then became euthyroid after treatment. In our case, the patient did not have levothyroxine replacement, and her medical history, there were no high-dose steroids, chemotherapy, or radiotherapy. During low-dose steroid treatment before starting rituximab, thyroid autoantibodies remained high.

In the prospective cohort study of Kaklamanos et al. (15), the first group with autoimmune rheumatic diseases was treated with rituximab, the second group with autoimmune rheumatic disease without treatment, and 3rd healthy group was compared for TSH, fT4, fT3, anti-Tg, and anti-TPO levels three times during 24 months. At the end of the study, for any period in which all groups had all evaluated parameters, no change indicates statistical significance. There was also no change in thyroid morphology in patients (15).

When the rituximab group was analyzed, at the beginning of the study, only 3 of 18 patients had anti-TPO positivity and 2 of them had anti-Tg positivity. If there were a greater number of patients with high thyroid autoantibody titers in the study would have been more informative regarding the mechanism of action of rituximab.

In recent years, rituximab has been used for the treatment of Graves' ophthalmopathies. Salvi et al. (16) reported in a review that 43 patients had received rituximab for ophthalmopathy so far. 91% of these patients had become inactive, 1/3rd had side effects that were recorded in the form of an infusion reaction (16).

Vannucchi et al. (17) conducted a study to understand the mechanism of action of rituximab in patients with Graves' ophthalmopathies. They found no changes in thyroid autoantibodies before and after treatment with rituximab, but they found increase in chemokine ligand -10 level which is a marker of B-cell lysis.

Researchers have defended the notion that rituximab exerts its effect not by reducing antibody levels but by increasing the lysis of B-cells, which interferes with antigen presentation to B-cells (17).

Due to the unavailability of follow-up data in our case, we were unable to determine the duration of the effect. To clarify the effect of rituximab on thyroid autoantibodies, more prospective controlled studies that involve more patients with positive thyroid autoantibodies are needed. However, on the basis of this case and data from previous studies, we can say that thyroid function tests and thyroid autoantibodies should be checked before and during rituximab treatment.

Ethics

Informed Consent: It was obtained.

Authorship Contributions

Concept: H.D., Design: H.D., Supervision: H.D., Materials: H.D., Data Collection or Processing: B.C., Analysis or Interpretation: H.D., Literature Search: E.A., Writing: H.D., Critical Review: H.D.

Conflict of Interest: No conflict of interest was declared by the authors.

Financial Disclosure: The authors declared that this study received no financial support.

REFERENCES

1. Leget GA, Czuczman MS. Use of rituximab, the new FDA-approved antibody. Curr Opin Oncol. 1998; 10: 548-51.
2. Edwards JC, Szczepanski L, Szechinski J, Filipowicz-Sosnowska A, Emery P, Close DR, et al. Efficacy of B-cell-targeted therapy with rituximab in patients with rheumatoid arthritis. N Engl J Med. 2004; 350: 2572-81.
3. Cohen SB, Emery P, Greenwald MW, Dougados M, Furie RA, Genovese MC, et al. Rituximab for rheumatoid arthritis refractory to anti-tumor necrosis factor therapy: Results of a multicenter, randomized, double-blind, placebo-controlled, phase III trial evaluating primary efficacy and safety at twenty-four weeks. Arthritis Rheum. 2006; 54: 2793-806.
4. Shiroky JB, Cohen M, Ballachey ML, Neville C. Thyroid dysfunction in rheumatoid arthritis: a controlled prospective survey. Ann Rheum Dis. 1993; 52: 454-56.
5. Magnus JH, Birketvedt T, Haga HJ. A prospective evaluation of antithyroid antibody prevalence in 100 patients with rheumatoid arthritis. Scand J Rheumatol. 1995; 24: 180-2.
6. Dayan CM, Daniels GH. Chronic autoimmune thyroiditis. N Engl J Med. 1996; 335: 99-107.
7. Lee DM, Weinblatt ME. Rheumatoid arthritis. Lancet. 2001; 358: 903-11.
8. Cragg MS, Walshe CA, Ivanov AO, Glennie MJ. The biology of CD20 and its potential as a target for mAb therapy. Curr Dir Autoimmun. 2005; 8: 140-74.
9. Weetman AP, McGregor AM. Autoimmune thyroid disease: further developments in our understanding. Endocr Rev. 1994; 15: 788-830.
10. Yu S, Dunn R, Kehry MR, Braley-Mullen H. B cell depletion inhibits spontaneous autoimmune thyroiditis in NOD.H-2h4 mice. J Immunol. 2008; 180: 7706-13.
11. Raterman HG, Simsek S, Lems WF, Meesters EW, Dijkmans BA, Nurmohamed MT. Rituximab and thyroid function. Arch Intern Med. 2009; 169: 1073-4.
12. Romaldini JH, Biancalana MM, Figueiredo DI, Farah CS, Mathias PC. Effect of L-thyroxine administration on antithyroid antibody levels, lipid profile, and thyroid volume in patients with Hashimoto's thyroiditis. Thyroid. 1996; 6: 183-8.
13. Kahara T, Iwaki N, Kaya H, Kurokawa T, Yoshida T, Ishikura K, et al. Transition of thyroid autoantibodies by rituximab treatment for thyroid MALT lymphoma. Endocr J. 2011; 58: 7-12.
14. Tamura K, Shimaoka K, Friedman M. Thyroid abnormalities associated with treatment of malignant lymphoma. Cancer. 1981; 47: 2704-11.
15. Kaklamanos M, Thomas D, Pikazis D, Christaki S, Kaltsas G. The effect of rituximab on thyroid function and autoimmunity. Thyroid. 2013; 23: 1044-5.
16. Salvi M, Vannucchi G, Beck-Peccoz P. Potential utility of rituximab for Graves' orbitopathy. J Clin Endocrinol Metab. 2013; 98: 4291-9.
17. Vannucchi G, Campi I, Bonomi M, Covelli D, Dazzi D, Currò N, et al. Rituximab treatment in patients with active Graves' orbitopathy: effects on proinflammatory and humoral immune reactions. Clin Exp Immunol. 2010; 161: 436-43.

GMJ 2024;35:452-456

DOI: http://dx.doi.org/10.12996/gmj.2024.3866

Metal Complexes and Their Role in Treatment of the Arthritis

Metal Kompleksleri ve Artrit Tedavisindeki Rolleri

Ejaz Ali[1], Kanwal Ashiq[1,2], Manhaz Ghulam Nabi[1], Maria Gul[3], Mubashra Gul[3]

[1]University of the Punjab University College of Pharmacy, Lahore, Pakistan
[2]Superior University Faculty of Pharmacy, Lahore, Pakistan
[3]Riphah International University Faculty of Pharmacy, Lahore, Pakistan

ABSTRACT

Worldwide, rheumatoid arthritis is a major cause of morbidity and mortality. In recent years, the domain of inorganic medicinal chemistry has shown more interest in metal-based drugs owing to their beneficial pharmacological activities. Since then, many useful anti-cancer metal-based drugs have been introduced. However, less attention has been paid to improving inflammatory drugs based on metal complexes. The objective of this review is to recapitulate previously published studies that concentrated on metal-based drugs used for the treatment of arthritis. It is anticipated that the current compilation of earlier studies will be helpful for the researcher to find the data and areas for future studies. The literature survey was done without any time limit using the help of various electronic databases, including ScienceDirect, SpringerLink, Web of Science, PubMed, and the Cochrane Library. Articles published in the English language are used for the current review. Only 20 studies were found to be pertinent to the present review. Metal complexes of non-steroidal anti-inflammatory drugs have been the subject of extensive research. To date, metal complexes of drugs such as aspirin, ibuprofen, anthranilic acid, methotrexate, indomethacin, and aceclofenac have been studied and evaluated for their possible antiarthritic activity. Gold metal complexes showed better efficacy and have been used in clinical practice as well. Due to their advantageous therapeutic properties, metals and their complexes are becoming more and more important today. To find new treatments for diseases, it is suggested that the mechanism of action and potential toxicity of metal complexes must be assessed.

Keywords: Rheumatoid arthritis, metal complexes, inflammation, NSAIDs, DMARs

ÖZ

Dünya çapında; romatoid artrit, morbidite ve mortalitenin önemli bir nedenidir. Son yıllarda, yararlı farmakolojik aktiviteleri nedeniyle inorganik tıbbi kimya alanında metal bazlı ilaçlara daha fazla ilgi gösterilmektedir. O zamandan beri, birçok yararlı kanser karşıtı metal bazlı ilaç piyasaya sürüldü. Ancak metal komplekslerine dayalı enflamatuvar ilaçların geliştirilmesine daha az ilgi gösterilmiştir. Bu derlemenin amacı, artrit tedavisinde kullanılan metal bazlı ilaçlara odaklanan daha önce yayınlanmış çalışmaları özetlemektir. Daha önce yapılmış çalışmaların mevcut derlemesinin, araştırmacılara gelecekteki çalışmalar için veri ve alan bulmada yardımcı olacağı öngörülmektedir. Literatür taraması ScienceDirect, SpringerLink, Web of Science, PubMed ve Cochrane Kütüphanesi gibi çeşitli elektronik veri tabanları kullanılarak herhangi bir zaman sınırlaması olmaksızın gerçekleştirildi. Mevcut inceleme için İngilizce dilinde yayınlanan makaleler kullanılmıştır. Mevcut incelemeyle ilgili olarak yalnızca 20 çalışma bulunmuştur. Non-steroidal anti-enflamatuvar ilaçların metal kompleksleri kapsamlı araştırmaların konusu olmuştur. Bugüne kadar aspirin, ibuprofen, antranilik asit, metotreksat, indometasin ve aseklofenak gibi ilaçların metal kompleksleri olası antiartritik aktiviteleri açısından incelenmiş ve değerlendirilmiştir. Altın metal kompleksleri daha iyi etkinlik göstermiş ve klinik uygulamada da kullanılmaya başlanmıştır. Metaller ve bunların kompleksleri, sağlığa yararlı özelliklerinden dolayı günümüzde giderek daha fazla önem kazanmaktadır. Hastalıklar için yeni tedaviler bulmak için, metal komplekslerinin etki mekanizmasının ve potansiyel toksisitesinin değerlendirilmesi önerilmektedir.

Anahtar Sözcükler: Romatoid artrit, metal kompleks, enflamasyon, NSAIDs, DMARs

Address for Correspondence/Yazışma Adresi: Kanwal Ashiq, PhD, University of the Punjab University College of Pharmacy; Superior University Faculty of Pharmacy, Lahore, Pakistan
E-mail / E-posta: kanwal.ashiq@superior.edu.pk
ORCID ID: orcid.org/0000-0001-8193-5147

Received/Geliş Tarihi: 28.04.2023
Accepted/Kabul Tarihi: 16.03.2024

INTRODUCTION

Rheumatoid arthritis (RA) is a chronic inflammatory disease that usually affects the joints. It is caused by systemic autoimmunity, which destroys the joint lining and can have a negative impact on patient quality of life, such as undeviating disability, treatment financial burden, and premature death rates. According to estimation, 5 out of 1000 are victims of RA who might be presented with relentless joint damage and permanent disability (1-3). Flurbiprofen, ketoprofen, aceclofenac, diclofenac sodium, ibuprofen, diclofenac, sodium salicylate, magnesium salicylate, acetylsalicylic acid, indomethacin, phenylbutazone, salsalate, diflunisal, sulindac, nabumetone, tolmetin sodium salt dihydrate, piroxicam, naproxen, meloxicam, lornoxicam, chlorfenamic acid, etoricoxib, parecoxib, celecoxib, and ketorolac are the most frequently utilized non-steroidal anti-inflammatory drugs (NSAIDs). Dexamethasone, hydrocortisone, prednisolone, beclometasone dipropionate, betamethasone and methylprednisolone are the frequently used glucocorticoids. Disease-modifying antirheumatic drugs (DMARDs) prevent bone damage by diminishing synovial inflammation to control joint growth and increase rheumatoid factor and C-reactive protein. They have a healing impact on the joints, they are also linked to low white blood cell counts, rash, severe liver and kidney damage, and vomiting. DMARDs, including auranofin, azathioprine, cyclophosphamide, D-penicillamine, methotrexate, sulfasalazine, hydroxychloroquine, and leflunomide, are usually used (4,5). New therapeutic modalities have dramatically changed how RA progresses. Although some patients do not respond well to treatment, many achieve remission if they are recognized early and receive adequate and consistent care. Early diagnosis, a treat-to-target strategy, and meticulous monitoring and management can increase the likelihood of remission in RA patients (6-8). Metals are frequently used in medicine and/or as diagnostic tools. Over the past 5,000 years, several human ailments have been treated using metals including iron, gold, and arsenic. There are now several medications with metals as ingredients. These materials contain a wide variety of metals, many of which are toxic to humans and can target DNA and/or proteins (9,10). Metal complexes have long been used in medicine to identify and treat various ailments. The discipline is undertaking a prototype modification; in the past, the major mechanism of action was examined after the discovery of a beneficial molecule; however, today, the mechanism of action is progressively employed to drive the innovation procedure. This method exploits the unique features of metal complexes, which can be modified to improve the metal compound's drug-like effects (11,12).

Recently, researchers have concentrated their attention on producing metal-based complexes to generate possible multi-targeted medicines due to the potential medical applications of metal complexes. This review's goal is to provide an overview of previously published research on arthritic treatments based on metal-based drugs. The literature was searched in the English language without any year limit using the help of various electronic databases, including ScienceDirect, SpringerLink, Web of Science, PubMed, and the Cochrane Library.

Metal Complexes of Drugs for the Treatment of Arthritis

Copper-Aspirin Metal Complex

NSAIDs are widely used to treat inflammatory disorders. Among NSAIDs class of the drugs, aspirin is commonly devoured to treat various inflammatory conditions, including arthritis. Aspirin causes a non-selective irremediable inhibition of the cyclooxygenase enzymes (COX-1 and COX-2) and, in return, blocks the synthesis of prostaglandin, which is essential to provoke an inflammatory response. COX-1 is found in many tissues, such as in the mucosa of the gastrointestinal tract, and it produces important prostaglandins. These prostaglandins exert cytoprotective effects by secreting mucus and protecting the stomach mucosa from the harmful effects of gastric hydrochloric acid. While COX-2 is turn out to be up-regulated in response to various inflammatory modulators that lead to the appearance of many symptoms of inflammatory disorders, such as RA and osteoarthritis. Hence, to treat inflammatory disorders it is recommended that COX-2-selective inhibitors should be used to avoid gastric ulceration and irritation (13,14). An attempt was made by researchers to bypass the harmful effects of aspirin by making its metal complex. This study proved that Cu-aspirin exhibited considerable inhibition of macrophages activated COX-2-mediated prostaglandin E_2 synthesis in contrast to aspirin. Further, the Cu-aspirin selectivity index was found to be 3.33 for COX-2 over COX-1 when compared to the selectivity index of aspirin which was 0.42. The outcome of the investigation demonstrated that the Cu-aspirin complex was seven times more selective for COX-2 than aspirin. The selective inhibition of the COX-2 by Cu-aspirin complex can be ascribed to the steric properties of the drug-metal complex and its interactions with inflammatory enzymes. Aspirin is a small molecule that can fit completely at cyclooxygenase enzymes (both COX-1 and COX-2) binding sites, which results in the non-selective inhibition of the enzyme. In contrast, selective COX-2 inhibitors like rofecoxib and celecoxib, have a bulky side chain of sulfanilamide in their structure, which prevents their interaction with the COX-1 enzyme. For the same reason, it is suggested that the Cu-aspirin complex is quite large compared with aspirin, which is why the drug-metal complex selectively inhibits COX-2. Further, aspirin, CuSO4, and the Cu-aspirin complex was tested in a control experiment. The results have shown that among all the tested chemicals, drug-metal complex exhibited an influential inhibition of COX-2 then CuSO4 and aspirin alone (15,16).

Metal Complexes of Anthranilic Acid

Iqbal et al. (17), reported that synthesis of transition metals Fe(II), Co(II), Mn(II), Ni(II), and Zn(II) with anthranilic acid and aldoses, whose description was done by different parameters. In an *in vivo* study, Mn(II) and Zn(II) complexes were administered in rats by oral route to assess the anti-inflammatory response in kaolin-induced paw edema. The COX-2/COX-1 selectivity index values were 0.34 to 0.52 and were similar to aspirin 7 values (0.41) (16,17).

Zinc-Aceclofenac Metal Complex

Kale et al. (18) conveyed that in 1992, the US FDA permitted aceclofenac, which was developed to overawe the un-wanted side effects associated with diclofenac. Gastric ulcer is still prevalent with aceclofenac, and to overcome this effect, zinc ions are most

best pronounced. The zinc ion has inherent antiarthritic activity, as well as a shield stomach. On this basis, an aceclofenac zinc complex was prepared. According to the findings of the *in vitro* hydrolysis investigation, the complex was more stable at acidic pH in the stomach than at alkaline pH in the intestine. The complex have anti-inflammatory effects as demonstrated by *in silico* analysis conducted using the Prediction of Activity Spectra of Substances software. This hypothesis was supported by an experiment on carrageenan-induced rat paw edema, the results of which included a decrease in the ulcer index and efficacy comparable to that of the parent medication. As a result, the aceclofenac-zinc complex and its derivatives can be used as anti-inflammatory agents as well as to treat ulcers (18).

Cobalt and Copper Metal Complexes of Mefenamic Acid

Cobalt (II) complexes with mefenamic acid have been created and studied, both with and without nitrogen donor heterocyclic ligands. Mefenamic acid appeared to function as a diprotonated monodentate ligand coupled to Co (II) ion, according to the experimental findings. CT-DNA can be bound by these metal complexes. When ethidium bromide and the complexes were evaluated in terms of how they bound to CT DNA, it became clear that the latter might outcompete the former by intercalating. These complexes can couple with human and bovine serum albumin, and complex 3 has the highest binding constant. Antioxidant activity is measured by their ability to repel reactive oxygen species (19). Cu-mefenamic acid complexes were also developed, characterized, and investigated. These complexes exhibited anti-inflammatory activity through interaction with CT-DNA. These complexes can effectively bind to albumin, and when reaching the target site, these complexes can easily dissociate (20).

Metal Complexes of Indomethacin

The inherent side effects of NSAIDs can be masked by the addition of beneficial effects by making a complex with the transition metals chromium and nickel. These complexes were screened for central, peripheral, and anti-inflammatory activity to identify potential pharmacological properties. 67.03% writhing inhibition and potent analgesic action was observed by nickel-indomethacin complex at a dose of 20 mg/kg. The anti-inflammatory profile of these compounds was conducted at 15 mg/kg dose, at 2 hr. inhibition of paw edema to 78.35% and 73.23%, respectively, which is comparable to the control indomethacin. Based upon the results, it can be expected that the chromium and nickel complexes of indomethacin have potential pharmacological effects that can be further verified by rigorous analysis (21,22).

Gold Metal Complexes

Various gold compounds of clinical importance, such as auranofin, solganal, and myochrysine, are being used in the treatment of arthritis. The indecisive picture about its innards procedure, it is assumed that its anti-inflammatory effects are due to certain reasons; gold(I), [Au(CN)2], or Au(III) are metabolites in the cell that can lead to the obsession of the selenium enzyme thioredoxin reductase. Auranofin is a new contender for the treatment of inflammation, cancer, and microbial infections because it inhibits inflammatory pathways and thiol redox enzymes (23).

Methotrexate Conjugated Gold Nanoparticles

Efficient drug delivery and therapeutic efficacy are the major interest of nanoparticles. The recent period is about nanoparticles, so methotrexate conjugated to gold nanoparticles (MTX-GNP), which have better antiarthritic potential than methotrexate alone in treating arthritis in experimental animal models. MTX-GNP was prepared by the adsorption method, and the particles formed were of 20-30 nm. The MTX-GNP was evaluated for its antiarthritic properties by studying urinary and serum parameters such as hydroxyproline, glucosamine, pyridoxine deoxypyridoxine, and serum cytokines. It has been revealed that MTX-GNP showed significant antiarthritic potential based on urinary and serum parameters than methotrexate alone. Therefore, it can be concluded that MTX-GNP has a better therapeutic advantage than MTX alone in the treatment of arthritis. A further detailed study is required on MTX-GNP (24).

Metal Complexes of Diclofenac

The most frequently prescribed therapeutic agents for RA are NSAIDs. Among the distinguished NSAIDs, diclofenac, a fenamic acid derivative, is generally administered due to its potency against pain and swelling in patients with RA. The synthesis of nociceptive prostaglandins in synovial tissue and blood and substance P, a pro-inflammatory neuropeptide, is inhibited by DCs, making it useful for the treatment of RA (25). Cobalt (II) diclofenac complexes were produced and categorized by chemical and spectroscopic analyses along with X-ray diffraction and thermal methods. The crystal structure was confirmed by spectroscopic and thermal data. The cobalt (II) coordination sphere has an octahedral structure with four waters and two diclofenac molecules. A polymeric chain extends down the crystal axis when an apical water molecule links two neighboring cobalt (II) ions. Compound 1 showed greater activity than diclofenac sodium, as revealed in the antioxidant activity experiments. The lower action of diclofenac sodium specifies that DPPH's lone pair of electrons most probably react with cobalt ions rather than sodium. The past investigations have shown comparable results (26). The interaction of [Cu(dicl)2(H_2O)2] (1), the copper(II) diclofenac complex, with the ligands N,N,N′,N′-tetramethylethylene-diamine (temed), propane-1,3-diamine (pn), ethylenediamine (en), unsymmetrical dimethylethylene-diamine (unsym-dmen), in methanol-water (4:1 v/v) produced the unique copper(II) complexes[Cu(temed)(dicl)2](2), [Cu(pn)2(H_2O)2](dicl)2·2H_2O(3), [Cu(en)2(H_2O)2](dicl)2·2H_2O(4) [Cu(unsym-dmen)2(H_2O)](dicl)2·H_2O_5), correspondingly. Spectroscopic (UV-vis, FT-IR) procedures were used to characterize each manufactured complex. The structures of complexes 2, 3, and 5 were explicitly discovered using single-crystal X-ray crystallography. The results exposed the ionic structures of complexes 4, 5 and the covalent structure of complex 2, and density functional theory calculations were used to improve the geometry of complex 3. The ability to bind to calf-thymus DNA of complexes 1-5 was observed through competitive studies with ethidium bromide and *in vitro* through cyclic voltammetry, viscosity measurements, and UV-vis spectroscopy. Fluorescence emission spectroscopy was utilized to find the interaction of complexes 1-5 with bovine serum albumin *in vitro* and the binding constants evaluated. The biological behaviors of complexes (1-5) was compared to those of previously described diclofenac complexes with Ni(II), Cu(II), and Mn(II). Complexes's (1-

5) current *in vitro* results with regard to their binding to CT-DNA and BSA might be encouraging for further biological study and their potential use as metallo-pharmaceutical compounds (27).

Ibuprofen and Naproxen Metal Complexes

Zinc can modify the body's natural defense mechanisms and is an effective antioxidant and anti-inflammatory agent. Zinc's role in accelerating wound healing, including ulcers, is widely accepted. The most extensively prescribed and utilized medicines are NSAIDs because of their several indications and widespread availability. Long-term and excessive use of NSAIDs can cause gastrointestinal impairment. As a result, in recent decades, increasing the curative indications of prevailing medicines has been top precedence. The metal complexes of NASAIDs have gotten a lot of attention in this area. The purpose of this research is to see how zinc complexation affects the naproxen and ibuprofen's ulcer-causing and anti-inflammatory effects in rats following intragastric injection. Anti-inflammatory activity was tested in male albino Wistar rats with inflammatory edema in the hindpaw initiated by carrageenan. In contrast to the control groups, both the complexes [zinc-naproxen and zinc-ibuprofen (20 mg/kg naproxen and ibuprofen)], as well as combinations with zinc hydroaspartate (in doses 14.37 and 16.05 mg/kg), and paternal drugs resulted in a substantial decrease in edema. After a single administration, there were insignificant statistical variations between the studied drugs. In contrast to control groups and parent NSAIDs, triple intragastric injection of the naproxen-ZHA and ibuprofen-ZHA mixture significantly improved anti-inflammatory action. Animals receiving ZHA and naproxen after 2 hours of carrageenan administration showed the most significant anti-inflammatory activity. Compared with the control group, these animals had 80.9 percent less edema. Ulcerations caused by parent NSAIDs were lessened by both mixtures of zinc hydroaspartate and zinc complexes combined with NSAIDs. However, following triple administration, the zinc hydroaspartate combinations of naproxen and ibuprofen were the minimum harmful. Based on these findings, by lowering the efficacious dosage of the paternal medicine while boosting its efficacy, zinc supplementation during NSAID treatment may assist to prevent and repair ulcers (28).

An innovative Zn (II)-naproxen combination [Zn(nap)2(dap)] has been synthesized. 1H NMR spectroscopy, elemental analysis, UV-Vis spectroscopy, and FT-IR were used to characterize the compound, which contained a 1,3-diamino propane ligand. X-ray crystallography was used to verify its single-crystal structure. *In vivo*, the Zn (II)-naproxen compound was tested for analgesic, ulcerogenic, and anti-inflammatory properties, as well as in vitro for antibacterial and antifungal properties. After 3 hours, the complex had a 57.8% edema inhibition rate, a 71 percent pain inhibition rate, and 8±1 as an ulcer index. The antioxidant and antibacterial actions of Zn(II)-Naproxen compound also examined and were found to be superior to naproxen (29).

Tenoxicam Metal Complexes

NSAIDs from the oxicam family, the most often used of which is tenoxicam, are one of the treatments for arthritis (30) and utilized to get rid of pain and swelling due to RA. TNX complexes of palladium(II), platinum(II), zinc(II), and copper(II) were produced in this study. They were characterized by analytical and instrumental procedures including differential thermal analysis, thermogravimetric analysis, UV-visible, inductively coupled plasma-optical emission spectrometry, and liquid chromatography-mass spectrometry. The complex FTIR spectra were calculated, and the results were reinforced by density functional theory calculations. [Pd(TNX)Cl2], [Pt(TNX)2], [Zn(TNX)2] and [Cu (TNX)2] are the proposed structures of these metal complexes. For the first time, the anti-inflammatory properties of the manufactured complexes were determined in comparison to the medication. The production of Tumor necrosis factor-alpha (TNF-α), a pro-inflammatory cytokine, was reduced more efficiently by metal complexes of the TNX as compared to tenoxicam alone. [Cu (TNX)2] exhibited the maximum anti-inflammatory activity. Molecular docking calculations showed the interactions amongst TNF-α and TNX complexes were of receptor-ligand type (31).

Folic Acid Conjugated Silver Nanoparticles

The origin of RA involves the invasion of inflammatory cells, particularly M1 macrophages that release a range of inflammatory cytokines. M1 macrophages should be removed/converted to the M2 phenotype (anti-inflammatory) to alleviate synovial inflammation. FA-AgNPs are folic-acid-based silver nanoparticles that can selectively transport into M1 macrophages. Effective RA treatment, they collaboratively decrease M1 macrophages and the polarization of M2 macrophages. The silver nanoparticles were simply made and then FA-modified to better comprehend M1 macrophage-focused transport through overexpressed folate receptors on their surface. FA-AgNPs melted after entering cells and freed Ag^{+} in reaction to intracellular glutathione, which is the main component for anti-inflammatory activities and hence helps in the management of RA. In high-biosafety mouse RA models, these nanoparticles may possibly gather into swollen joints, allowing for effective anti-inflammatory action and good healing. The body eventually rid itself of FA-AgNPs after treatment predominantly through feces, with no tissue accumulation and no long-term toxicity observed. This thesis is the first to apply bidirectional communication. The potential of folic acid-silver nanoparticles for RA treatment is highlighted in this study, which is the first study to use bioactive nanoparticles without the use of medicines (32).

CONCLUSION

Nowadays, the importance of metals and their complexes is increasing due to their beneficial therapeutic properties. However, little work has been reported previously on anti-arthritic metal complexes. It is suggested that the mechanism of action and possible toxicity of metal complexes must be evaluated to discover novel treatments against deadly ailments.

Ethics

Author Contributions

Concept: E.A., K.A., M.G.N., Ma.G., Mu.G., Design: E.A., K.A., M.G.N., Ma.G., Mu.G., Data Collection or Processing: E.A., K.A., M.G.N., Ma.G., Mu.G., Analysis or Interpretation: E.A., K.A., M.G.N., Ma.G., Mu.G., Literature Search: E.A., K.A., M.G.N., Ma.G., Mu.G., Writing: E.A., K.A., M.G.N., Ma.G., Mu.G.

Conflict of Interest: No conflict of interest is declared by the authors.

Financial Disclosure: The authors declared that this study received no financial support.

REFERENCES

1. Aletaha D, Smolen JS. Diagnosis and Management of Rheumatoid Arthritis: A Review. JAMA. 2018; 320: 1360-72.
2. Ashiq K, Bajwa MA, Tanveer S, Qayyum M, Ashiq S, Khokhar R, et al. A comprehensive review on gout: The epidemiological trends, pathophysiology, clinical presentation, diagnosis and treatment. J Pak Med Assoc. 2021; 71: 1234-8.
3. Ashiq K, Ashiq S, Shehzadi N. Hyperuricemia and its association with hypertension: risk factors and management. Pak Heart J. 2022; 55: 200-1.
4. Zhou S, Zou H, Chen G, Huang G. Synthesis and Biological Activities of Chemical Drugs for the Treatment of Rheumatoid Arthritis. Top Curr Chem (Cham). 2019; 377: 28.
5. Ashiq K, Ashiq S, Shehzadi N, Hussain K, Khan MT. Prevalence and Control of the Hypertension in Patients Suffering from Rheumatoid Arthritis. Pak Heart [Internet]. 2024; 55: 421-2.
6. Burmester GR, Pope JE. Novel treatment strategies in rheumatoid arthritis. Lancet. 2017; 389: 2338-48.
7. Ashiq K, Latif A, Ashiq S, Sundus A. A systematic review on the prevalence, pathophysiology, diagnosis, management and treatment of gout (2007-2018). GSC Biological and Pharmaceutical Sciences. 2018; 5: 50-5.
8. Cirri D, Fabbrini MG, Pratesi A, Ciofi L, Massai L, Marzo T, et al. The leading established metal-based drugs: a revisitation of their relevant physico-chemical data. Biometals. 2019; 32: 813-7.
9. Colotti G, Ilari A, Boffi A, Morea V. Metals and metal derivatives in medicine. Mini Rev Med Chem. 2013; 13: 211-21.
10. Barry NP, Sadler PJ. Challenges for metals in medicine: how nanotechnology may help to shape the future. ACS Nano. 2013; 7: 5654-9.
11. Boros E, Dyson PJ, Gasser G. Classification of Metal-based Drugs According to Their Mechanisms of Action. Chem. 2020; 6: 41-60.
12. Ashiq K, Naureen B, Ashiq S. Metal complexes and their potential therapeutic role against COVID-19: recent developments in drug designing. Sudan J Med Sci. 2021; 16: 540-5.
13. Jahnavi K, Reddy PP, Vasudha B, Narender B. Non-steroidal anti-inflammatory drugs: an overview. J Drug Deliv Ther. 2019; 9: 442-8.
14. Ngo SN, Addison CJ. Are COX-2 selective NSAIDs associated with less GI, renal, and cardiovascular side effects: evidence from animals treated with NSAIDs. Annual Res Rev Bio. 2018: 1-8.
15. Yun Y, Chen P, Zheng CL, Yang Y, Duan WG, Wang L, et al. Copper-aspirin complex inhibits cyclooxygenase-2 more selectively than aspirin. Yakugaku Zasshi. 2007; 127: 1869-75.
16. Leung CH, Lin S, Zhong HJ, Ma DL. Metal complexes as potential modulators of inflammatory and autoimmune responses. Chem Sci. 2015; 6: 871-84.
17. Iqbal MS, Khurshid SJ, Muhammad B. Anti-inflammatory and selective COX-2 inhibitory activities of metal complexes of Schiff bases derived from aldoses. Med Chem Res. 2013; 22: 861-8.
18. Kale MA, Shelke R, Nawale RB. Zinc-aceclofenac complex: synthesis, hydrolysis study and antiinflammatory studies. Antiinflamm Antiallergy Agents Med Chem. 2014; 13: 36-44.
19. Dimiza F, Papadopoulos AN, Tangoulis V, Psycharis V, Raptopoulou CP, Kessissoglou DP, et al. Biological evaluation of non-steroidal anti-inflammatory drugs-cobalt(II) complexes. Dalton Trans. 2010; 39: 4517-28.
20. Sharma RP, Kumar S, Venugopalan P, Ferretti V, Tarushi A, Psomas G, et al. New copper (II) complexes of the anti-inflammatory drug mefenamic acid: a concerted study including synthesis, physicochemical characterization and their biological evaluation. RSC Adv. 2016; 6: 88546-58.
21. Sukul A, Haque S, Poddar SK, Hossain MS, Niloy KK, Saha SK. Comparative physicochemical, anti-inflammatory, and analgesic activity assay of synthesized chromium and nickel complexes of indomethacin. Cogent Chem. 2017; 3: 1302312.
22. Lucas S. The pharmacology of indomethacin. J Headache Pain. 2016; 56: 436-46.
23. Madeira J, Gibson D, Kean W, Klegeris A. The biological activity of auranofin: implications for novel treatment of diseases. Inflammopharmacol. 2012; 20: 297-306.
24. Gomes A, Datta P, Sengupta J, Biswas A, Gomes A. Evaluation of anti-arthritic property of methotrexate conjugated gold nanoparticle on experimental animal models. J Nanopharm Drug Deliv. 2013; 1: 206-11.
25. Battu S, Yalavarthi PR, Gv SR, Radhakrishnan S, Thummaluru RMR, Konde A. Biopharmaceutical Process of Diclofenac Multi-particulate Systems for Chronotherapy of Rheumatoid Arthritis. Turkish J Pharm Sci. 2018; 15: 256.
26. Gacki M, Kafarska K, Wolf WM. A supramolecular polymeric chain in the cobalt (II) complex with diclofenac: Synthesis, crystal structure, spectroscopic, thermal and antioxidant activity. J Coord Chem. 2019; 72: 3481-94.
27. Kumar S, Sharma RP, Venugopalan P, Ferretti V, Perontsis S, Psomas G. Copper (II) diclofenac complexes: Synthesis, structural studies and interaction with albumins and calf-thymus DNA. J Inorganic Biochem. 2018; 187: 97-108.
28. Jarosz M, Szkaradek N, Marona H, Nowak G, Młyniec K, Librowski T. Evaluation of anti-inflammatory and ulcerogenic potential of zinc–ibuprofen and zinc–naproxen complexes in rats. Inflammopharmacol. 2017; 25: 653-63.
29. Chu YC, Wang TT, Wang LJ, Luo QY, Jia R, Hong TC, et al. Synthesis, characterization, and biological evaluation of a novel Zn (II)-Naproxen complex. Polyhedron. 2019; 163: 71-6.
30. Adam AMA. Ca (II), Sr (II) and Ba (II) ion interaction with the rheumatoid arthritis drug tenoxicam: Structural, thermal, and biological characterization. Applied Organometallic Chem. 2018; 32: e4055.
31. Muslu H, Kalaycıoğlu Z, Erdoğan T, Golcu A, Erim FB. Synthesis, characterization, anti-inflammatory evaluation, molecular docking and density functional theory studies of metal based drug candidate molecules of tenoxicam. Results Chem. 2021: 100111.
32. Yang Y, Guo L, Wang Z, Liu P, Liu X, Ding J, et al. Targeted silver nanoparticles for rheumatoid arthritis therapy via macrophage apoptosis and Re-polarization. Biomaterials. 2021; 264: 120390.

GMJ 2024;35:457-466

DOI: http://dx.doi.org/10.12996/gmj.2024.4182

Revolutionizing Ophthalmic Care: The Impact of Artificial Intelligence

Oftalmolojik Bakımda Devrim: Yapay Zekanın Etkisi

L. Subha[1], Atul Sharma[2], Anita Misra[3]

[1]Department of Ophthalmology, Sree Balaji Medical College and Hospital, Chennai, India
[2]Department of Ophthalmology, Padma Eye Care Center, Jabalpur, India
[3]Department of Ophthalmology, S.C.B Medical College and Hospital, Cuttack, India

ABSTRACT

Progress in digital health and telemedicine has brought forth instruments can enhance the accessibility and efficacy of eye care services. Current research shows how technology-enabled approaches are changing the way care is provided. Traditional diagnostic methods rely on physician expertise, resulting in high misdiagnosis rates and data inefficiency. Integrating ophthalmology with artificial intelligence (AI) promises to overhaul current diagnostic approaches, potentially making a significant clinical impact. Deep learning, an emerging facet of machine learning (ML), can uncover complex data structures without explicit rule specifications. The review centers on the revolutionary potential of AI in the identification and treatment of ocular disorders, such as diabetic retinopathy, degenerative maculopathy, retinal diseases, corneal diseases, anterior ocular region issues, and glaucoma. It explores AI-driven advancements in image analysis, pattern recognition, and ML techniques for individualized treatment plans, early diagnosis, and categorization. The difficulties with data standards, interpretability, and integration are discussed in this paper into clinical practice. It also emphasizes the potential of AI to enhance screening efficiency, reduce physician workload, and improve patient outcomes in ocular pathologies.

Keywords: Deep learning, glaucoma, diabetic retinopathy, ophthalmology, artificial intelligence, degenerative maculopathy

ÖZ

Dijital sağlık ve tele-tıp alanındaki ilerlemeler, göz bakımı hizmetlerinin erişilebilirliğini ve etkinliğini artırabilecek araçların ortaya çıkmasını sağladı. Güncel araştırmalar, teknoloji destekli yaklaşımların bakımın sağlanma biçimini nasıl değiştirdiğini gösteriyor. Geleneksel tanı yöntemleri hekim uzmanlığına dayandığından yanlış tanı oranları yüksek ve veri yetersizliği fazladır. Oftalmolojinin yapay zeka (YZ) ile bütünleştirilmesi, mevcut tanı yaklaşımlarını baştan aşağı değiştirmeyi ve önemli bir klinik etki yaratmayı vadediyor. Makine öğreniminin (ML) yeni ortaya çıkan bir alanı olan derin öğrenme, açık kural tanımlamaları olmadan karmaşık veri yapılarını ortaya çıkarabilir. Derlemede, diyabetik retinopati, dejeneratif makülopati, retina hastalıkları, kornea hastalıkları, ön göz bölgesi sorunları ve glokom gibi göz bozukluklarının tanımlanması ve tedavisinde YZ'nin devrim niteliğindeki potansiyeli ele alındı. Kişiye özel tedavi planları, erken tanı ve kategorizasyon için görüntü analizi, desen tanıma ve ML tekniklerindeki YZ destekli gelişmeleri araştırıyor. Bu makalede veri standartları, yorumlanabilirlik ve klinik uygulamaya entegrasyondaki zorluklar tartışılmaktadır. Ayrıca YZ'nin tarama verimliliğini artırma, hekim iş yükünü azaltma ve göz patolojilerinde hasta sonuçlarını iyileştirme potansiyeline de vurgu yapılıyor.

Anahtar Sözcükler: Derin öğrenme, glokom, diyabetik retinopati, göz hastalıkları, yapay zeka, dejeneratif makulopati

INTRODUCTION

Artificial intelligence (AI) uses computer algorithms to imitate the human intellect, which is becoming increasingly common in medicine. AI in medicine enables rapid and accurate analysis of medical data, which is beyond the ability of human doctors. Machine learning (ML), a subset of AI, adapts its parameters based on data to generate computer algorithms for making predictions and responding to data. The integration of AI is particularly advantageous in ophthalmology, where the field's extensive use of digital imaging techniques made many modalities to be used

Address for Correspondence/Yazışma Adresi: Anita Misra, MD, Department of Ophthalmology, S.C.B Medical College and Hospital, Cuttack, India
E-mail / E-posta: misraanita13@gmail.com
ORCID ID: orcid.org/orcid.org/0009-0000-5694-2126

Received/Geliş Tarihi: 02.04.2024
Accepted/Kabul Tarihi: 04.06.2024

together with quantifiable parameters such as visual acuity or foveal thickness. A significant dataset is made available by the growth of multi-modal digital images and electronic medical databases in ophthalmology for AI analysis. ML, which was originally introduced by Arthur Samuel in 1959, refers to an AI process in which a machine autonomously generates its programing and acquires the ability to execute tasks independently (1). In supervised ML models, the machine learns from pre-existing data containing accurate answers, making it particularly valuable for classification purposes, whether dealing with categorical values like "disease" or "no disease" or variables that may take on any value within a range, such as height or weight (2). The process involves utilizing a validation dataset to assess external validity. Conversely, unsupervised ML involves examining data without predefined answers, with the primary objective of modeling the data structure or distribution to gain insights. This method is especially useful for identifying associations among data. The integration of the capabilities of human doctors with those of deep learning (DL) algorithms is anticipated to reduce mistakes in diagnoses and therapies inherent in the existing systems (3,4). These models provide more accurate recommendations from basic eye care services provided in the community to professional ophthalmologists, ultimately optimizing diagnosis. Tele ophthalmology has significantly contributed to enhancing the availability of eye screening and facilitating distant expert evaluations in rural areas. This can be achieved via synchronous and mixed synchronous-asynchronous solutions (5) or "store, forward and video consultation" methods (6). However, despite the improved clinical outcomes shown by digital ophthalmology solutions, their growth potential is constrained by the need for more infrastructure and professionals to implement them. Unlike telemedicine and AI, which are not restricted to specific locations (such as to address the demand for eye hospitals that specialize in certain eye conditions or the availability of knowledgeable eye care professionals), these solutions may be combined with other technological advancements, such as imaging apparatus, to effectively deliver and improve primary care and eye screening services. Given the documented relationships between clinical features and disease severity in major eye issues, AI is particularly well-suited for use in eye screening. Early detection and treatment of ocular conditions are critical for preventing visual impairment and improving the general quality of life. Traditional diagnostic approaches rely heavily on doctors' expertise and limited expertise, leading to a significant occurrence of misdiagnosis and ineffective use of medical data. Integrating AI with ophthalmology can transform the disease diagnosis paradigm, yielding substantial clinical benefits. DL, an emerging facet of ML, can reveal intricate patterns within datasets without requiring explicit rule specifications. DL algorithms automatically learn the features of input data in an unsupervised manner, eliminating the need for manual segmentation and depiction of lesion areas (7). However, the training of DL algorithms requires a large dataset. Transfer learning involves retraining an algorithm that has undergone pretraining on many generic images, particularly on a focused dataset, and transferring the same for diagnosis usage. This methodology allows for a precise model with comparatively few training datasets. Heat maps can be used to identify pixels that impact image-level predictions. This method is particularly useful in the medical industry because heat maps help visualize and identify probable aberrant regions in input images. These regions can then be further reviewed and analyzed (8,9). This feature can provide immediate verification of computerized diagnoses during patient treatment. Several established DL techniques include convolutional neural networks (CNN), deep boltzmann machines, deep kernel machines, deep recurrent neural networks (NN), and models of both short-term and long-term memory.

AI's Importance in Ophthalmology

Over the last 5 to 10 years, advancements in computing ability and the accessibility of extensive datasets and the development of DL have been driven by AI. Recent research utilizing advanced AI methodologies, including DL, has demonstrated robust outcomes, surpassing human performance in various domains in medicine and healthcare. Unlike traditional ML methods, which require expert eye doctors to annotate specific clinical characteristics in images for AI model development (referred to as "supervised learning"), DL employs a different approach known as "unsupervised learning." DL eliminates the need for individual feature labeling by training the model on complete images annotated by professionals with clinical diagnosis or disease severity. This enables AI to generate norms by autonomously learning discriminative features to classify diagnoses or severity. When it comes to classifying ophthalmic imaging data-such as color fundus photography (CFP), which is used to identify various eye disorders like diabetic retinopathy (DR)-DL algorithms have demonstrated clinically acceptable performance. Compared to 2-dimensional CFPs, optical coherence tomography (OCT) imaging provides comprehensive 3-dimensional data, which can enhance the efficacy of existing CFP-based screening techniques. Finding retinal characteristics that match common eye disorders like glaucoma, age-related macular degeneration (AMD), and DR (10,11), and predict AMD progression using OCTs (12), as well as classifying glaucoma using ophthalmic imaging (13,14). These advancements mistake rates that are lower than generally acknowledged signify the promising role of DL in revolutionizing the field of ophthalmology. Despite the positive findings in research studies regarding the impressive performance of DL in clinical validation, there is a need for more investigations assessing its practical applications in real-world utilization. The concept of a "fully automated model" implies a system that operates independently without human provider or participation because the AI system itself takes the initiative to refer patients to ophthalmologists when necessary or to identify individuals suitable for ongoing community-based monitoring. On the other hand, a "semi-automated model" encompasses various scenarios involving human graders or ophthalmologists, collaborating with the DL to enhance patient classification and serving as a tool for triaging individuals. DL algorithms relying on AI can be incorporated into a "semi-automated model", wherein a human evaluator (such as a doctor or optometrist) intervenes in categorizing imaging data identified as abnormal by the AI. The computer-based machine learning (CML) methods used in AI diagnosis include decision trees, random forests (RF) (15), support vector machines (SVM) (16), Bayesian classifiers (17), k-nearest neighbors (18), k-means (19), linear discriminant analysis (20), and NN (21). Within this array, RF and SVM stand out as the most frequently employed CML technologies in the field of ophthalmology. DL, an emerging ML technology, possesses the capability to uncover intricate structures

within datasets without the necessity of explicitly specifying rules. DL algorithms autonomously learn features from unsupervised input data, eliminating the need for manual segmentation and depiction of lesion areas. Training the DL algorithm demands a substantial dataset. Transfer learning involves retraining an algorithm previously trained on a vast array for a dataset of diverse photos/images (22). This approach enables the creation of a very precise model even when using a relatively small training sample. Heat maps provide the potential to unveil the individual pixels that contribute to predictions made at the picture level. Within medicine, this visualization technique can accurately identify and highlight areas in the input picture that may be considered aberrant. This, in turn, makes it easier for medical professionals to evaluate and analyze these regions further. At the point of service, it might help with the instantaneous clinical validation of computerized diagnoses. Numerous techniques are used in DL, including CNN, deep Boltzmann machines, deep kernel machines, deep recurrent NN, and long- and short-term memory. A variety of CML techniques, such as decision trees, RF, support SVM, Bayesian classifiers, k-nearest neighbors, k-means, linear discriminant analysis, and NN, are used in the field of ophthalmology for AI diagnosis. The two CML technologies most frequently applied in the field of ophthalmology are RF and SVM Figure 1.

Diabetic Retinopathy

DR screening is essential for allowing early detection and treatment, which averts vision loss. AI has been investigated in the identification of DR using a variety of imaging modalities, such as OCT pictures, ultra-widefield (UWF) imaging, and even smartphone retinal photographs. The intraretinal fluid shown in OCT scans can be precisely identified by CNNs. With its ability to view up to 200° of the fundus, UWF imaging may be able to detect more peripheral diabetes conditions. The scarcity of imaging equipment and restricted accessibility are obstacles to efficient DR screening. An impressive solution is an offline AI system that runs on a smartphone and has a high accuracy in recognizing severe DR (23). In an effort to address this worldwide health issue, AI has been used to predict the risk of DR and its progression in people with diabetes. Recognizing particular irregularities, such as macular edema (24-27), With CML, exudates, microaneurysms, and neovascularization on the optic disk are made possible. To guarantee prompt attention and intervention, a system that focuses on rapid and effective proliferative DR detection has been created (28). DR identification was made possible by Gulshan et al.'s (24) groundbreaking work, which used DL and massive fundus imaging datasets to train a deep CNN. Using supervised learning, a deep CNN is trained. According to their research, DL methods have a high sensitivity and specificity and can identify referable DR with a great degree of accuracy (29). Furthermore, a CML-based computer-aided diagnostic (CAD) system that makes use of OCT angiography images was employed. It successfully identified non-proliferative DR with high accuracy automatically Figure 2.

Degenerative Maculopathy

Degenerative maculopathy is a prevalent contributor to vision impairment, affecting million individuals globally. Timely identification and intervention can significantly mitigate the risk of vision loss. Given the substantial impact of the disease, AI holds the potential to facilitate widespread screening through the analysis of retinal images and OCT, doing away with the requirement for in-person evaluations. The advancement of this domain has traces its origins from ML, utilizing datasets comprising fewer than 1000 images to the current state of a collection of more than 490,000 photos; the dataset demonstrates impressive sensitivity and specificity (30). Feeny et al. (31) developed a DL technique to identify abnormalities using over 130,000 pictures from 4,613 patients automatically. Their DL system had a remarkable accuracy rate of 92% in identifying persons with intermediate and advanced stages of diabetes mellitus. This was achieved using DL techniques, including examination of optical OCT, fundus pictures, and OCT angiography images, which improved the accuracy (32). A fluid volume measurement technique for neovascular diabetic macular edema patients has been created using AI. This efficiently tracks the favorable response to medical intervention. Furthermore, a number of significant characteristics linked to AMD, such as pigment epithelial detachment and intraretinal fluid and subretinal fluid, have been measured using

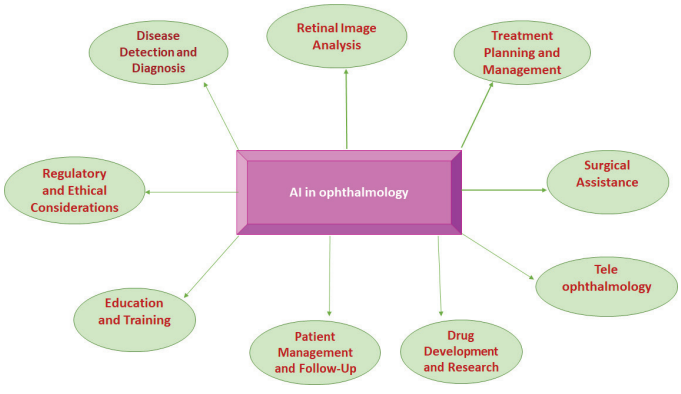

Figure 1. Various facets of AI in ophthalmology.

AI: Artificial intelligence.

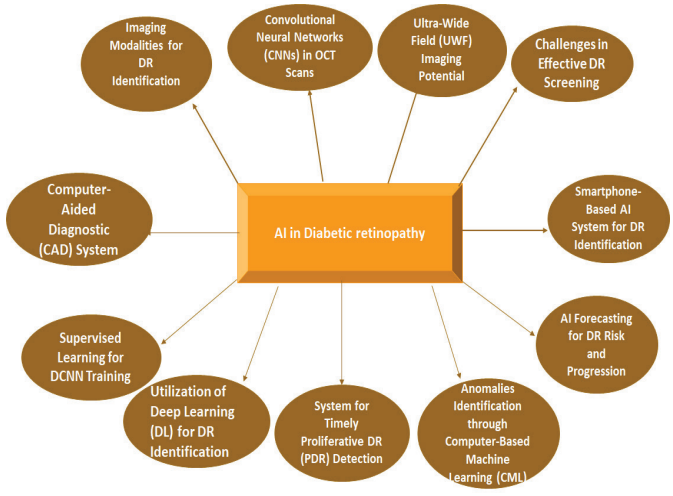

Figure 2. AI in diabetic retinopathy.

AI: Artificial intelligence, DR: Diabetic retinopathy, OCT: Optical coherence tomography, DCNN: Deep convolutional neural networks.

DL techniques. Research has focused on examining fundus images to identify drusen (33), fluid (34), reticular pseudodrusen (35), and geographic atrophy (36). With a usual accuracy rate of over 80%, the detection also includes the ability to forecast drusen regression, an important anatomical indicator distinguishing intermediate AMD and the beginning of severe AMD (37). This prediction is assisted by a specialized, fully automated ML algorithm. The process involves the application of automated image analysis techniques to recognize and characterize individual drusen at the initial assessment, with ongoing monitoring of their progression at subsequent visits. By leveraging this characterization and analysis, a survival analysis-based possibility of hazards and the anticipated deterioration of each individual drusen were determined using the ML method. Most importantly, automated retinal lesion detection and disease activity analysis demonstrate that it is feasible and holds considerable potential as a dependable tool in clinical practice Figure 3.

Other Retinal Disease

A DL model effectively identifies referable retinal illness using OCT images, exhibiting performance levels with retina subspecialists. This approach demonstrated competence in identifying diseases, including geographic atrophy, drusen, macular edema, macular holes, vitreomacular traction, central serous retinopathy, and epiretinal membrane membrane (38). The algorithm could accurately forecast retinal function in microperimetry for patients with stargardt disease by analyzing the structural characteristics of OCT using DL techniques. AI systems have shown the capacity to detect disorders, such as Macular telangiectasia, sickle cell disease, pachychoroid vasculopathy, and central serous retinopathy (39-42). Abnormal development of blood vessels in the retina is known as retinopathy of prematurity (ROP), which is a significant cause of juvenile blindness. The ETROP trial results highlight the critical need of early screening and intervention to improve visual outcomes for ROP (43). Recent developments suggest that AI may play a major role in ROP diagnosis, which would improve treatment outcomes. When evaluated on an independent dataset of 100 photos, a DL algorithm trained using wide-field retinal photographs outperformed six out of eight ROP experts in terms of diagnostic skill (44).

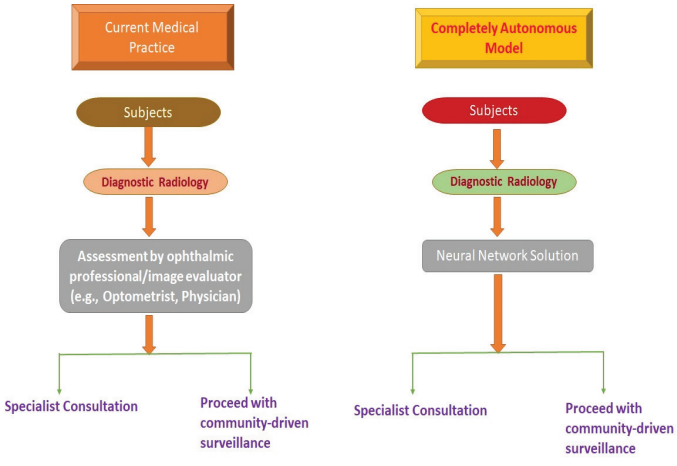

Figure 3. Degenerative maculopathy.

Corneal Disease

AI has lately been studied in anterior eye segment illnesses (45). It has shown promising results in accurately predicting the diagnosis of many corneal conditions, such as infectious keratitis (IK), keratoconus, pterygium, endothelial diseases, and difficulties associated with corneal transplantation. Dealing with clinical difficulties related to IK, such as accurately diagnosing the condition owing to variables including limited culture yield, absence of pathogen-specific characteristics, and infections caused by several microorganisms, continues to be an important element (46) for the treatment. Slit-lamp photos, often used in clinical settings to record and track IK and other disorders affecting the surface of the eye, have shown their ability to precisely diagnose different problems of the front part of the eye, such as IK, pterygium, conjunctivitis, and cataract (47). A unique DL system was created to automatically distinguish between fungal keratitis and non-fungal keratitis in corneal pictures (48). Furthermore, AI has shown its effectiveness in identifying corneal ectasia, namely keratoconus, by aiding in the early identification of suspected keratoconus, also known as forme fruste keratoconus, which can be difficult to diagnose. Numerous AI techniques, like automatic decision-tree classification (49), feedforward NN, CNN, and SVM learning, have been studied and proven to be successful (50). AI technologies, such as Keratodetect and ectasia status Index have been developed to diagnose keratoconus early and evaluate patients prior to refractive surgery. The anterior segment OCT, corneal topographies, and tomographies are used by these algorithms to analyze (51). Current endeavors have concentrated on formulating CNN algorithms that use numeric data matrices to enhance efficiency and flexibility for various topographical scenarios. AI has lately been used to investigate susceptibility genes linked to keratoconus. Hosoda et al. (52) identified particular gene regions linked to keratoconus susceptibility using IBM's Watson drug delivery. A genome-wide association study focusing on central corneal thickness was used to achieve this. DL algorithms have been applied to OCT images to distinguish between normal and edematous corneas (53). Fuchs endothelial corneal dystrophy was diagnosed using AI at an early stage (54). The clinical feature of using *in vivo* confocal microscopy images to evaluate the characteristics of the subbasal nerve plexus and establish connections with ocular and systemic illnesses has recently increased. The process of manually and partially automating the analysis of nerve fiber characteristics is well-recognized as arduous and time-intensive. However, the use of computer vision algorithms has greatly eased the automation of nerve analysis (55). Correlations between ocular nerves and diabetic neuropathy have been established using CNN-based approaches (56). The suggested technique entails the examination of three images from each eye, which allows for a thorough study similar to the clinical procedure performed by humans, eliminating the need for creating montages and acquiring additional images. Examining cataract pictures with computer-aided analysis is desirable. This entails automatically detecting and evaluating cataracts by fundus photography and/or slit-lamp photography. Although this method is perfect for identifying abnormalities of both the anterior and posterior segments concurrently, it must take into account any factors that could cause confusion, such as constricted pupils or vitreous opacities. Two SVM classifiers and a fully connected NN were used to identify and classify cataracts using resnet18 (Residual

Network) and Gray Level Co-occurrence Matrix. For discontinuous state transition, a deep NN with six grading levels was created as a result. The DST-ResNet and EDST-MLP models accurately detected and graded cataracts, respectively. Unlike cataracts in adults, cataracts in children show more variation. The choice of surgery is based on the likelihood of amblyopia, which is caused by a lack of visual stimulation (57). Performing pediatric tests presents difficulties, particularly in producing consistently high-quality slit-lamp pictures. The Apriori approach employs naive bayesian and RF prediction (58). After applying the synthetic minority oversampling approach to the datasets, three binary categories were resolved with average accuracy levels over 91%.

Anterior Ocular Region

Trachoma, a vision-threatening condition resulting from ocular infections with chlamydia trachomatis, was routinely investigated by analyzing eyelid images. There are two clinical trials: the PRET study, which focuses on eliminating trachoma in Niger, and the TANA trial, which aims to improve trachoma conditions in Northern Amhara (59). ML algorithms were used to identify trachomatous alterations (60) accurately. Furthermore, lacrimal scintigraphy (LS) has been established as a dependable and unbiased technique for evaluating tears and the lacrimal drainage system (61). ML and DL algorithms applied to LS images have demonstrated the ability to accurately diagnose lacrimal duct abnormalities in patients with a level of precision comparable to that of a skilled oculoplastic specialist. Ocular infections can cause trachoma, a disorder that can seriously impair vision. Thoracomatous alterations were successfully categorized using AI techniques, which let computers learn from experience and get better at it without having to be explicitly programed. LS has become a reliable and impartial technique for assessing tear flow and the lacrimal drainage system (62). Making use of DL and machine algorithms on LS images proved successful in classifying lacrimal duct pathology in patients, demonstrating accuracy on par with that of a proficient oculoplastic expert. The significance of meibomian glands (MGs) in maintaining ocular surface health is widely acknowledged, and the diagnostic technique involving the photographic documentation of eyelid MGs using Transillumination, often known as infrared light, is frequently employed for assessing and managing MG dysfunction. A DL approach was implemented to digitally partition and quantify the degree of MG atrophy in mimography images, thereby offering quantitative insights into gland atrophy. The algorithm demonstrated an impressive 95.6% accuracy in terms of grading meiboscores (63). An ML segmentation algorithm was employed to assess tear OCT and to measure meniscus thickness to quantify the amount of tear film (64). Although the sample size was small, the method consistently produced predictable findings. The researchers collected corneal topography data over time to develop a DL system for diagnosing keratoconus, a non-inflammatory condition of the cornea characterized by astigmatism and stromal thinning. The resulting model was able to predict cases of subclinical keratoconus with notable accuracy, and it also showed decent accuracy in keratoconus screening. A “NN”, designed and put into use by Dos Santos et al. (65), dubbed CorneaNet, especially for corneal OCT image segmentation. This algorithm was created to measure corneal thickness in patients with keratoconus and those with normal ocular conditions. The corneal thickness, primary layers (epithelium, bowman’s layer, and the middle stroma). The models exhibited comparable performance in detecting keratoconus, achieving an accuracy of validation levels between 99.45% and 99.57%. The application of DL was effective in identifying and classifying eyes with keratoconus, including the staging of the disease. Keratoconus is an irreversible condition that affects both eyes and is characterized by corneal weakening, protrusion, and scarring (66). Initially, it shows one-sided characteristics that may later develop, affecting both sides, except in uncommon situations (67). Identification of subclinical corneal ectasia poses a significant challenge. Both topography and tomography offer intricate data for each cornea to ophthalmologists. Despite the wealth of information distinguishing the several examined parameters, the distinctions between normal and subclinical keratoconus remain highly challenging for ophthalmologists. The Orbscan data employed SVM, multiple-layer perceptron classifiers, and radial basis function NN are examples of machine learning classifiers (MLC) (68). Each of these classifiers demonstrated proficiency in recognizing the previously mentioned corneal anomalies. Data from Scheimpflug tomography were selected over Orbscan information (69). Data from devices using Scheimpflug tomography-which generated three-dimensional, touch-free reconstructions of the anterior segment of the eye-were collected for the comparisons. After ML successfully differentiates between obvious corneal disorders, research efforts are directed toward creating AI that can recognize the subclinical features of corneal ectasia (70). Cataract, a condition characterized by a cloudy lens, affects many elderly individuals. Timely identification and intervention can significantly enhance the well-being of those with cataracts. ML techniques, including SVM and RF, have been used to detect and evaluate cataracts based on fundus photographs, ultrasound photographs, and visible wavelength photographs of the eye (71). Liu et al. (72) developed the first CAD system to classify and evaluate juvenile cataracts using CNNs. Additionally, a cloud-based platform with AI connectivity designed to promote cooperation between numerous hospitals has been developed. It is possible to design software for ophthalmologists and patients to use clinically, and the Zhong Shan Ophthalmic Center has documented the use of the program (72). These techniques are essential for creating surgical plans for horizontal strabismus and evaluating corneal power following myopia and corneal refractive surgery (73).

Glaucoma

Glaucoma is the second primary cause of permanent blindness globally. Detecting early-stage glaucoma has been proven effective in minimizing vision loss (74). The utilization of digital photography to capture images has been a prevalent technique for screening glaucoma, and its efficacy has been demonstrated in many telemedicine glaucoma programs. An extensive evaluation of persons suspected of having glaucoma may include gonioscopy, perimetry, tonometry, pachymetry, and spectral domain (SD) OCT (75). CFP of the optic nerve is an accessible and affordable way to check for glaucoma. Images of the optic nerve have been altered to help detect early signs of glaucoma more accurately thanks to ML. It is feasible to automate the early detection of glaucoma by integrating these algorithms into teleglaucoma screening protocols. Accompanying color fundus imaging with optic nerve OCT imaging has accelerated the creation of accurate DL algorithms for

glaucomatous nerve damage detection. When DL algorithms are trained to assess monoscopic optic nerve pictures using SD-OCT, they outperform glaucoma specialists in identifying glaucomatous optic nerve damage. Standard automated perimetry evaluation is one application of ML that seems promisinged (76). Many datasets are available, including findings from an extensive visual field (VF) test that was carried out over a long period of time. With a high degree of reliability, AI can anticipate glaucoma up to four years ahead of official raw VF data needed for diagnosis. The progression of patterns, a vibrational ML classifier, outperformed guided progression analysis in identifying the progression of glaucomatous optic neuropathy in patients with glaucoma and those suspected of having the disease (77). With the use of screening and monitoring datasets, AI seeks to produce affordable decision support systems that are as sensitive and specific as or more so than current techniques. The optic cup-to-disc ratio (CDR) is a useful marker for glaucoma identification (78). AI algorithms can compute the CDR to assist in the diagnosis of early-stage glaucoma by using automated optic nerve head location and optic disc/cup extraction from retinal images (79). The most likely patch on OCT images was precisely identified by the SVM model during training to provide a reference plane for computing the CDR (80) by approximating the coarse disc margin using a spatial correlation smoothness constraint. As glaucoma worsens, defects in the VF play a major role in the deterioration of visual function. Early in the disease, changes in the central VF may manifest, which is consistent with findings from imaging studies (81). Therefore, early detection of glaucomatous changes in the VF is essential for both the diagnosis and management of glaucoma.

Challenges and Future Research

AI utilization and contemporary applications in research represent significant advances in optimizing and enhancing efficiency. As the number of electronic medical record increases, healthcare providers and medical facilities find themselves with an extensive patient data repository. AI plays a crucial and central function in this context, as creating computer-generated algorithms or the appropriate training of automated systems for bulk processing of patient information results is a substantially faster data collection process than manual methods. Ophthalmology, a medical discipline characterized by swift access to ophthalmic imaging and objective markers, is particularly well-suited for managing vast datasets. The Smart Eye Database is a database that holds electronic health information about patients with ophthalmology, arranged according to the conditions that affect each patient's eyes (82). IRIS and the Smart Eye Database are two instances of datasets, which enables the identification of subtle correlations, the execution of multicenter studies, the integration of multimodal analyses, the discovery of novel imaging patterns, and increased statistical power in research. These capabilities are challenging to achieve with smaller datasets (83). Modifications to these machines were confined to those foreseen and considered during pre-programing. Since humans programed the machine, its capabilities were restricted by the technological knowledge of the individuals who drafted the programing. The caliber of the dataset that an AI algorithm uses for training and validation determines the effectiveness of the program will be estimating the optimal number of training images within a dataset poses a challenge, as there is a common belief that a larger number of images leads to better outcomes. However, an excessively large dataset can impede the efficiency of the training process and potentially result in overfitting the MLC to the training dataset. Variations between machines from different brands may introduce subtle differences that can impact assessment accuracy. Restricting the number of categories in a program to those with significant predictive importance may be beneficial given the size of the dataset and the complexity of the algorithm (84). Establishing standards for reporting in future research is crucial for minimizing heterogeneity across studies. If AI improves medical care, it becomes imperative to ensure that these improvements reach populations facing financial constraints. A significant obstacle in deploying proven, the need for AI solutions is essential for a complete solution designed for practical use. Achieving this goal may involve integrating DL, implementing solutions that demonstrate satisfactory performance in a clinical setting, and ensuring that the solution can effectively handle pictures of different quality levels from regularly used equipment. There is a requirement for developing clinical guidelines that support the provision of patients with the DL system classifications and supporting their choice of patient. It is important to remember that the majority of DL systems in use today have only been independently validated for the classification of one eye condition at a time. For providers without technical AI or software skills, maintaining and switching between different DL systems for every possible eye condition is impractical and represents a considerable challenge. It is crucial to establish supportive systems and processes to rectify misclassifications among patients, including instances of incorrect classifications or errors in either direction. This emphasizes the importance of adopting standardized practices in the entire lifecycle of AI, encompassing development, validation, reporting and implementation. Such measures are essential to prevent misclassification issues, especially when AI is applied to diverse target populations. Ethical and legal dilemmas arise when employing DL systems to classify clinical data, particularly due to their lack of ability to explain. Addressing these challenges requires a focus on appropriate training data and external validation. Overcoming this obstacle is essential for ensuring the generalizability and practical application of these solutions. The challenge lies in the arduous task of labeling collected data throughout the training process, which requires the participation of skilled practitioners. By carefully selecting patients, the imaging datasets are repetitively labeled to calibrate the DL system, with each new set population potentially causing delays in adoption and contributing to setup costs. The inherent characteristics of AI and the absence of comprehensibility in DL methods provide substantial technical obstacles that must be resolved. Advancements in AI development for picture classification include using techniques like "soft attention" (85). New approaches like "weighted error scoring" are being created to compare the effects of inaccurate automated classification AI decisions to human grading (86). AI techniques have proven effective in the healthcare industry for identifying a range of illnesses. By easing the sharing of specialist expertise and optimizing limited resources, AI applications can greatly aid in the support of patients in remote areas. However, model accuracy frequently decreased as the frequency of disease increased. In order to enhance the use of AI in clinical settings, funding must be allocated toward developing intelligent systems capable of accurately diagnosing a broad spectrum of illnesses.

Reliance on a small number of abnormalities identified by a single imaging method may not guarantee accurate diagnosis of certain retinal diseases in clinical practice, such as glaucoma or DR. including a number of clinical images, including fundus, angiography, OCT, and VF imaging, is essential for constructing a robust AI system that ensures more reliable diagnostic outcomes. Despite the availability of various datasets, the fundamental challenge lies in the insufficient representation of the multitude of diseases that humans experience. Images depicting severe or rare diseases are notably lacking in these datasets. Therefore, when selecting input data, factors such as demographic features, the existence of various systemic illnesses, and the numerous physical traits of diseases should be considered. For more robust validation, larger datasets from diverse patient cohorts encompassing different settings, conditions, ethnicities, and environments are imperative for some automated diagnosis systems that have shown promising outcomes. Significant reliance on data quality should not be overlooked. The diversity of imaging devices, imaging procedures, and inherent noise in the data can substantially impact data quality, thereby exerting considerable influence on model performance. AI faces challenges in ophthalmological dyslexia by needing nuanced data for accurate recognition, understanding, and aiding dyslexic individuals (87). AI confronts significant challenges when it comes to enhancing wearable eye sensor gadgets tailored for eye-related diagnostic applications (88). The challenges lie in refining sensor precision, minimizing device size while maximizing data accuracy, addressing connectivity issues, ensuring seamless integration with AI algorithms, and fostering user trust regarding data security and privacy. AI confronts significant hurdles when it comes to enhancing wearable sensor gadgets tailored for eye-related applications. The challenges lie in refining sensor precision, minimizing device size while maximizing data accuracy, addressing connectivity issues, ensuring seamless integration with AI algorithms, and fostering user trust regarding data security and privacy. AI must overcome variability in symptoms, adapt to diverse language patterns, and provide personalized interventions. Ensuring inclusivity, privacy and ethical use while enhancing accessibility remain pivotal challenges in AI for dyslexia support. AI needs to revolutionize cancer diagnosis (89) for eye diseases, employing advanced algorithms to analyze medical images swiftly and accurately. In radiology, AI helps interpret complex optic scans, enhancing early detection and personalized treatment for ophthalmology.

CONCLUSION

AI and DL capabilities are advancing swiftly, presenting potential solutions to technical challenges. In the realm of ophthalmology, research on AI has moved away from creating and validating tools to their practical implementation. This crucial transition aims to identify and address practical and sociocultural challenges, tailoring solutions to the specific needs of users, including patients and healthcare providers. In conclusion, AI exhibits great promise in enhancing the capacity of health systems for eye screening in well-defined areas. This involves automating the classification of diseases, such as DR, across various clinical applications. There is a growing degree of preparedness as technology advances from clinical validation to translation; however, new difficulties arise when incorporating AI solutions into clinical care pathways and healthcare infrastructures. Current studies are in progress to tackle the issues mentioned and provide focused remedies.

Ethics

Author Contributions

Concept: L.S., Design: L.S., Analysis or Interpretation: A.S., Literature Search: A.S., A.M., Writing: A.S.

Conflict of Interest: No conflict of interest is declared by the authors.

Financial Disclosure: The authors declared that this study received no financial support.

REFERENCES

1. Demir S, Paksoy T. Ai, robotics and autonomous systems in scm. Logistics. 2020 Dec 17;4:156.
2. Chen RC, Dewi C, Huang SW, Caraka RE. Selecting critical features for data classification based on machine learning methods. Journal of Big Data. 2020; 7: 52.
3. Dilsizian SE, Siegel EL. Artificial intelligence in medicine and cardiac imaging: harnessing big data and advanced computing to provide personalized medical diagnosis and treatment. Curr Cardiol Rep. 2014; 16: 441.
4. Patel VL, Shortliffe EH, Stefanelli M, Szolovits P, Berthold MR, Bellazzi R, et al. The coming of age of artificial intelligence in medicine. Artif Intell Med. 2009; 46: 5-17.
5. Massie J, Block SS, Morjaria P. The role of optometry in the delivery of eye care via telehealth: a systematic literature review. Telemedicine and e-Health. 2022 Dec 1; 28: 1753-63.
6. Ting DS, Gunasekeran DV, Wickham L, Wong TY. Next generation telemedicine platforms to screen and triage. Br J Ophthalmol. 2020; 104: 299-300.
7. Gurunath Bharathi PG, Agrawal A, Sundaram P, Sardesai S. Combination of hand-crafted and unsupervised learned features for ischemic stroke lesion detection from Magnetic Resonance Images. Biocybern Biomed Eng. 2019; 39: 410-25.
8. Hitchings RA, Spaeth GL. The optic disc in glaucoma. I: Classification. Br J Ophthalmol. 1976; 60: 778-85.
9. Davis MD, Gangnon RE, Lee LY, Hubbard LD, Klein BE, Klein R, et al. The Age-Related Eye Disease Study severity scale for age-related macular degeneration: AREDS Report No. 17. Arch Ophthalmol. 2005; 123: 1484-98.
10. Grassmann F, Mengelkamp J, Brandl C, Harsch S, Zimmermann ME, Linkohr B, et al. A Deep Learning Algorithm for Prediction of Age-Related Eye Disease Study Severity Scale for Age-Related Macular Degeneration from Color Fundus Photography. Ophthalmology. 2018; 125: 1410-20.
11. Govindaiah A, Smith RT, Bhuiyan A. A New and Improved Method for Automated Screening of Age-Related Macular Degeneration Using Ensemble Deep Neural Networks. Annu Int Conf IEEE Eng Med Biol Soc. 2018; 2018: 702-5.
12. Russakoff DB, Lamin A, Oakley JD, Dubis AM, Sivaprasad S. Deep Learning for Prediction of AMD Progression: A Pilot Study. Invest Ophthalmol Vis Sci. 2019; 60: 712-22.
13. Jammal AA, Thompson AC, Mariottoni EB, Berchuck SI, Urata CN, Estrela T, et al. Human Versus Machine: Comparing a Deep Learning Algorithm to Human Gradings for Detecting Glaucoma on Fundus Photographs. Am J Ophthalmol. 2020; 211: 123-31.

14. Al-Aswad LA, Kapoor R, Chu CK, Walters S, Gong D, Garg A, et al. Evaluation of a Deep Learning System for Identifying Glaucomatous Optic Neuropathy Based on Color Fundus Photographs. J Glaucoma. 2019; 28: 1029-34.
15. Rokach L, Maimon O. Top-down induction of decision trees classifiers - a survey. IEEE Trans Syst Man Cybern C. 2005; 35: 476-87.
16. Breiman L. Random forests. Mach Learn. 2001; 45: 5-32.
17. Chang CC, Lin CJ. LIBSVM: a library for support vector machines. ACM Trans Intell Syst Technol. 2011; 2: 1-27.
18. Quan Y. Development of computer aided classroom teaching system based on machine learning prediction and artificial intelligence KNN algorithm. Journal of Intelligent & Fuzzy Systems. 2020 Jan 1; 39: 1879-90.
19. Keller JM, Gray MR, Givens JA. A fuzzy K-nearest neighbor algorithm. IEEE Trans Syst Man Cybern. 2012; SMC-15: 580-5.
20. Kanungo T, Mount DM, Netanyahu NS, Piatko CD, Silverman R, Wu AY. An efficient k-means clustering algorithm: analysis and implementation. IEEE Trans Pattern Anal Mach Intell. 2002; 24: 881-92.
21. Ye J. Two-dimensional linear discriminant analysis. Adv Neural Inf Process Syst. 2005; 17: 1431-41.
22. Phillips NA, Rajpurkar P, Sabini M, Krishnan R, Zhou S, Pareek A, et al. CheXphoto: 10,000+ photos and transformations of chest X-rays for benchmarking deep learning robustness. InMachine Learning for Health 2020; pp. 318-27.
23. Khilji AFUR, Sinha U, Singh P, Ali A, Dadure P, Manna R, et al. Multimodal recipe recommendation system using deep learning and rule-based approach. SN Comput Sci. 2023; 4: 421.
24. Gulshan V, Peng L, Coram M, Stumpe MC, Wu D, Narayanaswamy A, et al. Development and validation of a deep learning algorithm for detection of diabetic retinopathy in retinal fundus photographs. JAMA. 2016; 316: 2402-10.
25. Hassan T, Akram MU, Hassan B, Syed AM, Bazaz SA. Automated segmentation of subretinal layers for the detection of macular edema. Appl Opt. 2016; 55: 454-61.
26. Lee CS, Tyring AJ, Deruyter NP, Wu Y, Rokem A, Lee AY. Deep-learning based, automated segmentation of macular edema in optical coherence tomography. Biomed Opt Express. 2017; 8: 3440-8.
27. Roy AG, Conjeti S, Karri SPK, Sheet D, Katouzian A, Wachinger C, et al. ReLayNet: retinal layer and fluid segmentation of macular optical coherence tomography using fully convolutional networks. Biomed Opt Express. 2017; 8: 3627-42.
28. Akram MU, Tariq A, Khan SA, Javed MY. Automated detection of exudates and macula for grading of diabetic macular edema. Comput Methods Programs Biomed. 2014; 114: 141-52.
29. Welikala RA, Dehmeshki J, Hoppe A, Tah V, Mann S, Williamson TH, et al. Automated detection of proliferative diabetic retinopathy using a modified line operator and dual classification. Comput Methods Programs Biomed. 2014; 114: 247-61.
30. Wong TY, Bressler NM. Artificial intelligence with deep learning technology looks into diabetic retinopathy screening. JAMA. 2016; 316: 2366-7.
31. Feeny AK, Tadarati M, Freund DE, Bressler NM, Burlina P. Automated segmentation of geographic atrophy of the retinal epithelium via random forests in AREDS color fundus images. Comput Biol Med. 2015; 65: 124-36.
32. Hosny A, Parmar C, Quackenbush J, Schwartz LH, Aerts HJWL. Artificial intelligence in radiology. Nat Rev Cancer. 2018; 18: 500-10.
33. Ran A, Cheung CY. Deep learning-based optical coherence tomography and optical coherence tomography angiography image analysis: an updated summary. Asia Pac J Ophthalmol (Phila). 2021; 10: 253-60.
34. Chen Q, Leng T, Zheng L, Kutzscher L, Ma J, de Sisternes L, et al. Automated drusen segmentation and quantification in SD-OCT images. Med Image Anal. 2013; 17: 1058-72.
35. Bogunovic H, Montuoro A, Baratsits M, Karantonis MG, Waldstein SM, Schlanitz F, et al. Machine learning of the progression of intermediate age-related macular degeneration based on OCT imaging. Invest Ophthalmol Vis Sci. 2017; 58: BIO141-50.
36. van Grinsven MJ, Buitendijk GH, Brussee C, van Ginneken B, Hoyng CB, Theelen T, et al. Automatic identification of reticular pseudodrusen using multimodal retinal image analysis. Invest Ophthalmol Vis Sci. 2015; 56: 633-9.
37. Jonas JB, Cheung CMG, Panda-Jonas S. Updates on the epidemiology of age-related macular degeneration. Asia Pac J Ophthalmol (Phila). 2017; 6: 493-7.
38. Ly A, Yapp M, Nivison-Smith L, Assaad N, Hennessy M, Kalloniatis M. Developing prognostic biomarkers in intermediate age-related macular degeneration: their clinical use in predicting progression. Clin Exp Optom. 2018; 101: 172-81.
39. Schulze S, Hoerle S, Mennel S, Kroll P. Vitreomacular traction and exudative age-related macular degeneration. Acta Ophthalmol. 2008; 86: 470-81.
40. Ko J, Han J, Yoon J, Park JI, Hwang JS, Han JM, et al. Assessing central serous chorioretinopathy with deep learning and multiple optical coherence tomography images. Sci Rep. 2022; 12: 1-8.
41. Chou YB, Hsu CH, Chen WS, Chen SJ, Hwang DK, Huang YM, et al. Deep learning and ensemble stacking technique for differentiating polypoidal choroidal vasculopathy from neovascular age-related macular degeneration. Sci Rep. 2021; 11: 1-9.
42. Cai S, Han IC, Scott AW. Artificial intelligence for improving sickle cell retinopathy diagnosis and management. Eye (Lond). 2021; 35: 2675-84.
43. Loo J, Cai CX, Choong J, Chew EY, Friedlander M, Jaffe GJ, et al. Deep learning-based classification and segmentation of retinal cavitations on optical coherence tomography images of macular telangiectasia type 2. Br J Ophthalmol. 2022; 106: 396-402.
44. Early Treatment for Retinopathy of Prematurity Cooperative Group; Good WV, Hardy RJ, Dobson V, Palmer EA, Phelps DL, Tung B, et al. Final visual acuity results in the early treatment for retinopathy of prematurity study. Arch Ophthalmol. 2010; 128: 663-71.
45. Yang J, Fong S, Wang H, Hu Q, Lin C, Huang S, et al. Artificial intelligence in ophthalmopathy and ultra-wide field image: A survey. Expert Syst Appl. 2021; 182: 115068.
46. De Fauw J, Ledsam JR, Romera-Paredes B, Nikolov S, Tomasev N, Blackwell S, et al. Clinically applicable deep learning for diagnosis and referral in retinal disease. Nat Med. 2018; 24: 1342-50.
47. Khoo P, Cabrera-Aguas MP, Nguyen V, Lahra MM, Watson SL. Microbial keratitis in Sydney, Australia: risk factors, patient outcomes, and seasonal variation. Graefes Arch Clin Exp Ophthalmol. 2020; 258: 1745-55.
48. Dahlgren MA, Lingappan A, Wilhelmus KR. The clinical diagnosis of microbial keratitis. Am J Ophthalmol. 2007; 143: 940-4.
49. Kuo MT, Hsu BW, Yin YK, Fang PC, Lai HY, Chen A, et al. A deep learning approach in diagnosing fungal keratitis based on corneal photographs. Sci Rep. 2020; 10: 14424.
50. Issarti I, Consejo A, Jiménez-García M, Hershko S, Koppen C, Rozema JJ. Computer aided diagnosis for suspect keratoconus detection. Comput Biol Med. 2019; 109: 33-42.

51. Bansal M, Goyal A, Choudhary A. A comparative analysis of K-nearest neighbor, genetic, support vector machine, decision tree, and long short term memory algorithms in machine learning [journal]. Decision Analytics Journal. 2022; 3: 100071.
52. Hosoda Y, Miyake M, Meguro A, Tabara Y, Iwai S, Ueda-Arakawa N, et al. Keratoconussusceptibility gene identification by corneal thickness genome-wide association study and artificial intelligence IBM Watson. Commun Biol. 2020; 3: 410.
53. Yasuno Y, Madjarova VD, Makita S, Akiba M, Morosawa A, Chong C, et al. Three-dimensional and high-speed swept-source optical coherence tomography for in vivo investigation of human anterior eye segments. Opt Express. 2005; 13: 10652-64.
54. Zéboulon P, Ghazal W, Gatinel D. Corneal edema visualization with optical coherence tomography using deep learning: proof of concept. Cornea. 2021; 40: 1267-75.
55. Eleiwa T, Elsawy A, Özcan E, Abou Shousha M. Automated diagnosis and staging of Fuchs'endothelial cell corneal dystrophy using deep learning. Eye Vis (Lond). 2020; 7: 44.
56. Dabbah MA, Graham J, Petropoulos IN, Tavakoli M, Malik RA. Automatic analysis of diabetic peripheral neuropathy using multi-scale quantitative morphology of nerve fibres in corneal confocal microscopy imaging. Med Image Anal. 2011; 15: 738-47.
57. Zetterström C, Lundvall A, Kugelberg M. Cataracts in children. Journal of Cataract & Refractive Surgery. 2005 Apr 1; 31: 824-40.
58. Papageorgiou E, Asproudis I, Maconachie G, Tsironi EE, Gottlob I. The treatment of amblyopia: current practice and emerging trends. Graefes Arch Clin Exp Ophthalmol. 2019; 257: 1061-78.
59. Zhang K, Liu X, Jiang J, Li W, Wang S, Liu L, et al. Prediction of postoperative complications of pediatric cataract patients using data mining. J Transl Med. 2019; 17: 2.
60. Socia D, Brady CJ, West SK, Cockrell RC. Detection of trachoma using machine learning approaches. PLoS neglected tropical diseases. 2022 Dec 7; 16: e0010943.
61. Kim MC, Okada K, Ryner AM, Amza A, Tadesse Z, Cotter SY, et al. Sensitivity and specificity of computer vision classification of eyelid photographs for programmatic trachoma assessment. PLOS ONE. 2019; 14: e0210463.
62. Oklar M, Yazıcıoglu T, Talan M. Modified Horner-Duverney's muscle plication in the treatment of functional epiphora. Graefes Arch Clin Exp Ophthalmol. 2023; 261: 2971-8.
63. Amanat LA, Hilditch TE, Kwok CS. Lacrimal scintigraphy. III. Physiological aspects of lacrimal drainage. Br J Ophthalmol. 1983; 67: 729-32.
64. Wang J, Yeh TN, Chakraborty R, Yu SX, Lin MC. A deep learning approach for Meibomian gland atrophy evaluation in meibography images. Transl Vis Sci Technol. 2019; 8: 37.
65. Dos Santos VA, Schmetterer L, Stegmann H, Pfister M, Messner A, Schmidinger G, et al. CorneaNet: fast segmentation of cornea OCT scans of healthy and keratoconic eyes using deep learning. Biomed Opt Express. 2019; 10: 622-41.
66. Dogan L, Arslan GD. Evaluation of the tear meniscus using optical coherence tomography in Meibomian gland dysfunction. Ocul Immunol Inflamm. 2023; 31: 1785-91.
67. Krachmer JH, Feder RS, Belin MW. Keratoconus and related noninflammatory corneal thinning disorders. Surv Ophthalmol. 1984; 28: 293-22.
68. Holland DR, Maeda N, Hannush SB, Riveroll LH, Green MT, Klyce SD, et al. Unilateral keratoconus. Incidence and quantitative topographic analysis. Ophthalmology. 1997; 104: 1409-13.
69. Kamiya K, Ayatsuka Y, Kato Y, Fujimura F, Takahashi M, Shoji N, et al. Keratoconus detection using deep learning of colour-coded maps with anterior segment optical coherence tomography: a diagnostic accuracy study. BMJ Open. 2019; 9: e031313.
70. Sy ME, Ramirez-Miranda A, Zarei-Ghanavati S, Engle J, Danesh J, Hamilton DR. Comparison of posterior corneal imaging before and after LASIK using dual rotating scheimpflug and scanning slit-beam corneal tomography systems. J Refract Surg. 2013; 29: 96-101.
71. Yang JJ, Li J, Shen R, Zeng Y, He J, Bi J, et al. Exploiting ensemble learning for automatic cataract detection and grading. Comput Methods Programs Biomed. 2016; 124: 45-57.
72. Liu X, Jiang J, Zhang K, Long E, Cui J, Zhu M, et al. Localization and diagnosis framework for pediatric cataracts based on slit-lamp images using deep features of a convolutional neural network. PLoS One. 2017; 12: e0168606.
73. Almeida JDSD, Silva AC, Teixeira JAM, Paiva AC, Gattass M. Surgical planning for horizontal strabismus using support vector regression. Comput Biol Med. 2015; 63: 178-86.
74. Leske MC, Heijl A, Hussein M, Bengtsson B, Hyman L, Komaroff E; Early Manifest Glaucoma Trial Group. Factors for glaucoma progression and the effect of treatment: the early manifest glaucoma trial. Arch Ophthalmol. 2003; 121: 48-56.
75. Martucci A, Toschi N, Cesareo M, Giannini C, Pocobelli G, Garaci F, et al. Spectral domain optical coherence tomography assessment of macular and optic nerve alterations in patients with glaucoma and correlation with visual field index. J Ophthalmol. 2018; 2018: 6581846.
76. Balyen L, Peto T. Promising artificial intelligence-machine learning-deep learning algorithms in ophthalmology. Asia Pac J Ophthalmol (Phila). 2019; 8: 264-72.
77. Haleem MS, Han L, van Hemert J, Li B. Automatic extraction of retinal features from colour retinal images for glaucoma diagnosis: a review. Comput Med Imaging Graph. 2013; 37: 581-96.
78. Tangelder GJ, Reus NJ, Lemij HG. Estimating the clinical usefulness of optic disc biometry for detecting glaucomatous change over time. Eye (Lond). 2006; 20: 755-63.
79. Raja C, Gangatharan N. A hybrid swarm algorithm for optimizing glaucoma diagnosis. Comput Biol Med. 2015; 63: 196-207.
80. Shehryar T, Akram MU, Khalid S, Nasreen S, Tariq A, Perwaiz A, et al. Improved automated detection of glaucoma by correlating fundus and SD-OCT image analysis. Int J Imaging Syst Technol. 2020; 30: 1046-65.
81. Hood DC, Raza AS, de Moraes CG, Johnson CA, Liebmann JM, Ritch R. The Nature of Macular Damage in Glaucoma as Revealed by Averaging Optical Coherence Tomography Data. Transl Vis Sci Technol. 2012; 1: 3.
82. Kortüm KU, Müller M, Kern C, Babenko A, Mayer WJ, Kampik A, et al. Using Electronic Health Records to Build an Ophthalmologic Data Warehouse and Visualize Patients' Data. Am J Ophthalmol. 2017; 178: 84-93.
83. Lee CS, Brandt JD, Lee AY. Big data and artificial intelligence in ophthalmology: where are we now? Ophthalmol Sci. 2021; 1: 100036.
84. Han SS, Lim W, Kim MS, Park I, Park GH, Chang SE. Interpretation of the Outputs of a Deep Learning Model Trained with a Skin Cancer Dataset. J Invest Dermatol. 2018; 138: 2275-7.
85. Nguyen VD, Bui ND, Do HK. Skin Lesion Classification on Imbalanced Data Using Deep Learning with Soft Attention. Sensors (Basel). 2022; 22: 7530.

86. Kermany DS, Goldbaum M, Cai W, Valentim CCS, Liang H, Baxter SL, et al. Identifying medical diagnoses and treatable diseases by image-based deep learning. Cell. 2018; 172: 1122-31.
87. Shalileh S, Ignatov D, Lopukhina A, Dragoy O. Identifying dyslexia in school pupils from eye movement and demographic data using artificial intelligence. Plos one. 2023; 18: e0292047.
88. Mandal D, Bag S. Smart Health Monitoring Using Wearable Device Sensors: A Brief Review. Int J Pharm Sci. 2023; 14: 46-61.
89. Ali WM, Alhumaidi MS. Artificial Intelligence for Cancer Diagnosis & Radiology. International Journal of Trends in OncoScience. 2023: 13-8.